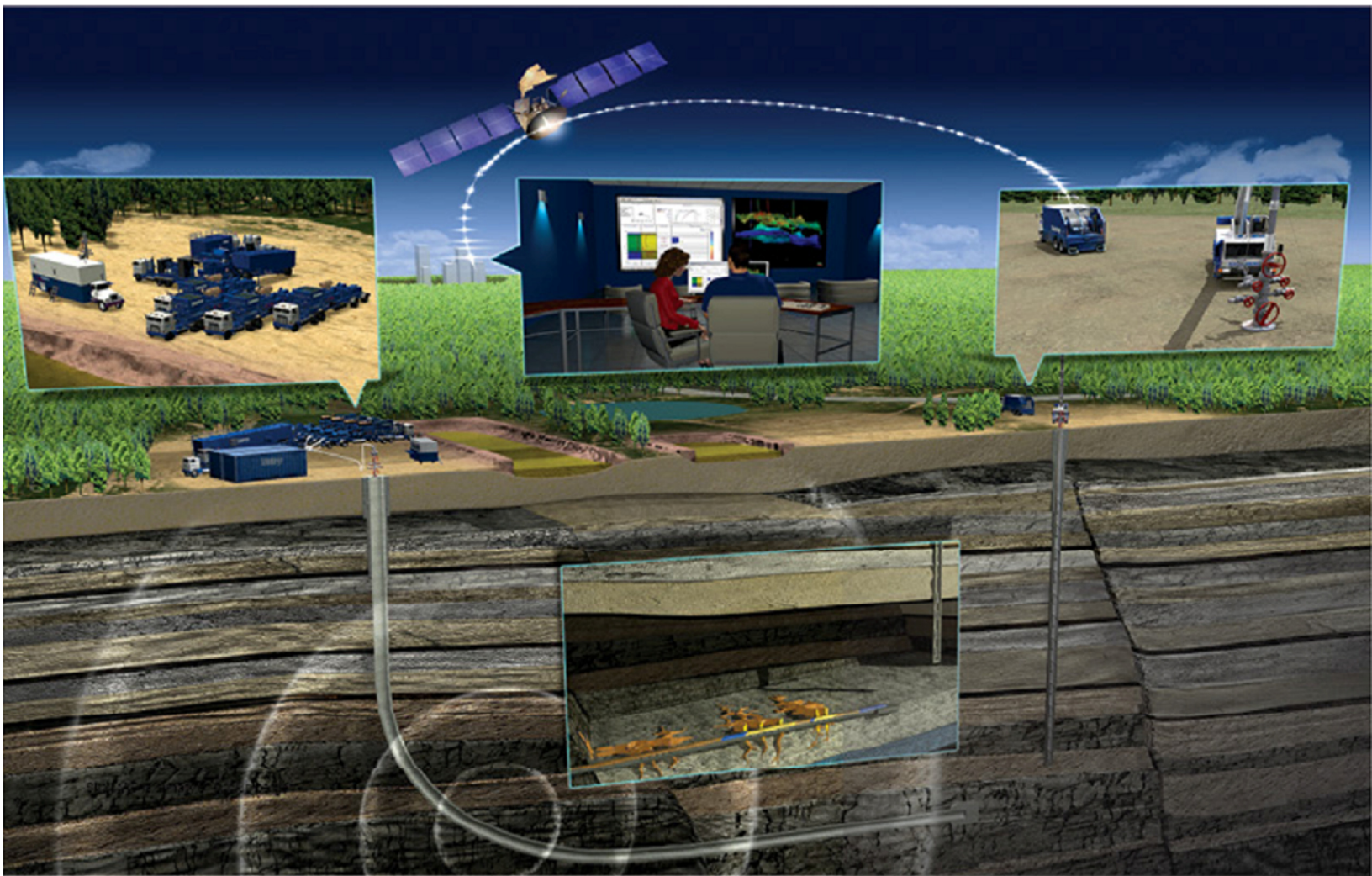


Schlumberger Microseismic Services Evaluation Report

URS Energy and Construction Inc.

Marcellus Shale
COP 324A #6HM
Clearfield County, PA

Jul 15, 2013 - Jul 19, 2013



Schlumberger Microseismic Services Evaluation Report

**COP 324A #6HM
Clearfield County, PA
Marcellus Shale**

**Prepared for
URS Energy and Construction Inc.**

**Prepared by
Schlumberger**

Aug 26, 2013

Steve Reese
Evaluation Engineer

Craig Woerpel/Tim Osburg
Geophysicists

Robert Downie
Microseismic Interpretation Manager
North America

For contact link and information about Schlumberger hydraulic fracture monitoring service, please go to:
http://www.slb.com/services/completions/stimulation/hydraulic_fracture_monitoring.aspx

Disclaimer Notice

This information is presented in good faith, but no warranty is given by and Schlumberger assumes no liability for advice or recommendations made concerning results to be obtained from the use of any product or service. The results given are estimates based on calculations produced by a computer model including various assumptions on the well, reservoir and treatment. The results depend on input data provided by the Operator and estimate as to unknown data and can be no more accurate than the model, the assumptions and such input data. The information presented is Schlumberger's best estimate of the actual results that may be achieved and should be used for comparison purposes rather than absolute values. The quality of input data, and hence results, may be improved through the use of certain tests and procedures which Schlumberger can assist in selecting.

Freedom from infringement of patents of Schlumberger or others is not to be inferred.

Summary	1
1 Microseismic Monitoring Configuration and Quality Control for Evaluation	4
1.1 Project Overview	4
1.2 Monitoring Well Data	4
1.3 Quality Control of the Microseismic Events for Evaluation	5
1.4 Magnitude versus Distance	11
2 Completion Design and Execution Summary.....	12
2.1 Treatment Well Data	12
2.2 Completion and Stimulation Design	13
2.3 Execution Results and Microseismic Estimates of Dimensions and Stimulated Volumes	14
3 Microseismic Length and Azimuth.....	15
4 Microseismic Height	18
5 Microseismic Volume (Event-Density)	21
6 Seismic Moment Applications.....	24
7 Time-Dependent Behavior	29
8 Treatment Data and Microseismic Events Summary by Stage	34
8.1 Stage 01.....	34
8.2 Stage 02.....	38
8.3 Stage 03.....	42
8.4 Stage 04.....	46
8.5 Stage 05.....	50
8.6 Stage 06.....	54
8.7 Stage 07.....	58
8.8 Stage 08.....	62
8.9 Stage 09.....	66
8.10Stage 10.....	70
8.11Stage 11.....	74
8.12Stage 12.....	78
8.13Stage 13.....	82
9 Geophysics Processing Report	86
Calibration Overview	87
Velocity Model Construction and Calibration.....	89
Velocity Model	89

Calibration Shots Results	91
Calibration Shot Waveforms.....	92
Quality Indicators.....	93
Signal-to-noise ratio	94
Magnitude.....	96
Confidence Factor	99
Example Waveforms	100
Uncertainty	103
Source Dimension	105

Summary

Schlumberger Microseismic Services acquired microseismic events data during the completion of the Marcellus formation in the COP 324A 6HM well. The well is located in the Clearfield County, Pennsylvania. Schlumberger provided fracturing services during the project. A total of 13 stimulation stages were monitored and evaluated.

The objectives of the evaluation are as follows:

- Evaluation of fracture geometry
- Stimulated volume of each treatment stage
- Discussion of fracture containment and height growth

This report contains the following evaluations. Stage-by-stage summaries and a geophysical processing report are attached.

1. Monitoring configuration and quality control of the detected microseismic events used in the evaluation
2. Completion and stimulation treatment summary
3. Microseismic length and azimuth
4. Microseismic height
5. Microseismic estimate of stimulated volumes using event-density calculation methods
6. Cumulative seismic moment evaluation
7. Time-dependent and depth-dependent behavior

Discussion

The microseismic events extended generally northeast and southwest of the treatment well with apparent asymmetry to the southeast. The azimuths shown are based on the locations of the microseismic events. Azimuth estimates for stages 11-13 are less well defined than previous treatments as seen in Figure 1. The average total length of the event clouds is about 2,300 feet. However, much of this apparent length appears to take place in the Hamilton formation. The average length based on evaluation of seismic moment and deformation is approximately one half the total length that is generated using event locations. The latter figure is considered more representative of fracture geometry.

Each of the treatment stages appears to be very well contained by the Tully Limestone formation above zone, which historically has proved to be a fairly competent barrier to upward height growth. The Onondaga Limestone formation, which is also usually a competent barrier, seems to lose some integrity after Stage 4 of the job. After Stage 4, many events are observed within the Onondaga and below to the Helderberg formation. It is important to note that all perforations were shot down at 0 degree phasing from Stage 5 on. Possible fault contact has been identified during stage 5 and stage 6 and coincides with the change in observed fracture height growth. Figure 2 is a summary of height estimates from the microseismic events.

The time-dependent behavior of the microseismic events shows that the treatments that are contained against downward growth by the Onondaga (stages 1-4) have increased height growth and microseismic activity in the Hamilton during the later portion of the stimulation treatment. The activity in the Hamilton appears to spread to greater distances laterally from the treatment well than events in the Marcellus. A more conservative estimate of fracture length based on moment-density is shown in Figure 3. Figure 3 also shows the event locations for comparison purposes.

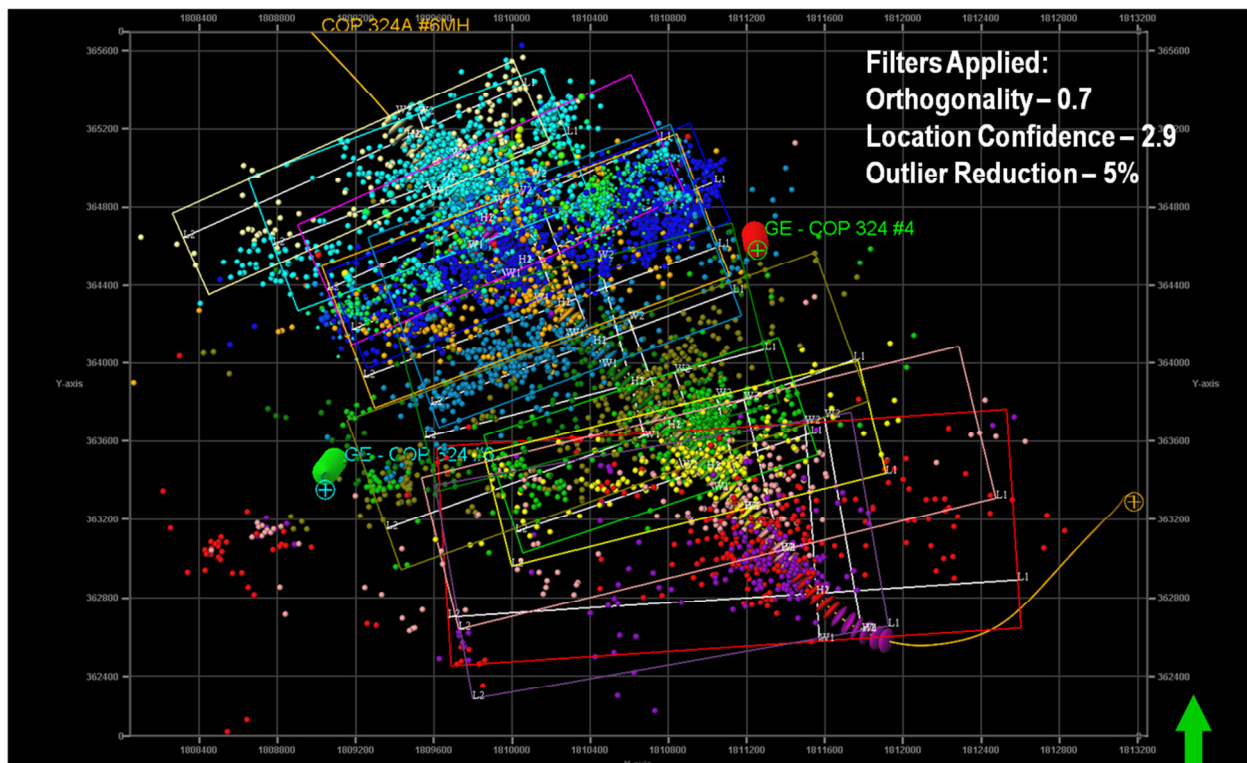


Figure 1 – Microseismic estimate of fracture length and azimuth

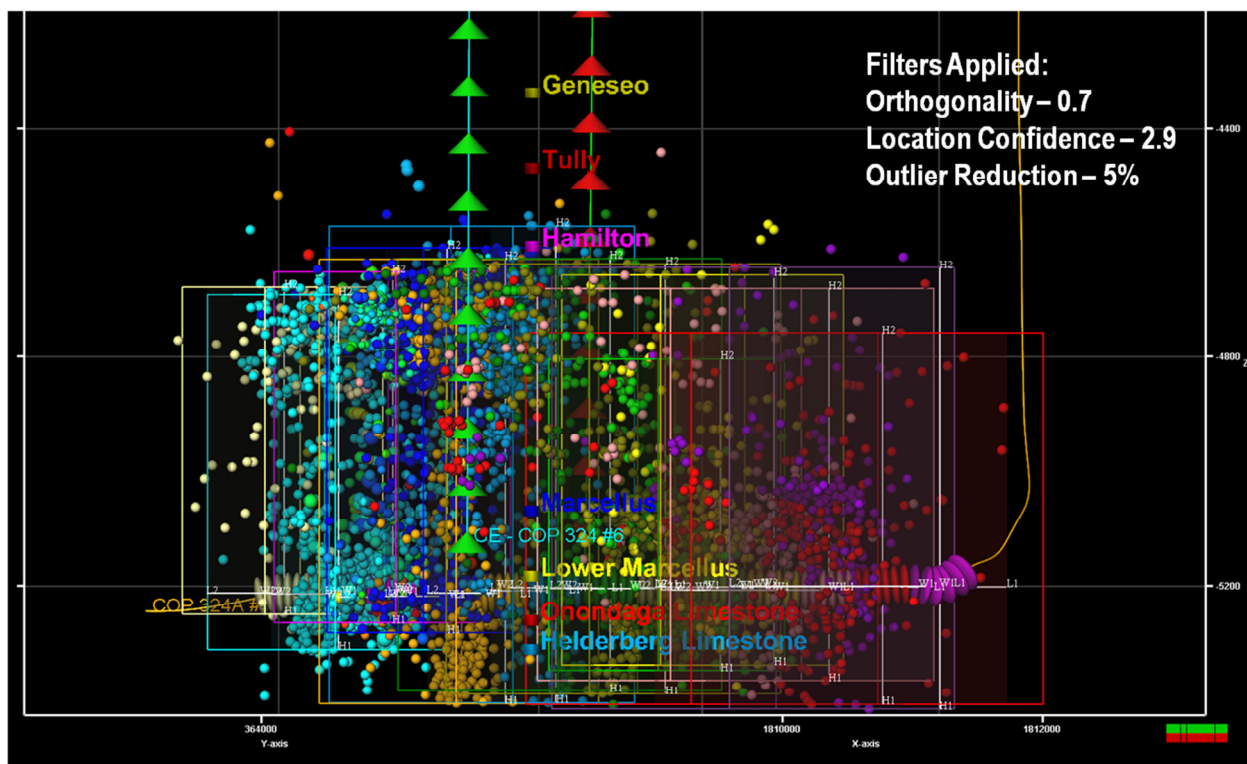


Figure 2 – Fracture height estimate using event locations

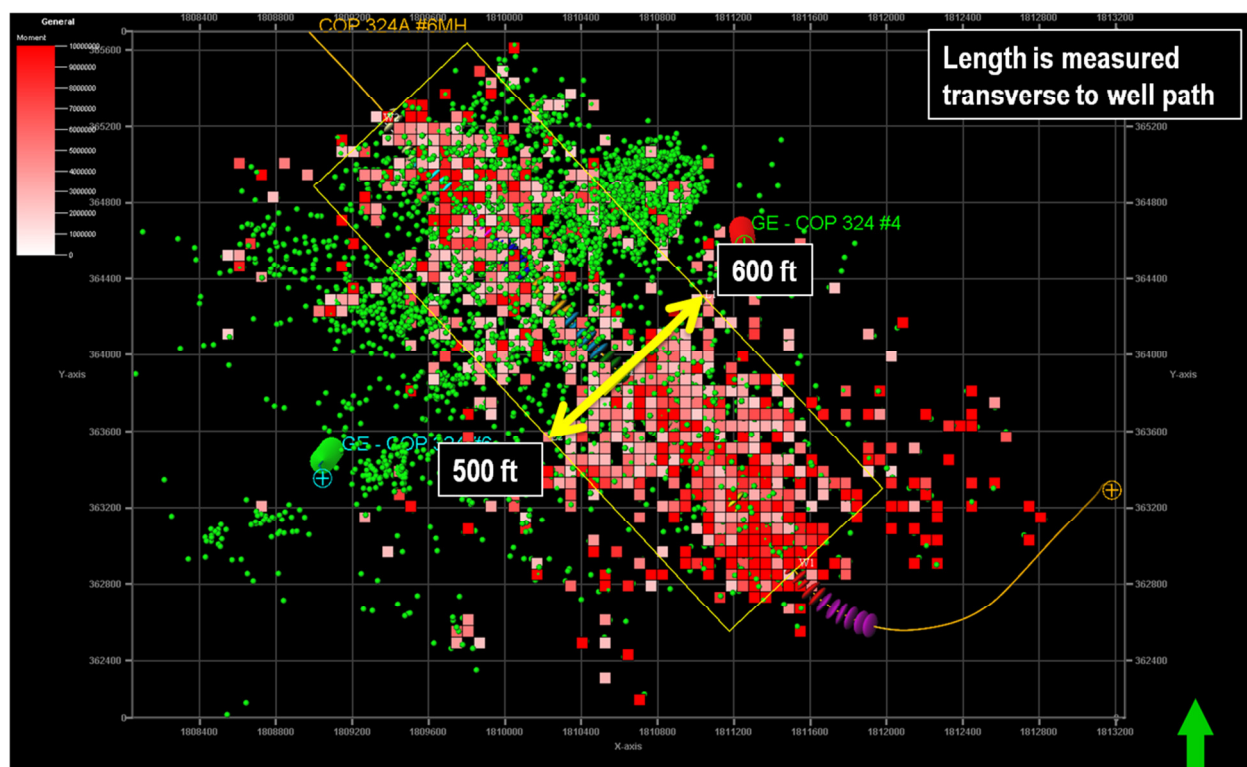


Figure 3 – Fracture length estimate using moment-density compared to event locations

Conclusions and Recommendations

The following conclusions based on the stated objectives have been reached:

- The average total microseismic lengths based on the 3D mapping of deformation using the seismic moment of the microseismic events is about 1,100 feet. Note that this estimate of length is less than 50% of the estimates obtained from the event locations.
- Microseismic activity in the Hamilton increases when there is good containment against downward growth by the Onondaga. There is no corresponding increase in the observed fracture length in the Marcellus. A reduction in total fluid volume and modified proppant scheduling might be considered.
- Comparisons of cumulative moment values for the treatment stages with key treatment parameters such as total fluid volume, final shut-down pressures, and completion sequence did not reveal any observable trends. It should be noted that the static pressure in the well immediately prior to starting each treatment was not recorded and therefore no interpretation of induced stresses could be made. The absence of observable trends with the treatment data and completion sequence suggest that the observed microseismic activity is heavily influenced by other factors that might relate to the landing point of the well within the vertical section, faults, or other structural features. A detailed geological model that includes surfaces taken from seismic data, if available, might resolve some of the uncertainties surrounding the causes of the observed fracture behavior.

1 Microseismic Monitoring Configuration and Quality Control for Evaluation

1.1 Project Overview

This report contains the evaluation of Schlumberger Microseismic Services microseismic data acquired during completion of the Marcellus formation in the COP 324A 6HM well. The well is located in Clearfield County, Pennsylvania. Schlumberger provided fracturing services during the project. A total of 13 treatment stages were monitored.

1.2 Monitoring Well Data

Two monitoring wells were used to acquire microseismic events. Each monitoring array consisted of 12 VSI geophones spaced 100 feet apart. The geophones were placed in a vertical configuration as shown in Figure 1.1. The depths of the monitoring tools are listed in Table 1.1. The average monitoring distance from the center of the geophone array to the mid-perforation location of selected treatment stages are also shown.

Table 1.1 - Geophone depths and spacing in Syczyn-OU1

Monitor Well	First stage monitored	Last stage monitored	Number of geophones	Top geophone depth (MD) (ft)	Spacing (ft)	Orientation
GE-COP 324 #4	Stage 1	Stage 13	12	6200	100	Vertical
GE-COP 324 #6	Stage 1	Stage `3	12	6200	100	Vertical

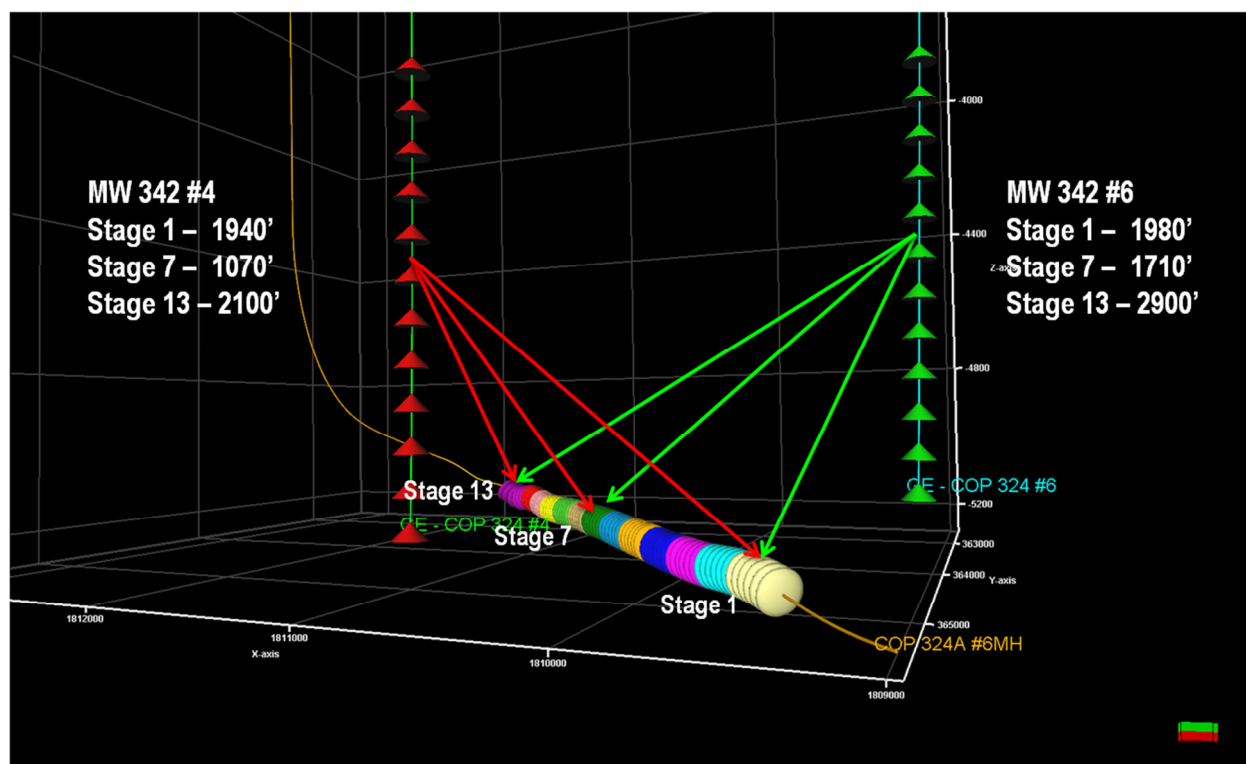


Figure 1.1 - Location of the treatment and monitor wells

1.3 Quality Control of the Microseismic Events for Evaluation

Microseismic events that are detected during any monitoring project must possess sufficient signal quality and amplitude to be located. The accuracy of the event locations is subject to a number of factors related to the waveforms themselves, the performance of the monitoring tools, and the background noise environment. For these reasons the located events are filtered by the processing geophysicist and evaluation engineer to produce a data set with consistent quality for the various evaluations. The selection of filters and their settings might be different depending on the type of analysis that is being performed.

A co-location process that produces a single estimated hypocenter for any event detected by both monitoring arrays has been used during the project. Events detected by one of the two monitor arrays are also included and merged with the co-located events.

The number of detected events for each treatment stage, the filter settings used, and numbers of events used for the evaluation contained within this report are listed in table 1.2. Any changes to the filter settings are noted where applicable. Additional information related to the detection and location of microseismic events can be found in the Geophysical Processing Report.

Table 1.2 – Located events, filter settings, and QC'd event counts

Treatment Stage	Detected Events	P/S Orthogonality (minimum value)	Location Confidence (minimum value)	QC'd Events
1	201	0.7	2.9	124
2	1697	0.7	2.9	1354
3	1446	0.7	2.9	1199
4	1139	0.7	2.9	874
5	475	0.7	2.9	354
6	1006	0.7	2.9	478
7	463	0.7	2.9	158
8	510	0.7	2.9	370
9	1684	0.7	2.9	557
10	421	0.7	2.9	270
11	299	0.7	2.9	177
12	618	0.7	2.9	293
13	376	0.7	2.9	199

Figure 1.2 and Figure 1.3 are map and depth views of the located microseismic events. Figure 1.4 and Figure 1.5 are the uncertainty ellipsoids for all located events.

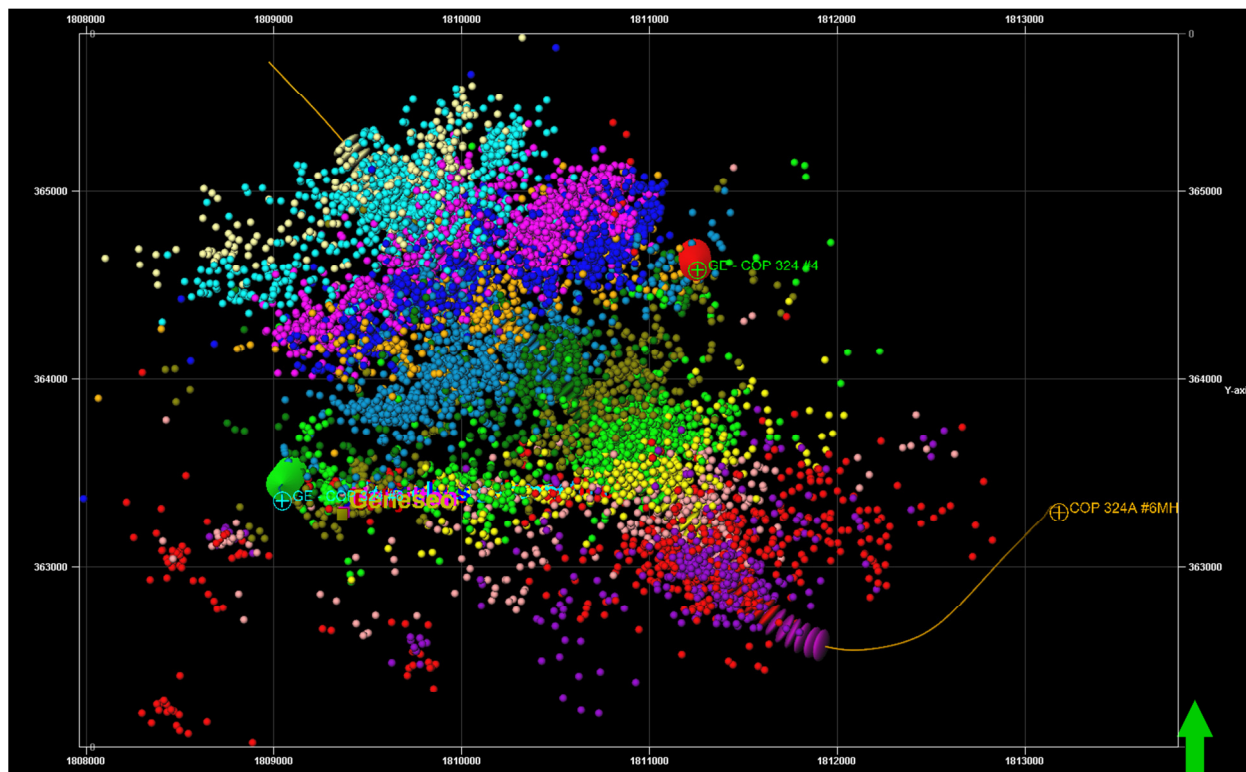


Figure 1.2 – Map view of all located events

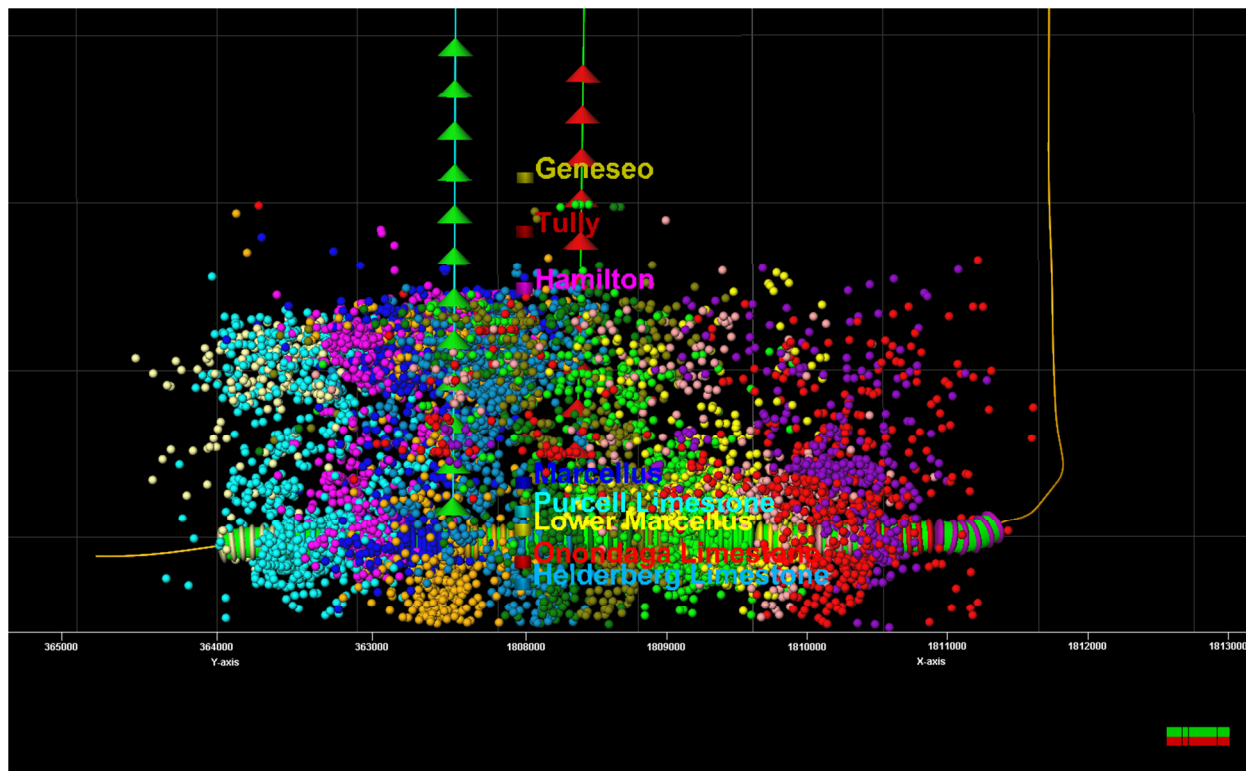


Figure 1.3 – Depth view of all located events

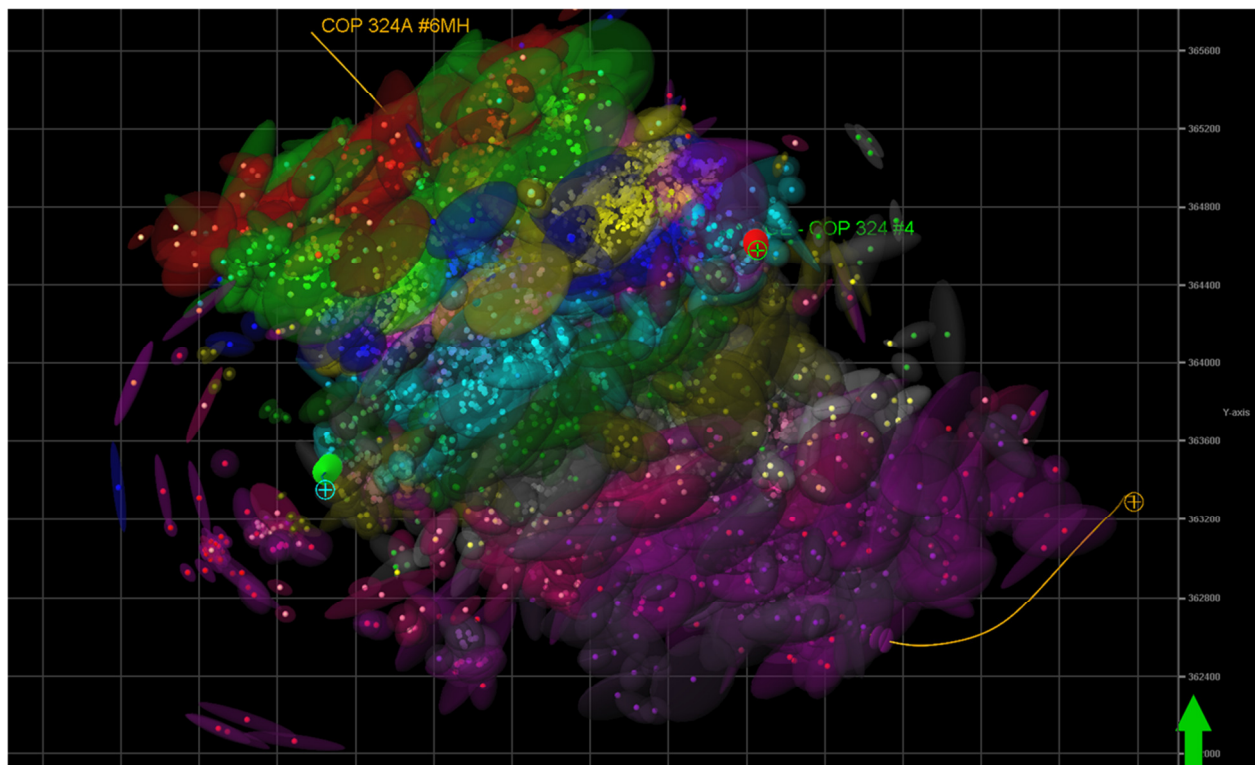


Figure 1.4 – Map view of uncertainty ellipsoids for all located events

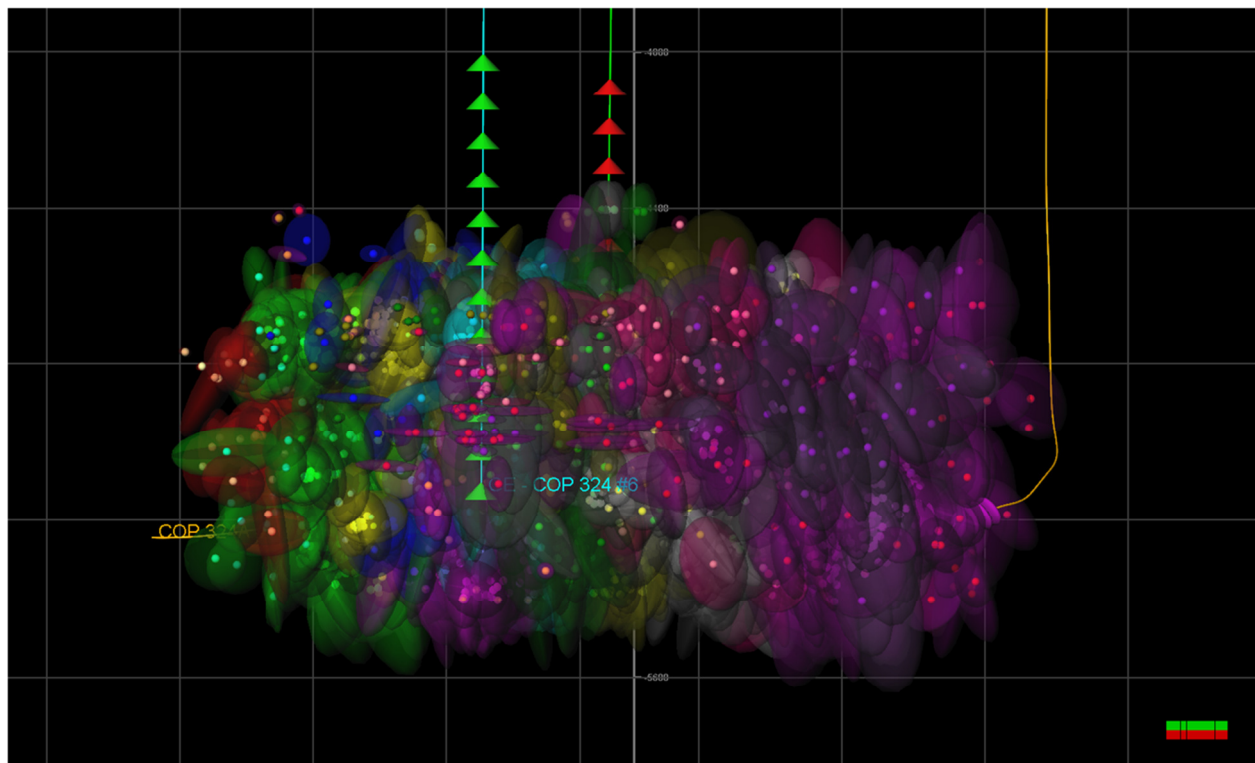


Figure 1.5 - Depth view of uncertainty ellipsoids for all located events

Figure 1.6 and Figure 1.7 are map and depth views of the filtered microseismic events. Figure 1.8 and Figure 1.9 are the uncertainty ellipsoids for the filtered events.

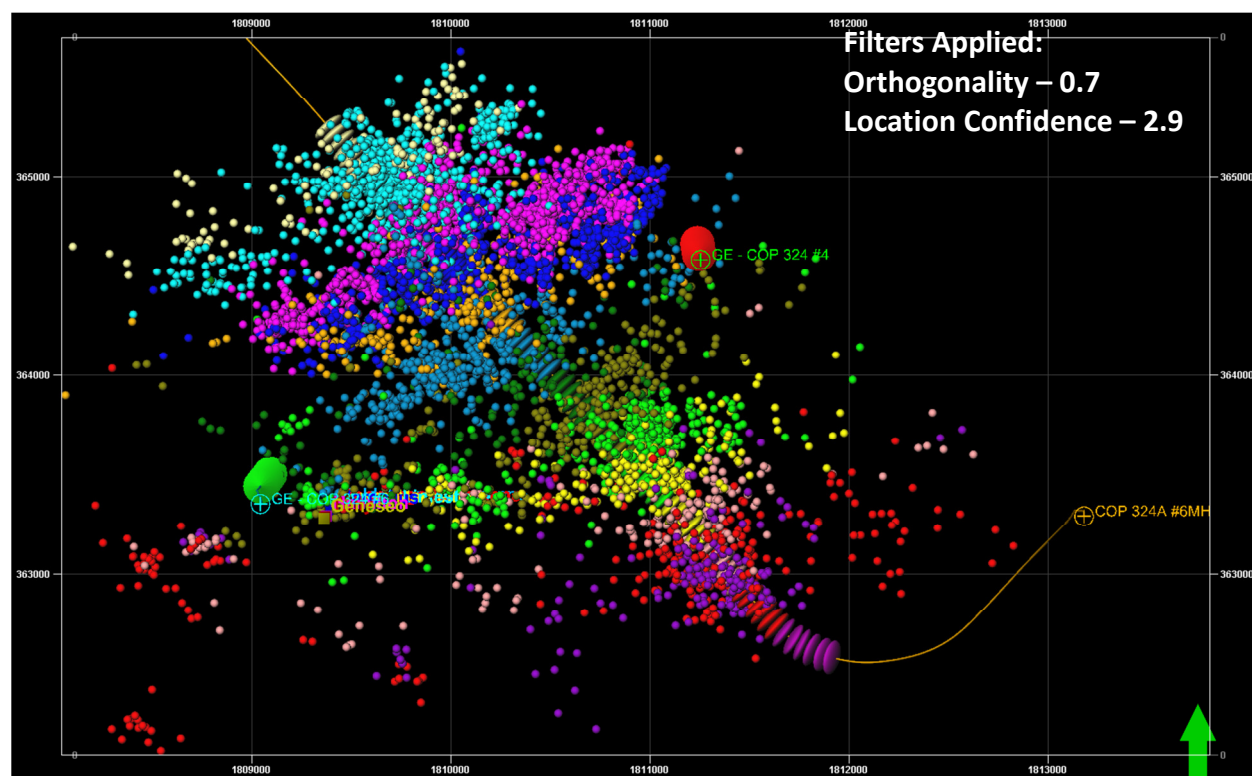


Figure 1.6 – Map view of QC filtered events

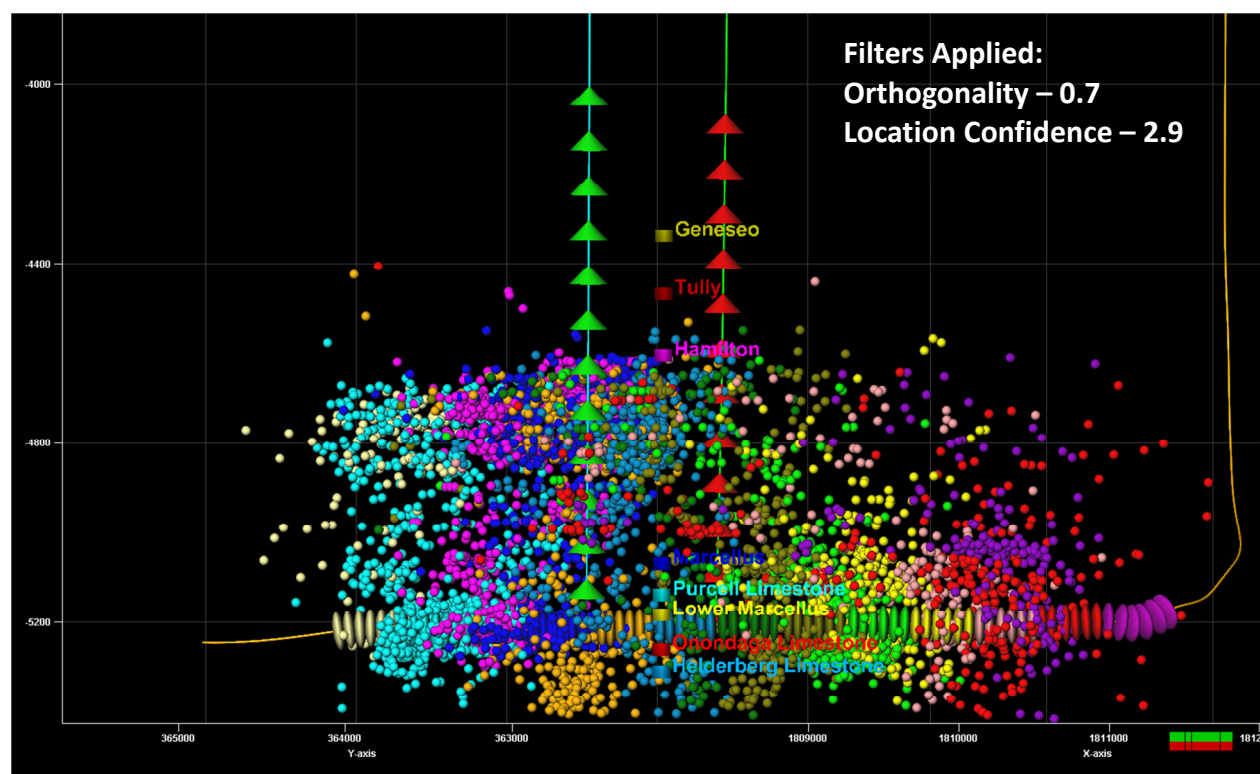


Figure 1.7 – Depth view of QC filtered events

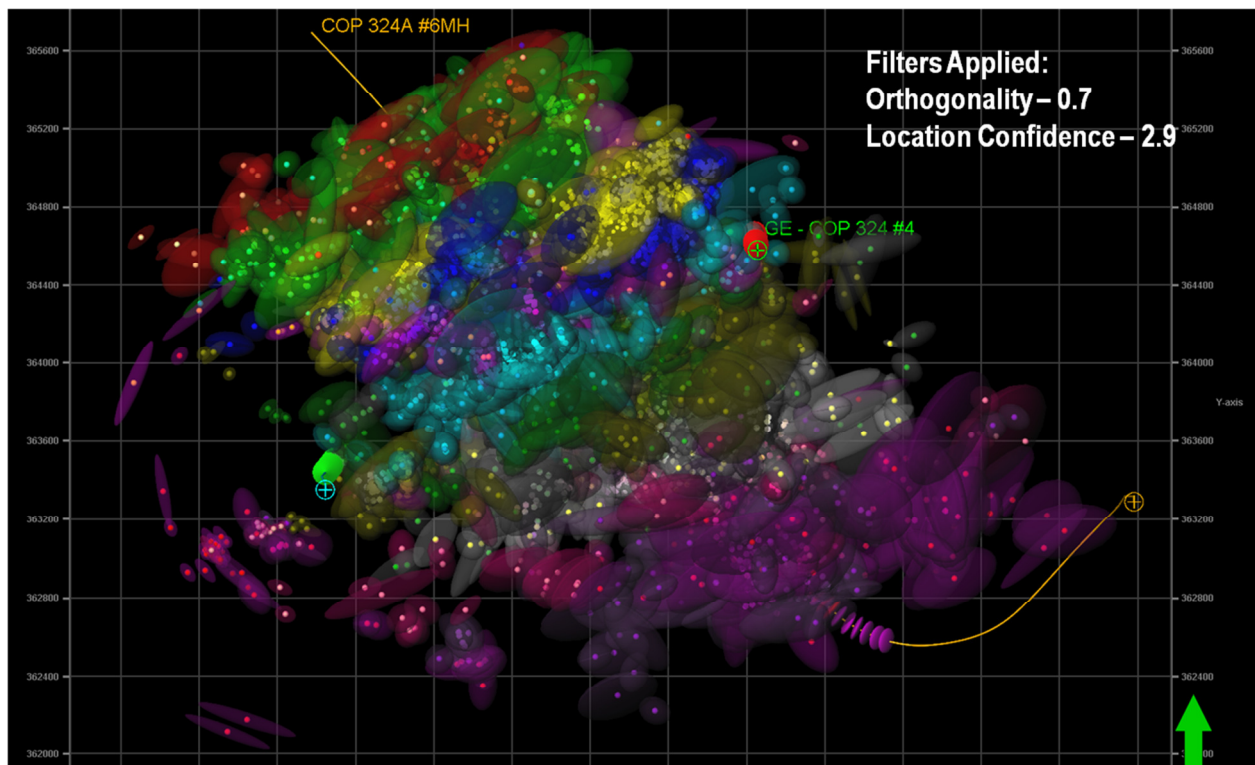


Figure 1.8 – Map view of uncertainty ellipsoids for QC filtered events

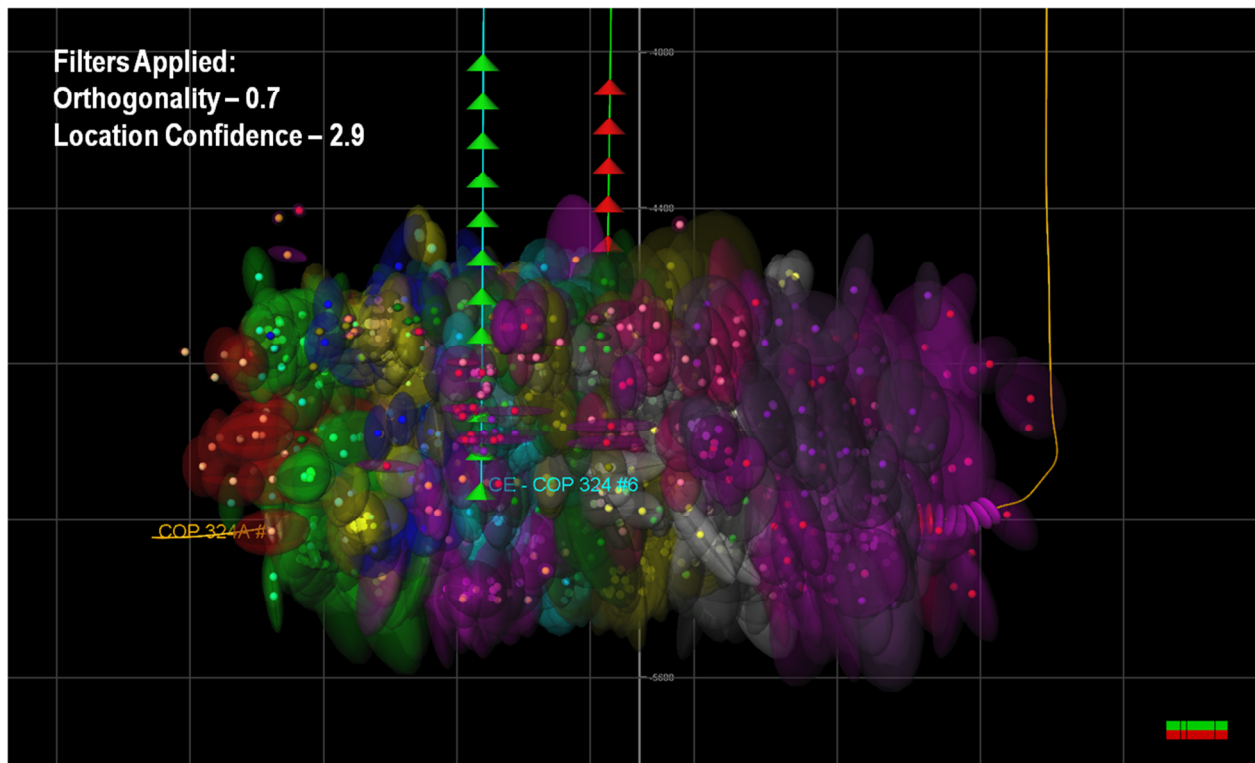


Figure 1.9 - Depth view of uncertainty ellipsoids for QC filtered events

1.4 Magnitude versus Distance

The magnitude versus distance plot is used for both quality assurance and for evaluation. The detection threshold is the minimum magnitude necessary to locate a microseismic event at a given distance. A consistent detection threshold indicates that the microseismic event location acquisition and processing has been consistent. Changes in the detection threshold might be caused by environmental conditions such as background noise or changing reservoir properties. Anomalies are reviewed prior to conducting the interpretation.

The magnitude versus distance plot for all monitored completion stages is shown below in Figure 1.10.

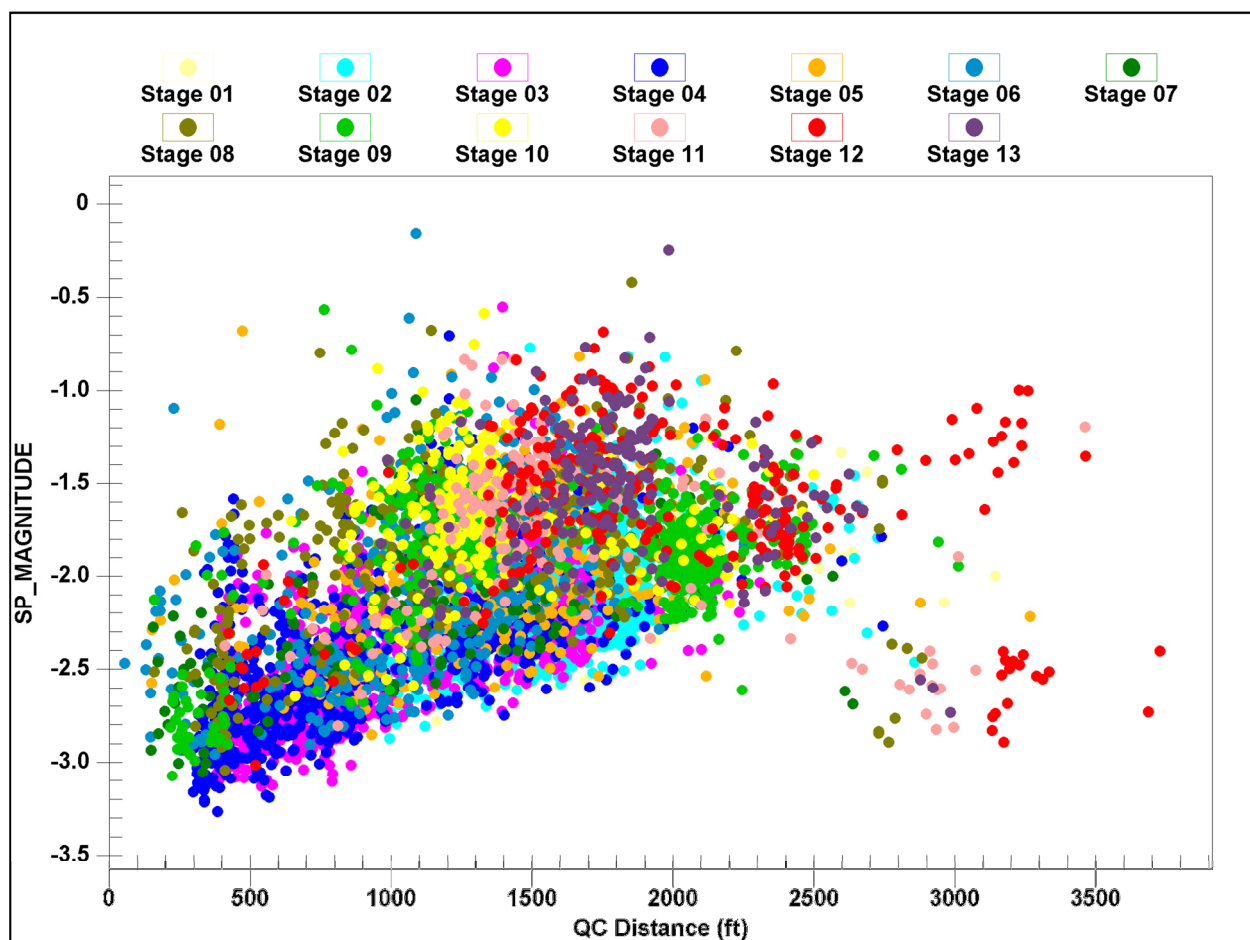


Figure 1.10 - Magnitude versus distance plot

2 Completion Design and Execution Summary

2.1 Treatment Well Data

11 fracture stimulation treatments were monitored during the completion of the COP 324A 6HM. The stage 6 perforations were stimulated with acid only and are not included in this evaluation.

The well data is shown in Table 2.1.

Table 2.1 - Treatment well data

Treatment wells	COP 324A #6HM
Well type	Horizontal
Completion	Plug & Perf
Kelly bushing - KB (ft)	2146
Total measured depth - MD (ft)	12682
Maximum vertical depth - TVD (ft)	7390

2.2 Completion and Stimulation Design

Table 2.2 lists the overall perforation intervals, number of perforation clusters, and design parameters for the fracturing treatments.

Table 2.2 - Completion design summary

Stage	Bottom perf (MD) (ft)	Top perf (MD) (ft)	Clusters	Total fluid (1000_gal)	Total proppant (1000_lbm)	Desired rate (bbl/min)
Stage 01	12075	11835	6	607.7	600.5	95
Stage 02	11788	11550	6	607.7	600.5	95
Stage 03	11502	11272	6	607.7	600.5	95
Stage 04	11217	10983	10	607.7	600.5	95
Stage 05	10901	10695	6	607.7	600.5	95
Stage 06	10642	10419	6	607.7	600.5	95
Stage 07	10363	10131	6	607.7	600.5	95
Stage 08	10070	9843	6	607.7	600.5	95
Stage 09	9782	9555	6	607.7	600.5	95
Stage 10	9506	9268	6	607.7	600.5	95
Stage 11	9220	8982	6	607.7	600.5	95
Stage 12	8939	8698	6	607.7	600.5	95
Stage 13	8650	8375	6	607.7	600.5	95

2.3 Execution Results and Microseismic Estimates of Dimensions and Stimulated Volumes

Table 2.3 summarizes the actual volumes pumped, average rates and pressures, microseismic estimates of dimensions, and estimated stimulated volumes for each treatment stage that was monitored.

Table 2.3 - Stimulation execution summary with microseismic evaluation results

Stage	Total fluid (1000_gal)	Total proppant (1000_lbm)	ISIP (psi)	Total MS length (ft)	Total MS height (ft)	MS volume (MM- ft3)	Fracture azimuth (deg)
Stage 01	685.9	N/A	3865	1910	572	11.2	66
Stage 02	617.9	N/A	4945	1604	620	132.0	69
Stage 03	682.8	N/A	4165	1871	614	110.4	66
Stage 04	599.9	N/A	4485	2005	673	79.3	68
Stage 05	655.8	N/A	5290	1938	778	51.8	70
Stage 06	602.4	N/A	4054	1651	835	58.1	70
Stage 07	598.4	N/A	4310	1799	757	15.8	75
Stage 08	584.1	N/A	3954	2542	752	58.1	70
Stage 09	680.6	N/A	4198	1590	544	70.8	72
Stage 10	585.1	N/A	4072	1973	680	48.0	76
Stage 11	596.3	N/A	4196	2828	685	26.1	76
Stage 12	583.3	N/A	4260	2921	649	41.9	86
Stage 13	592.4	N/A	4025	2160	773	33.3	80

3 Microseismic Length and Azimuth

Interpretation of hydraulic fracture length and orientation are based on the locations of the microseismic events that occur during stimulation treatments. The dimensions that are presented are based on Principal Component Analysis of the event locations. The analysis is constrained so that the height, length, and width are oriented appropriately in space. Azimuth is taken from the length and is reported as an angle relative to grid north. The dimensions are referenced initially to the centroid of the event cloud. An additional step moves this center coordinate the mid-perforation location so that length and height can be referenced to the location of the treatment well.

The lengths and azimuths that are reported are subject to an additional outlier filter. A specified percentage of the total number of events located at the greatest distance from the centroid of the event cloud is not included in the dimensions or azimuths. In the results shown the outlier filter has been set at 5% of the displayed events. The outlier filter is used to improve the visualization and produce more meaningful results for qualitative comparisons of the monitored treatments.

A visual representation of the microseismic lengths and azimuths is shown in Figure 3.1. The arrow on the plot indicates the direction of grid north.

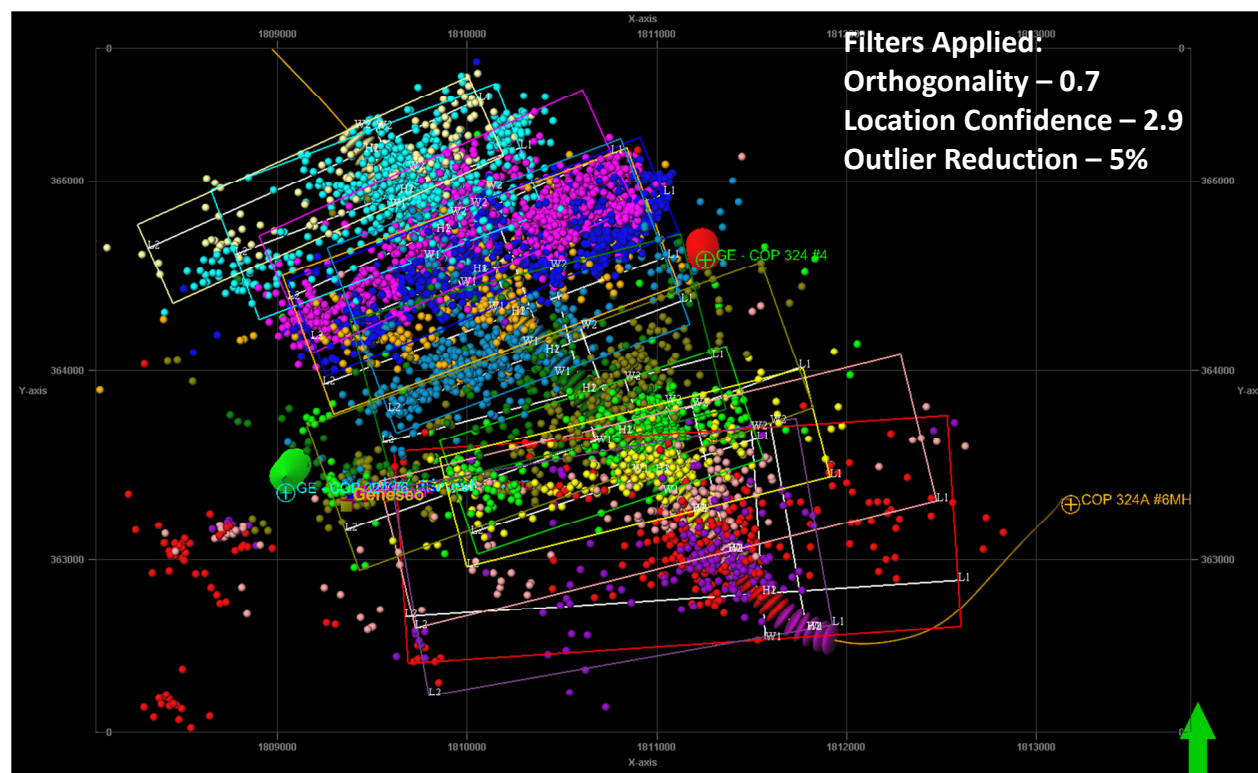


Figure 3.1 - Map view of microseismic lengths and azimuths

Figure 3.2 is a bar chart that compares the total lengths from tip to tip. Figure 3.3 displays the lengths on either side of the treatment well to determine if and to what extent length asymmetry might be present.

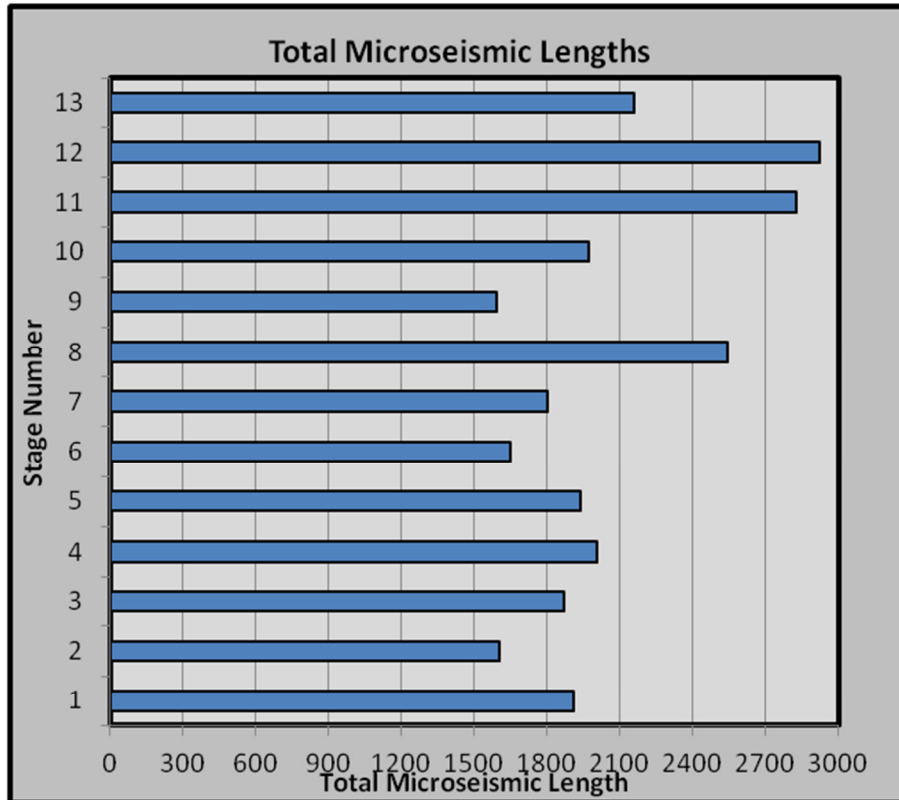


Figure 3.2 – Total microseismic lengths. Average total length is 2,060 feet.

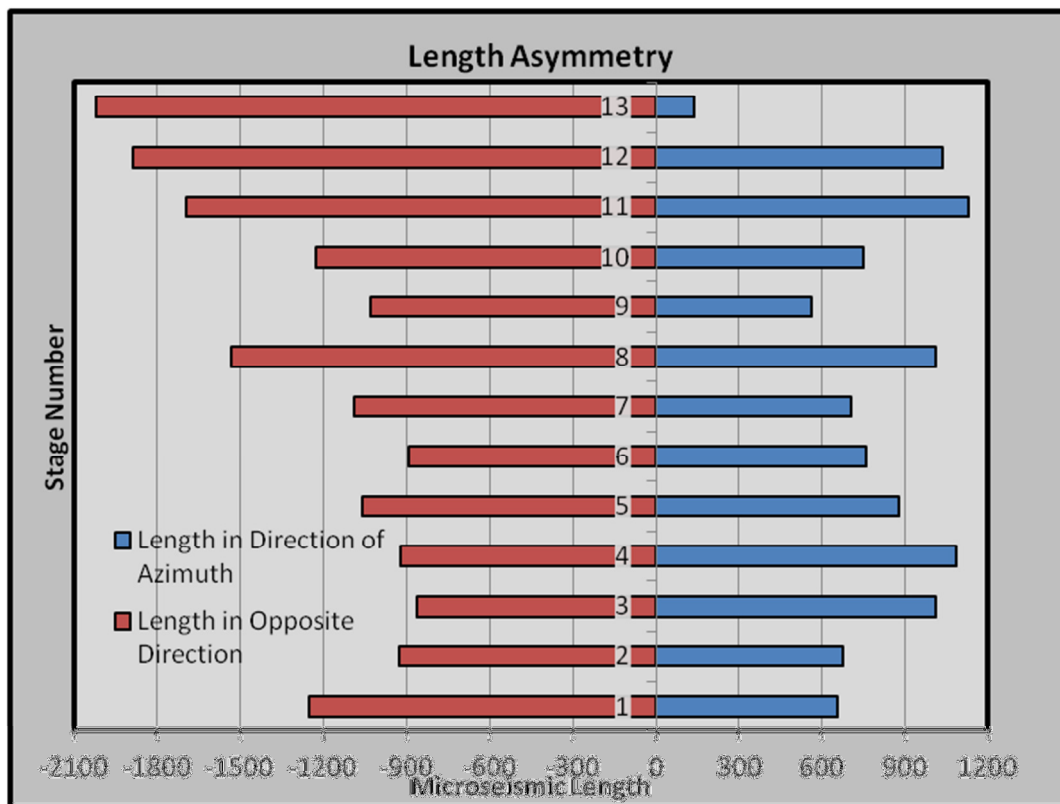


Figure 3.3 – Microseismic length asymmetry relative the perforations. Average length in the direction of the azimuth (east) is 800 feet. Average length in the opposite direction is 1,260 feet.

Table 3.1 Summarizes the length estimates and lists the azimuths determined from the locations of the microseismic events for each treatment stage.

Table 3.1 – Summary of microseismic lengths and azimuths

Treatment Stage	Total Microseismic Length (ft)	Easterly Extension (ft)	Westerly Extension (ft)	Fracture Azimuth (deg)
Stage 1	1910	656	1254	66
Stage 2	1604	675	929	69
Stage 3	1871	1010	861	66
Stage 4	2005	1082	923	68
Stage 5	1937	876	1061	70
Stage 6	1651	760	891	70
Stage 7	1799	707	1092	75
Stage 8	2543	1011	1532	70
Stage 9	1590	561	1029	72
Stage 10	1973	747	1226	76
Stage 11	2828	1131	1697	76
Stage 12	2921	1033	1888	86
Stage 13	2160	138	2022	80

4 Microseismic Height

Microseismic estimates of fracture height growth are taken from the event location subject to the constraints described for computation of lengths and azimuths. It should be noted that the height that is reported is a maximum height, up or down, and might not be constant along the length of the fracture. Evaluation of height that is based on microseismic event source parameters can provide additional information to determine the potential severity of height growth.

A visual representation of the microseismic height estimates is shown in Figure 4.1. The location of the treatment well and formation surfaces is also shown.

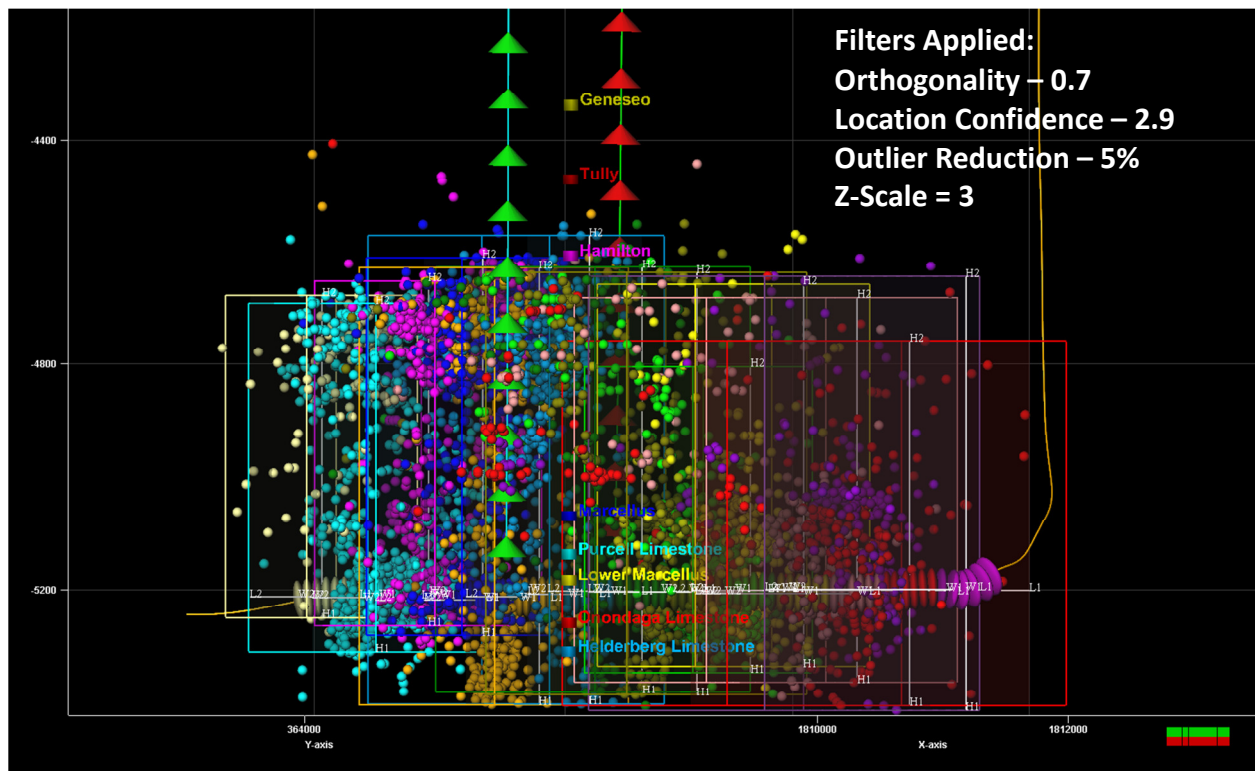


Figure 4.1 - Depth view of microseismic heights

Figure 4.2 displays the microseismic heights as viewed from the toe of the well. The visualization in Figure 4.2 provides improved reference to the formation tops.

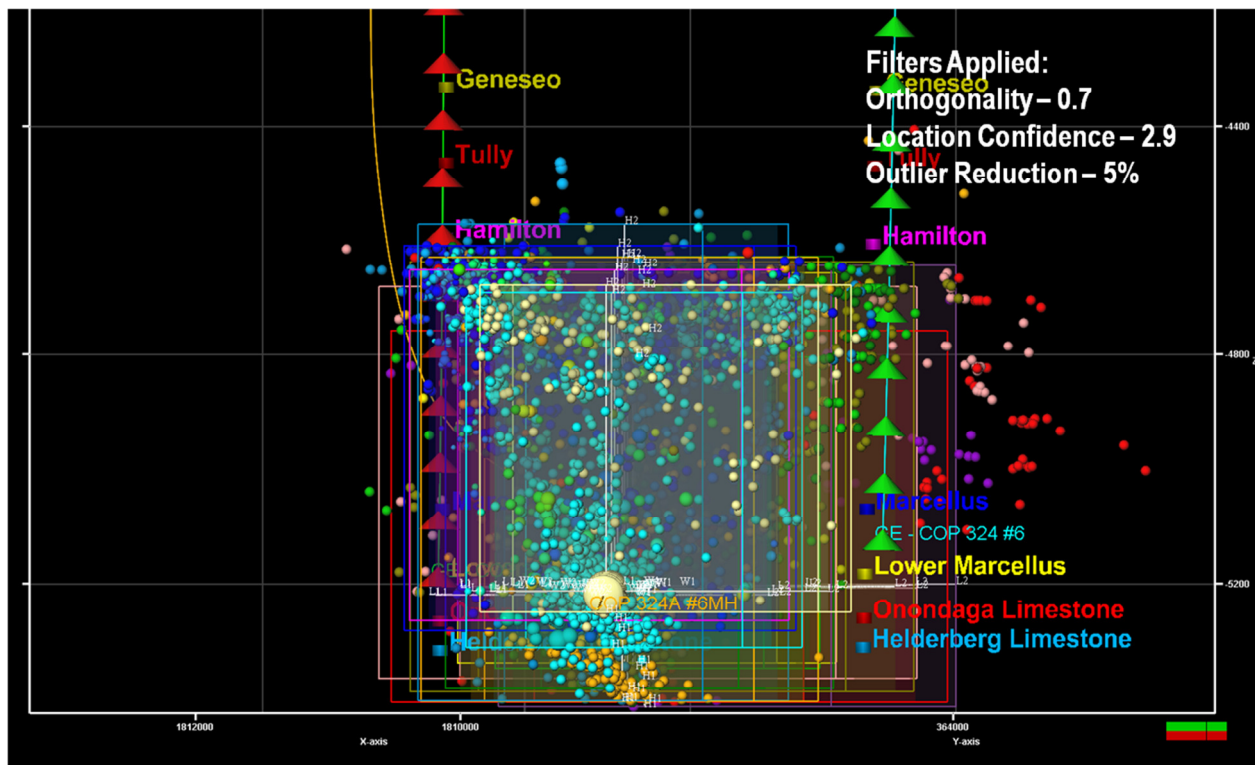


Figure 4.2 – Distribution of event depths along the length of a fracture (stage 5 is shown)

Figure 4.3 is a bar chart of upward and downward height growth relative to the treatment well. The depths shown in Figure 4.2 are True Vertical Depth (TVD).

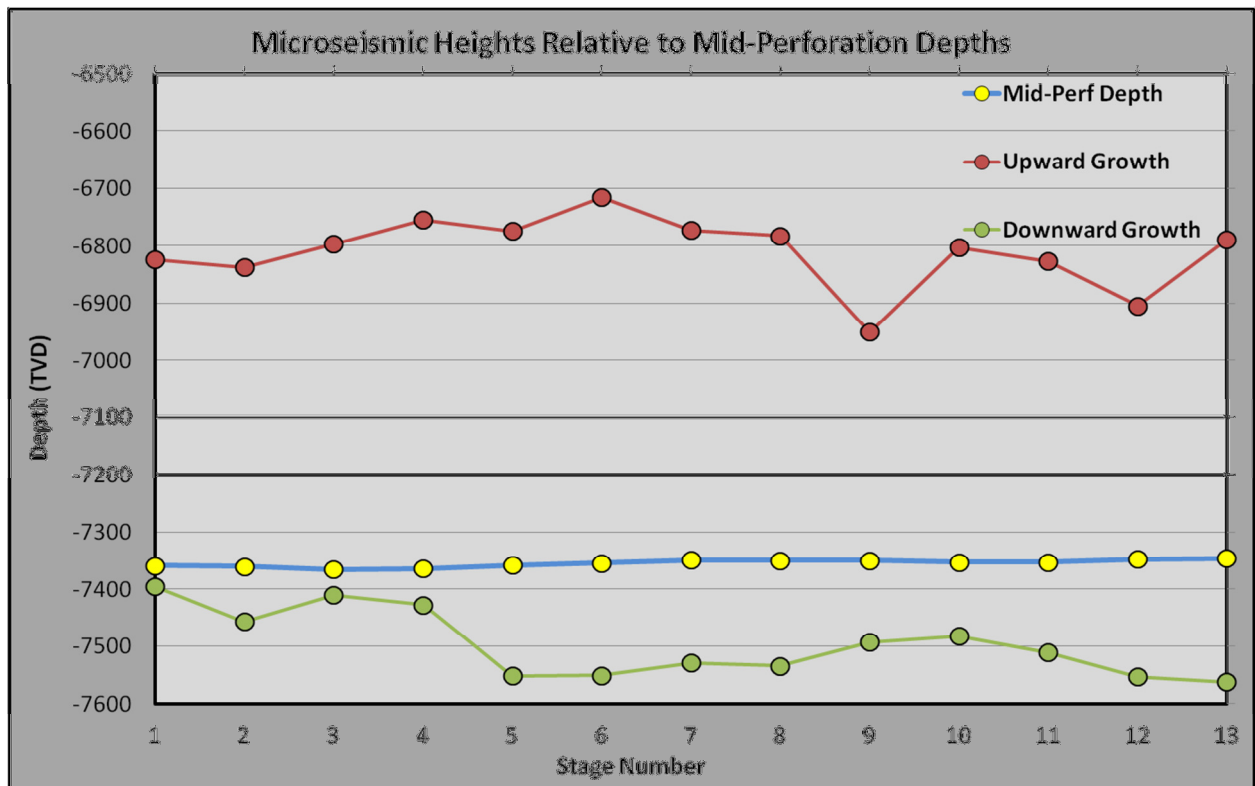


Figure 4.2 – Height growth relative to the treatment well

Table 4.1 summarizes the results in numerical form. Upward growth and downward growth are reported relative to the mid-perforation depth of each treatment stage.

Table 4.1 – Summary of microseismic heights

Treatment Stage	Total Microseismic Height (ft)	Upward Height Growth (ft)	Downward Height Growth (ft)
Stage 1	572	37	535
Stage 2	619	97	522
Stage 3	613	45	568
Stage 4	673	64	609
Stage 5	778	194	584
Stage 6	835	197	638
Stage 7	757	181	576
Stage 8	752	185	567
Stage 9	543	144	399
Stage 10	680	130	550
Stage 11	684	158	526
Stage 12	649	206	443
Stage 13	773	216	557

5 Microseismic Volume (Event-Density)

Microseismic volumes, also known as Stimulated Reservoir Volume (SRV) or Estimated Stimulated Volume (ESV) are sometimes used for qualitative evaluation of fracture stimulation treatments. The method used to extract the volumes reported below are based on a computation that uses the density of microseismic events and a user-defined cell size in an iso-density calculation.

Microseismic volumes are intended to be used qualitatively only. The volume that is represented in the tables and charts are non-unique values that depend on the user settings used for the computation. Microseismic volumes are also sensitive to monitor well bias and should not be used for reservoir engineering applications or production forecasting.

The microseismic event density uses the locations of the events only and does not include any adjustment for the source parameters such as magnitude of the microseismic events. Detection bias cannot be estimated when using co-located events.

Figure 5.1 is a visual representation of the microseismic volumes shown in map view. Figure 5.2 displays the microseismic volumes in depth view. A list of microseismic volumes is included in Table 5.1.

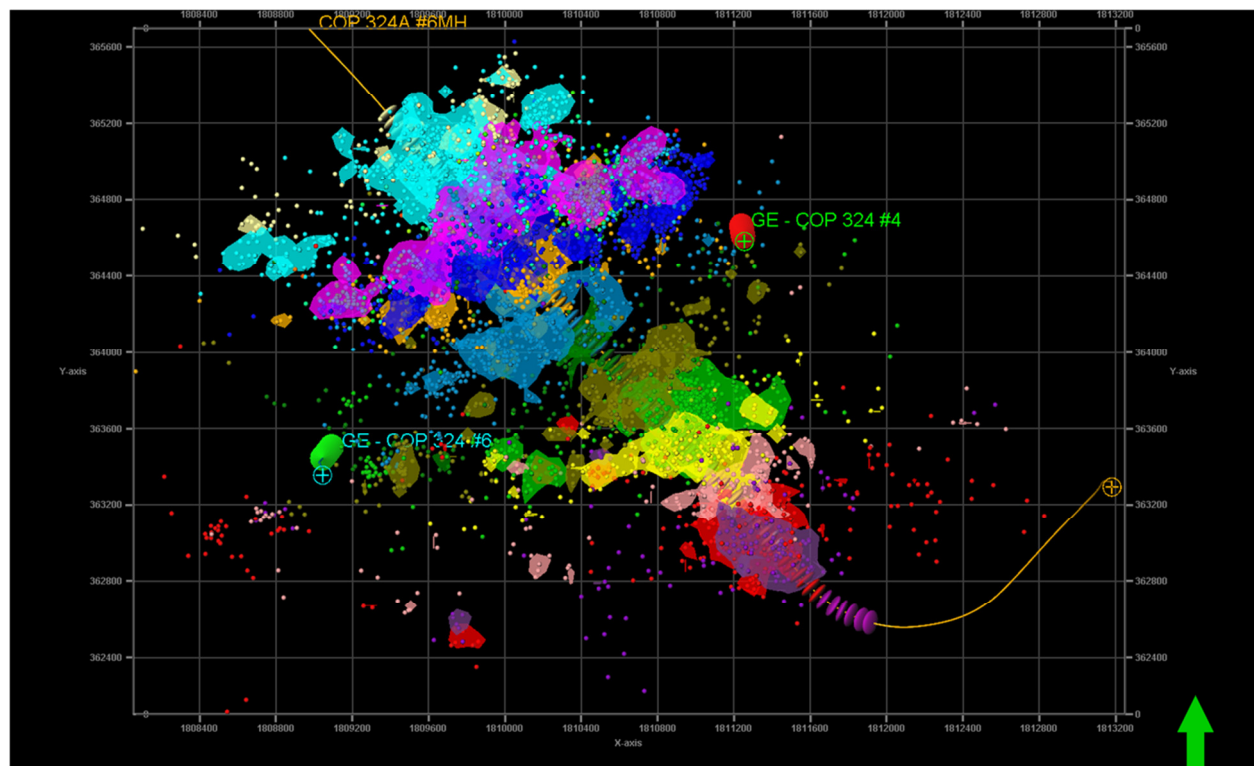


Figure 5.1 – Map view of microseismic volumes

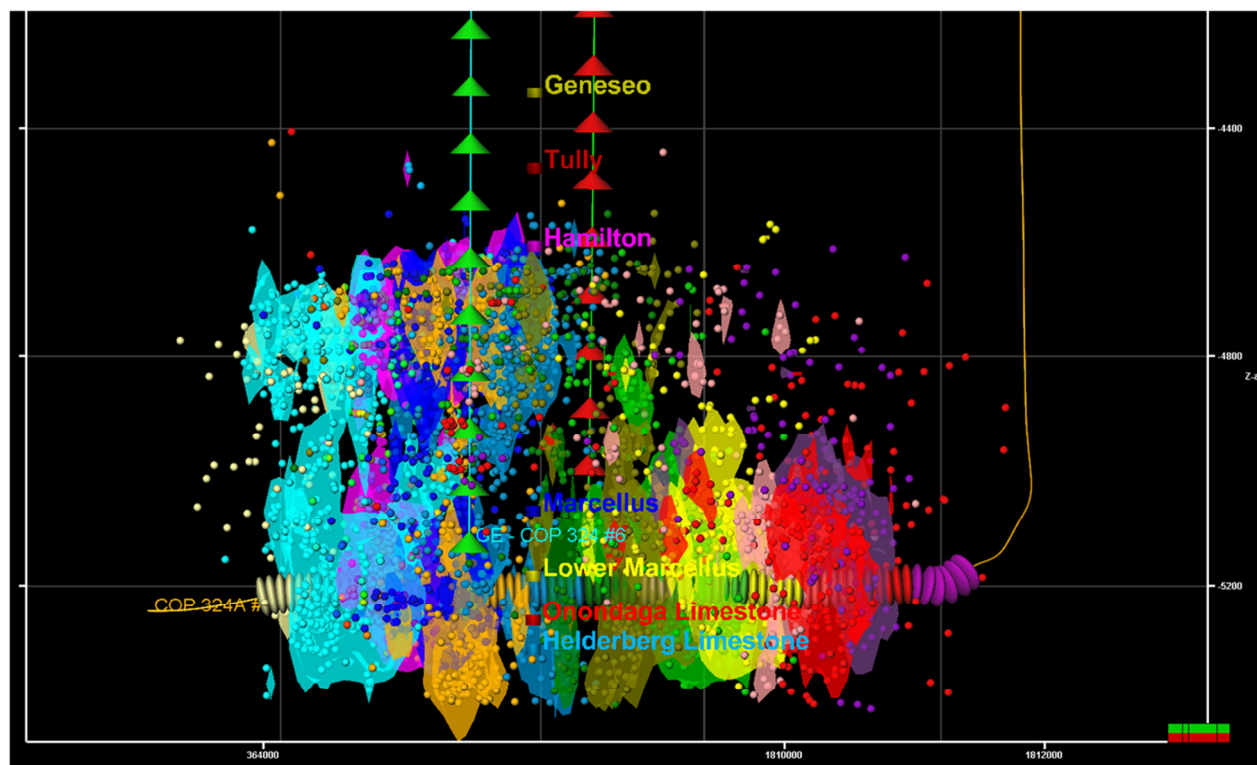


Figure 5.2 - Depth view of microseismic volumes

Table 5.1 – Summary of microseismic volumes

Treatment Stage	Microseismic Volume (MM_ft3)
Stage 1	11.2
Stage 2	132.0
Stage 3	110.4
Stage 4	79.3
Stage 5	51.8
Stage 6	58.1
Stage 7	15.8
Stage 8	58.1
Stage 9	70.8
Stage 10	48.0
Stage 11	26.1
Stage 12	41.9
Stage 13	33.3

6 Seismic Moment Applications

Seismic moment is a source parameter that is computed using the amplitudes and frequency content of the detected horizontal shear and compressional waves. Moment values can be interpreted as the deformation associated with the source mechanisms of the individual microseismic events. Seismic moment (M_0) is converted to moment-magnitude (M_w) for magnitude versus distance plots and visual displays.

Seismic moment is a useful evaluation tool and can be used in a number of different applications that use the computed totals, known as the cumulative moment, and normalized comparisons based on the percentage of deformation that occurs in temporal or spatial dimensions.¹ Evaluations that are based on cumulative moment and deformation are less sensitive to monitor bias when compared to microseismic volumes.

Figure 6.1 is a visualization of moment values within a 3D grid. The moment values of any events within a grid cell are totalized to determine the total deformation in each cell. The color scale is used to compare where relatively high deformation has been detected compared to cells where there is less deformation.

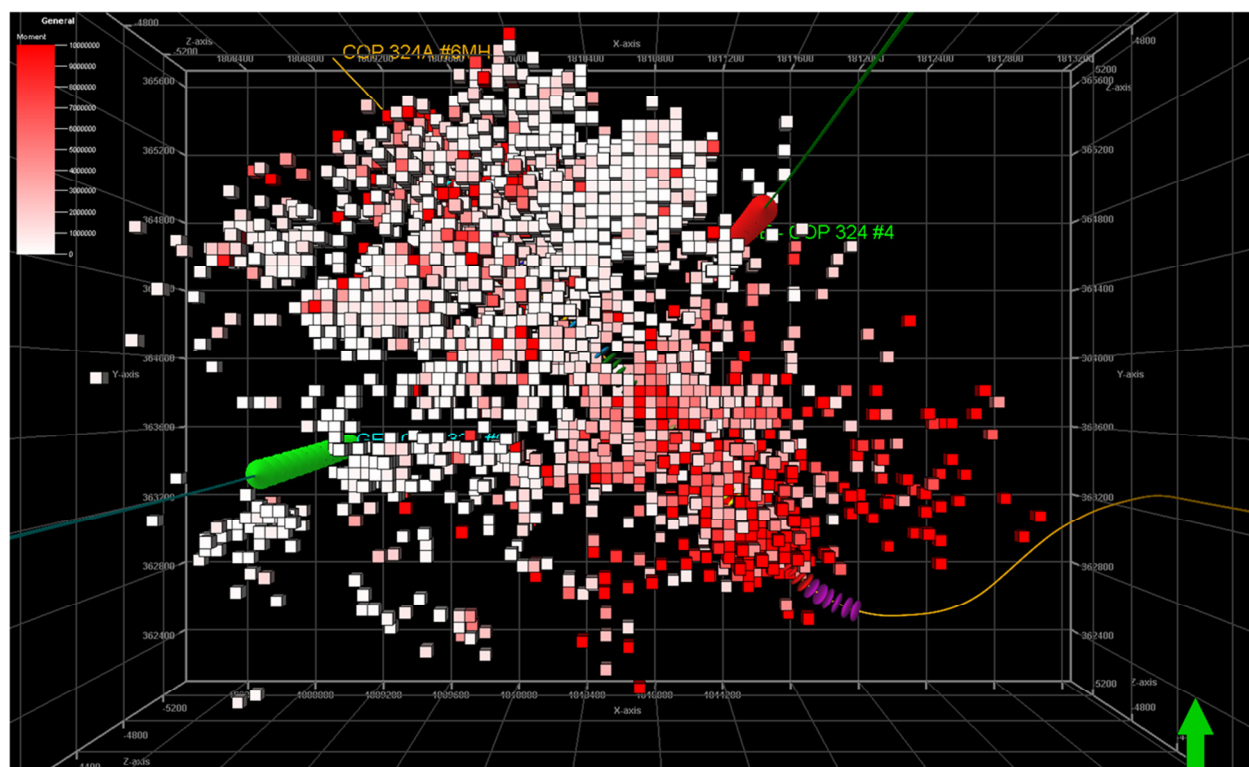


Figure 6.1 – Pillar grid populated with seismic moment values of the microseismic events

It is possible to improve the visualization by disabling cells with relatively low cumulative moment values. This process improves the qualitative evaluation of deformation and minimizes detection bias. Figure 6.2 shows the pillar grid after disabling all cells whose cumulative moment is less than 2 MN-m. Note that the apparent lateral extent of the region with highest

¹ For more information about seismic moment applications please see Downie et al, SPE 163873, available at www.spe.org

moment density is much less after disabling the grid cells with relatively low levels of deformation.

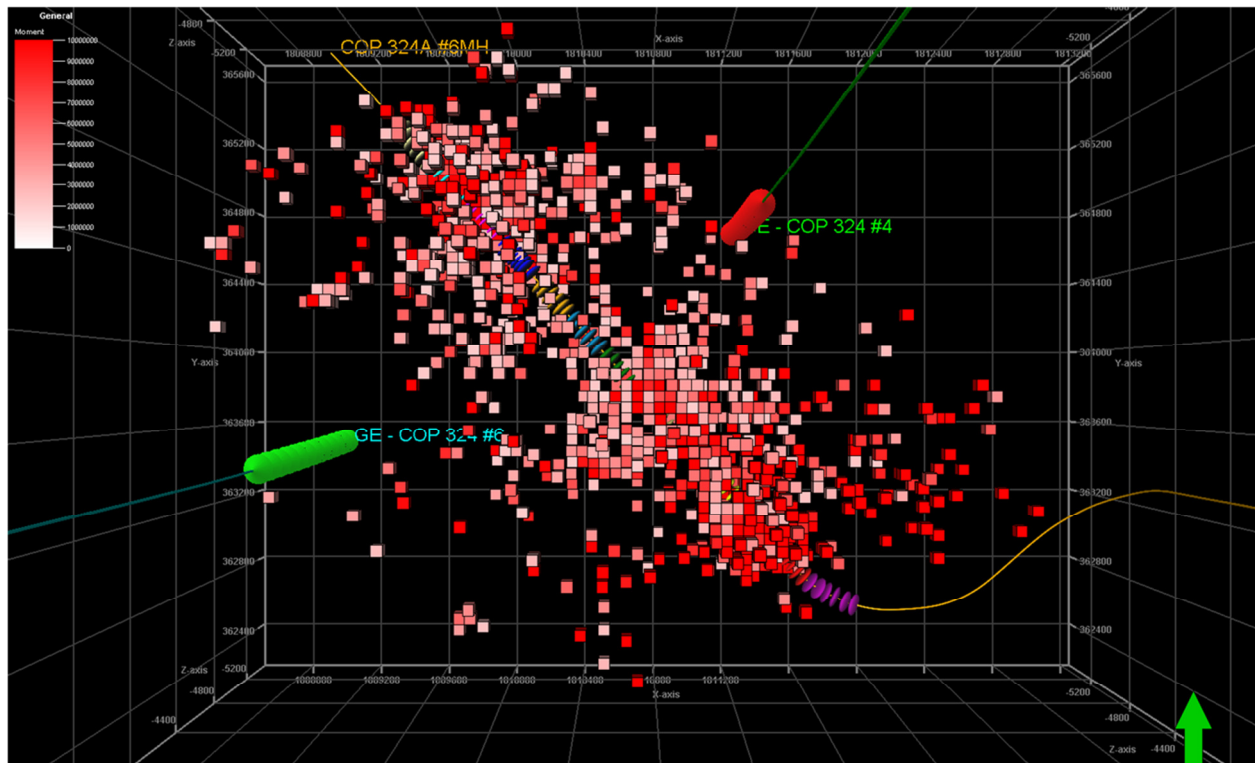


Figure 6.2 – Visual estimation of the regions with high moment density

Figure 6.3 adds an approximation of the average length of the microseismic event cloud using all populated cells in the 3D grid. Figure 6.4 displays the interpretation of average length after disabling the cells with less than 2 MN-m total seismic moment. The lengths shown are referenced to location of the treatment well.

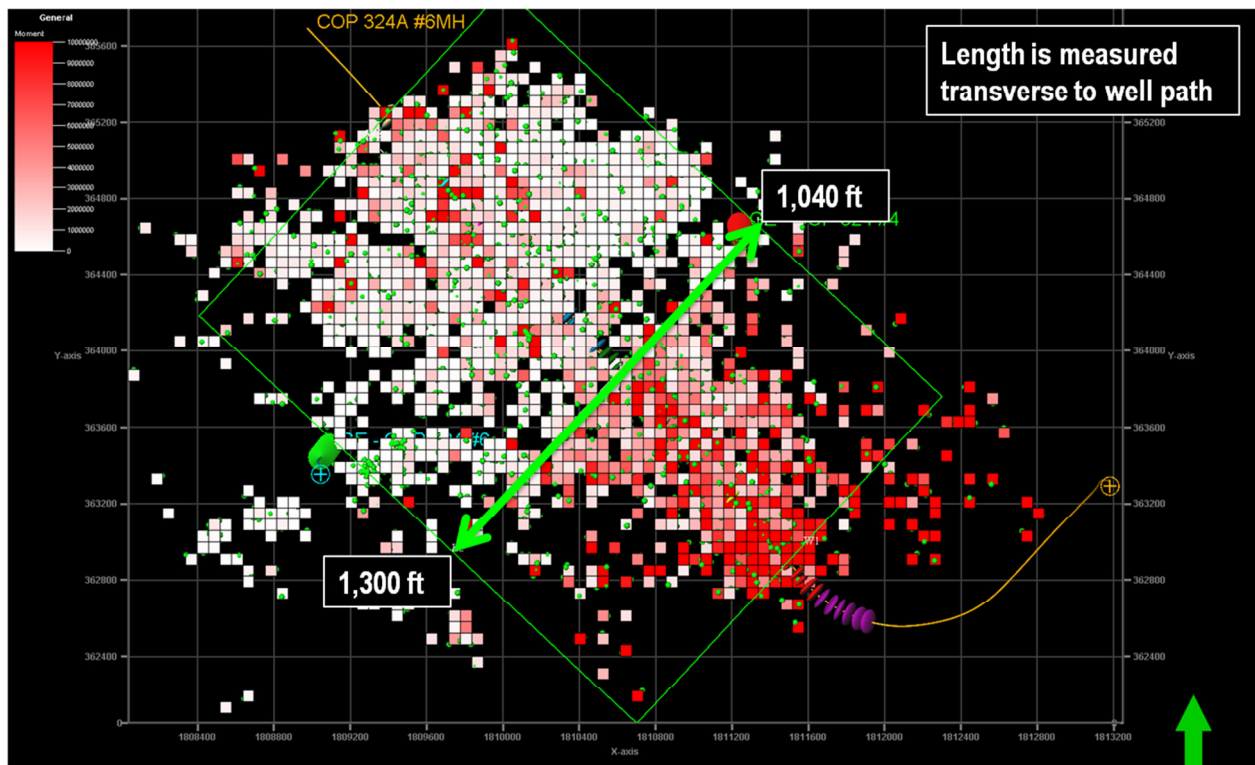


Figure 6.3 – Estimate of fracture length based on moment-density

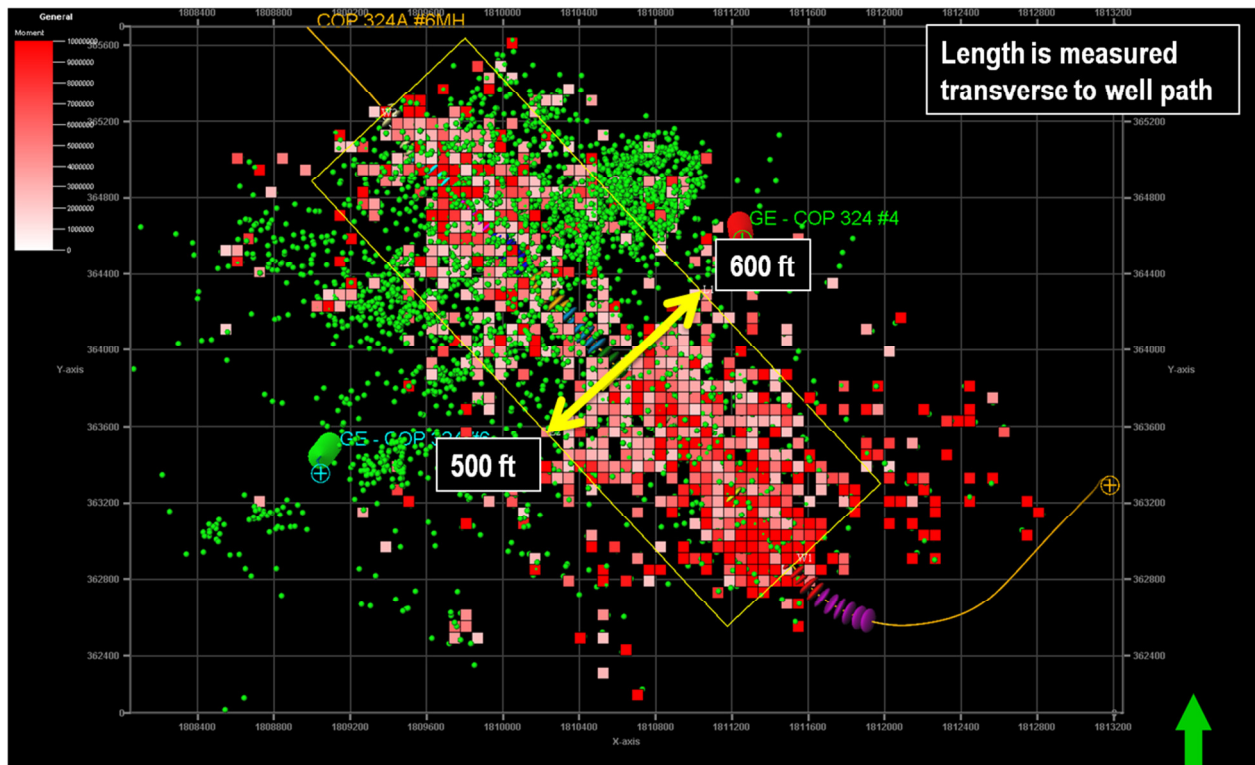


Figure 6.4 – Revised estimate of fracture length after removal of low-deformation cells

Figure 6.5 and Figure 6.6 are height growth estimates based on moment density, using all populated cells and with low-deformation cells disabled. Upward and downward growth is

referenced to the average depth of the treatment well. Note that the vertical scale has been increased relative to the horizontal scale.

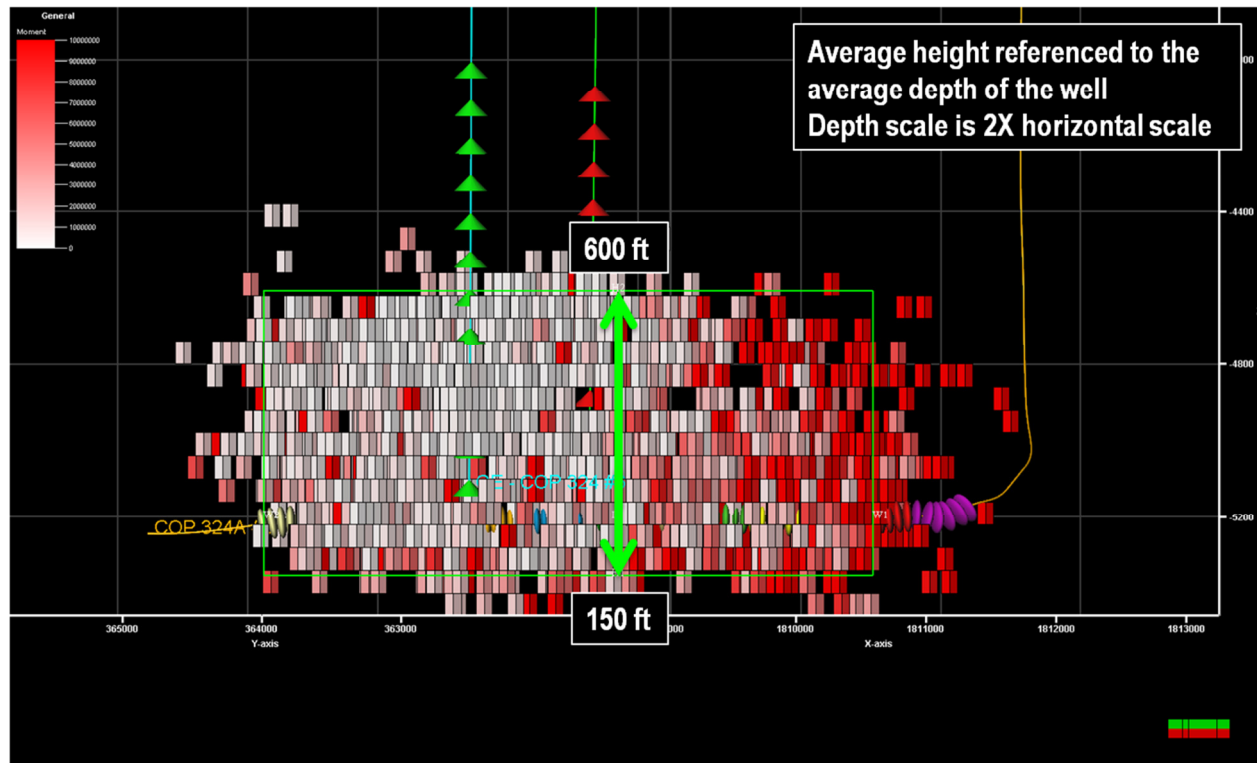


Figure 6.5 – Estimated height growth from moment-density

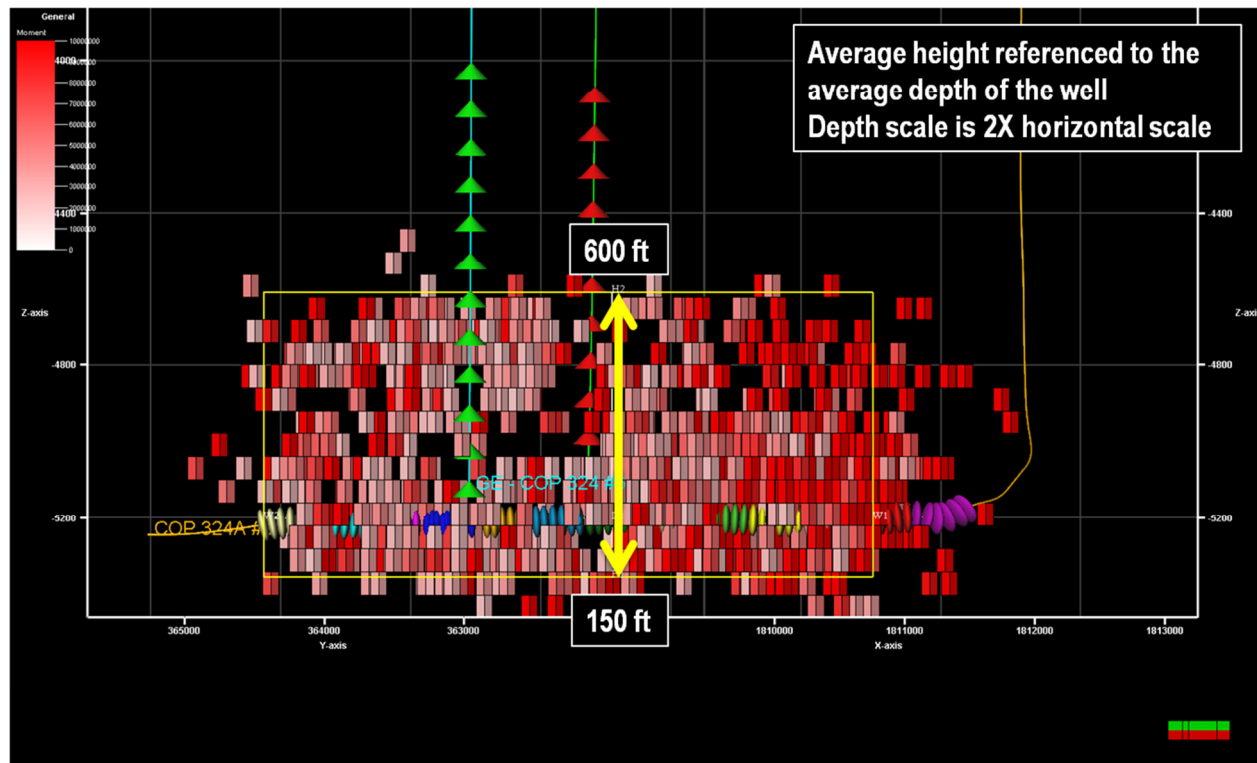


Figure 6.6 – Estimated height growth with low-deformation cells disabled

Mapping of the seismic moment in the 3D grid shows that interpretation of the fracture lengths is somewhat problematic due to the presence of large numbers of cells with relatively low deformation. Height growth and containment are more easily estimated. The greatest difference in the interpretation of fracture length occurs during the first five treatment stages and suggests that there are significant differences in the treatment procedures or rock properties within the reservoir or bounding zones that cause a visible difference in fracture behavior.

Cumulative seismic moment can also be used to construct diagnostic plots that compare the total deformation observed during the stimulation treatments to various aspects of the pumping schedules, pressure measurements, and other aspects of the completion such as the time between successive treatment stages. Figure 6.7 is a compilation of diagnostic plots that compare the cumulative moment totals of individual treatment stages to various treatment parameters.

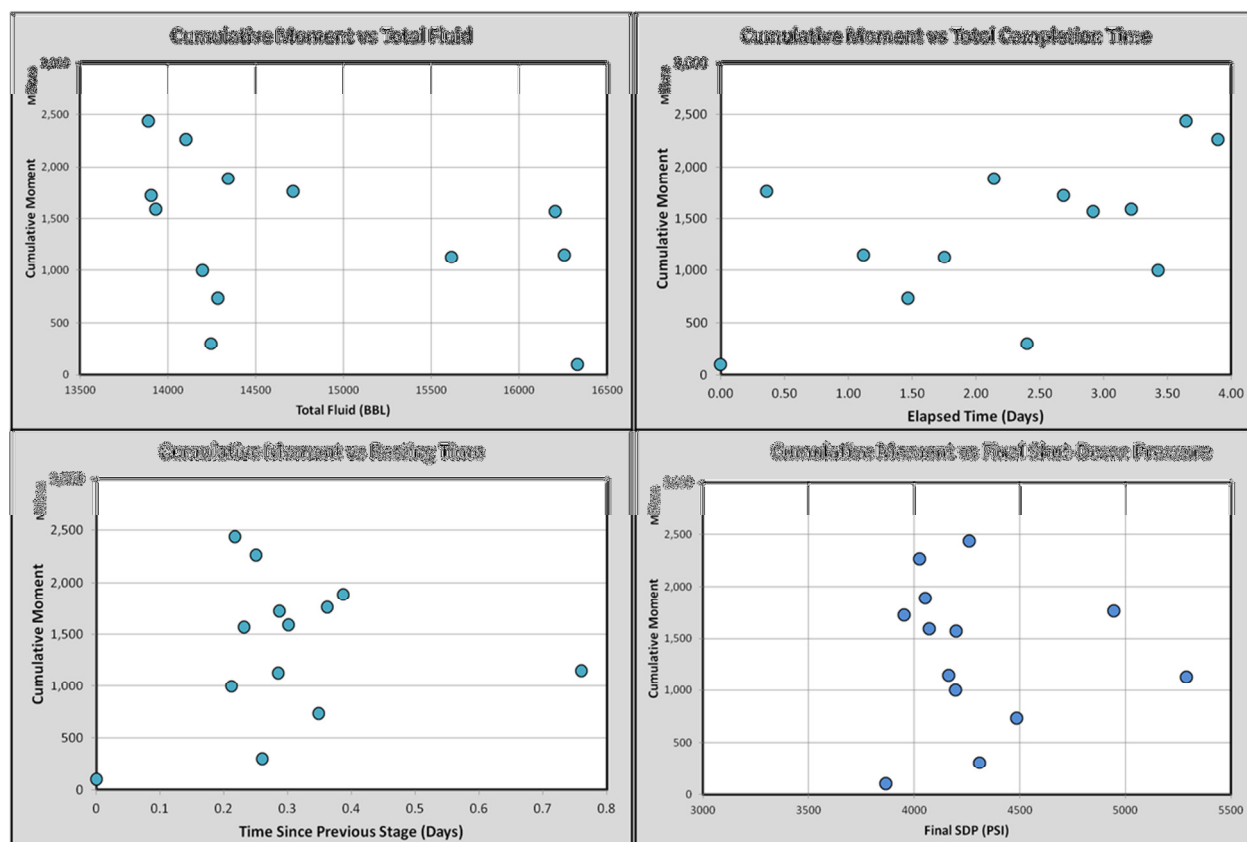


Figure 6.7 – Cumulative moment diagnostic plots

In this example there are not distinct trends in the data that would indicate that cumulative moment is related to the completion sequence (time between stages and total completion time) or net pressure development inferred from the final shut-down pressures of the individual treatment stages. The lack of any observable trend between cumulative moment and final shut-down pressure also suggests that the apparent reduction in cumulative moment that is observed when the total fluid increases is probably not a true trend. The absence of any trends then leads to the interpretation that the observed microseismic responses are affected by factors related to reservoir geology, geohazards, depletion from offset wells (if present), or the landing point of the well within the vertical section.

7 Time-Dependent Behavior

The time dependent behavior of the stimulation treatments can be evaluated using a number of techniques. Dimensions and volumes that have been computed from the event locations as shown in Section 3, Section 4, and Section 5 can be compared to the stimulation treatment data and microseismic event rates.

Figure 7.1 is an example from stage 2 of the completion, where limited height growth below the Onondaga was noted. Upward height growth into the Hamilton can be seen almost immediately upon beginning the stimulation treatment. Many of the events that occur late in the stage or after pumping is finished are offset from these early events.

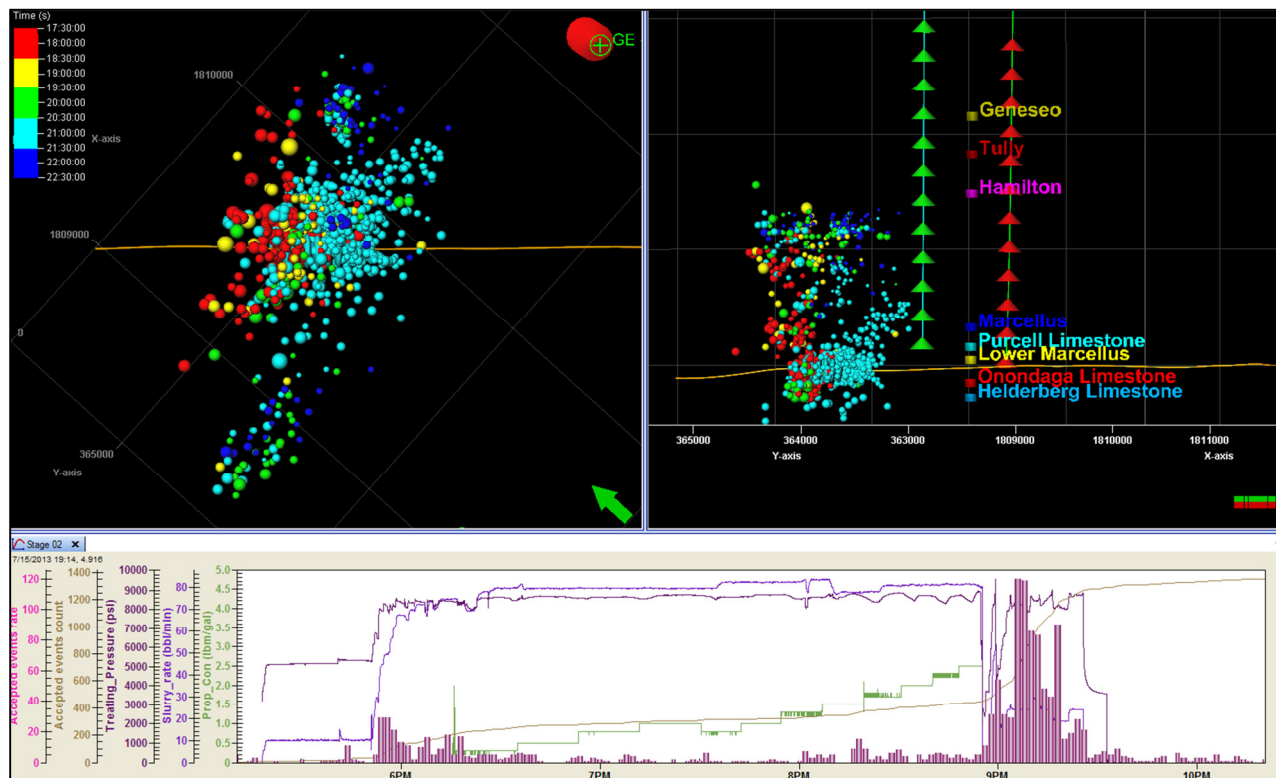


Figure 7.1 – Stage 02 colored by time and sized by magnitude (-2.9 to -0.6)

Figure 7.2 shows the events from stage 10, when the treatment grows down further into the Onondaga. Note that upward height growth appears to be reduced. Again, it is important to remember that Stages 5-13 were perforated with 0 degree phasing that was oriented down, which.

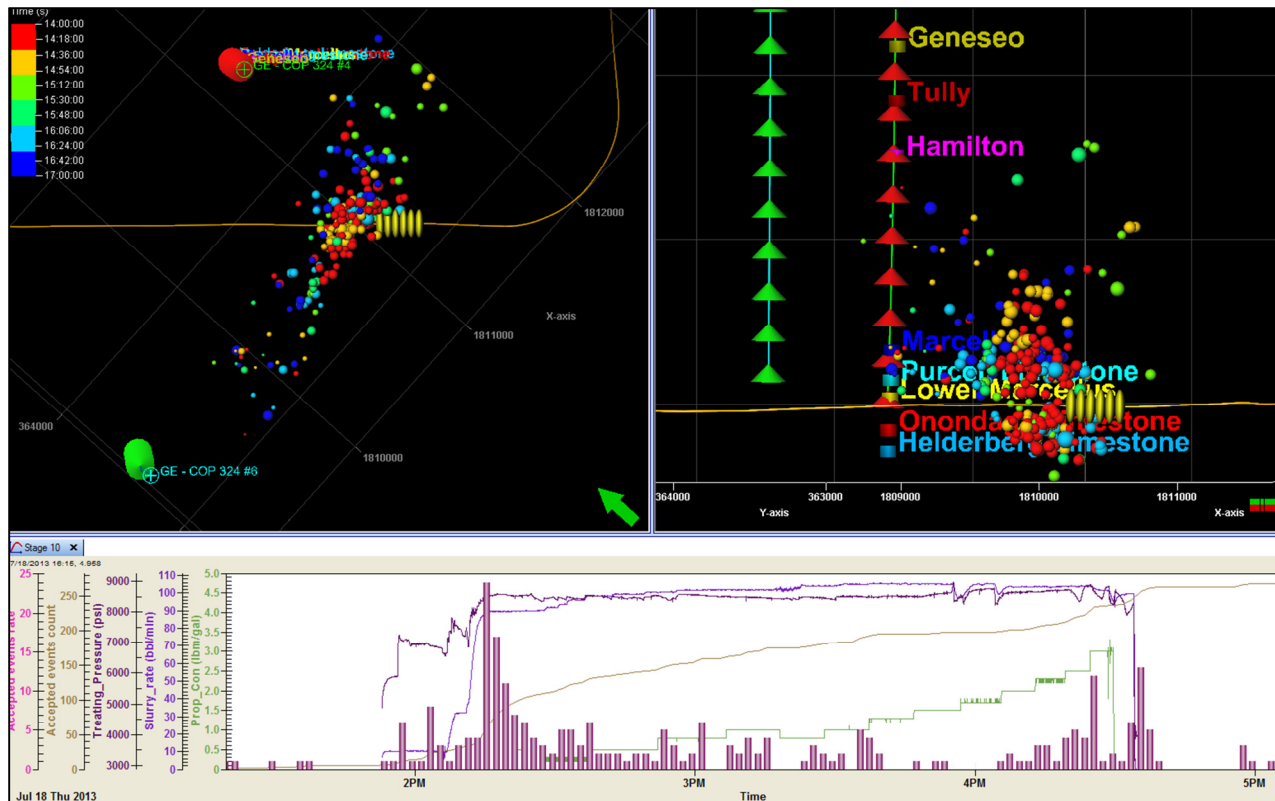


Figure 7.2 – Stage 10 colored by time and sized by magnitude (-2.6 to -0.6)

The variations in time-dependent behavior can be observed using cumulative seismic moment versus time, and versus depth. These qualitative assessment that are based on the observed deformation that produces the microseismic events can show changes in fracture behavior that are difficult to identify when comparing visual images of the events as shown in Figure 7.1 and Figure 7.2.

For qualitative comparison the cumulative moment has been normalized by converting the values to percentages of the total cumulative moment. This permits comparison of the percentage of deformation versus time and depth on a common vertical scale. Deformation versus time for the stimulation treatments is shown in Figure 7.3.

Stages 1 through 5 all display an increase in deformation that occurs during the latter portion of each treatment, as identified in Figure 7.1. This increase in observed deformation consists to a large extent of increased activity in the Hamilton. The events in the Hamilton extend much further from the lateral than the events in the Marcellus and therefore are the source of the increased total fracture length observed during those treatments in the moment-density evaluations.

Treatment stages 6, 7, and 10 all have the highest percentage of total deformation during the first part of the treatment stage. There are some similarities between these treatments and stages 11, 12, and 13. The observed time-dependent behavior of this group of treatments is distinctly different than stages 1 through 5. Stages 6 and 9 will be examined further through comparisons of deformation versus depth as shown in Figure 7.4, Figure 7.5, and Figure 7.6.

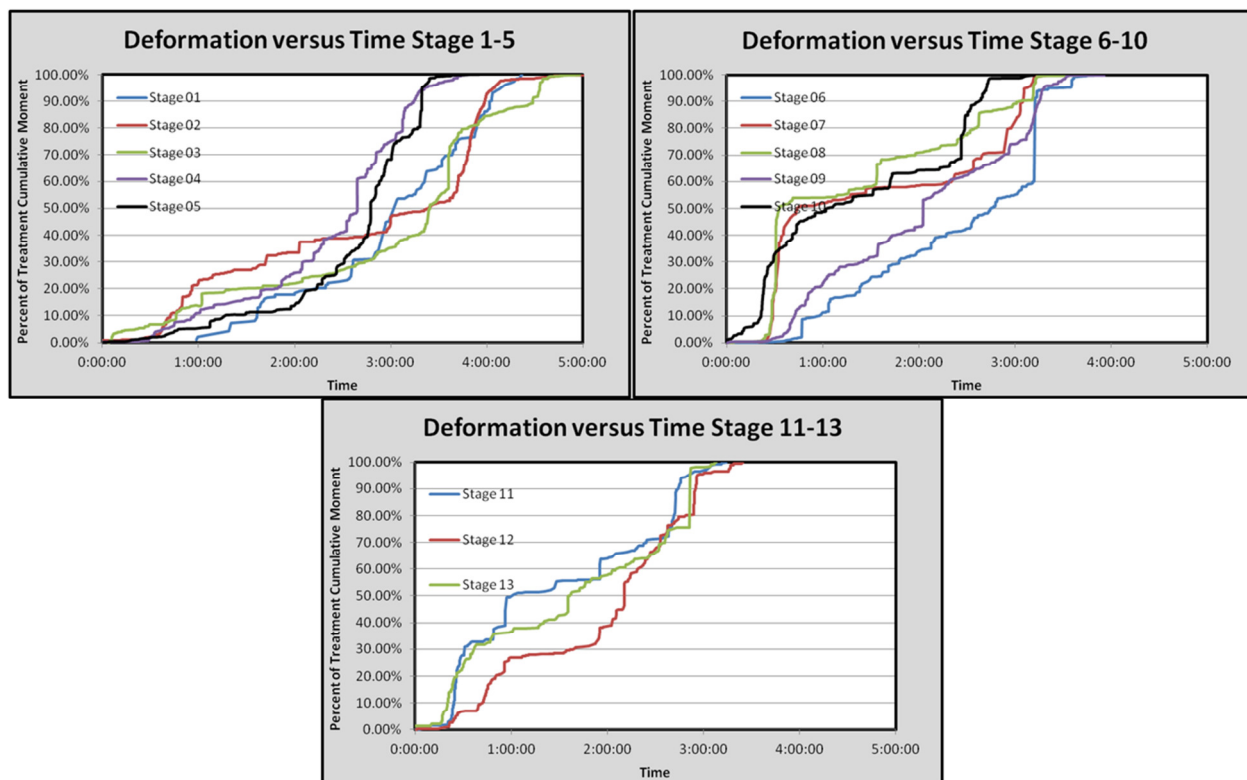


Figure 7.3 – Deformation versus time

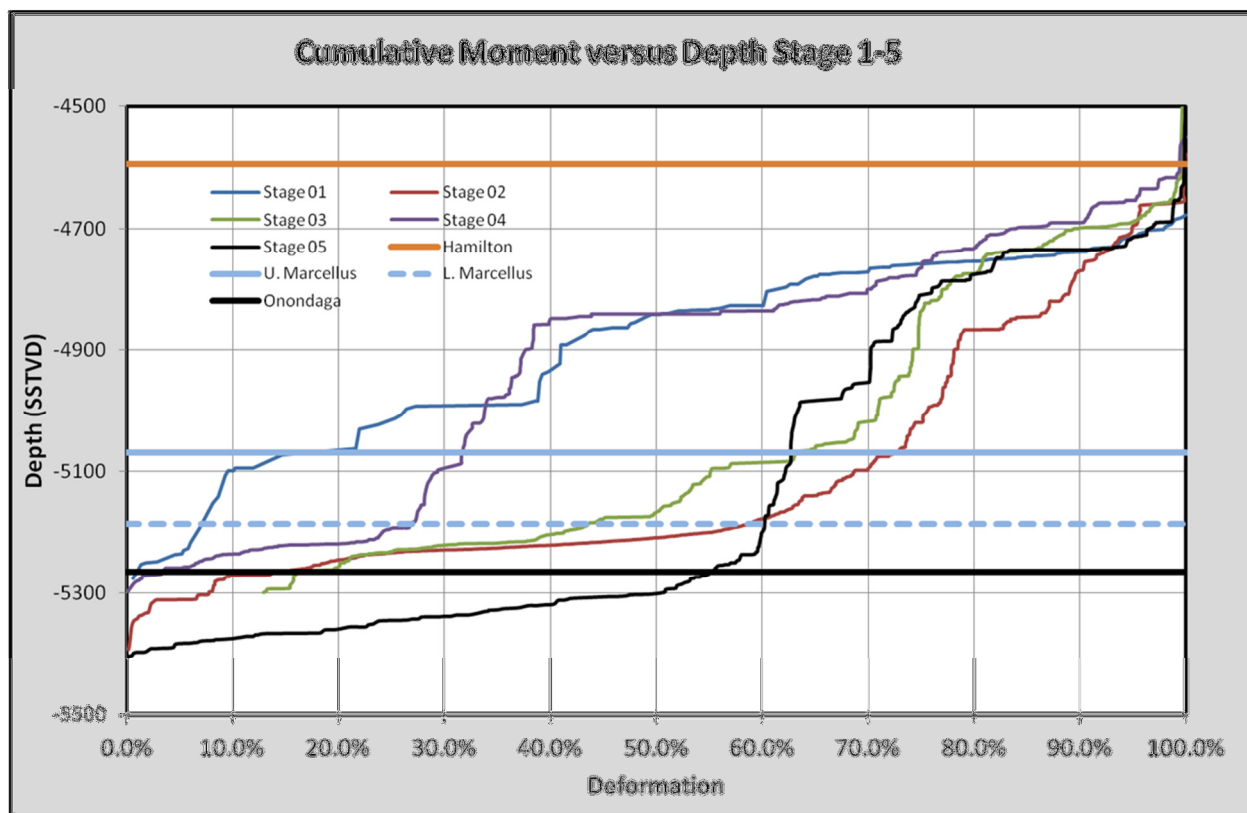


Figure 7.4 – Deformation versus depth, stages 1-5

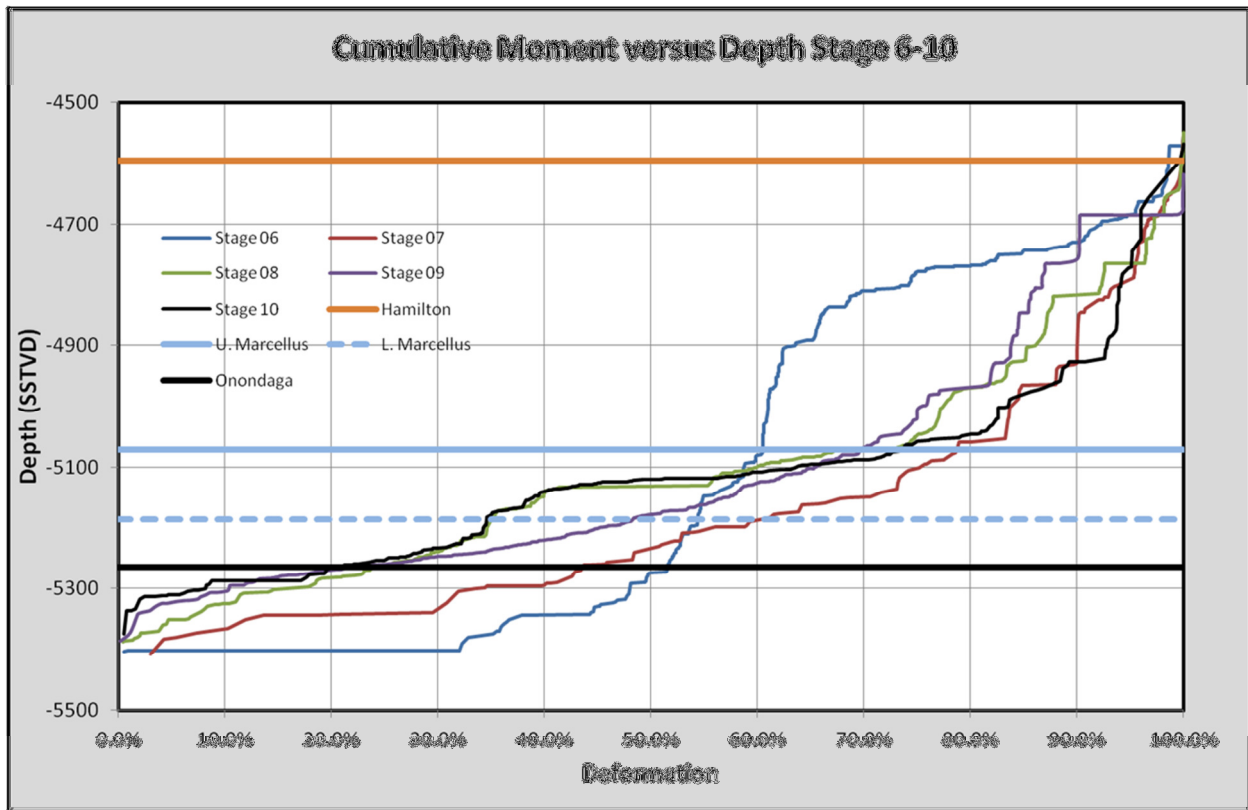


Figure 7.5 – Deformation versus depth, stages 6-10

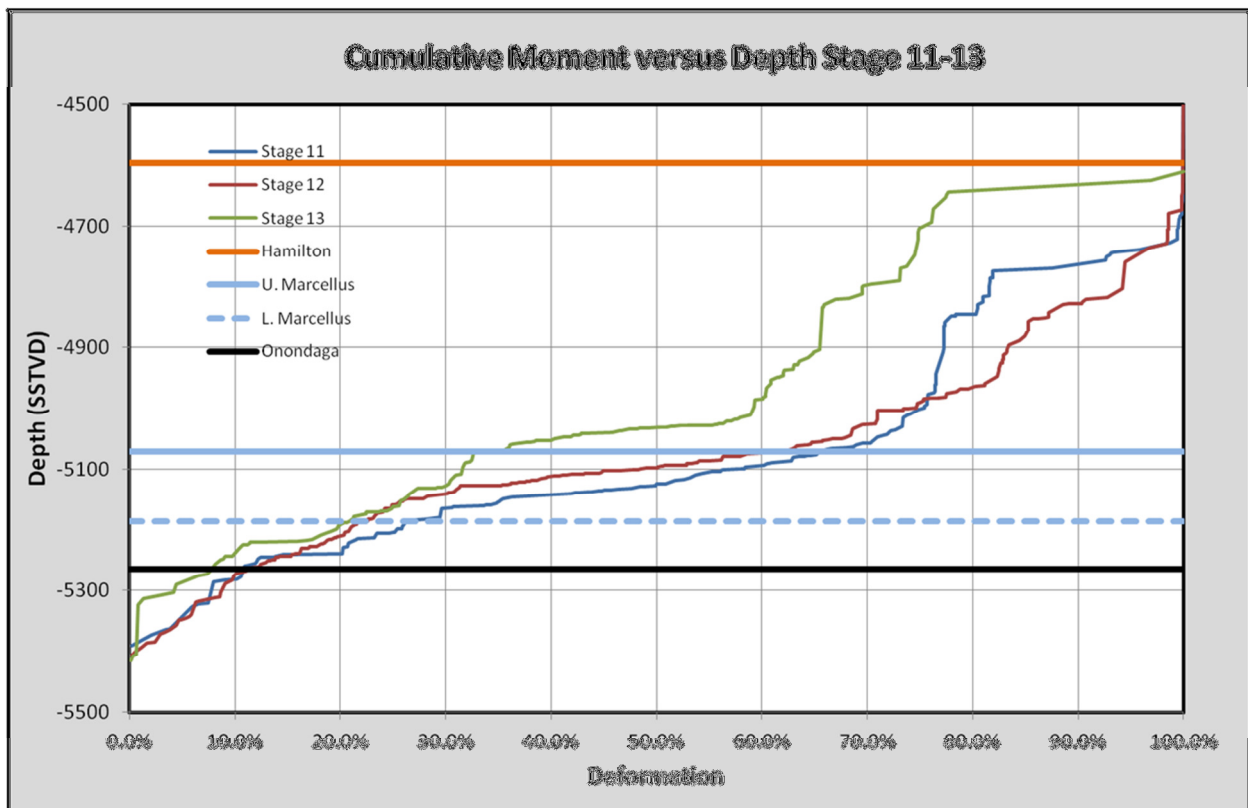


Figure 7.6 – Deformation versus depth, stages 11-13

Comparison of the moment versus depth plots of stages 6 and 9 with adjacent treatment stages shows that stage 9 does not differ significantly from the stages 7 through 13. Stage 6 is distinctly different and has very little deformation in the Marcellus. Stage 6 is also unusual in that it has the highest final shut-down pressure and relatively high levels of microseismic activity following the conclusion of the stimulation treatment. Stage 5 has similar moment versus depth distribution as stage 6.

The results of the time-dependent and depth-dependent evaluations are that the stimulation treatments behave differently during stages 1-4 compared to stages 7-13. This observation coincides with an increase in microseismic activity in the Onondaga during stages 7-13. The unusual behavior of stage 5 and stage 6 might be related to contact with a small fault. A map of identified faults near the treatment well is shown in Figure 7.7

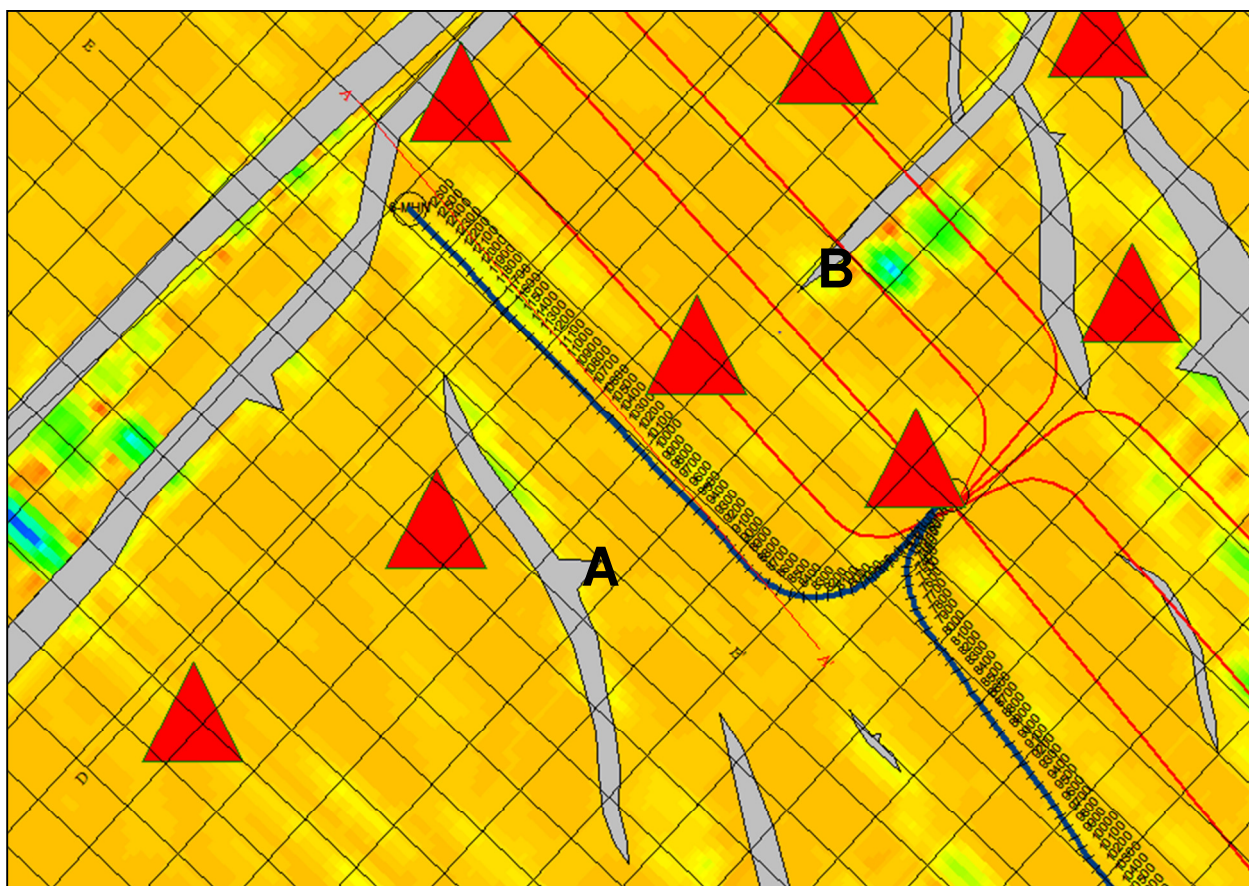


Figure 7.7 – COP 324 Seismic Map

It is not clear if fault A or B are the source of the unusual behavior that has been identified during stages 5 and 6. Other stimulation treatments might also be affected but the responses of these two treatments display the highest evidence of fault re-activation. Note that the presumed contact with one or more faults does not affect height growth, only the distribution of deformation within the fracture for those two treatments.

8 Treatment Data and Microseismic Events Summary by Stage

8.1 Stage 01

The Stage 01 treatment data and microseismic event rate are shown below. The microseismic events are color coded according to time as shown in the legend for each figure.

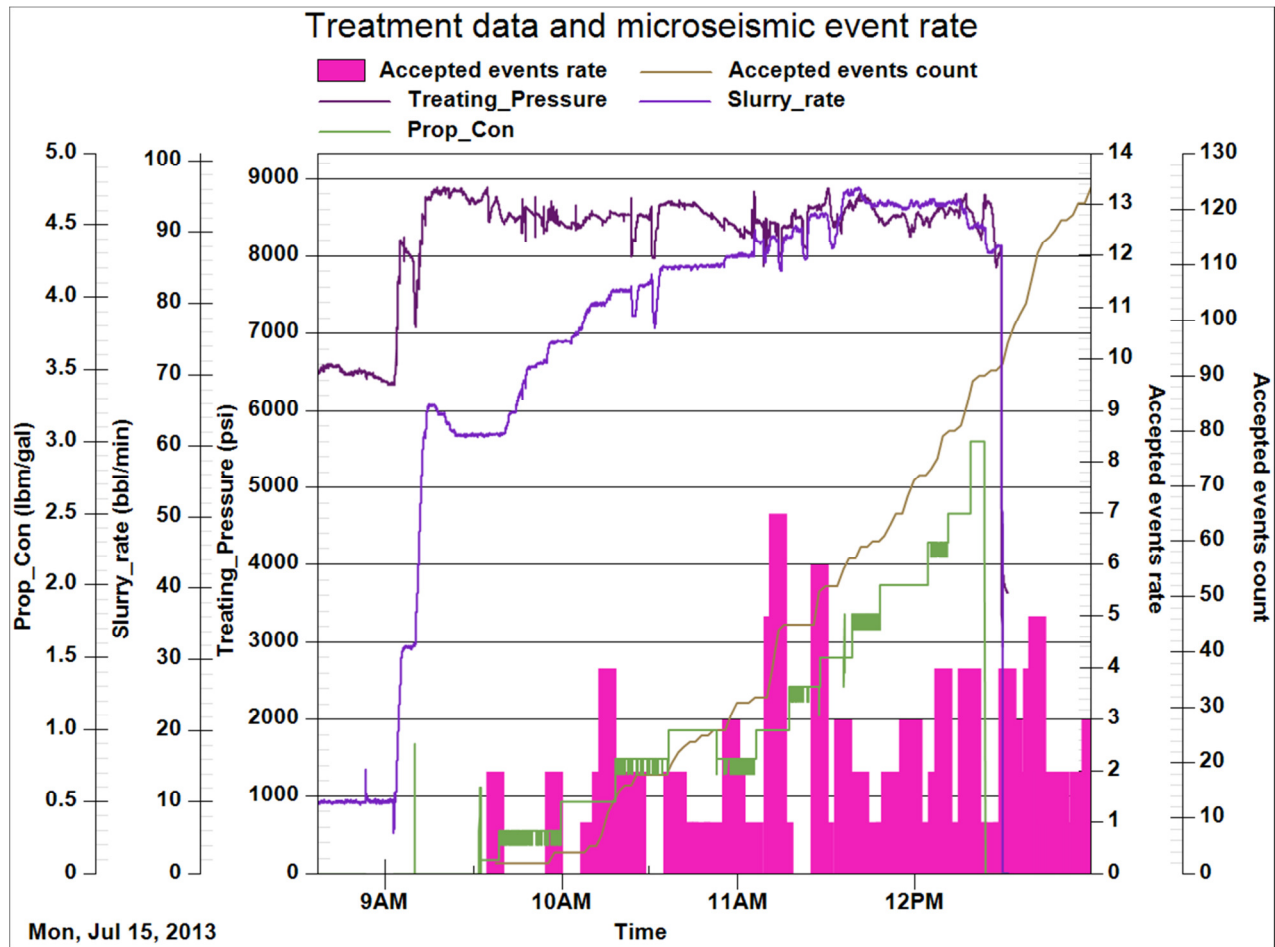


Figure 8.1 - Stage 01 treatment data and microseismic event rate

Table8.1 - Stage 01 fracture treatment volumes

Description	Designed	Placed
Total fluids (gal)	607700	685902
Total proppants (lbm)	600500	Not used

Table 8.2 - Stage 01 treatment data summary

Description	Value
Average rate (bbl/min)	N/A
Average pressure (psi)	N/A
Pre-treatment ISIP (psi)	N/A
Post-treatment ISIP (psi)	N/A
Maximum PPA (lbm/gal)	N/A

Table 8.3 - Stage 01 microseismic event geometry

Description	Microseismic geometry
Fracture azimuth (deg)	66
MS length (ft)	1910
MS height (ft)	572
MS volume (ft3)	11231999.7

The microseismic data from Stage 01 is shown below in map and transverse views. The microseismic events are color coded according to time as shown on the plot legend. The microseismic dimensions are also shown.

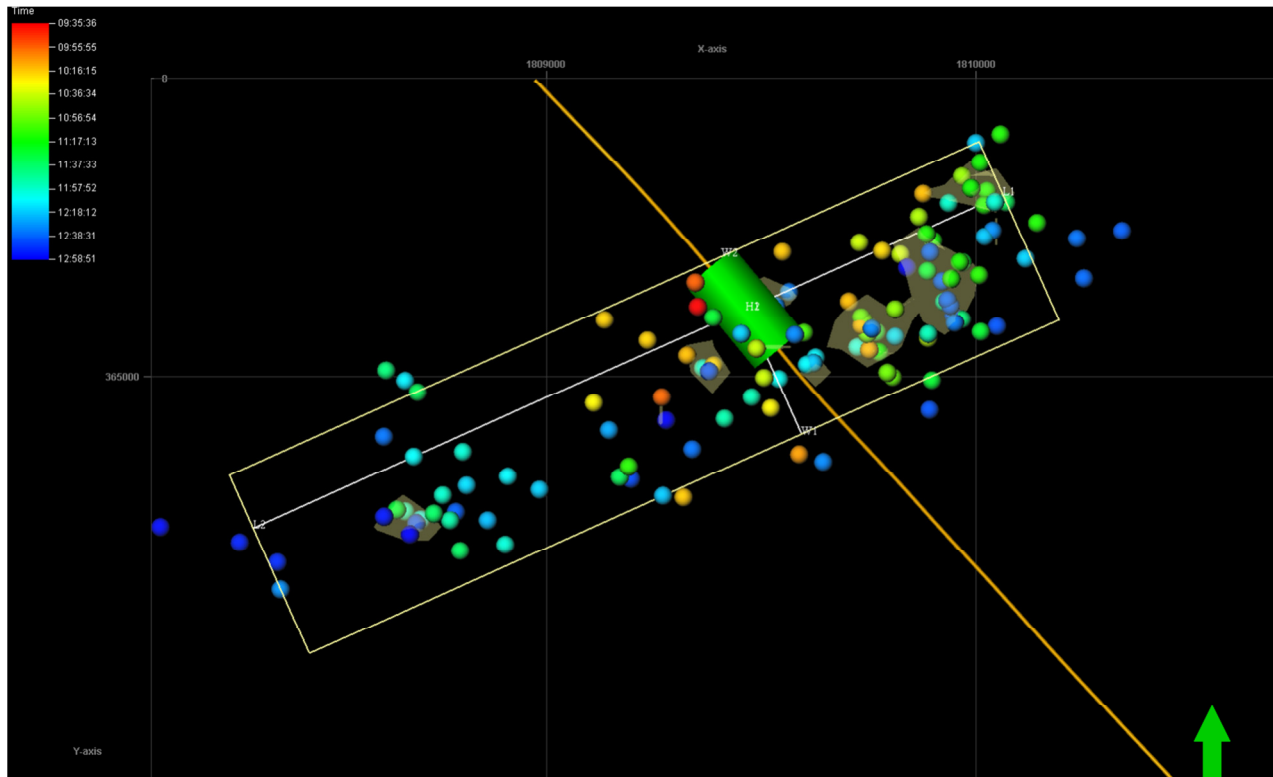


Figure.2 - Stage 01 map view (length and width)

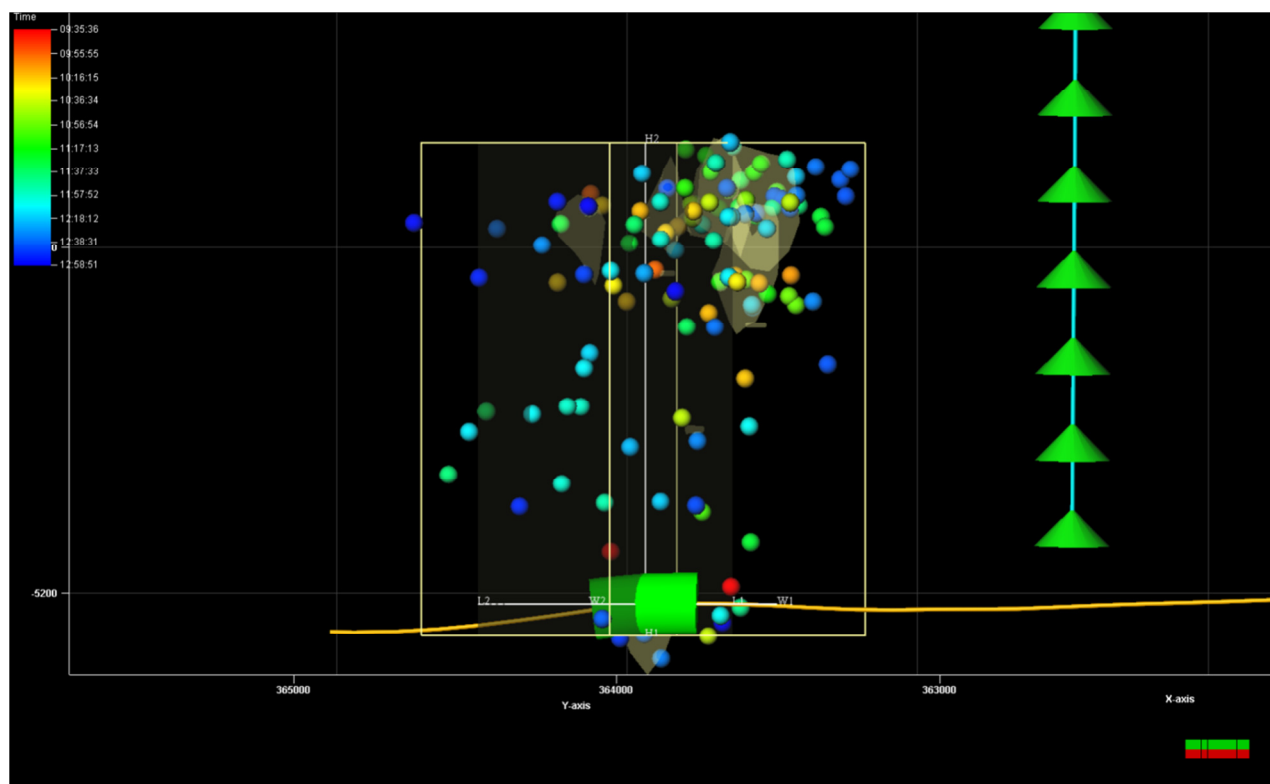


Figure.3 - Stage 01 transverse view (height and width)

The microseismic event location uncertainty ellipsoids for Stage 01 are shown below in map and transverse views.

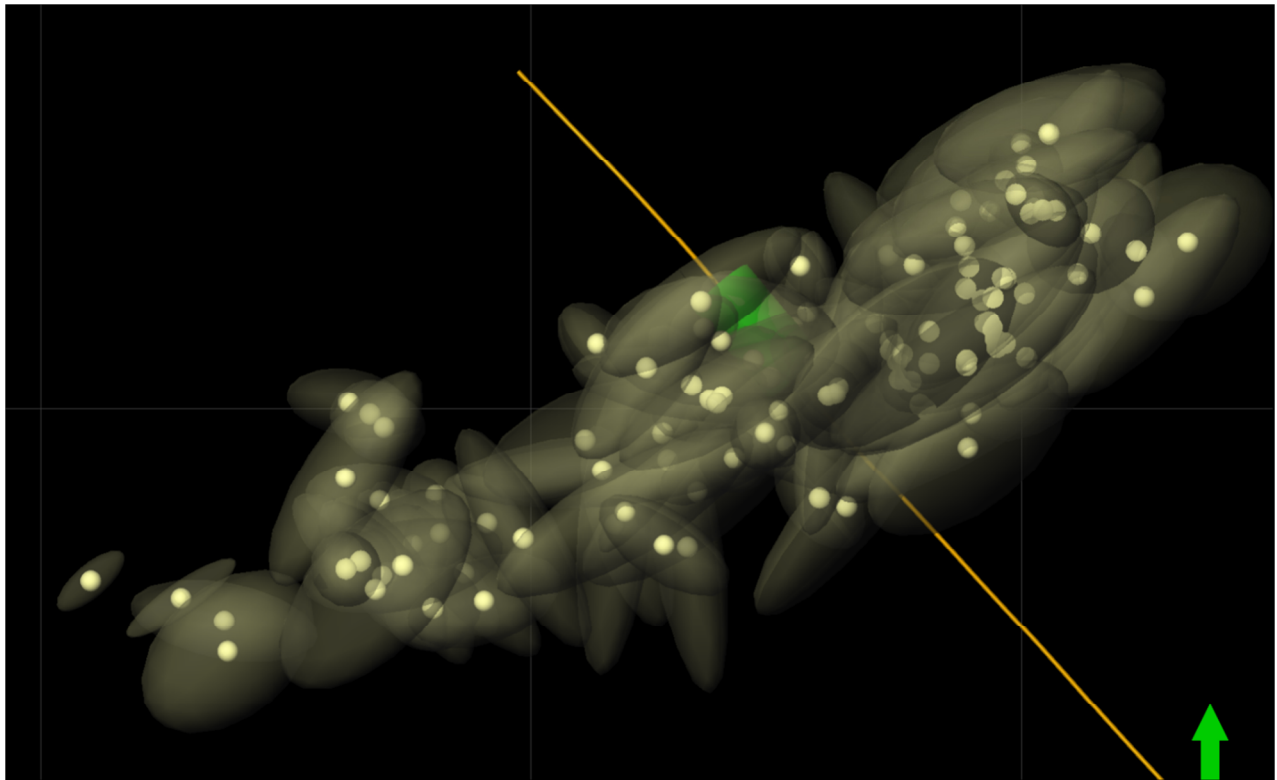


Figure.4 - Stage 01 event location uncertainty ellipsoids – map view

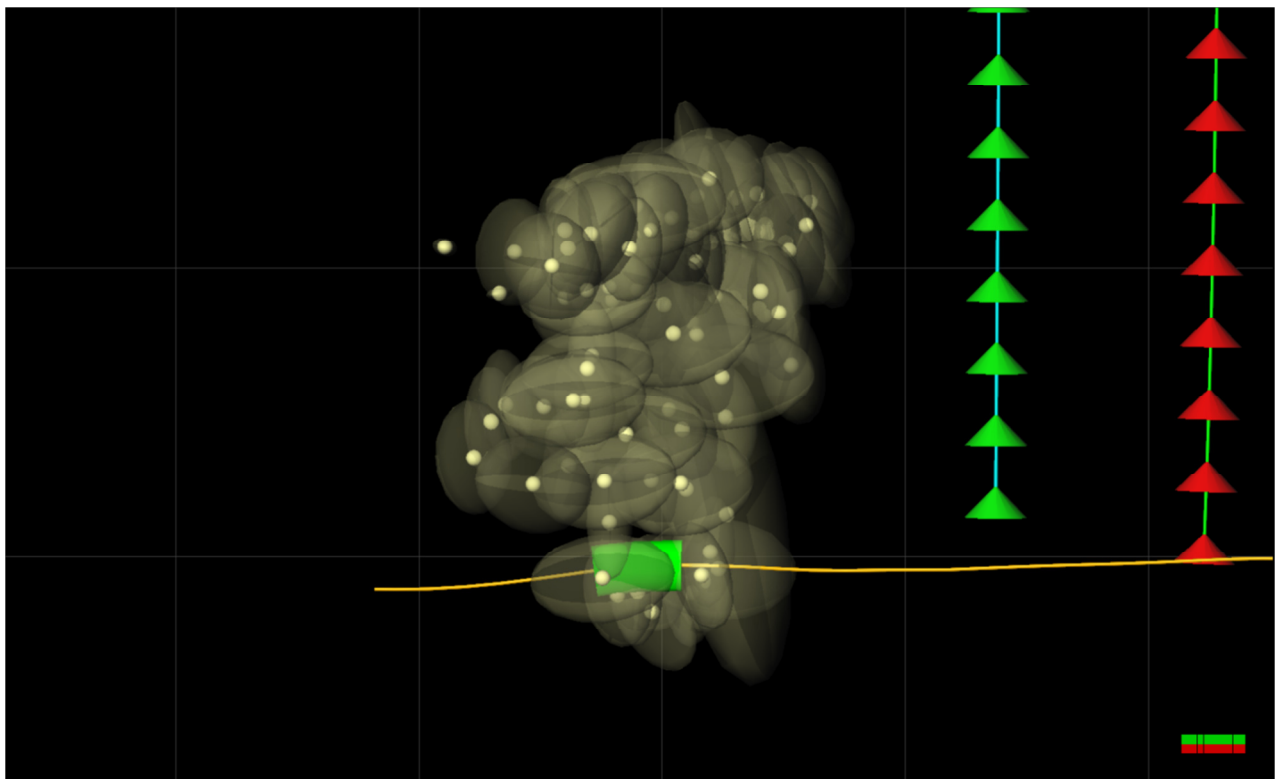


Figure.5 - Stage 01 event location uncertainty ellipsoids – side view

8.2 Stage 02

The Stage 02 treatment data and microseismic event rate are shown below. The microseismic events are color coded according to time as shown in the legend for each figure.

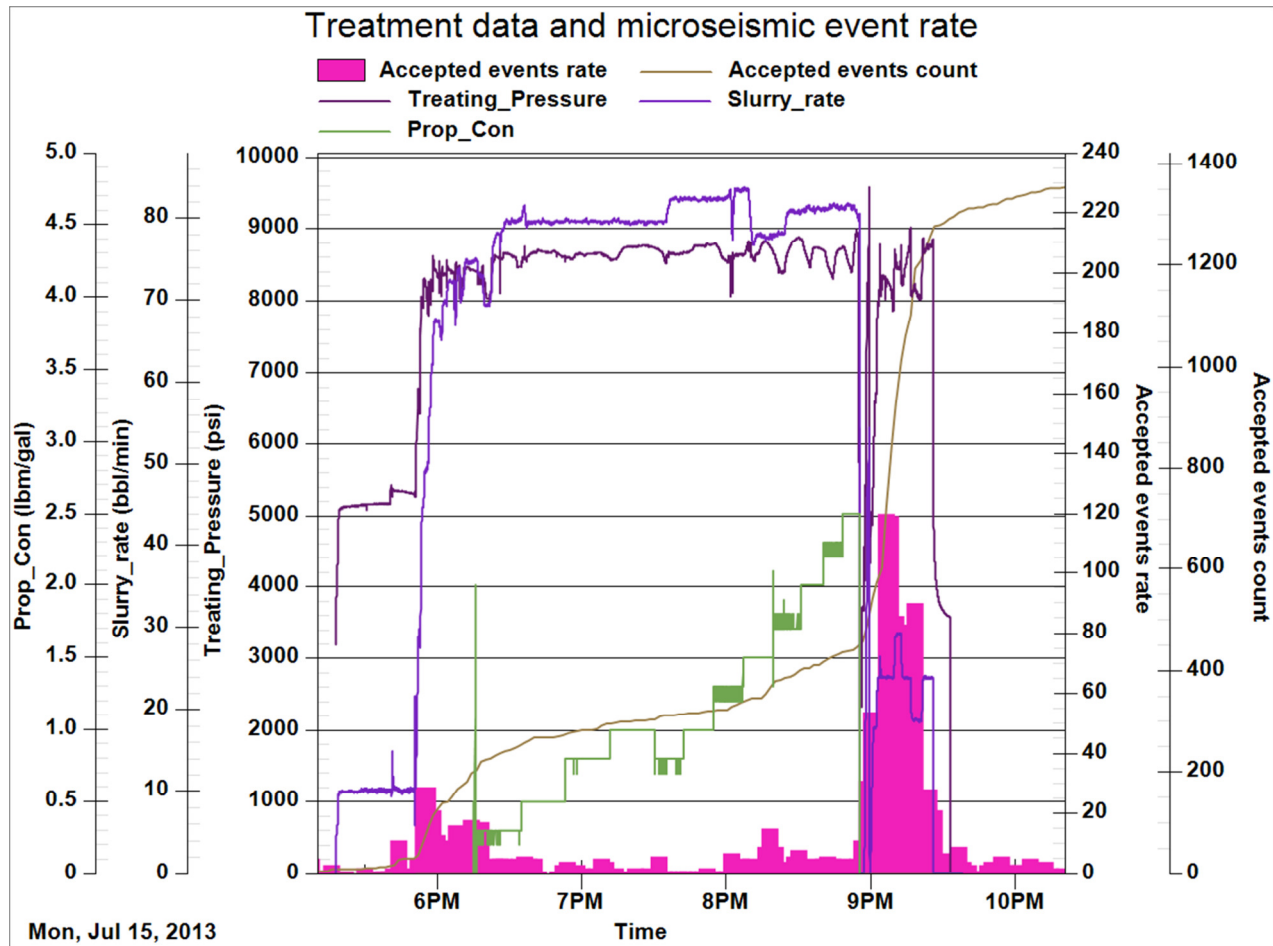


Figure.6 - Stage 02 treatment data and microseismic event rate

Table 8.4 - Stage 02 fracture treatment volumes

Description	Designed	Placed
Total fluids (gal)	607700	617904
Total proppants (lbm)	600500	Not used

Table 8.5 - Stage 02 treatment data summary

Description	Value
Average rate (bbl/min)	N/A
Average pressure (psi)	N/A
Pre-treatment ISIP (psi)	N/A
Post-treatment ISIP (psi)	N/A
Maximum PPA (lbm/gal)	N/A

Table 8.6 - Stage 02 microseismic event geometry

Description	Microseismic geometry
Fracture azimuth (deg)	69
MS length (ft)	1604
MS height (ft)	620
MS volume (ft3)	131976003.7

The microseismic data from Stage 02 is shown below in map and transverse views. The microseismic events are color coded according to time as shown on the plot legend. The microseismic dimensions are also shown.

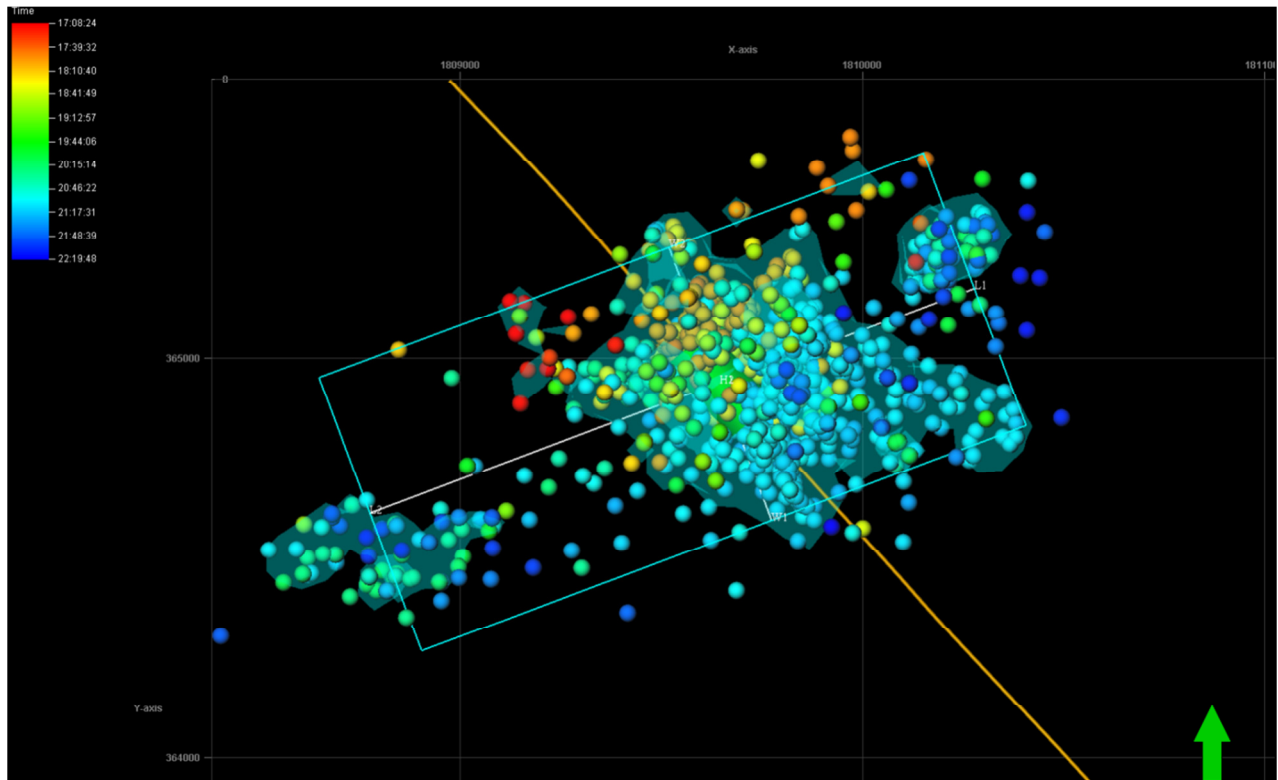


Figure 8.7 - Stage 02 map view (length and width)

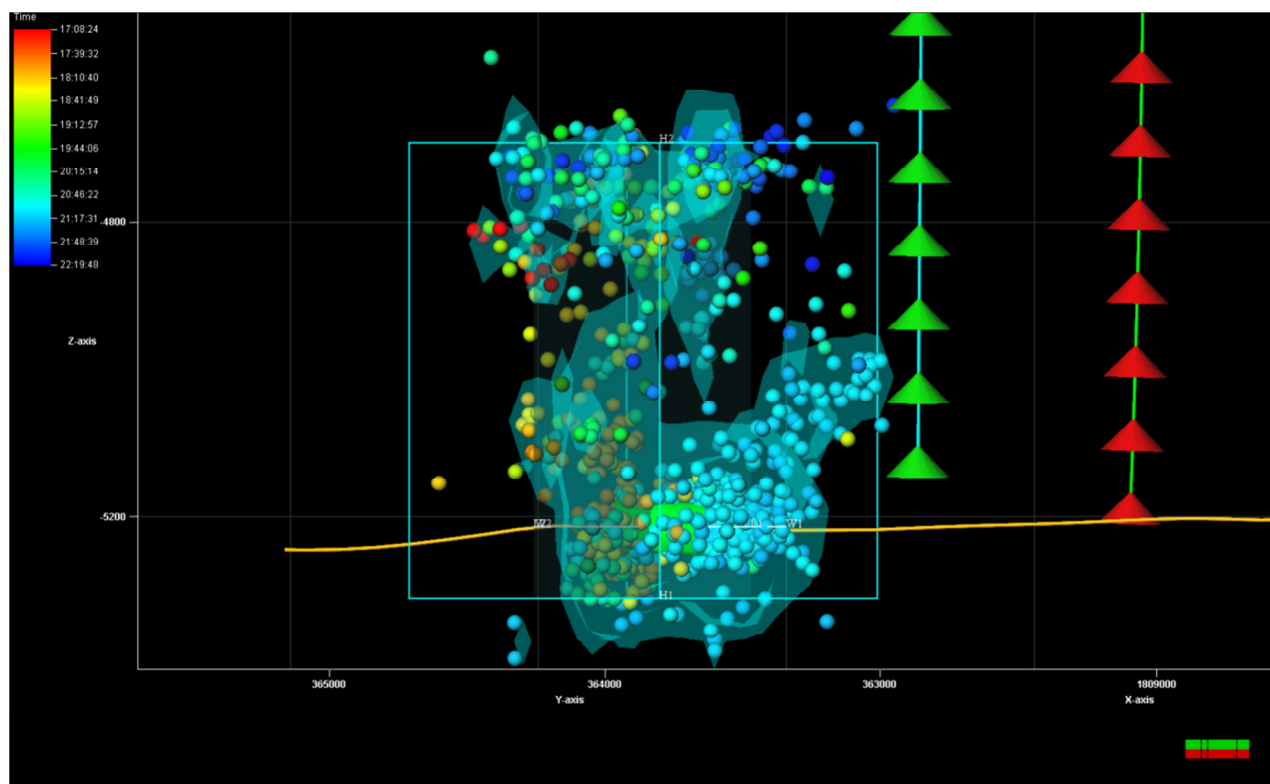


Figure 8.8 - Stage 02 transverse view (height and width)

The microseismic event location uncertainty ellipsoids for Stage 02 are shown below in map and transverse views.

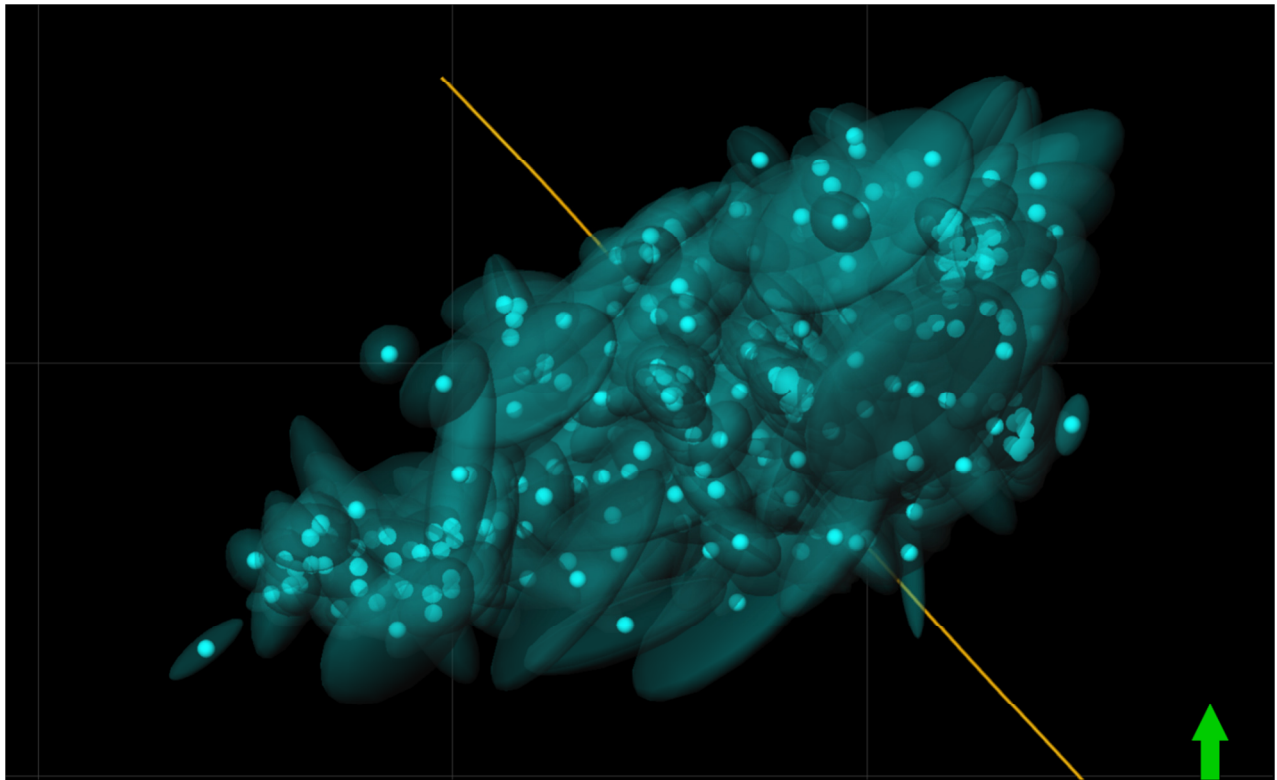


Figure 8.9 - Stage 02 event location uncertainty ellipsoids – map view

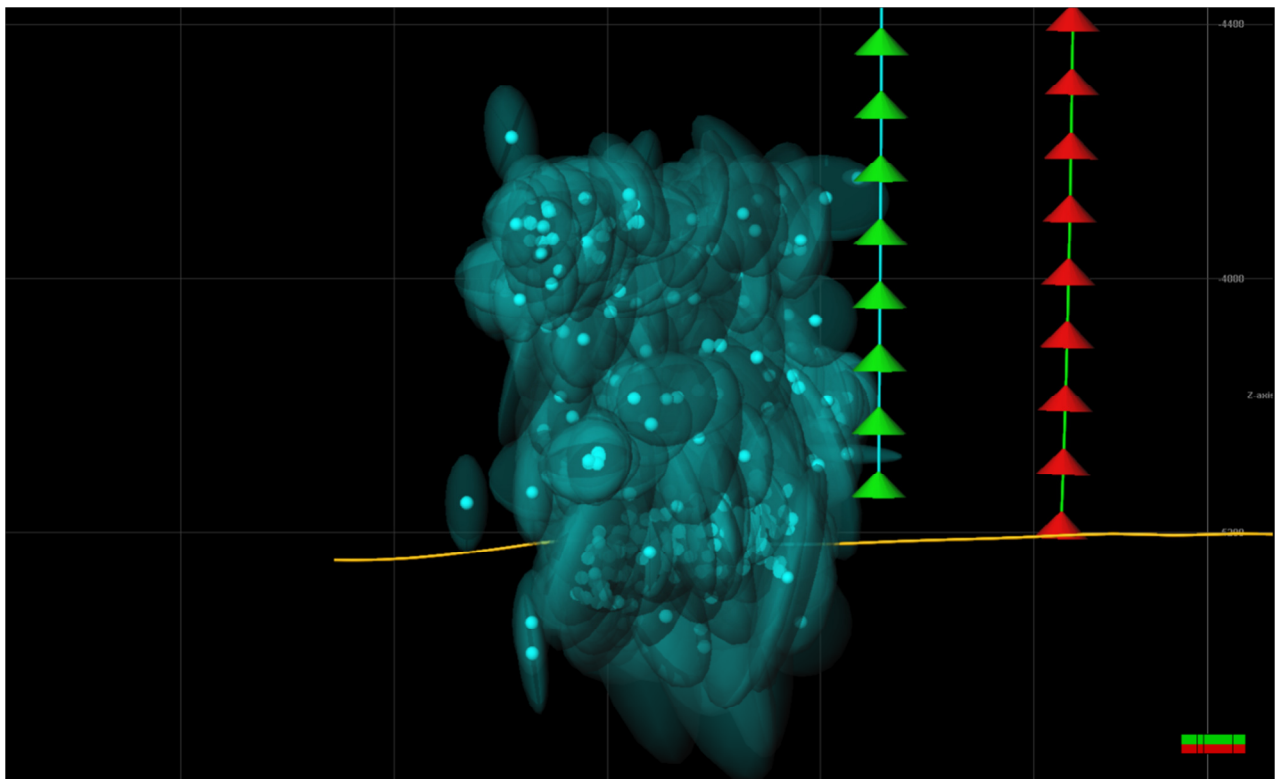


Figure 8.10 - Stage 02 event location uncertainty ellipsoids – side view

8.3 Stage 03

The Stage 03 treatment data and microseismic event rate are shown below. The microseismic events are color coded according to time as shown in the legend for each Figure 8.

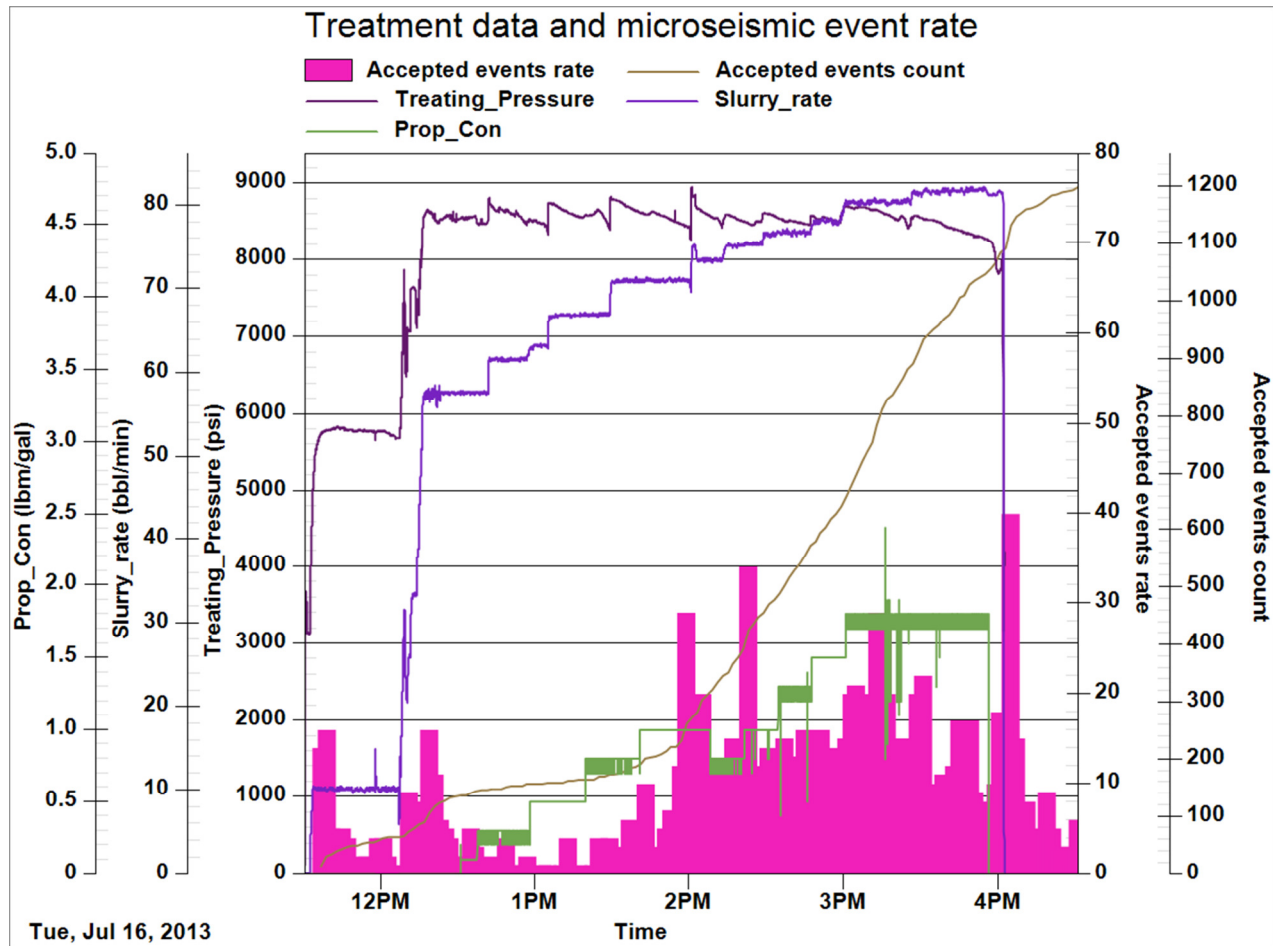


Figure 8.11 - Stage 03 treatment data and microseismic event rate

Table 8.7 - Stage 03 fracture treatment volumes

Description	Designed	Placed
Total fluids (gal)	607700	682836
Total proppants (lbm)	600500	Not used

Table 8.8 - Stage 03 treatment data summary

Description	Value
Average rate (bbl/min)	N/A
Average pressure (psi)	N/A
Pre-treatment ISIP (psi)	N/A
Post-treatment ISIP (psi)	N/A
Maximum PPA (lbm/gal)	N/A

Table 8.9 - Stage 03 microseismic event geometry

Description	Microseismic geometry
Fracture azimuth (deg)	66
MS length (ft)	1871
MS height (ft)	614
MS volume (ft3)	110375999.7

The microseismic data from Stage 03 is shown below in map and transverse views. The microseismic events are color coded according to time as shown on the plot legend. The microseismic dimensions are also shown.

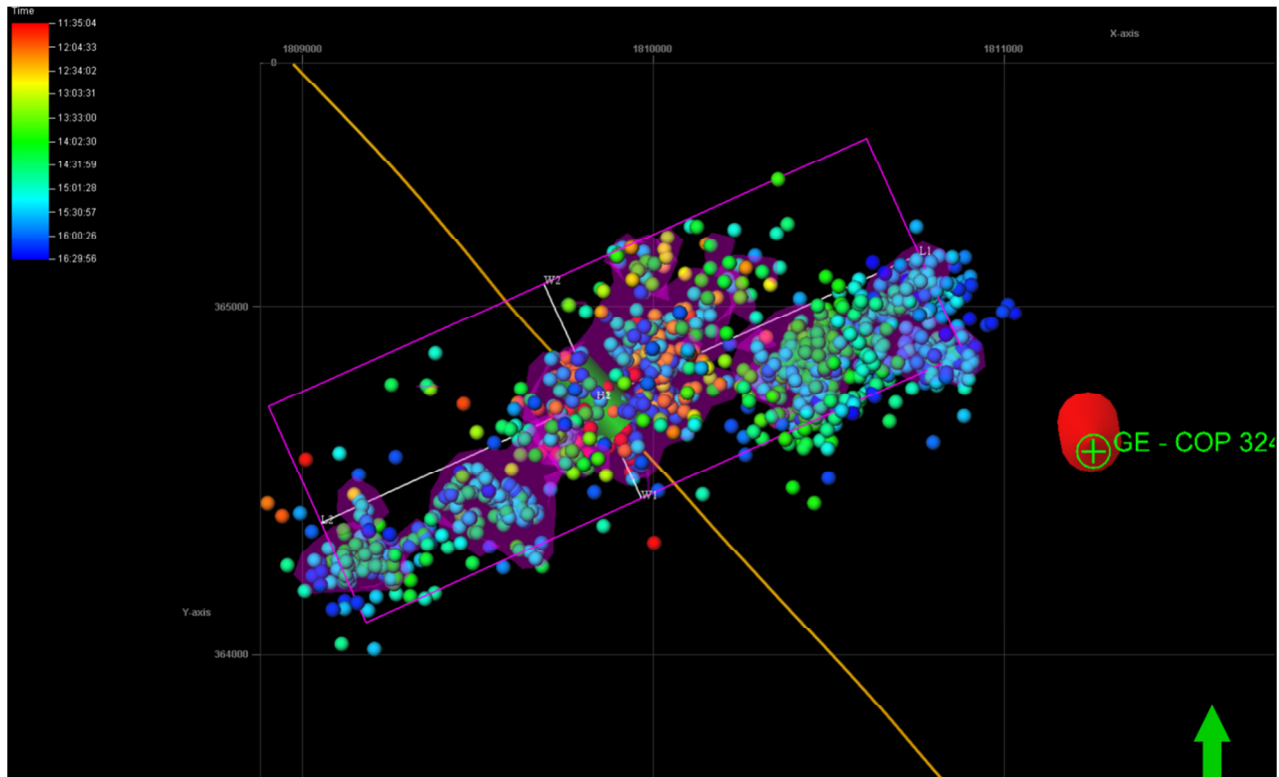


Figure 8.12 - Stage 03 map view (length and width)

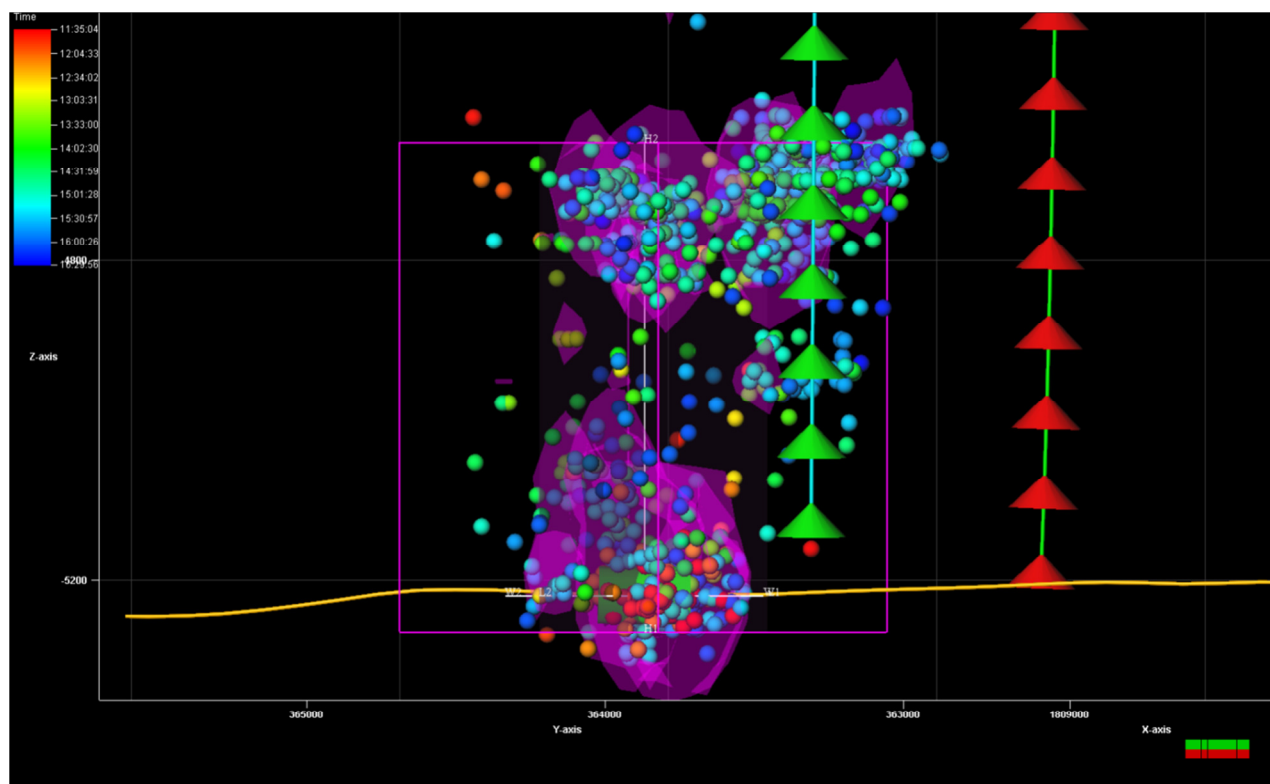


Figure 8.13 - Stage 03 transverse view (height and width)

The microseismic event location uncertainty ellipsoids for Stage 03 are shown below in map and transverse views.

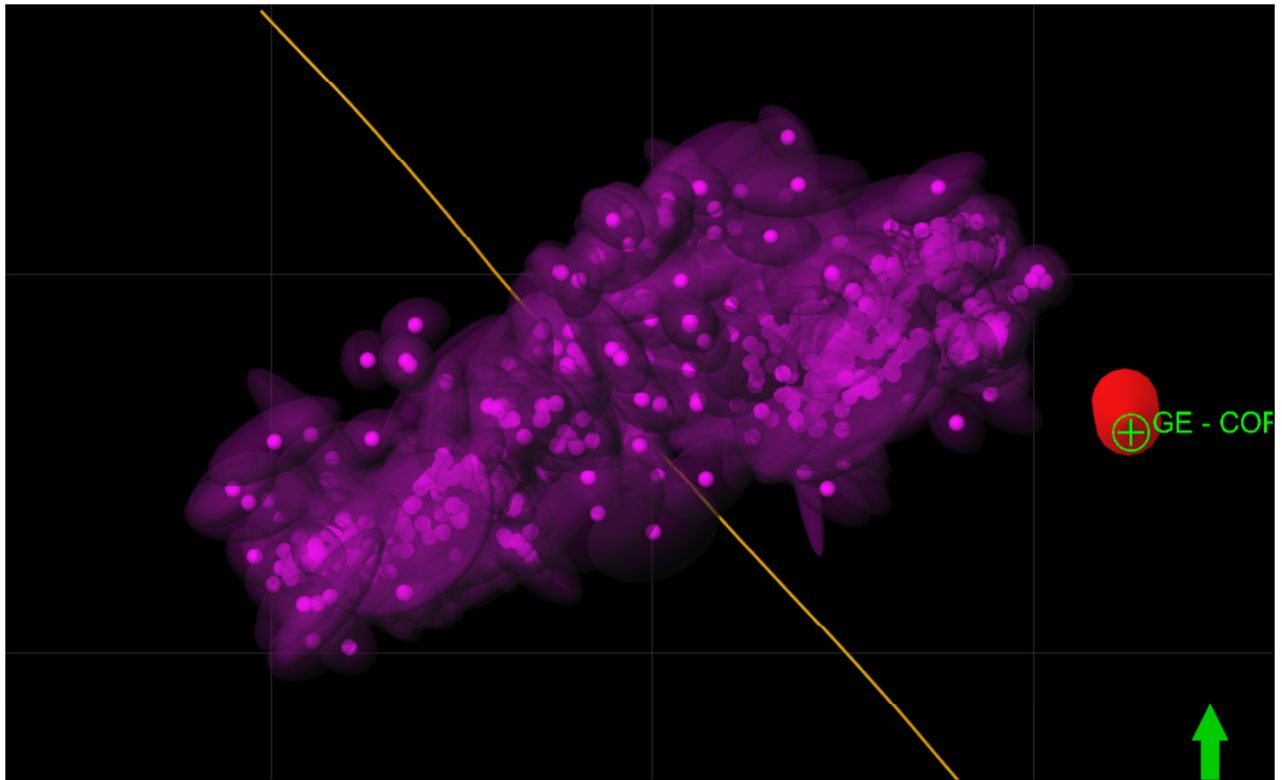


Figure 8.14 - Stage 03 event location uncertainty ellipsoids – map view

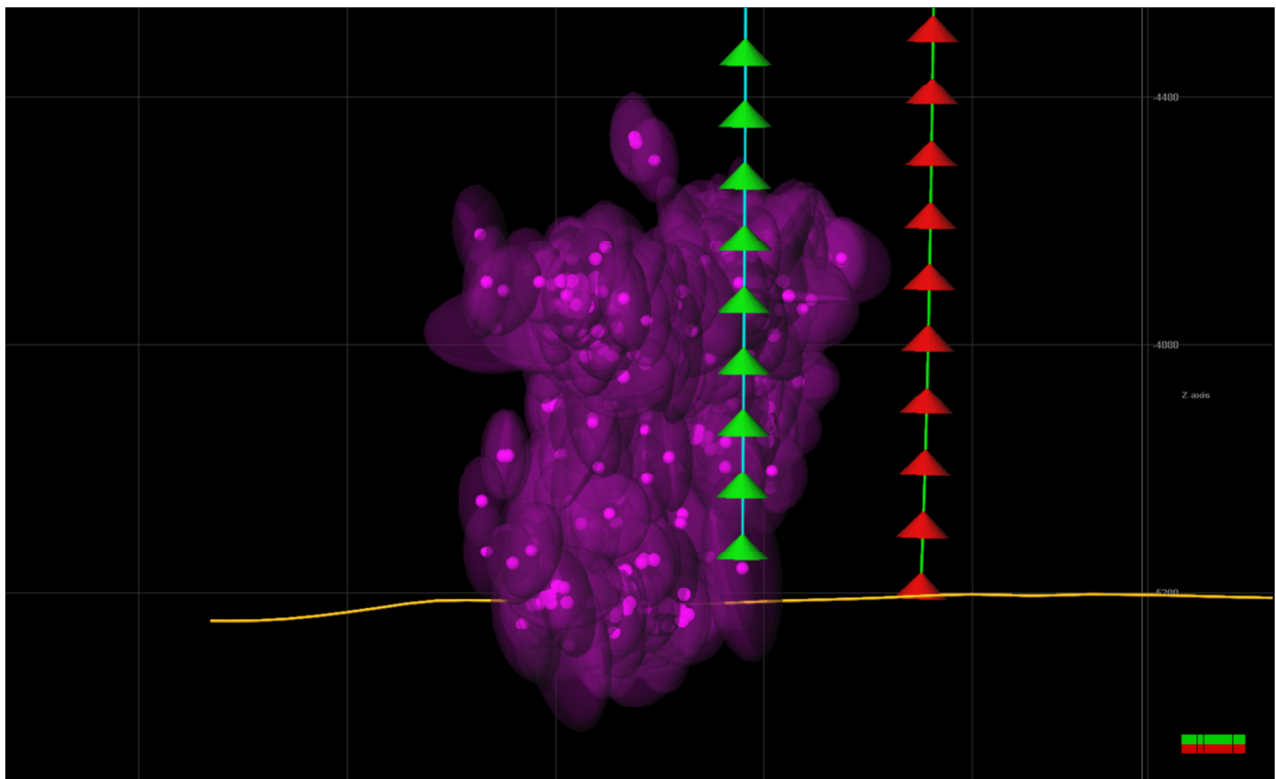


Figure 8.15 - Stage 03 event location uncertainty ellipsoids – side view

8.4 Stage 04

The Stage 04 treatment data and microseismic event rate are shown below. The microseismic events are color coded according to time as shown in the legend for each Figure 8.

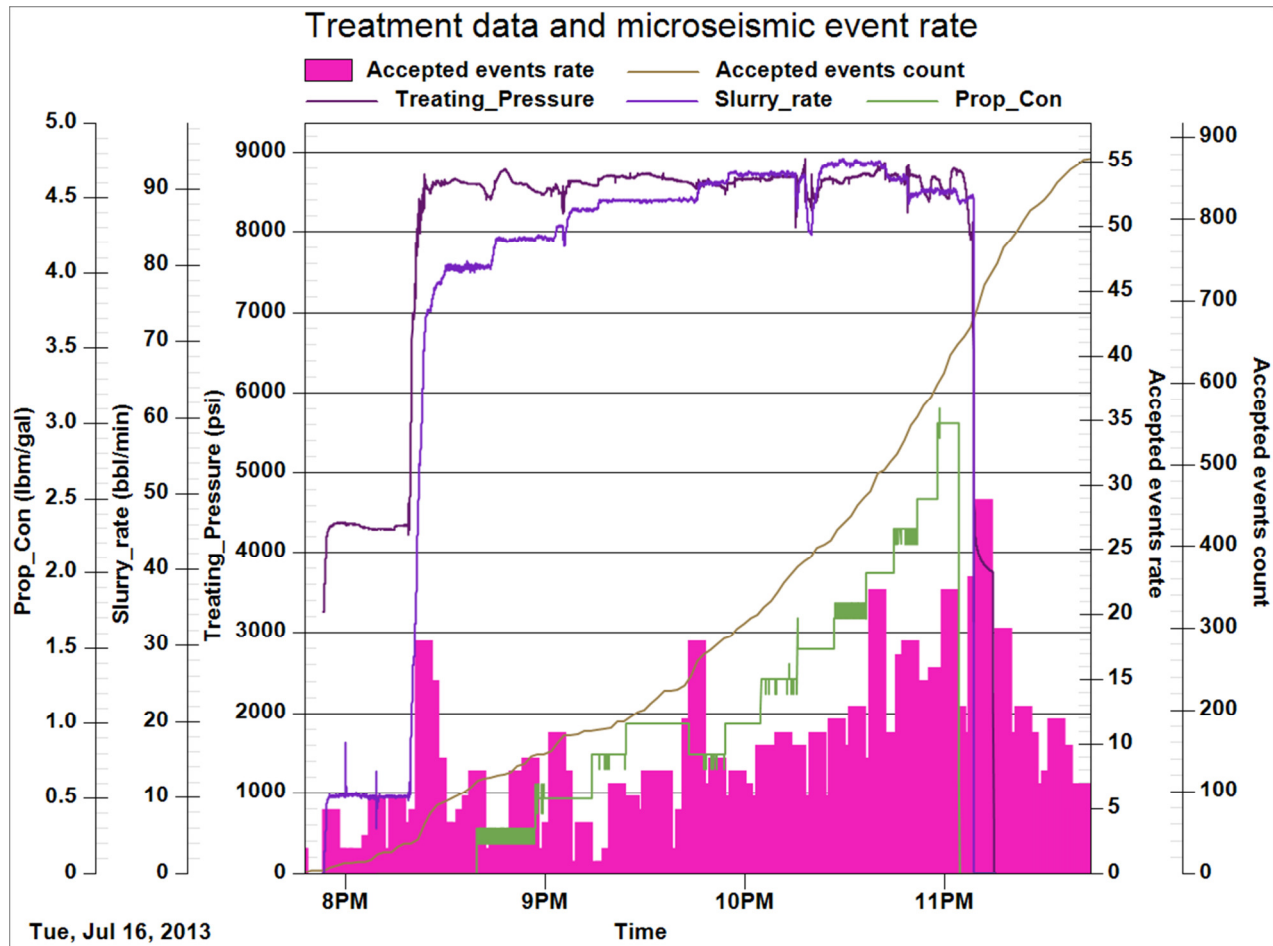


Figure 8.16 - Stage 04 treatment data and microseismic event rate

Table 8.10 - Stage 04 fracture treatment volumes

Description	Designed	Placed
Total fluids (gal)	607700	599928
Total proppants (lbm)	600500	Not used

Table 8.11 - Stage 04 treatment data summary

Description	Value
Average rate (bbl/min)	N/A
Average pressure (psi)	N/A
Pre-treatment ISIP (psi)	N/A
Post-treatment ISIP (psi)	N/A
Maximum PPA (lbm/gal)	N/A

Table 8.12 - Stage 04 microseismic event geometry

Description	Microseismic geometry
Fracture azimuth (deg)	68
MS length (ft)	2005
MS height (ft)	673
MS volume (ft3)	79271997.8

The microseismic data from Stage 04 is shown below in map and transverse views. The microseismic events are color coded according to time as shown on the plot legend. The microseismic dimensions are also shown.

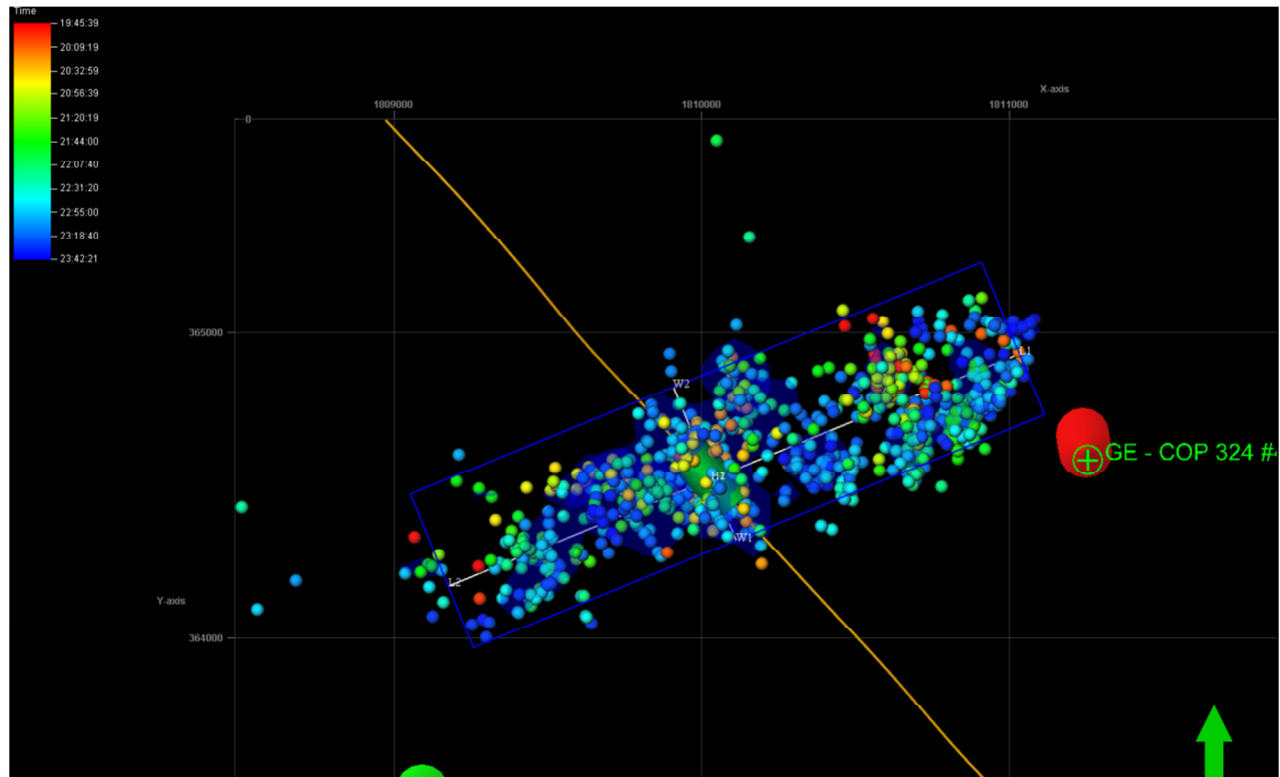


Figure 8.17 - Stage 04 map view (length and width)

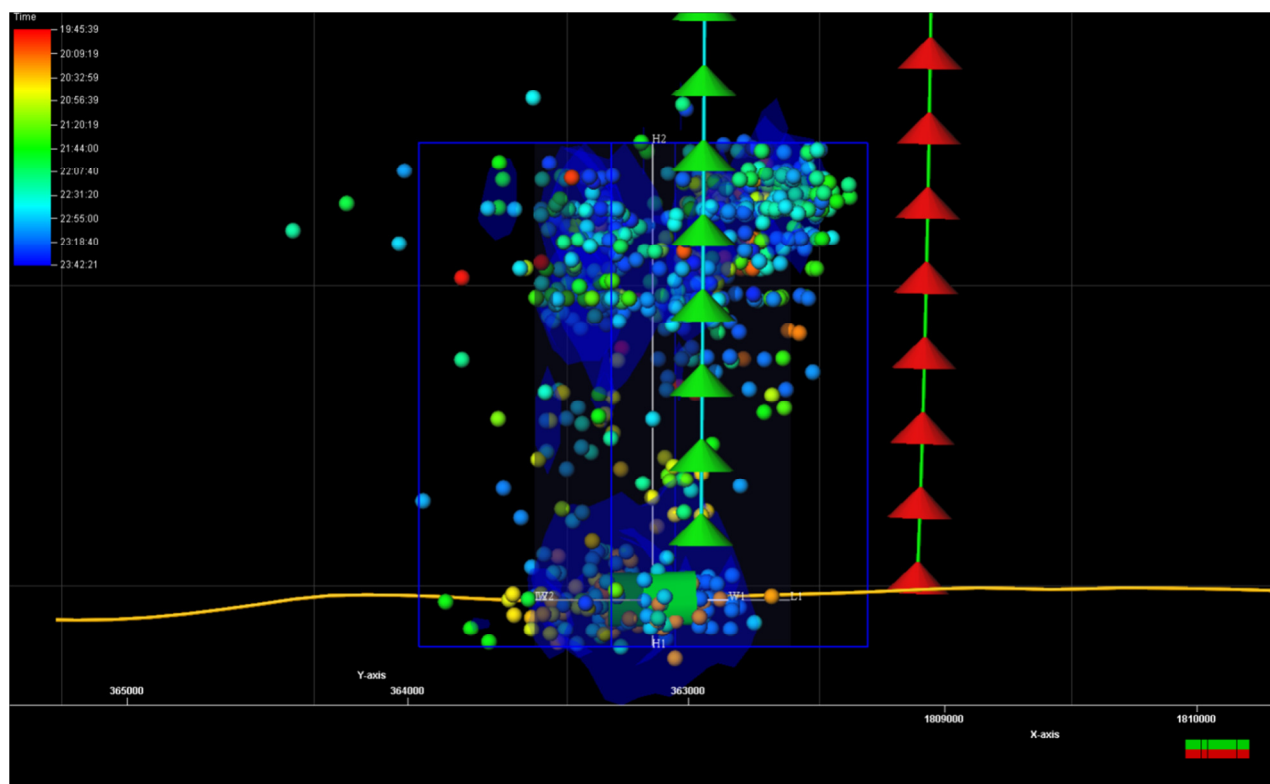


Figure 8.18 - Stage 04 transverse view (height and width)

The microseismic event location uncertainty ellipsoids for Stage 04 are shown below in map and transverse views.

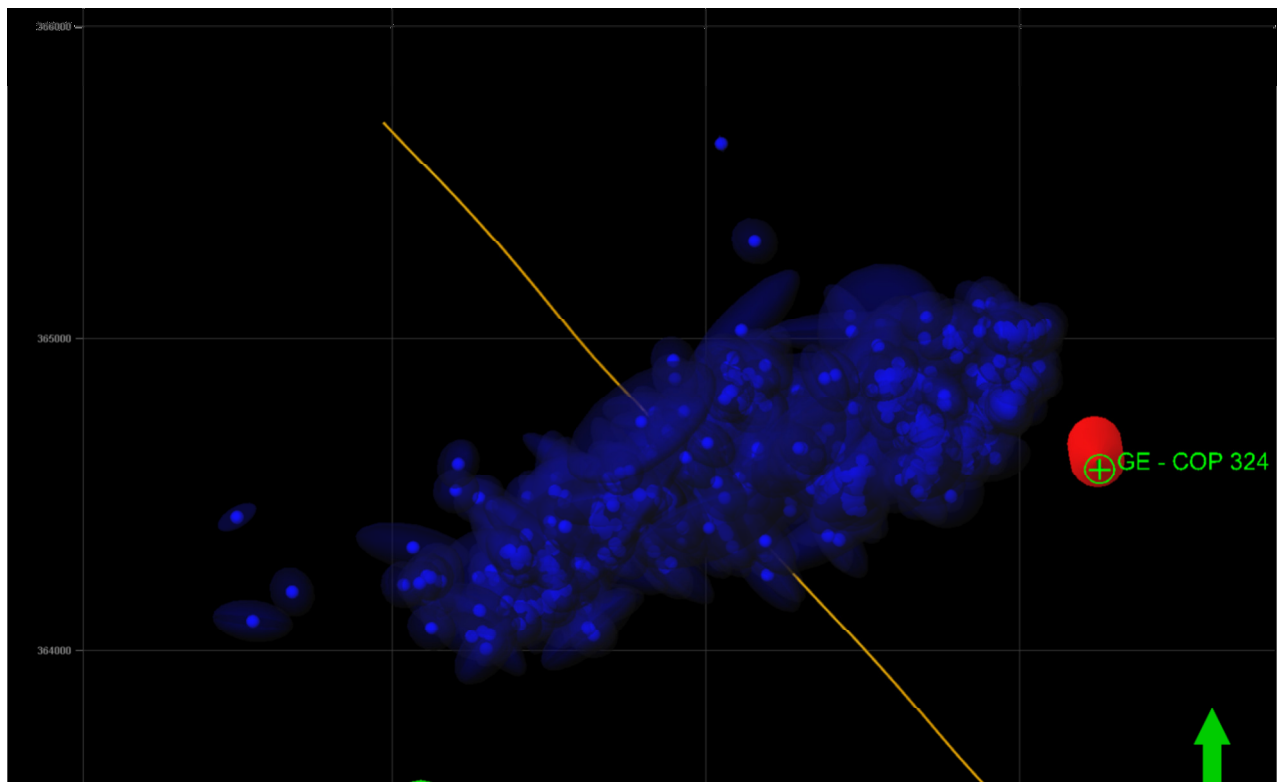


Figure 8.19 - Stage 04 event location uncertainty ellipsoids – map view

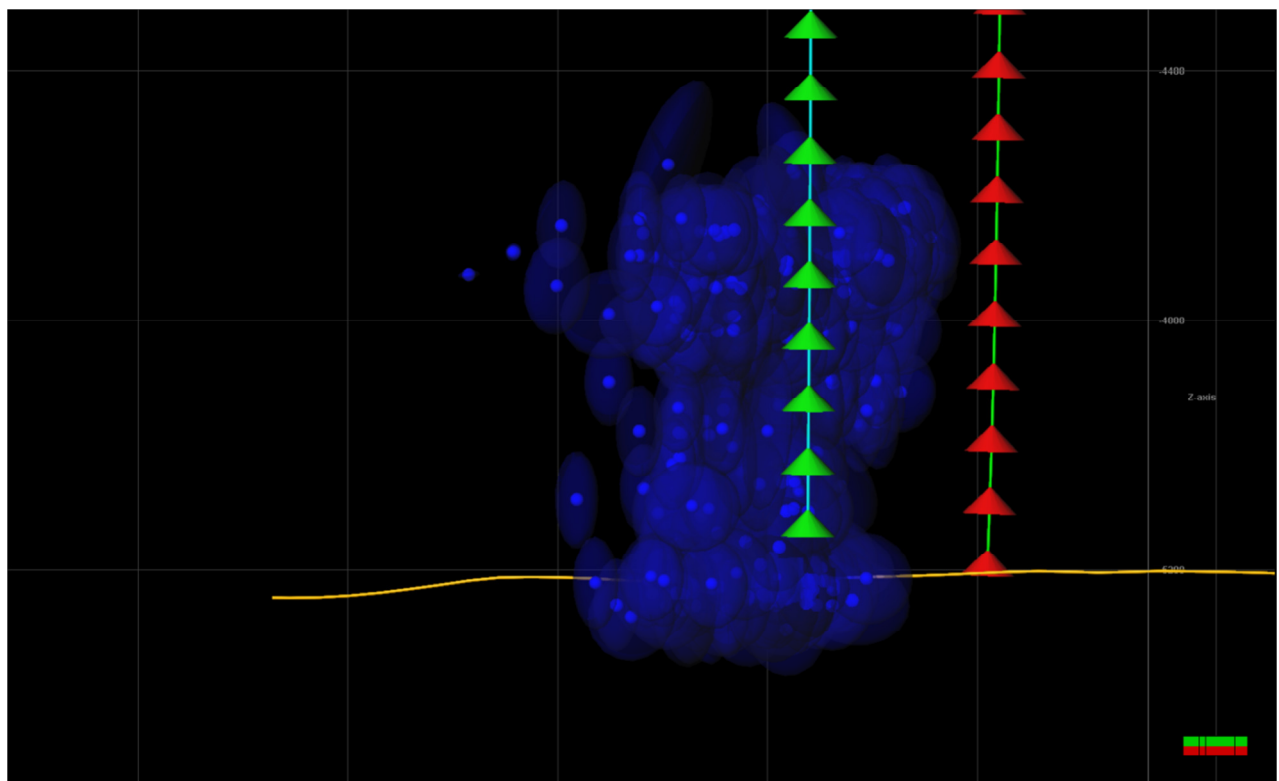


Figure 8.20 - Stage 04 event location uncertainty ellipsoids – side view

8.5 Stage 05

The Stage 05 treatment data and microseismic event rate are shown below. The microseismic events are color coded according to time as shown in the legend for each Figure 8.

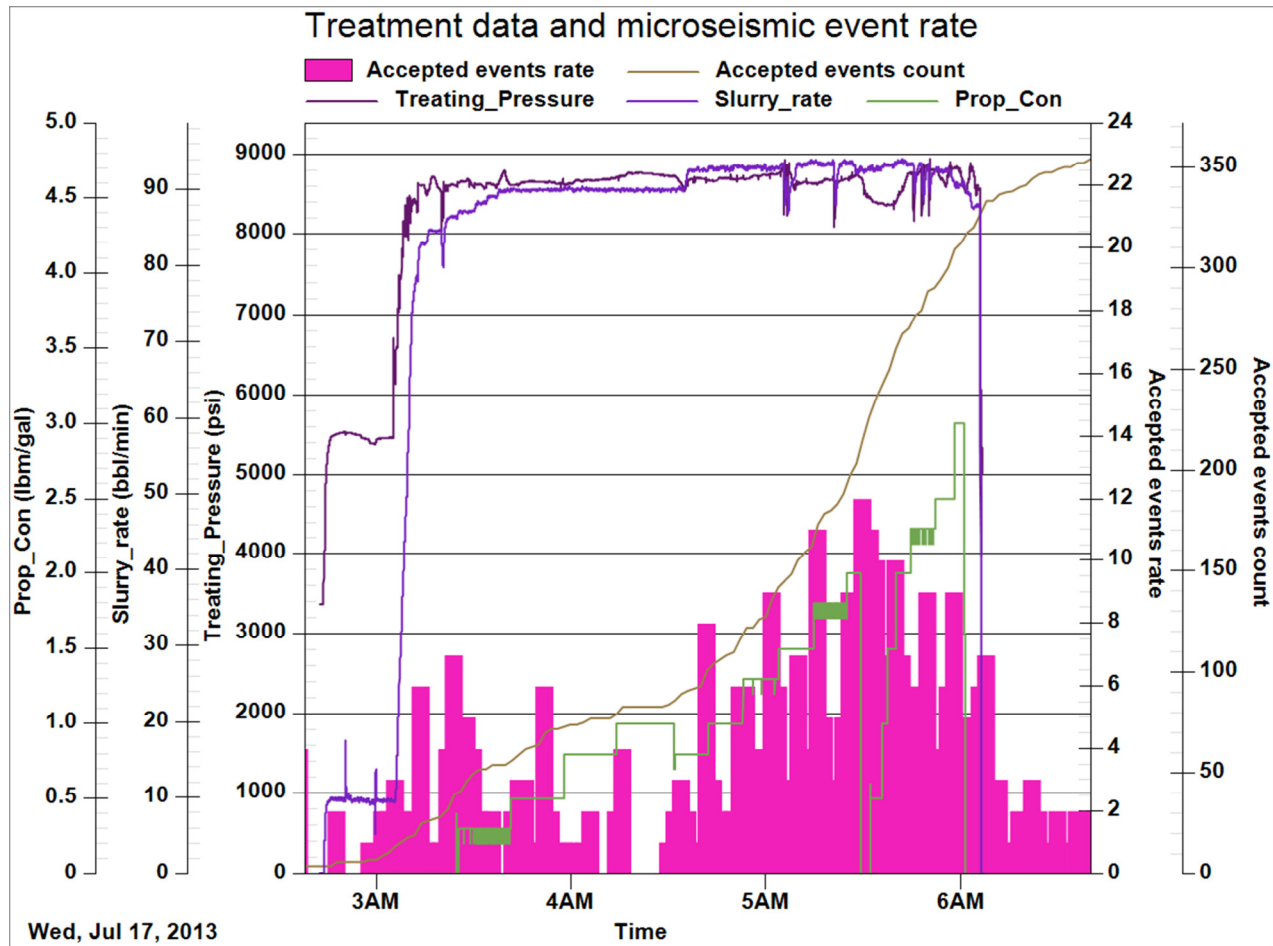


Figure 8.21 - Stage 05 treatment data and microseismic event rate

Table 8.13 - Stage 05 fracture treatment volumes

Description	Designed	Placed
Total fluids (gal)	607700	655788
Total proppants (lbm)	600500	Not used

Table 8.14 - Stage 05 treatment data summary

Description	Value
Average rate (bbl/min)	N/A
Average pressure (psi)	N/A
Pre-treatment ISIP (psi)	N/A
Post-treatment ISIP (psi)	N/A
Maximum PPA (lbm/gal)	N/A

Table 8.15 - Stage 05 microseismic event geometry

Description	Microseismic geometry
Fracture azimuth (deg)	70
MS length (ft)	1938
MS height (ft)	778
MS volume (ft3)	51840001.7

The microseismic data from Stage 05 is shown below in map and transverse views. The microseismic events are color coded according to time as shown on the plot legend. The microseismic dimensions are also shown.

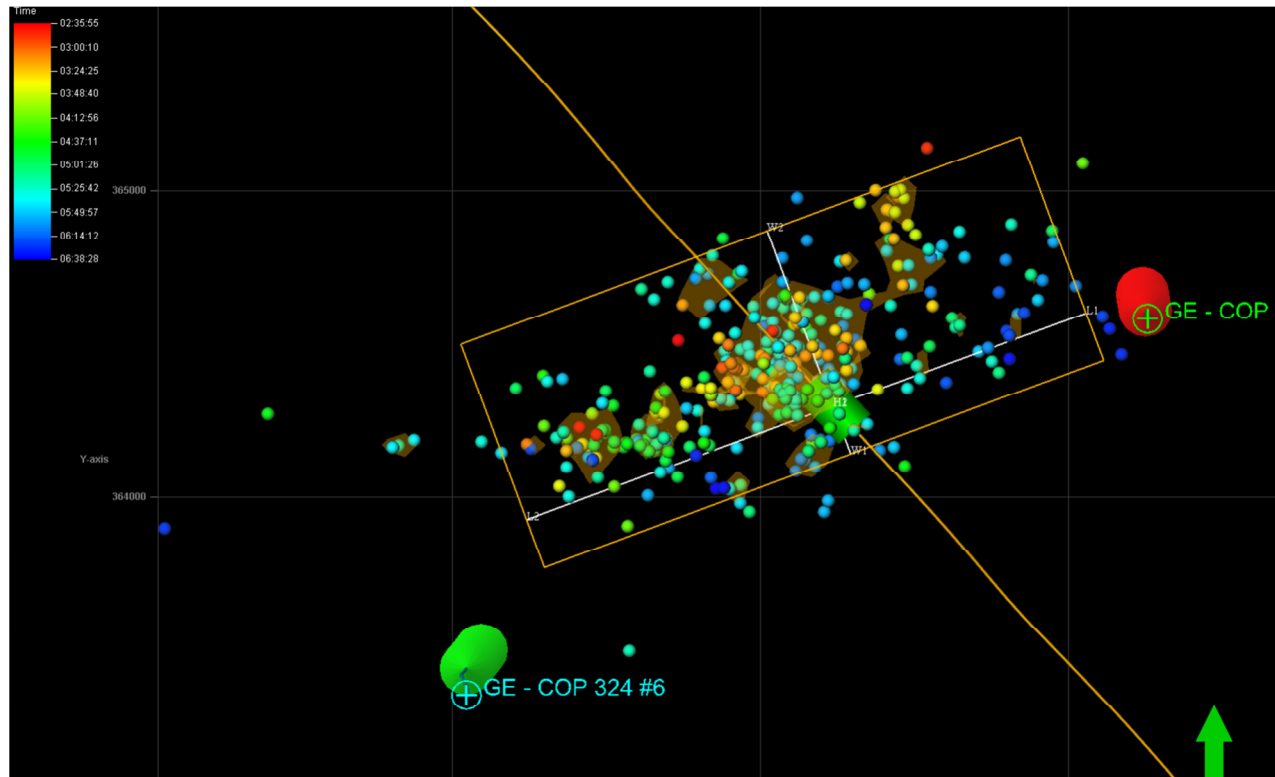


Figure 8.22 - Stage 05 map view (length and width)

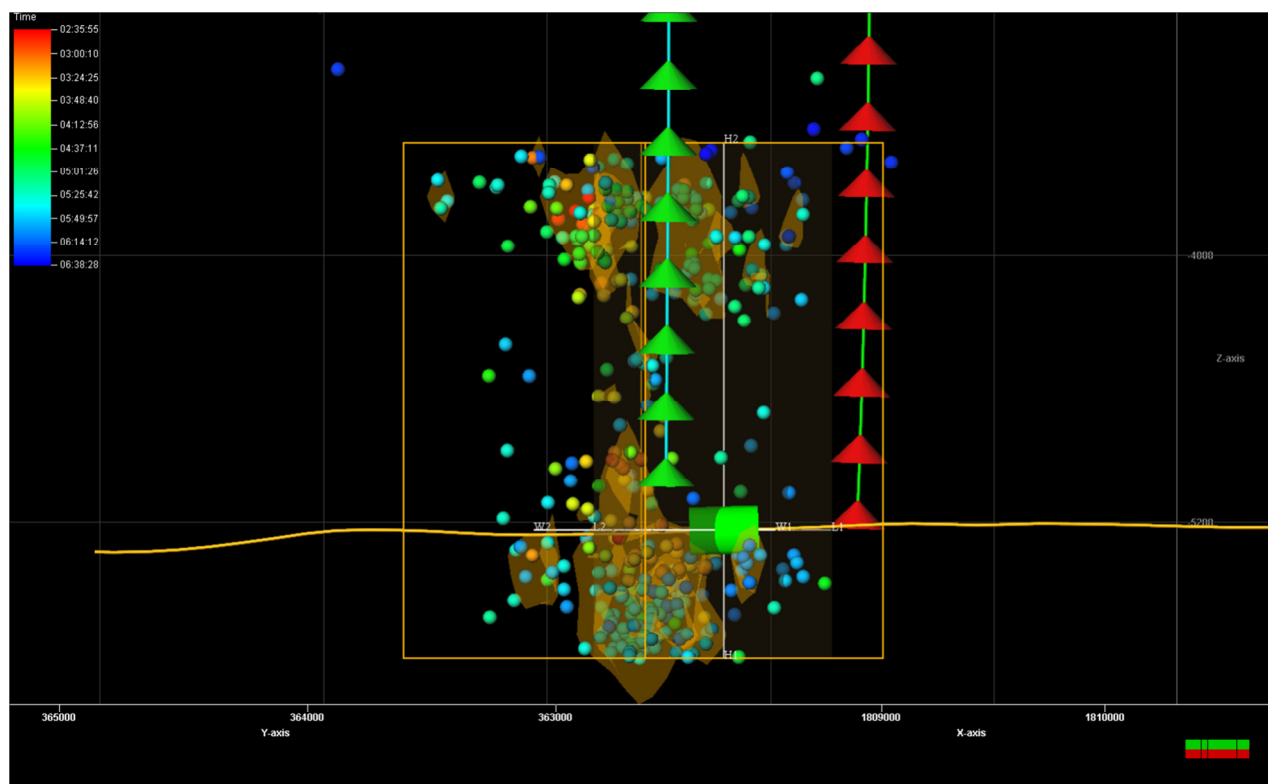


Figure 8.23 - Stage 05 transverse view (height and width)

The microseismic event location uncertainty ellipsoids for Stage 05 are shown below in map and transverse views.

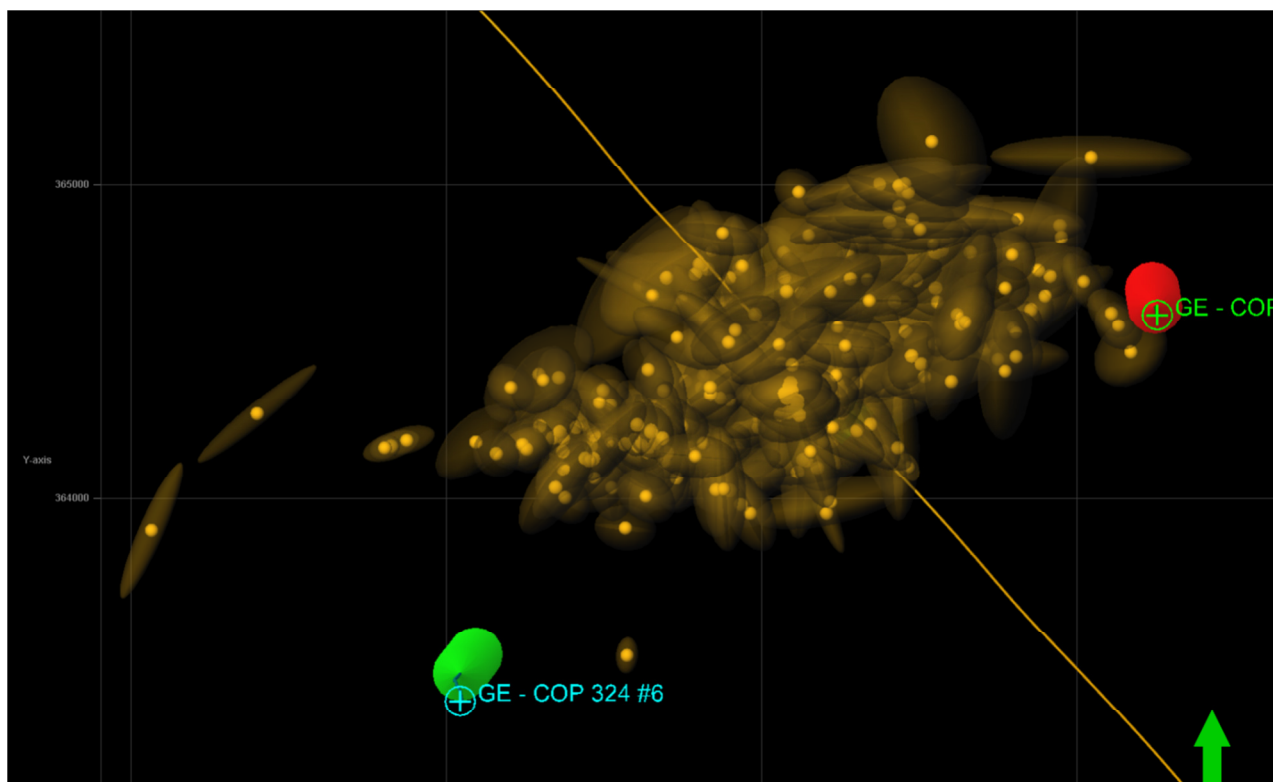


Figure 8.24 - Stage 05 event location uncertainty ellipsoids – map view

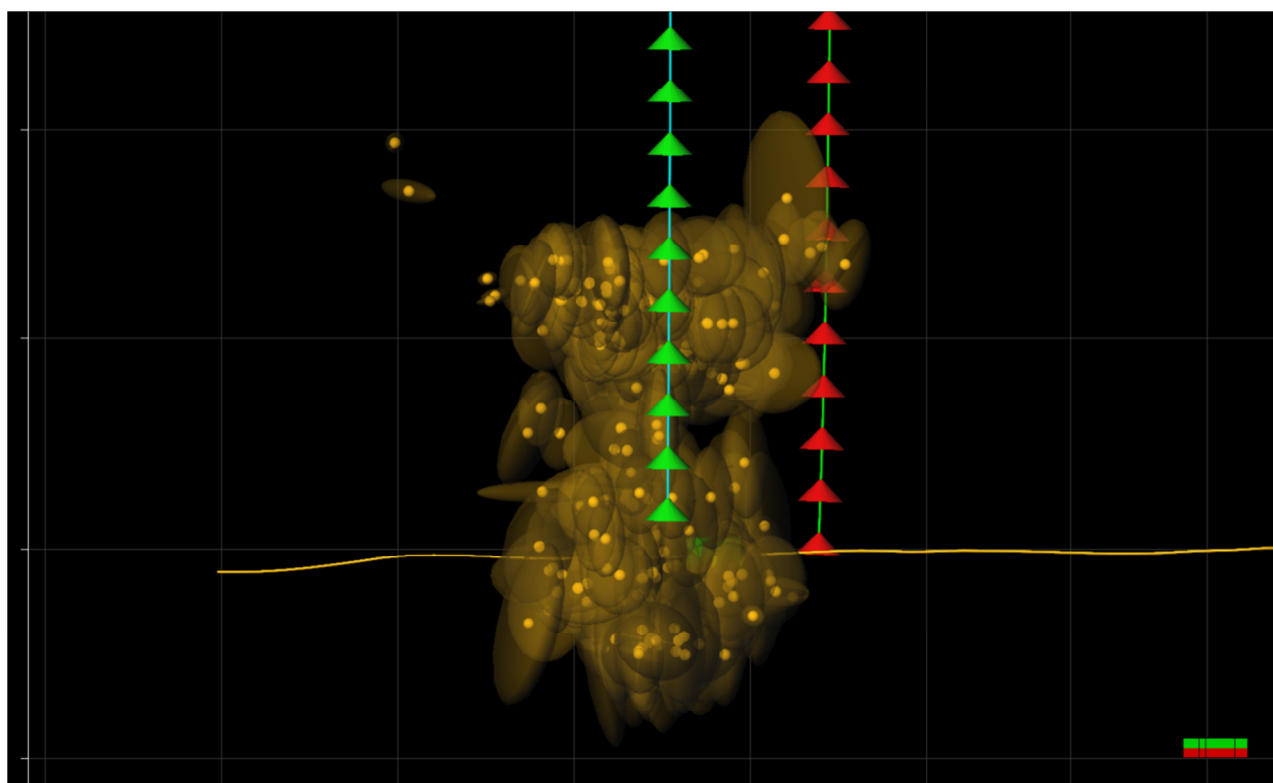


Figure 8.25 - Stage 05 event location uncertainty ellipsoids – side view

8.6 Stage 06

The Stage 06 treatment data and microseismic event rate are shown below. The microseismic events are color coded according to time as shown in the legend for each Figure 8.

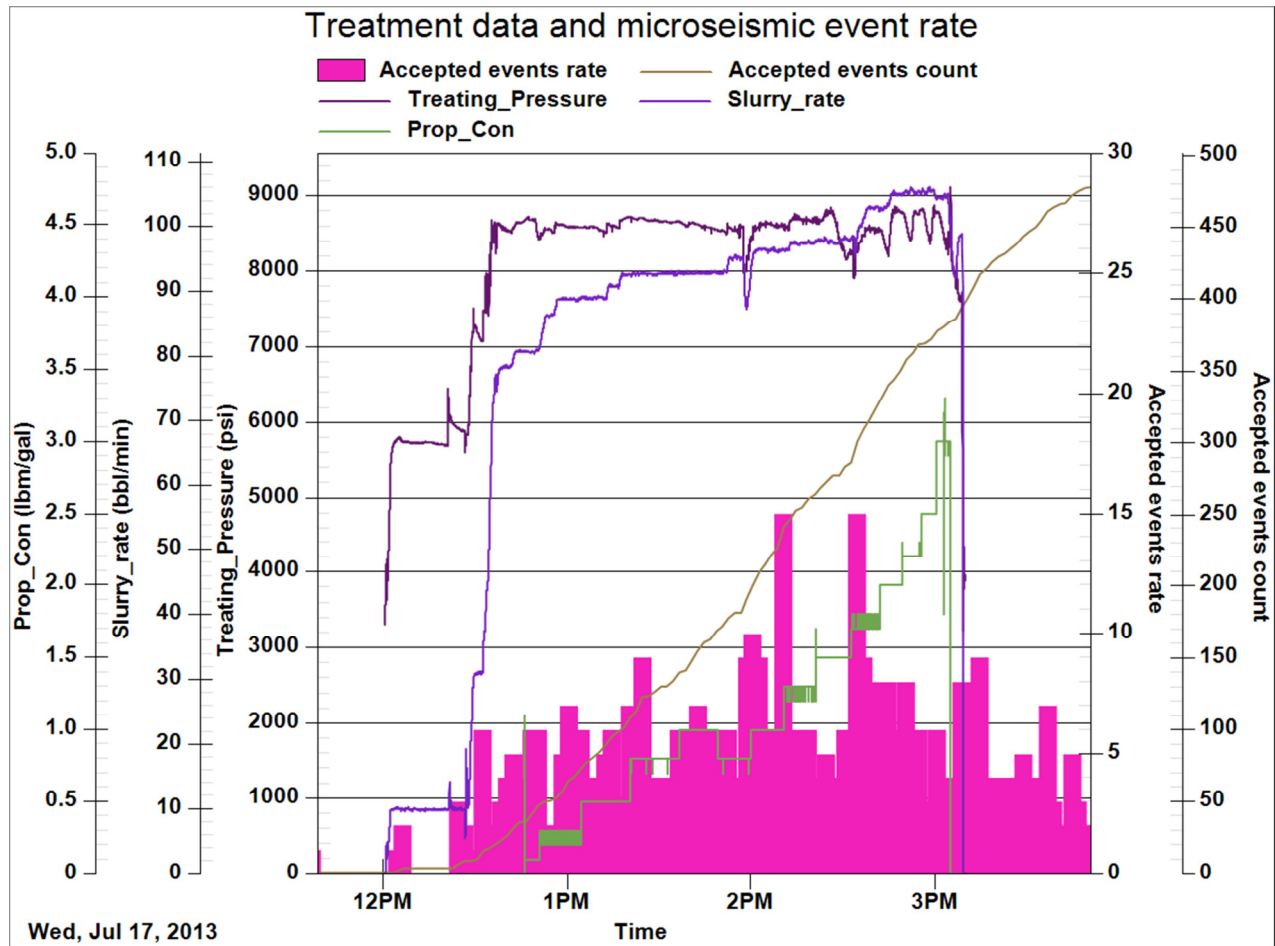


Figure 8.26 - Stage 06 treatment data and microseismic event rate

Table 8.16 - Stage 06 fracture treatment volumes

Description	Designed	Placed
Total fluids (gal)	607700	602448
Total proppants (lbm)	600500	Not used

Table 8.17 - Stage 06 treatment data summary

Description	Value
Average rate (bbl/min)	N/A
Average pressure (psi)	N/A
Pre-treatment ISIP (psi)	N/A
Post-treatment ISIP (psi)	N/A
Maximum PPA (lbm/gal)	N/A

Table 8.18 - Stage 06 microseismic event geometry

Description	Microseismic geometry
Fracture azimuth (deg)	70
MS length (ft)	1651
MS height (ft)	835
MS volume (ft3)	58104002.5

The microseismic data from Stage 06 is shown below in map and transverse views. The microseismic events are color coded according to time as shown on the plot legend. The microseismic dimensions are also shown.

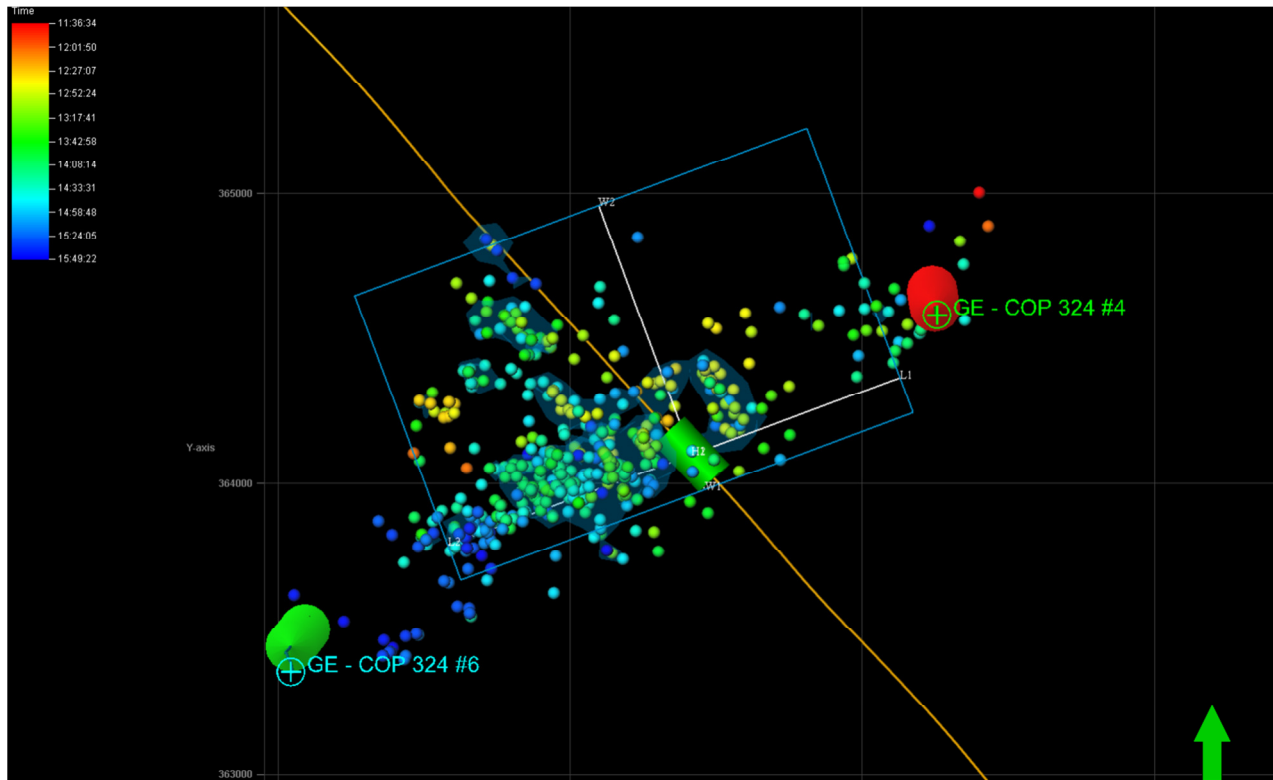


Figure 8.27 - Stage 06 map view (length and width)

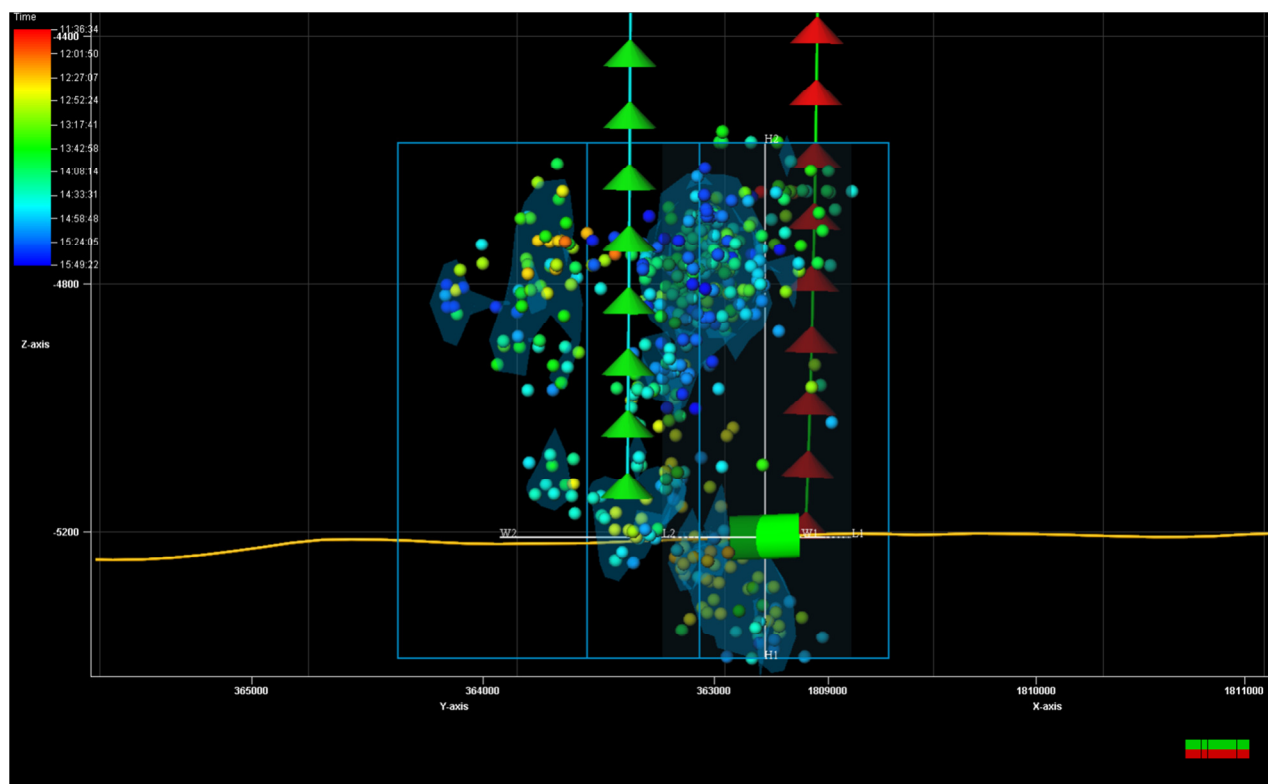


Figure 8.28 - Stage 06 transverse view (height and width)

The microseismic event location uncertainty ellipsoids for Stage 06 are shown below in map and transverse views.

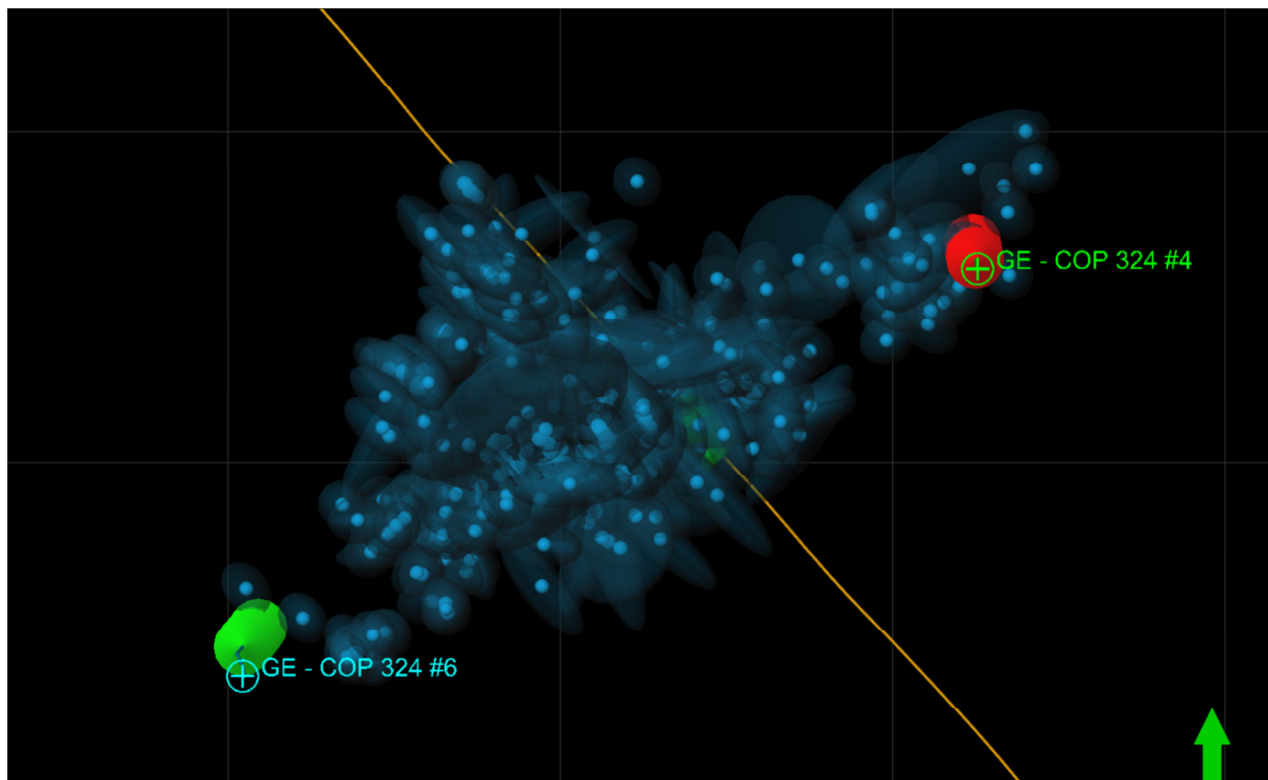


Figure 8.29 - Stage 06 event location uncertainty ellipsoids – map view

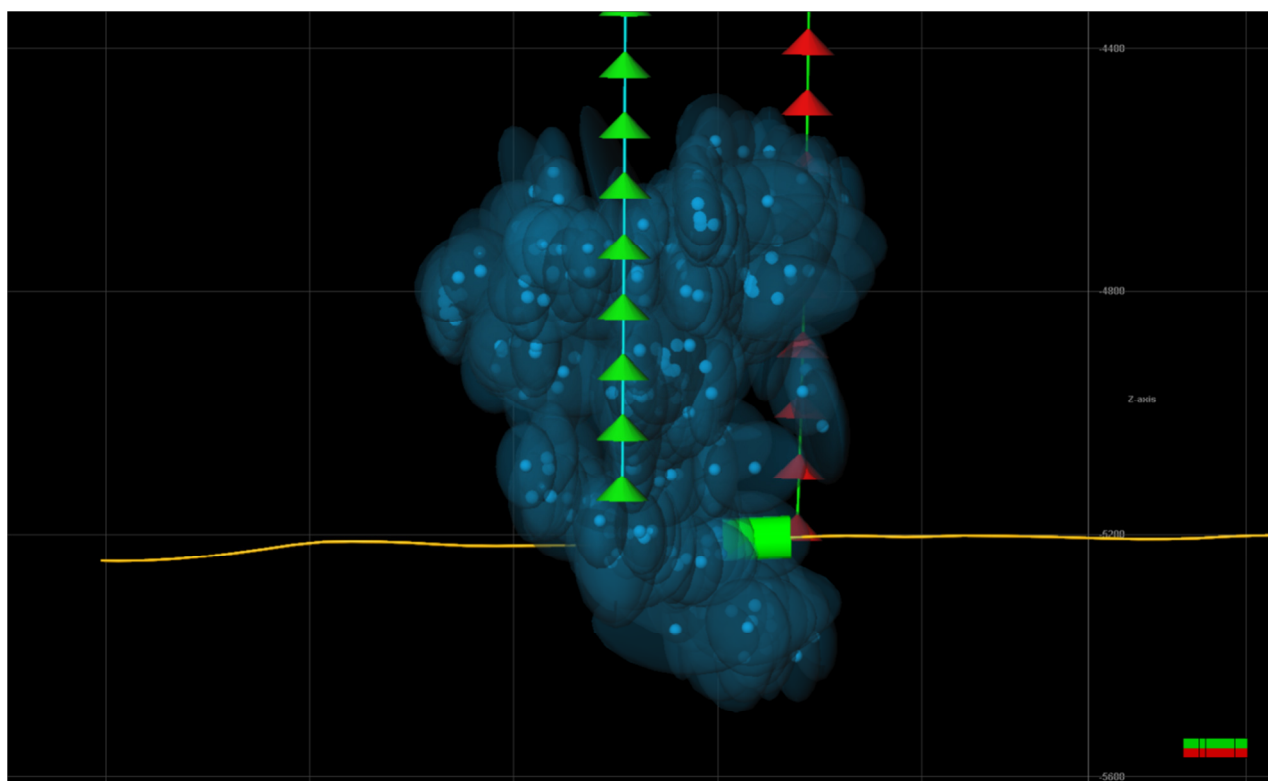


Figure 8.30 - Stage 06 event location uncertainty ellipsoids – side view

8.7 Stage 07

The Stage 07 treatment data and microseismic event rate are shown below. The microseismic events are color coded according to time as shown in the legend for each Figure 8.

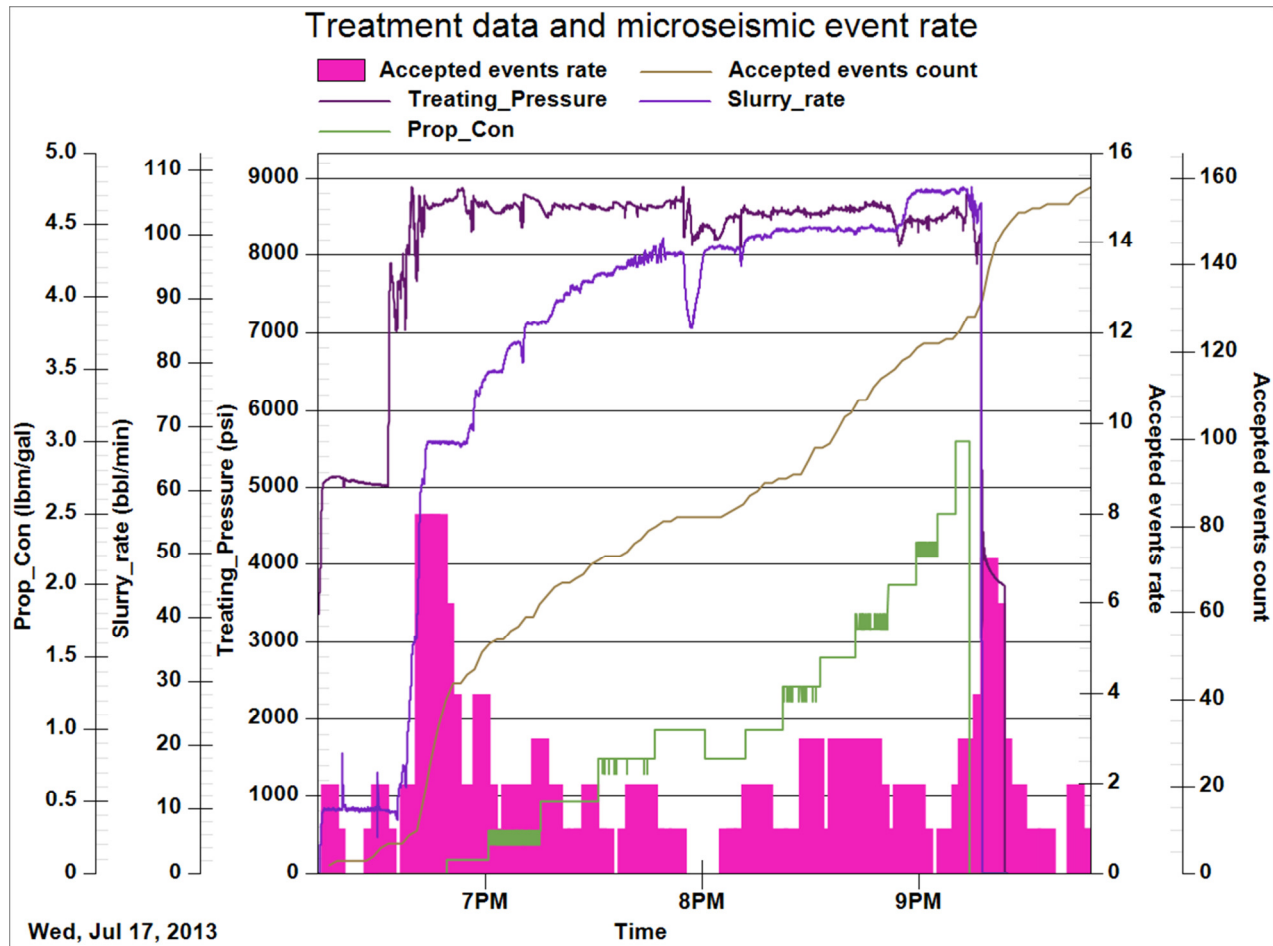


Figure 8.31 - Stage 07 treatment data and microseismic event rate

Table 8.19 - Stage 07 fracture treatment volumes

Description	Designed	Placed
Total fluids (gal)	607700	598374
Total proppants (lbm)	600500	Not used

Table 8.20 - Stage 07 treatment data summary

Description	Value
Average rate (bbl/min)	N/A
Average pressure (psi)	N/A
Pre-treatment ISIP (psi)	N/A
Post-treatment ISIP (psi)	N/A
Maximum PPA (lbm/gal)	N/A

Table 8.21 - Stage 07 microseismic event geometry

Description	Microseismic geometry
Fracture azimuth (deg)	75
MS length (ft)	1799
MS height (ft)	757
MS volume (ft3)	15768000.9

The microseismic data from Stage 07 is shown below in map and transverse views. The microseismic events are color coded according to time as shown on the plot legend. The microseismic dimensions are also shown.

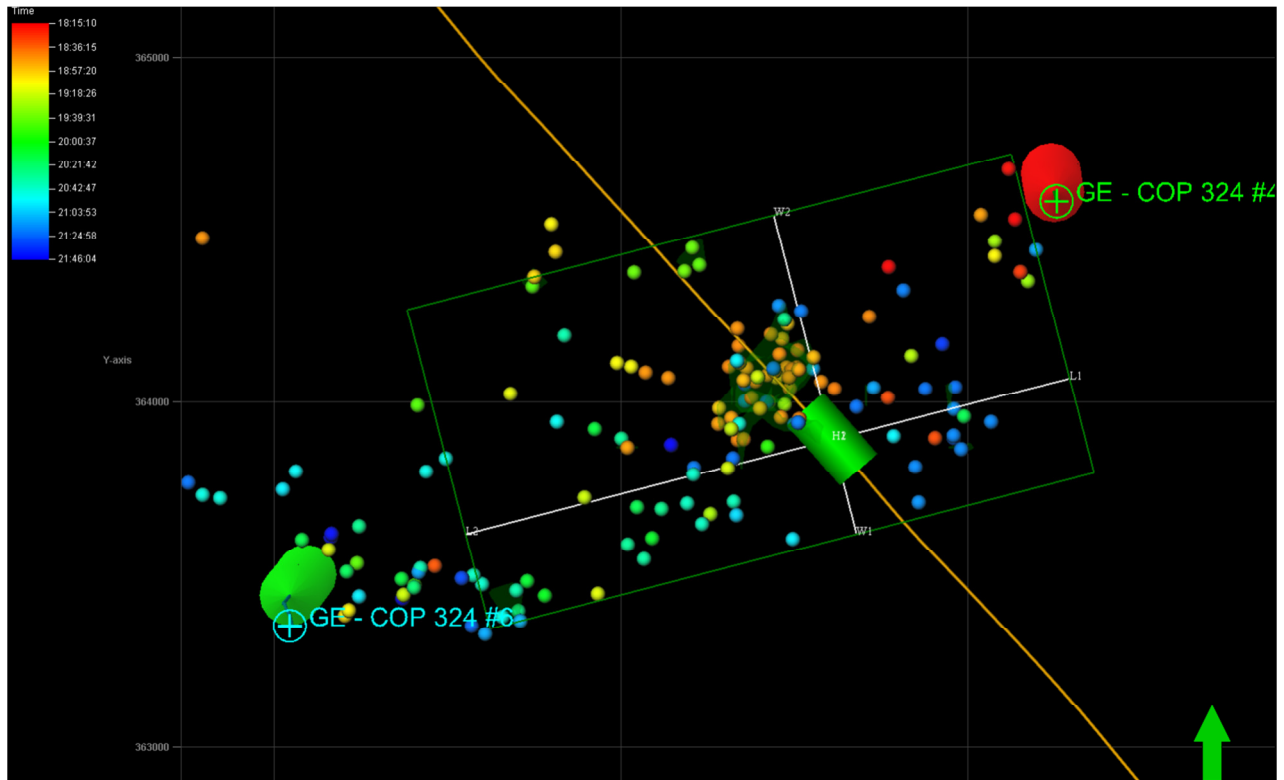


Figure 8.32 - Stage 07 map view (length and width)

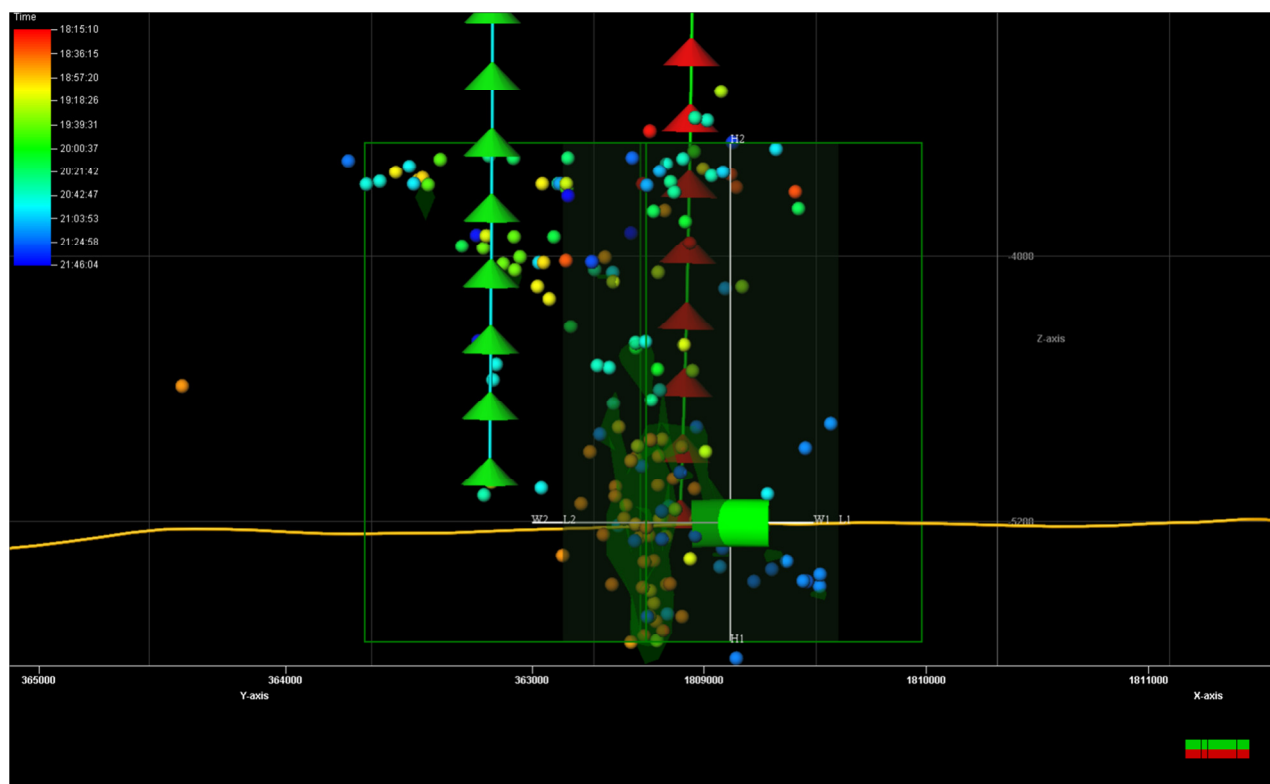


Figure 8.33 - Stage 07 transverse view (height and width)

The microseismic event location uncertainty ellipsoids for Stage 07 are shown below in map and transverse views.

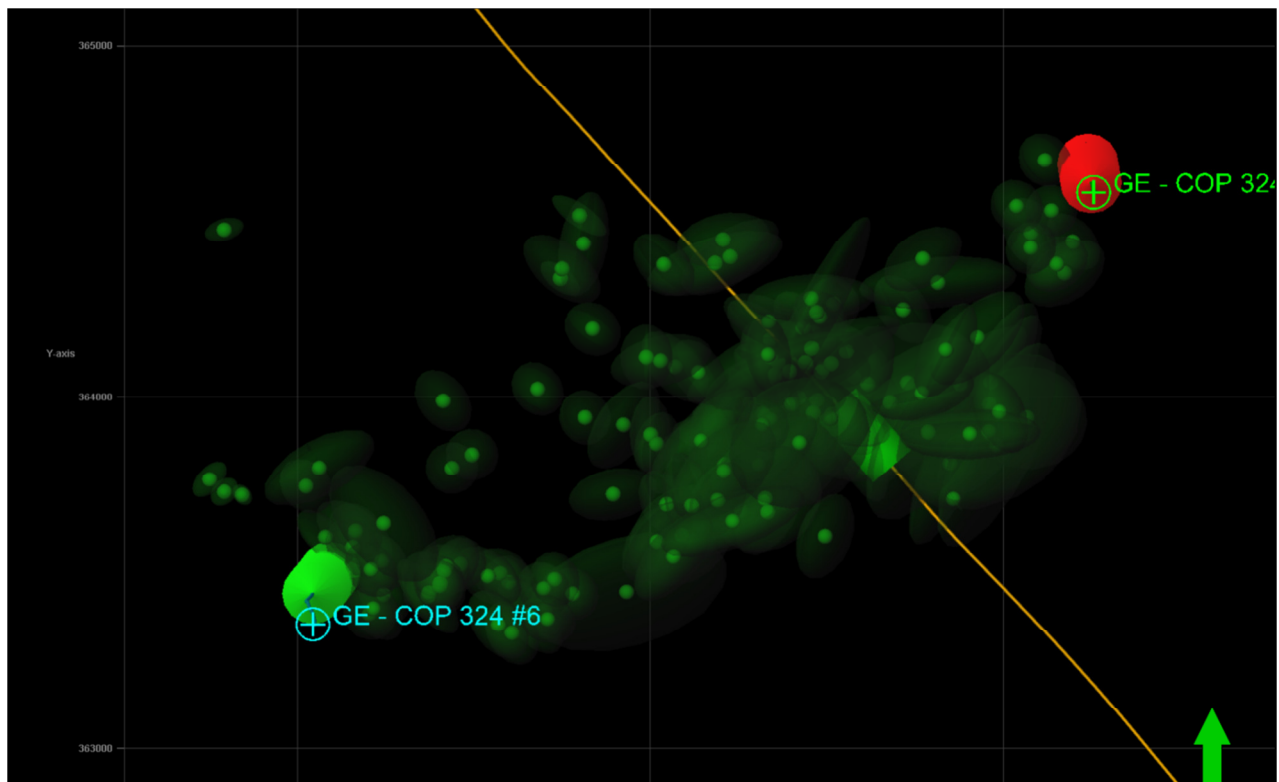


Figure 8.34 - Stage 07 event location uncertainty ellipsoids – map view

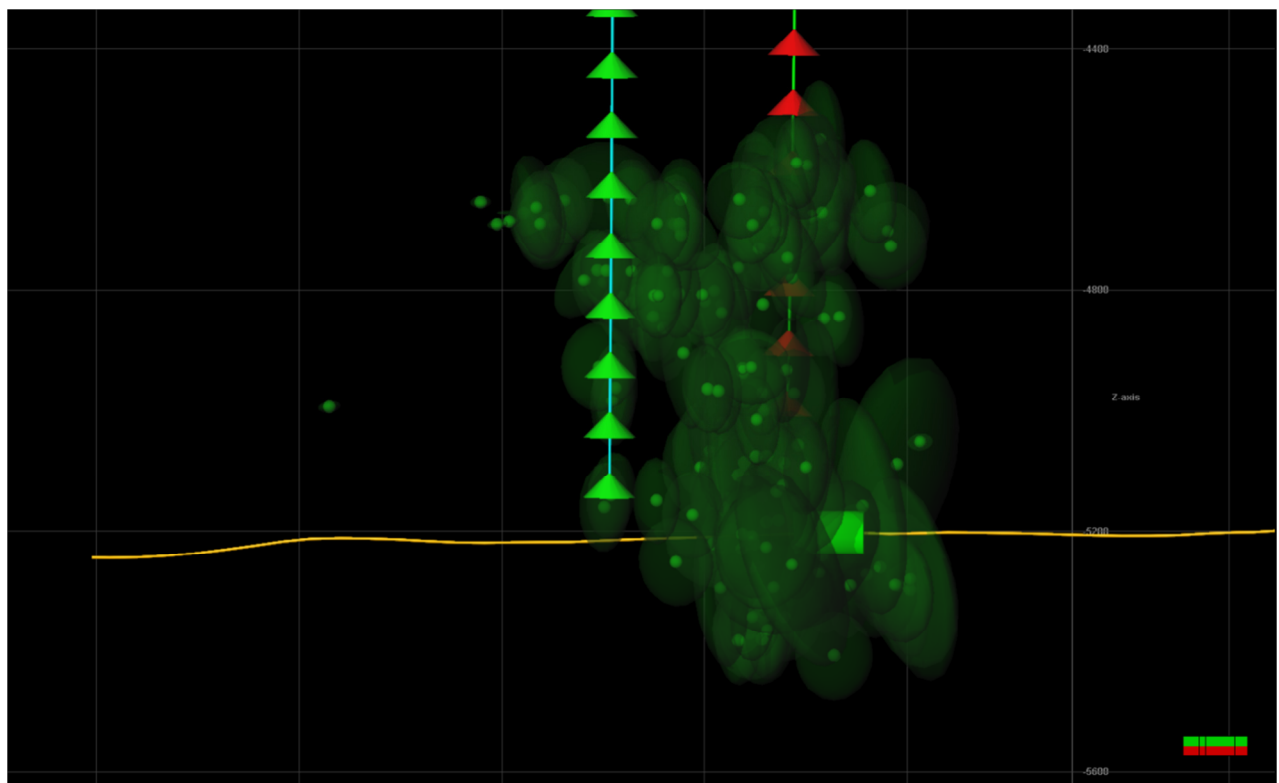


Figure 8.35 - Stage 07 event location uncertainty ellipsoids – side view

8.8 Stage 08

The Stage 08 treatment data and microseismic event rate are shown below. The microseismic events are color coded according to time as shown in the legend for each Figure 8.

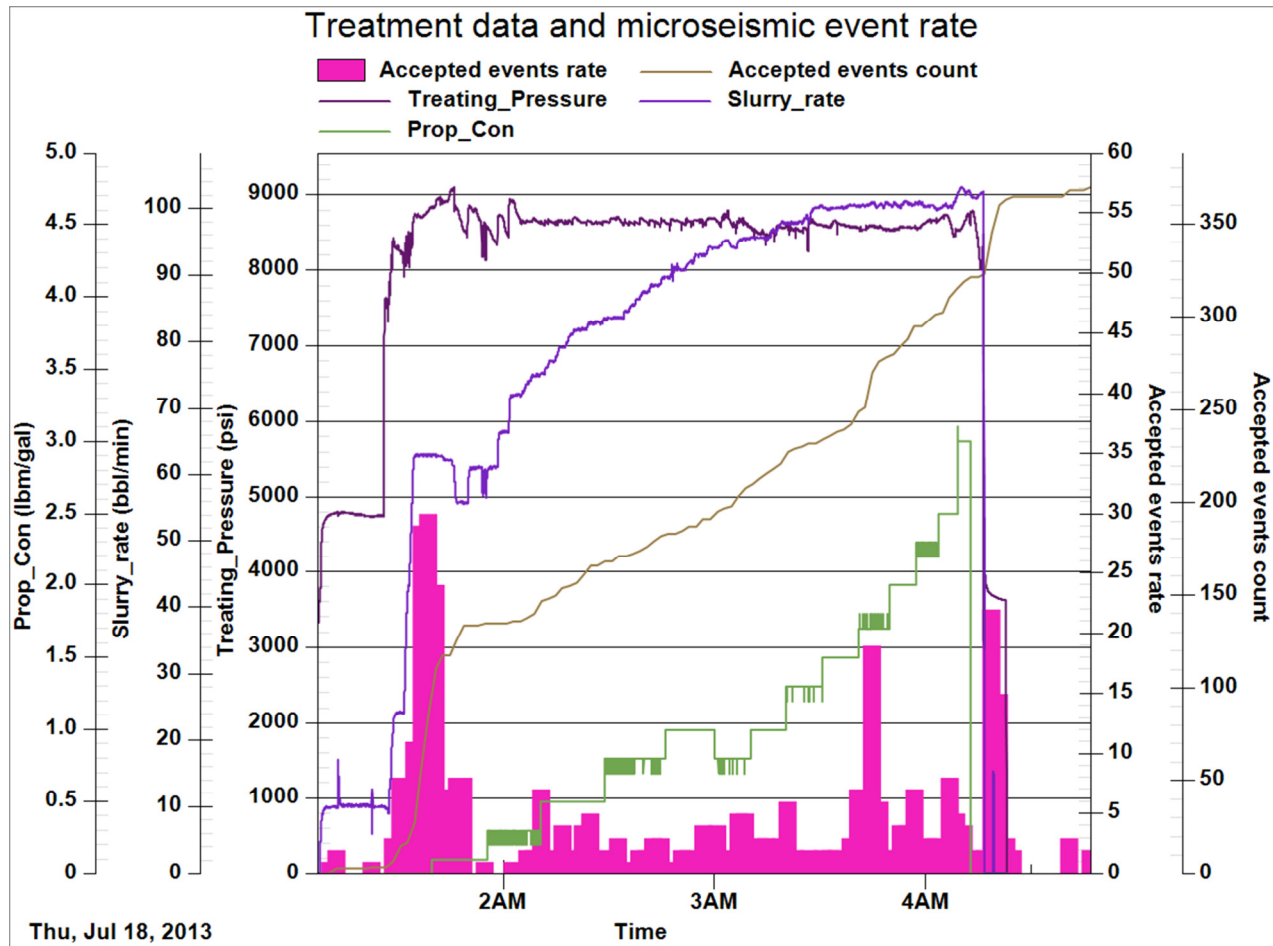


Figure 8.36 - Stage 08 treatment data and microseismic event rate

Table 8.22 - Stage 08 fracture treatment volumes

Description	Designed	Placed
Total fluids (gal)	607700	584094
Total proppants (lbm)	600500	Not used

Table 8.23 - Stage 08 treatment data summary

Description	Value
Average rate (bbl/min)	N/A
Average pressure (psi)	N/A
Pre-treatment ISIP (psi)	N/A
Post-treatment ISIP (psi)	N/A
Maximum PPA (lbm/gal)	N/A

Table 8.24 - Stage 08 microseismic event geometry

Description	Microseismic geometry
Fracture azimuth (deg)	70
MS length (ft)	2542
MS height (ft)	752
MS volume (ft3)	58104002.5

The microseismic data from Stage 08 is shown below in map and transverse views. The microseismic events are color coded according to time as shown on the plot legend. The microseismic dimensions are also shown.

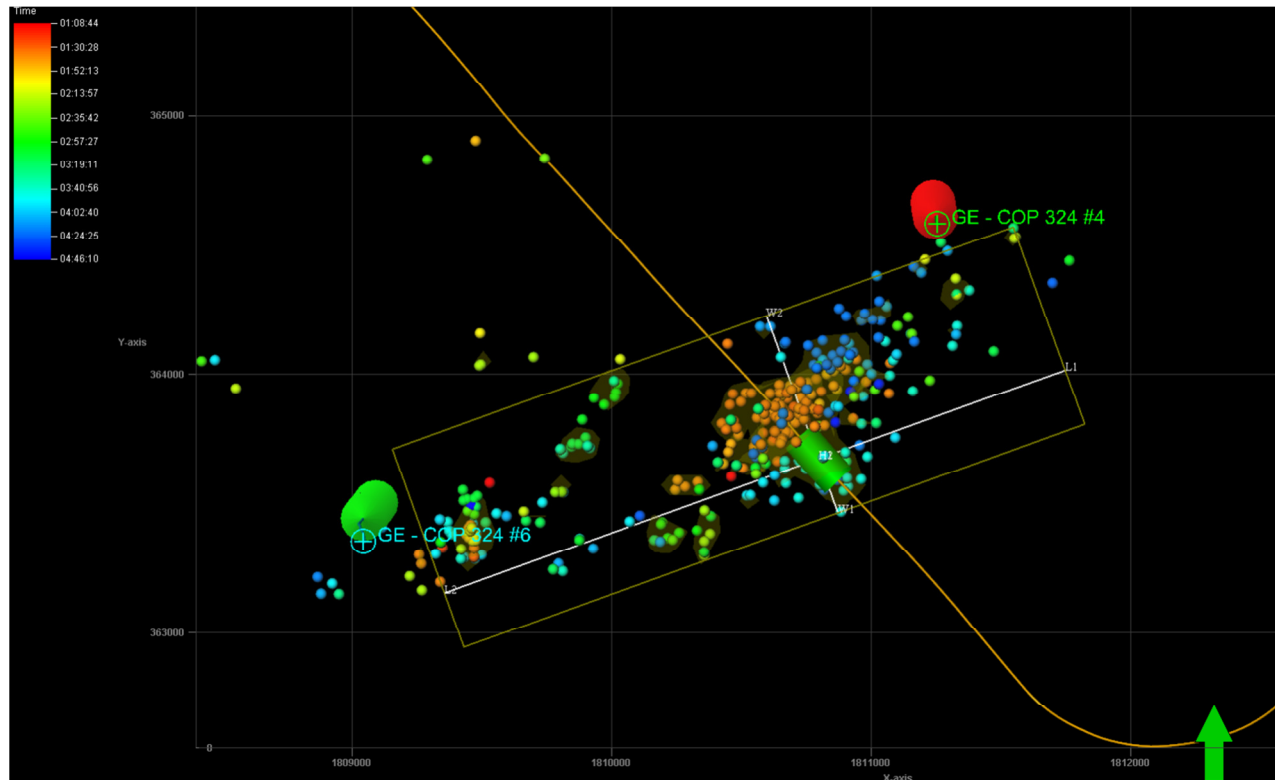


Figure 8.37 - Stage 08 map view (length and width)

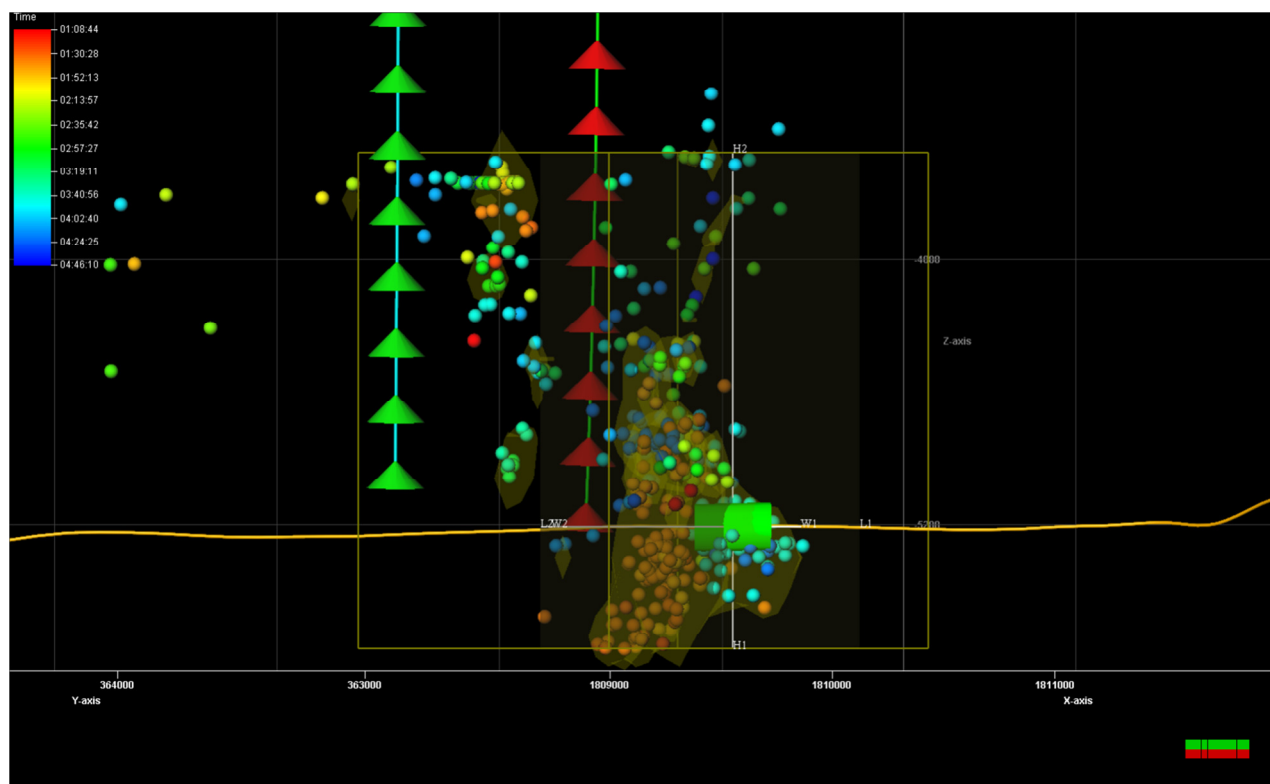


Figure 8.38 - Stage 08 transverse view (height and width)

The microseismic event location uncertainty ellipsoids for Stage 08 are shown below in map and transverse views.

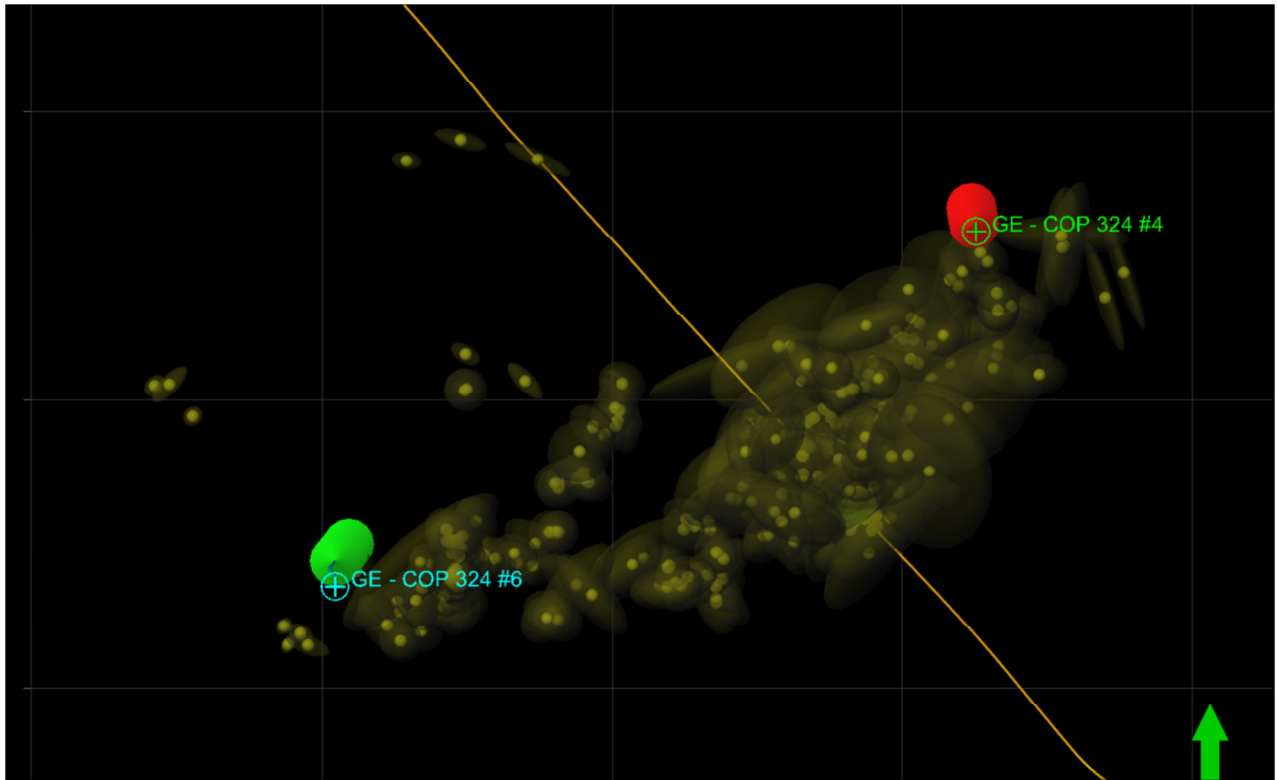


Figure 8.39 - Stage 08 event location uncertainty ellipsoids – map view

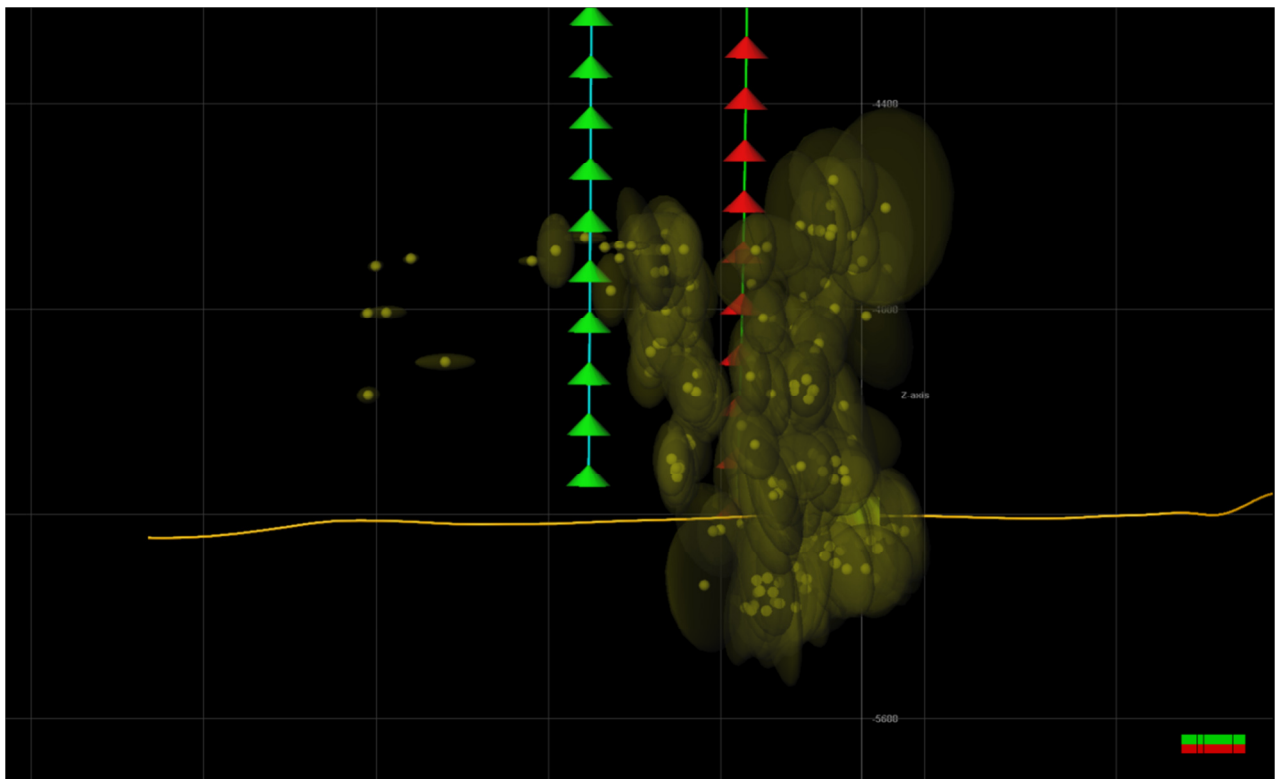


Figure 8.40 - Stage 08 event location uncertainty ellipsoids – side view

8.9 Stage 09

The Stage 09 treatment data and microseismic event rate are shown below. The microseismic events are color coded according to time as shown in the legend for each Figure 8.

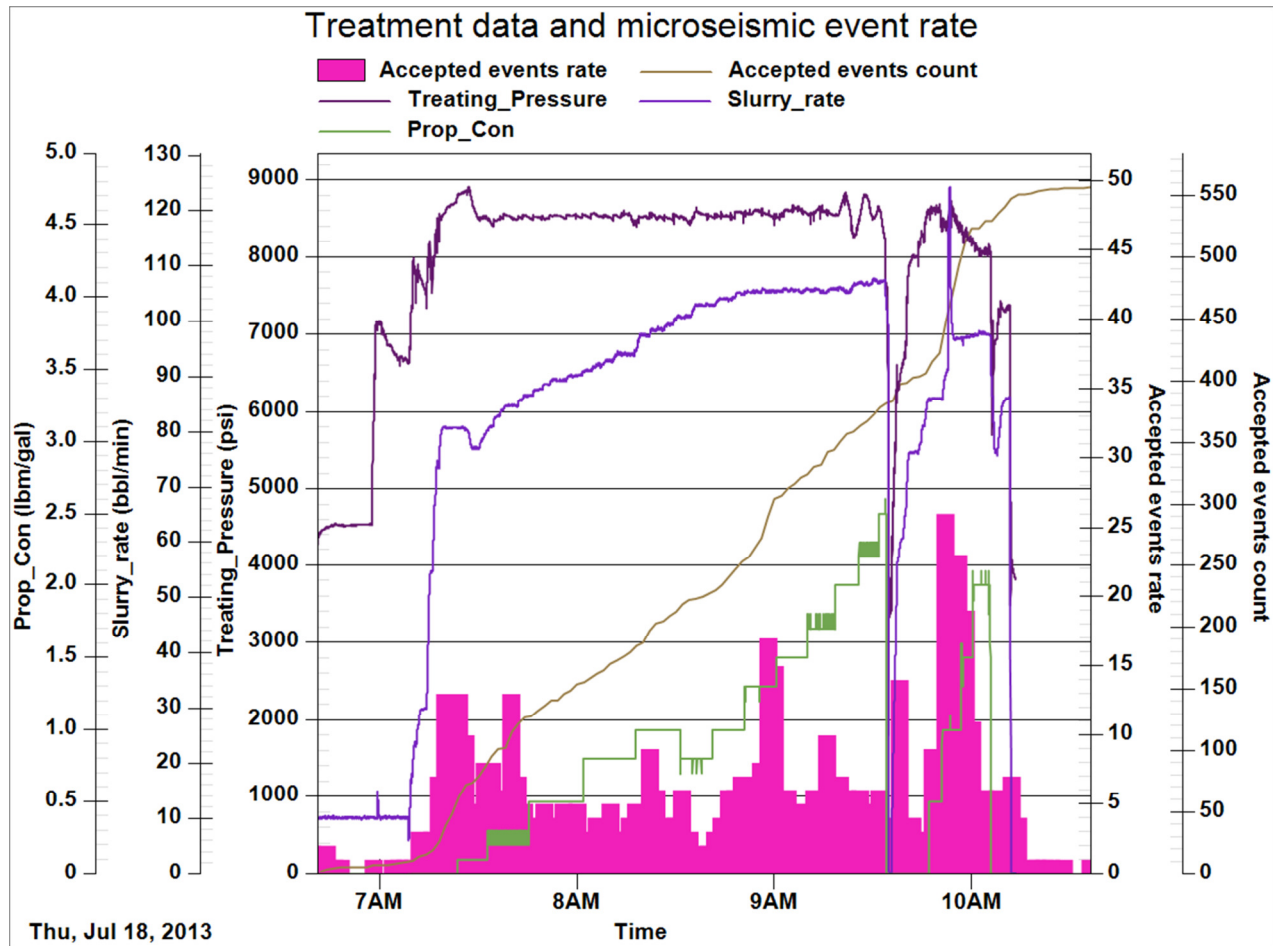


Figure 8.41 - Stage 09 treatment data and microseismic event rate

Table 8.25 - Stage 09 fracture treatment volumes

Description	Designed	Placed
Total fluids (gal)	607700	680568
Total proppants (lbm)	600500	Not used

Table 8.26 - Stage 09 treatment data summary

Description	Value
Average rate (bbl/min)	N/A
Average pressure (psi)	N/A
Pre-treatment ISIP (psi)	N/A
Post-treatment ISIP (psi)	N/A
Maximum PPA (lbm/gal)	N/A

Table 8.27 - Stage 09 microseismic event geometry

Description	Microseismic geometry
Fracture azimuth (deg)	72
MS length (ft)	1590
MS height (ft)	544
MS volume (ft3)	70847997.4

The microseismic data from Stage 09 is shown below in map and transverse views. The microseismic events are color coded according to time as shown on the plot legend. The microseismic dimensions are also shown.

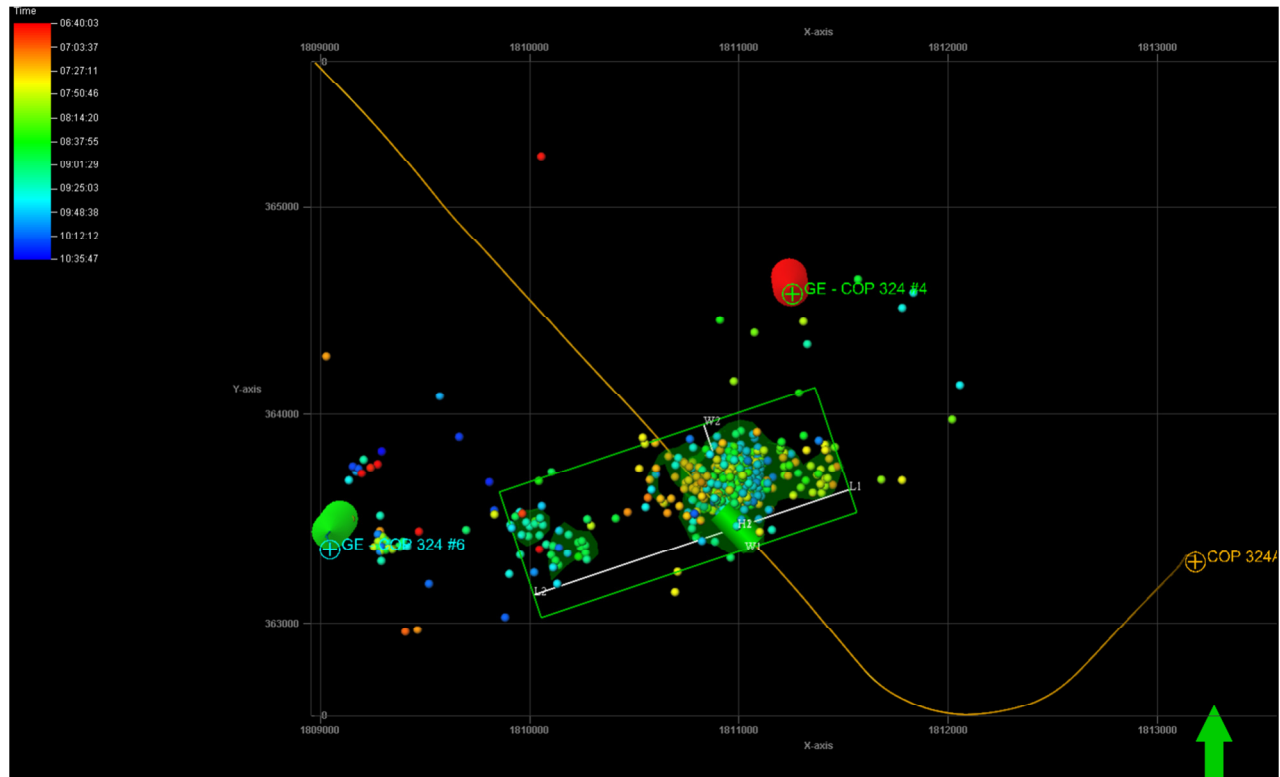


Figure 8.42 - Stage 09 map view (length and width)

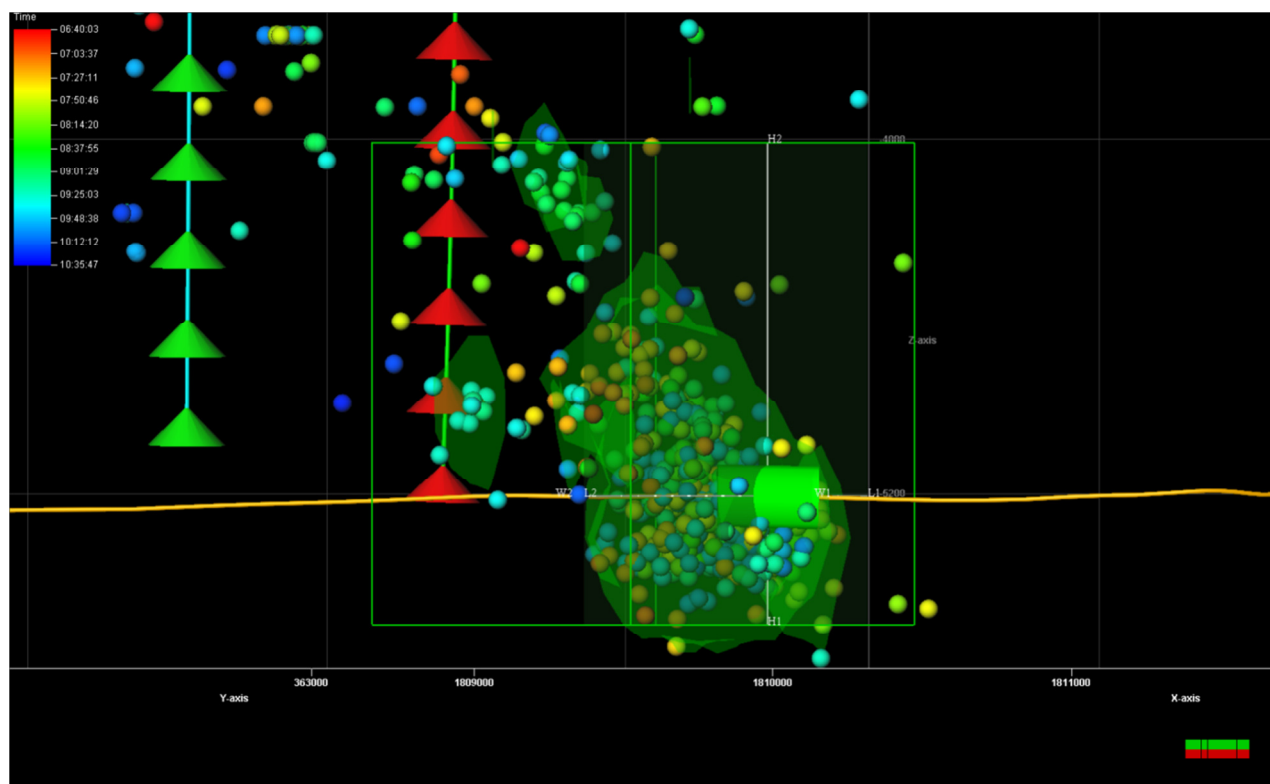


Figure 8.43 - Stage 09 transverse view (height and width)

The microseismic event location uncertainty ellipsoids for Stage 09 are shown below in map and transverse views.

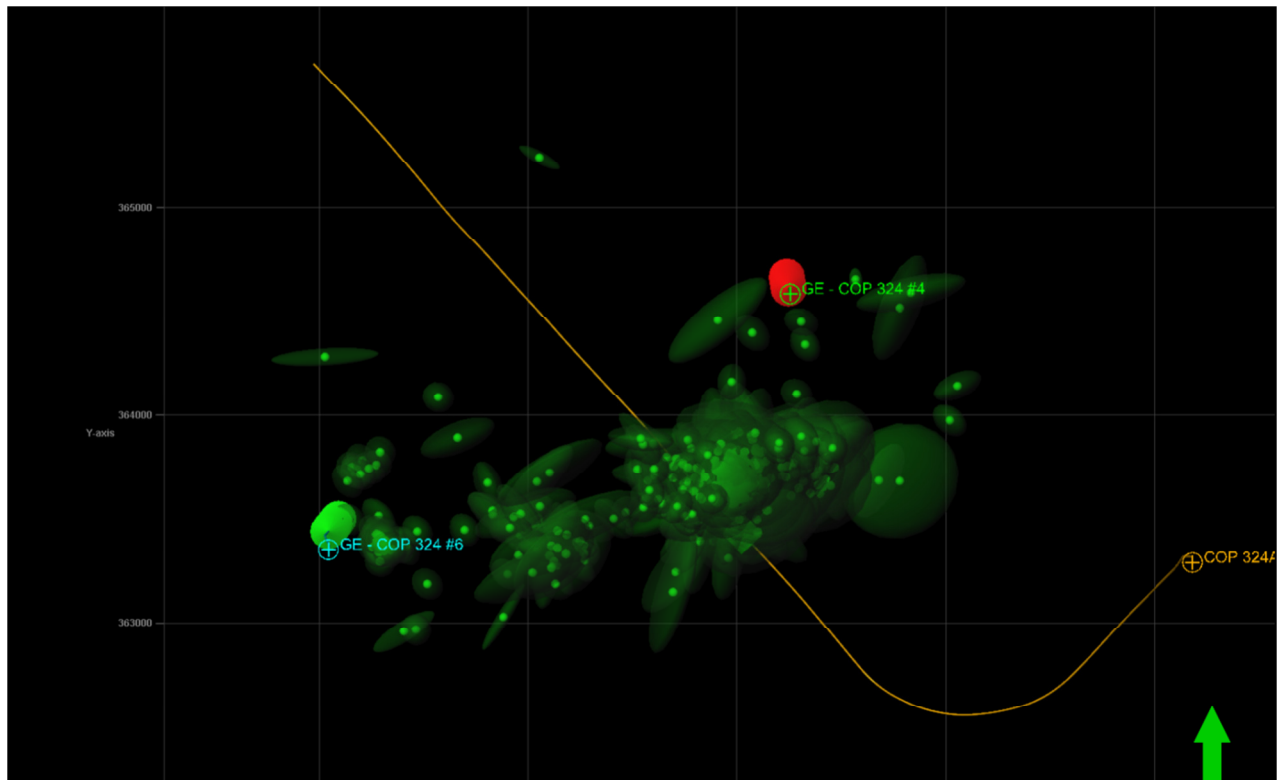


Figure 8.44 - Stage 09 event location uncertainty ellipsoids – map view

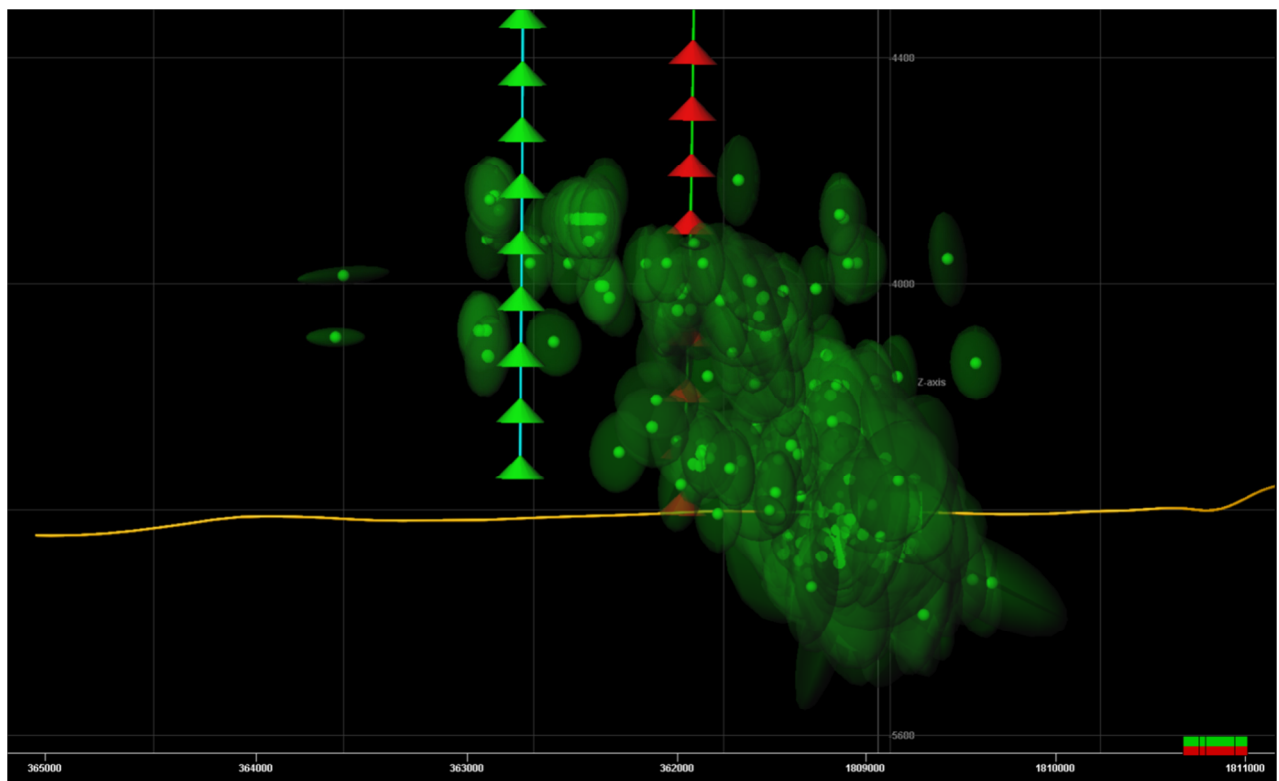


Figure 8.45 - Stage 09 event location uncertainty ellipsoids – side view

8.10 Stage 10

The Stage 10 treatment data and microseismic event rate are shown below. The microseismic events are color coded according to time as shown in the legend for each Figure 8.

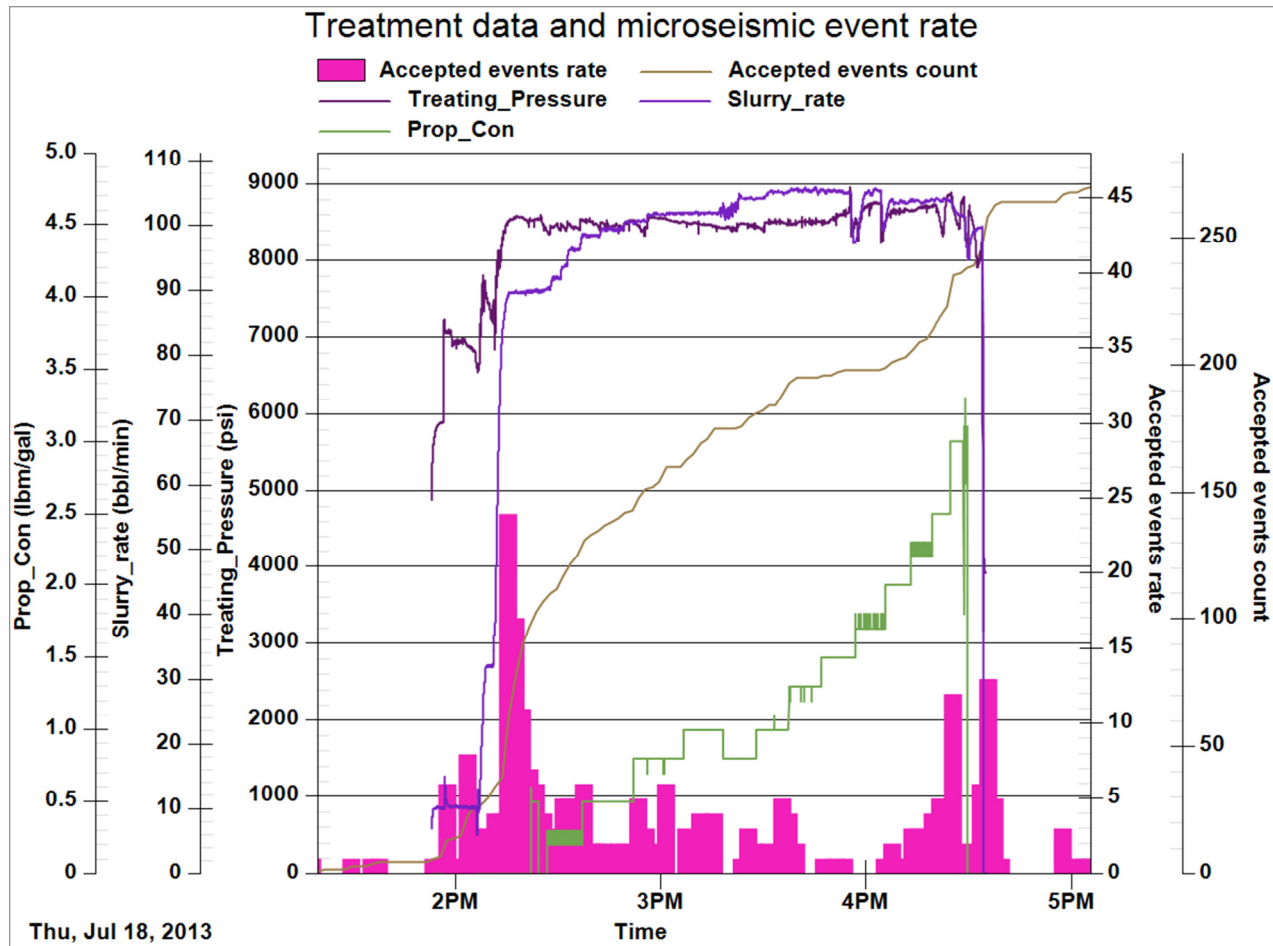


Figure 8.46 - Stage 10 treatment data and microseismic event rate

Table 8.28 - Stage 10 fracture treatment volumes

Description	Designed	Placed
Total fluids (gal)	607700	585144
Total proppants (lbm)	600500	Not used

Table 8.29 - Stage 10 treatment data summary

Description	Value
Average rate (bbl/min)	N/A
Average pressure (psi)	N/A
Pre-treatment ISIP (psi)	N/A
Post-treatment ISIP (psi)	N/A
Maximum PPA (lbm/gal)	N/A

Table 8.30 - Stage 10 microseismic event geometry

Description	Microseismic geometry
Fracture azimuth (deg)	76
MS length (ft)	1973
MS height (ft)	680
MS volume (ft3)	47951998.1

The microseismic data from Stage 10 is shown below in map and transverse views. The microseismic events are color coded according to time as shown on the plot legend. The microseismic dimensions are also shown.

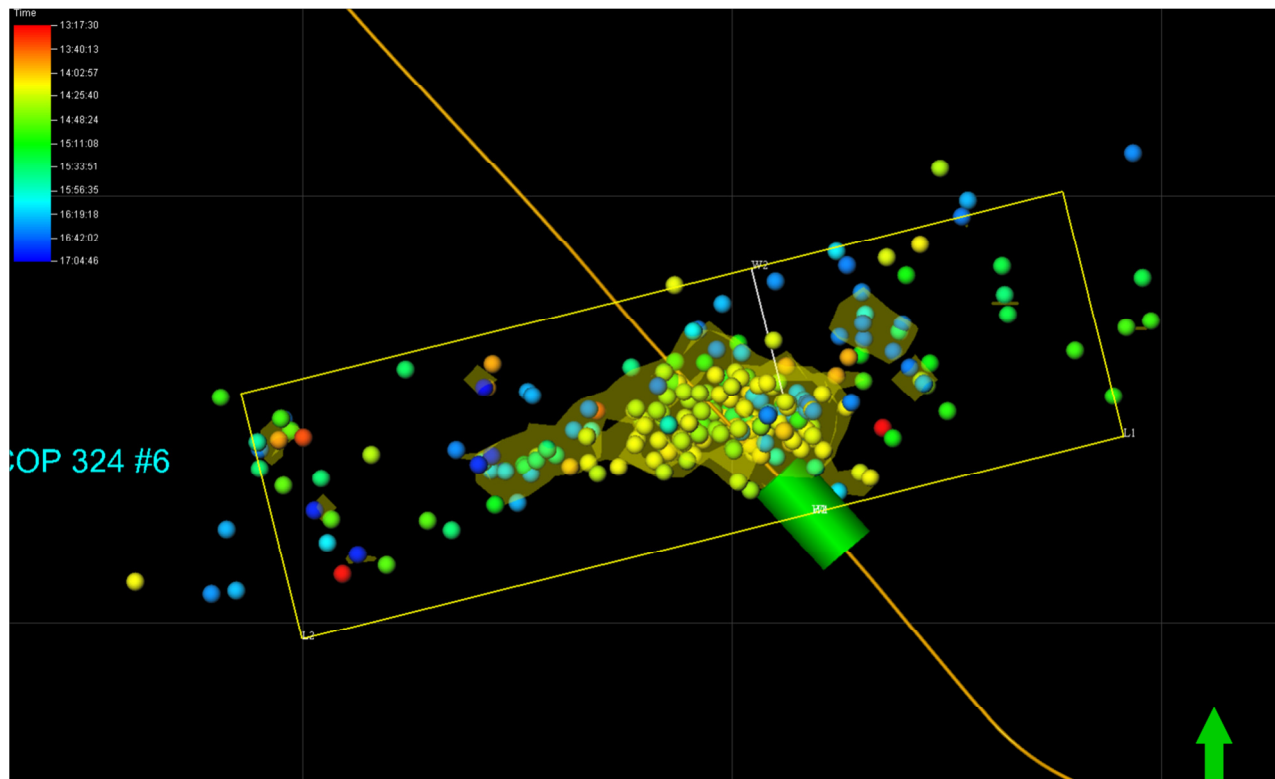


Figure 8.47 - Stage 10 map view (length and width)

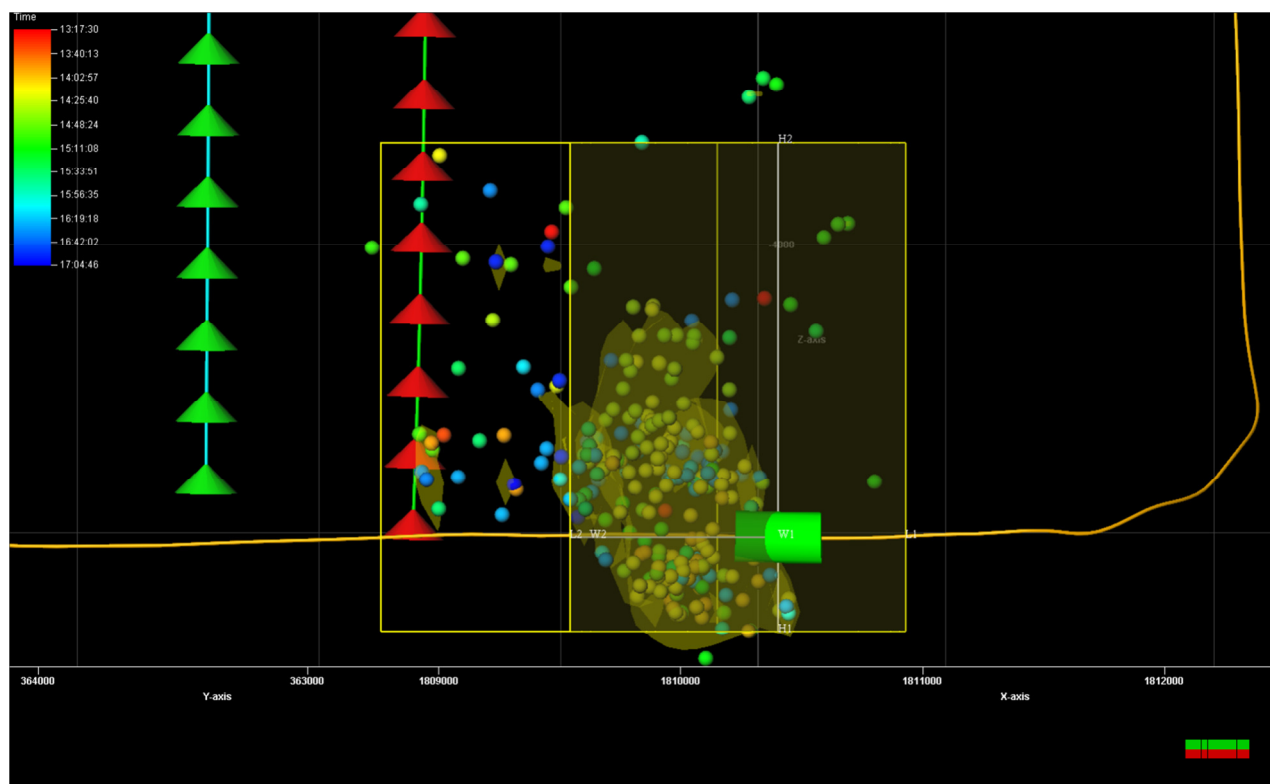


Figure 8.48 - Stage 10 transverse view (height and width)

The microseismic event location uncertainty ellipsoids for Stage 10 are shown below in map and transverse views.

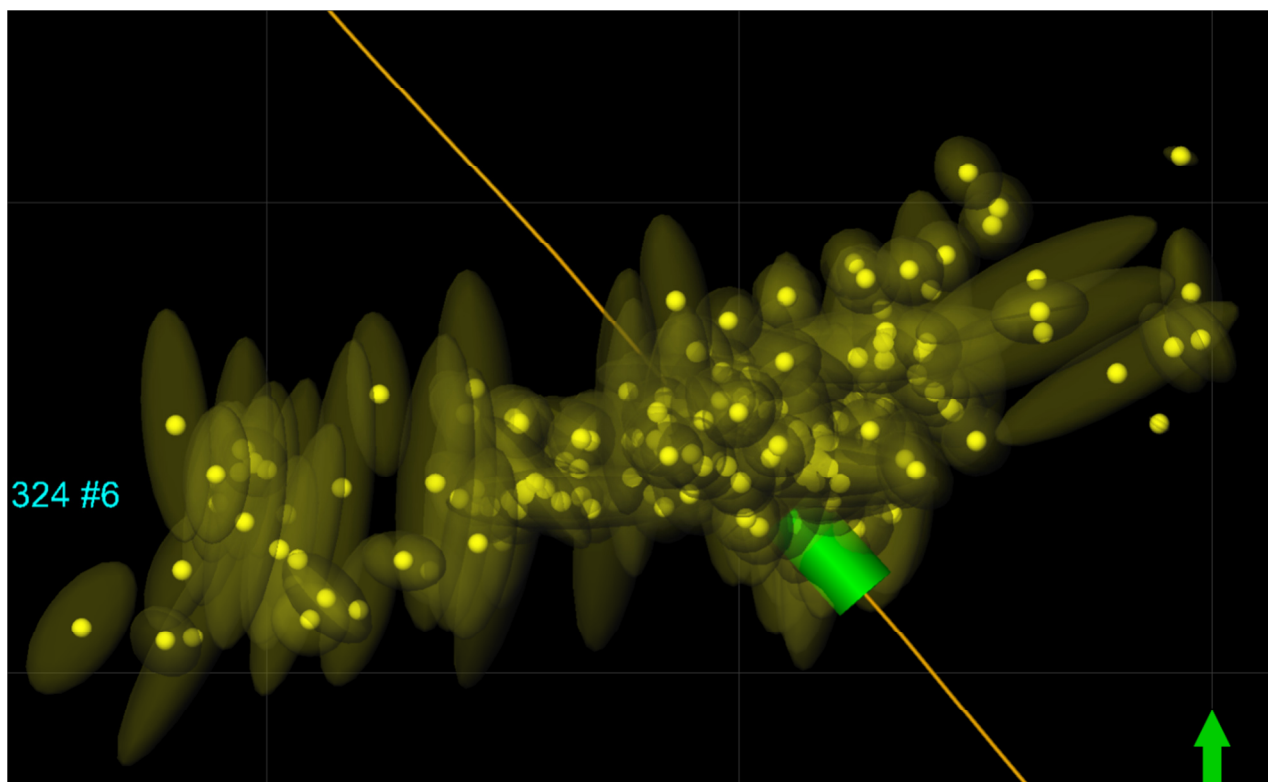


Figure 8.49 - Stage 10 event location uncertainty ellipsoids – map view

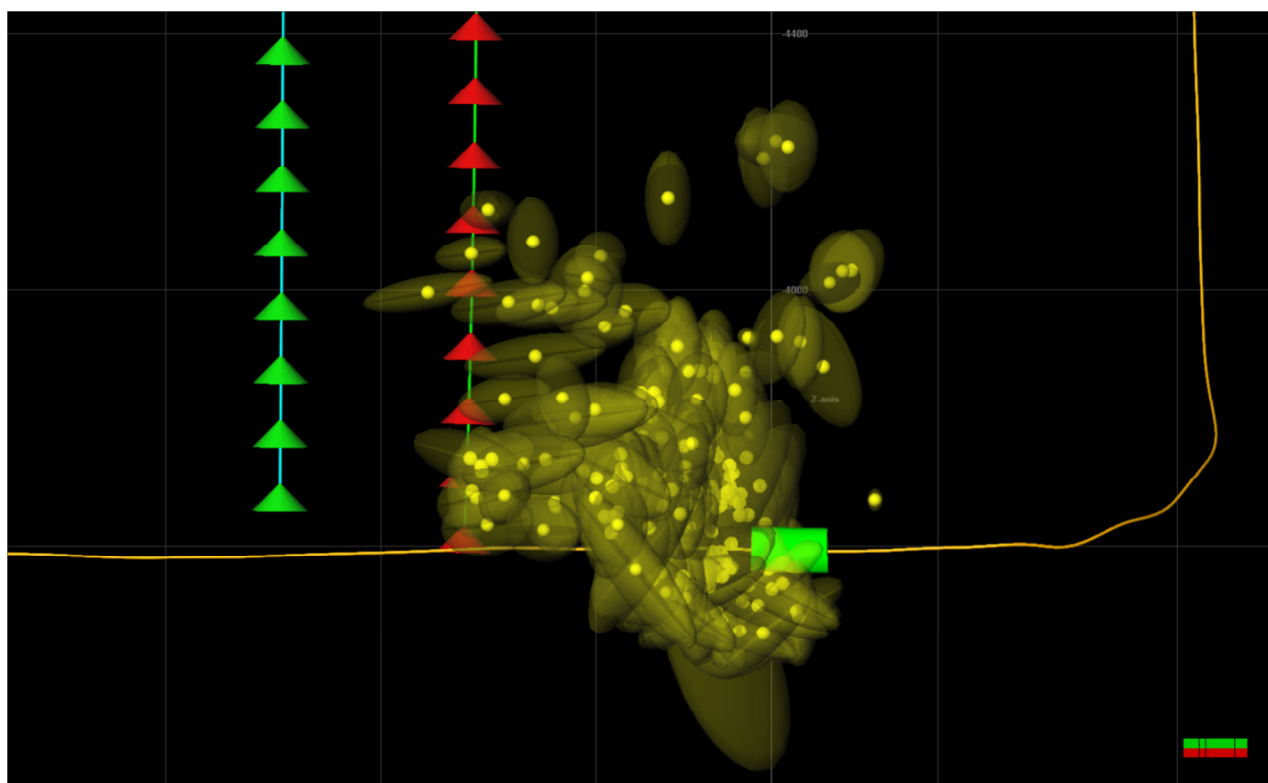


Figure 8.50 - Stage 10 event location uncertainty ellipsoids – side view

8.11 Stage 11

The Stage 11 treatment data and microseismic event rate are shown below. The microseismic events are color coded according to time as shown in the legend for each Figure 8.

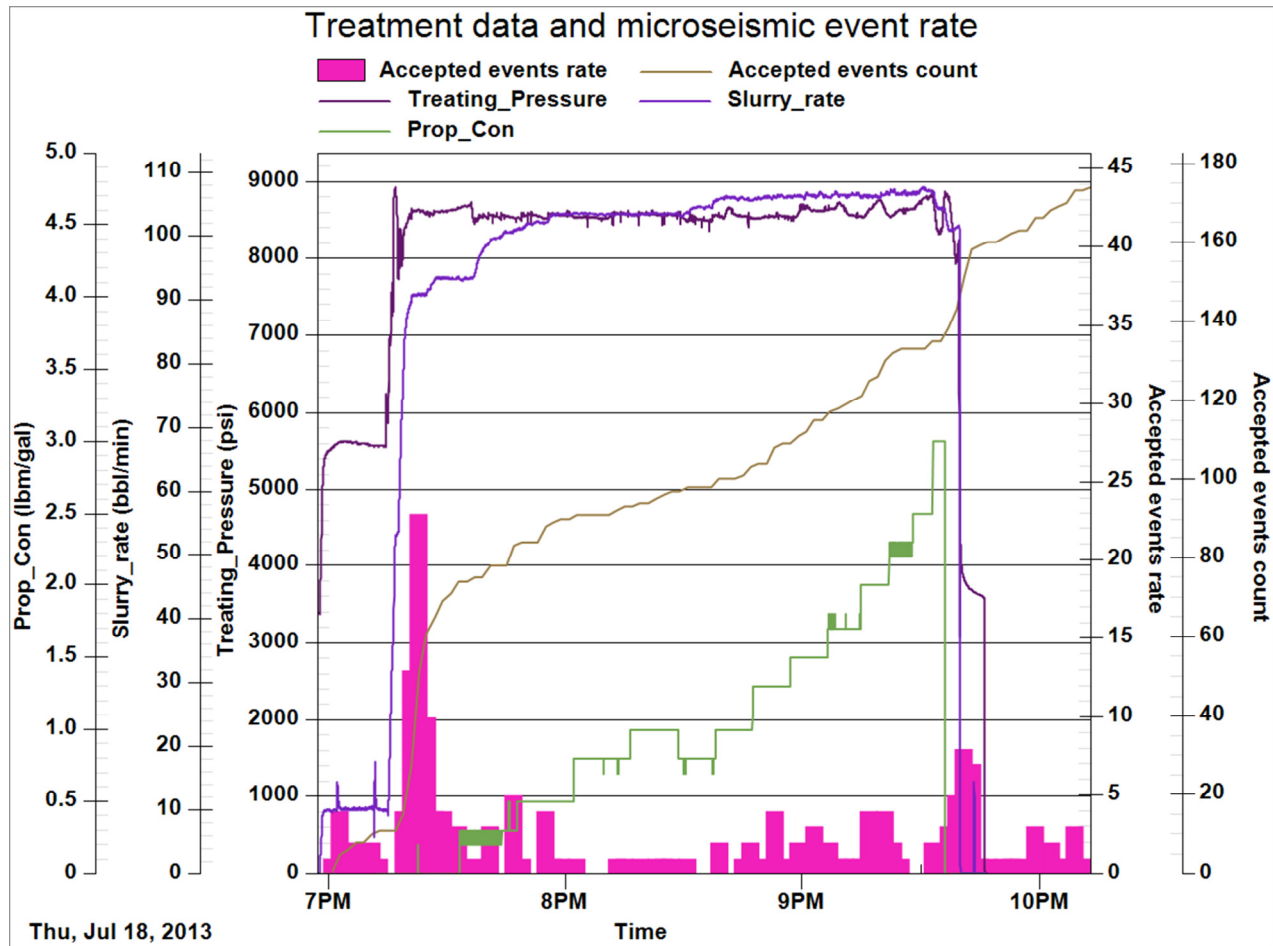


Figure 8.51 - Stage 11 treatment data and microseismic event rate

Table 8.31 - Stage 11 fracture treatment volumes

Description	Designed	Placed
Total fluids (gal)	607700	596274
Total proppants (lbm)	600500	Not used

Table 8.32 - Stage 11 treatment data summary

Description	Value
Average rate (bbl/min)	N/A
Average pressure (psi)	N/A
Pre-treatment ISIP (psi)	N/A
Post-treatment ISIP (psi)	N/A
Maximum PPA (lbm/gal)	N/A

Table 8.33 - Stage 11 microseismic event geometry

Description	Microseismic geometry
Fracture azimuth (deg)	76
MS length (ft)	2828
MS height (ft)	685
MS volume (ft3)	26135998.6

The microseismic data from Stage 11 is shown below in map and transverse views. The microseismic events are color coded according to time as shown on the plot legend. The microseismic dimensions are also shown.

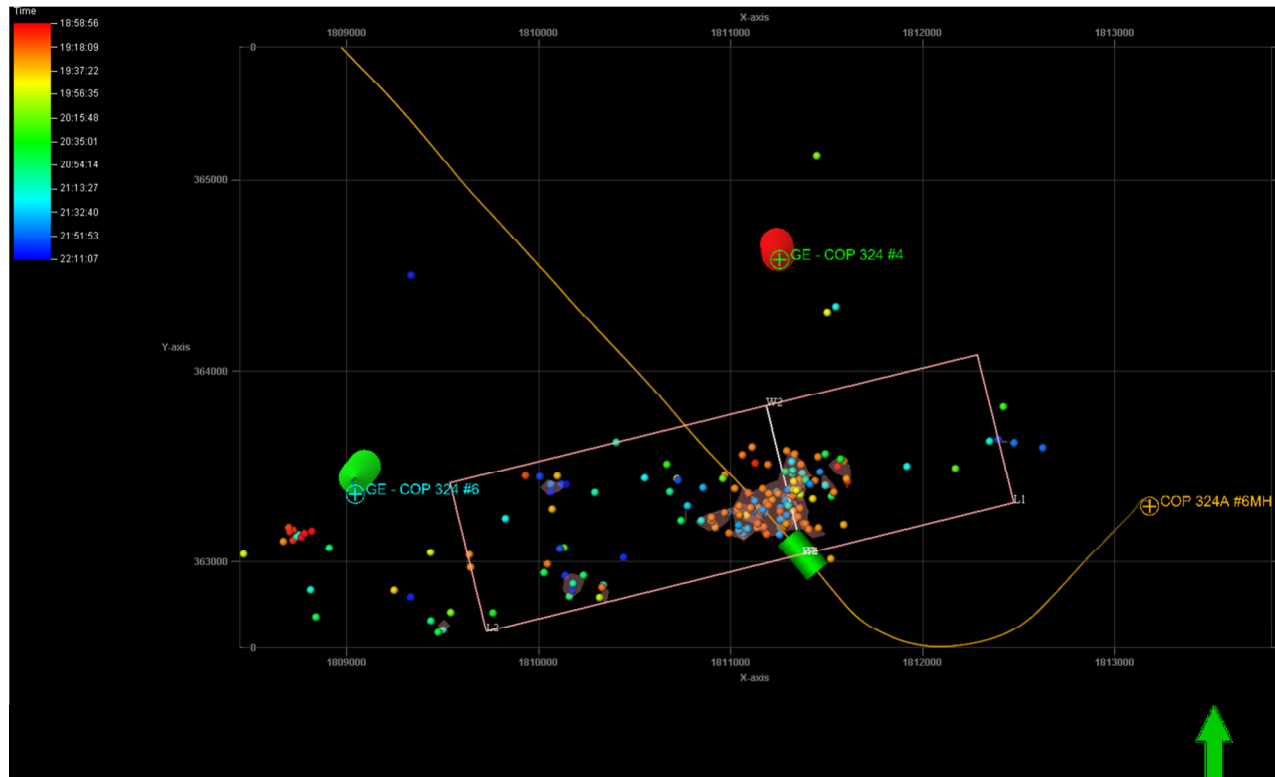


Figure 8.52 - Stage 11 map view (length and width)

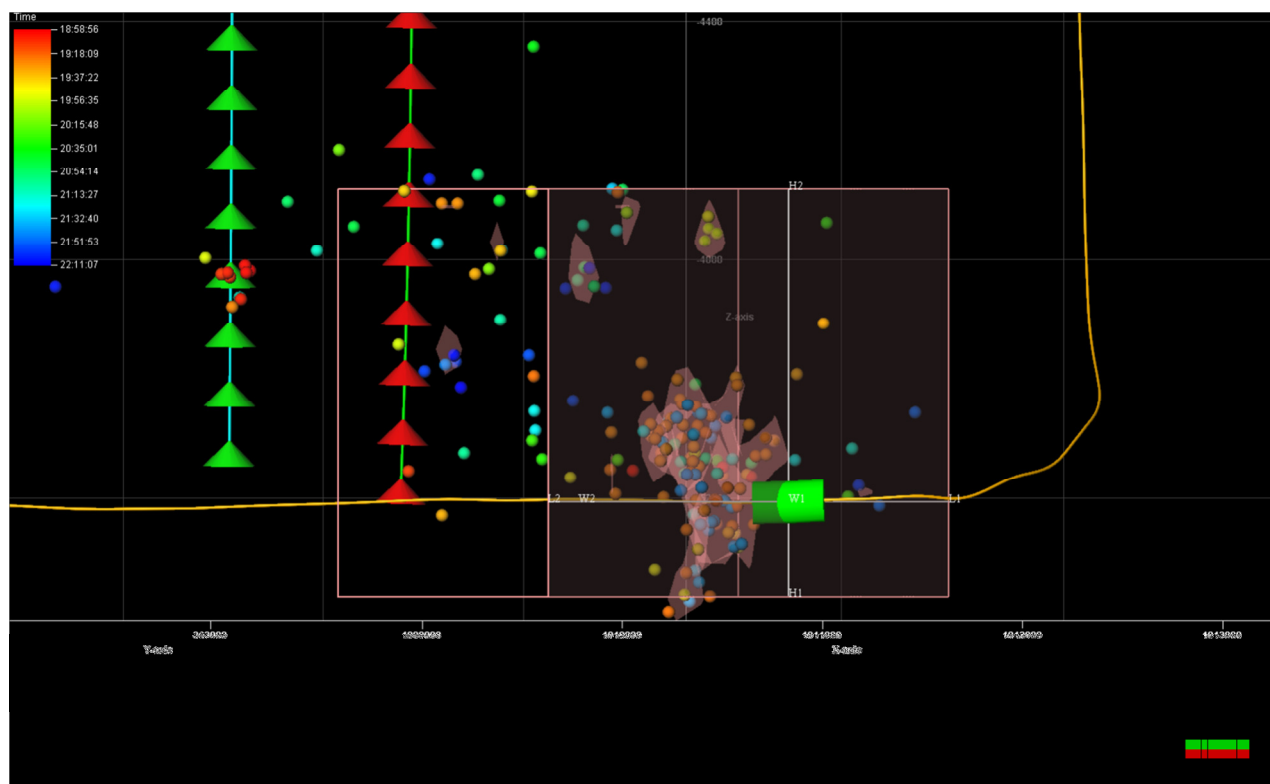


Figure 8.53 - Stage 11 transverse view (height and width)

The microseismic event location uncertainty ellipsoids for Stage 11 are shown below in map and transverse views.

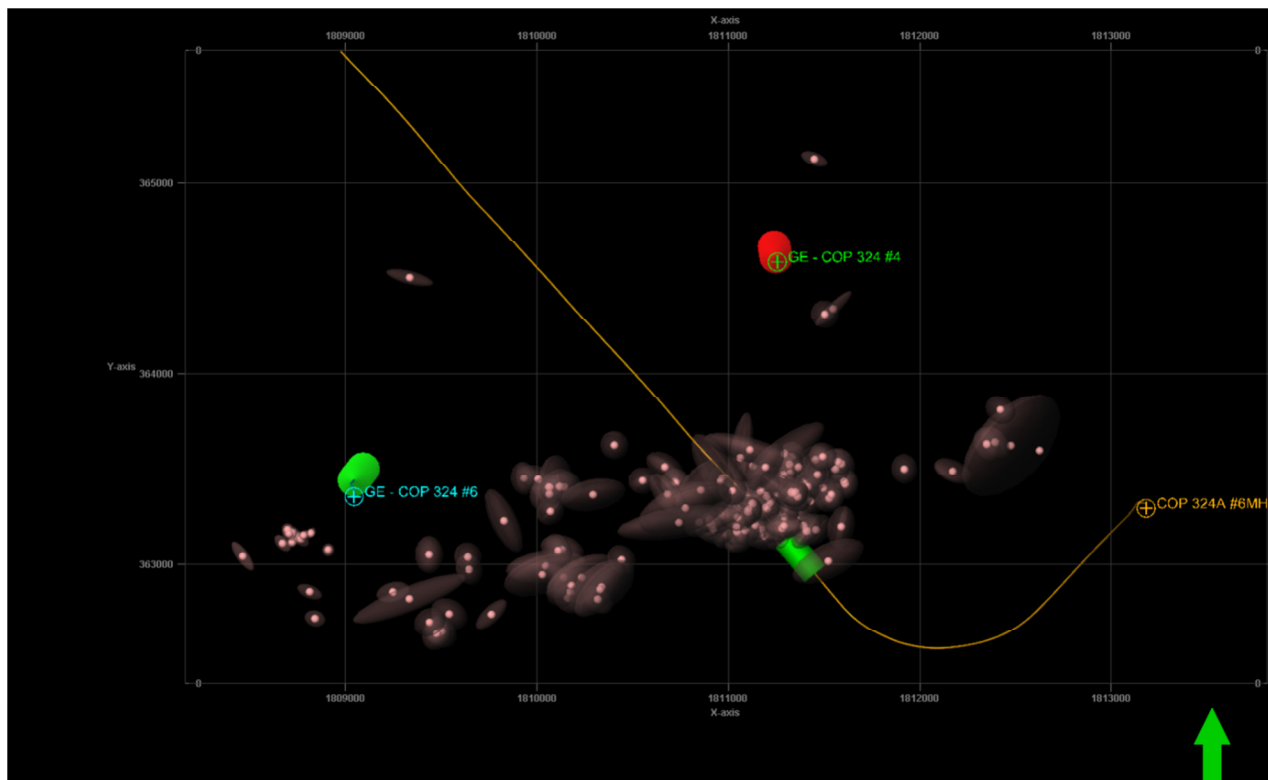


Figure 8.54 - Stage 11 event location uncertainty ellipsoids – map view

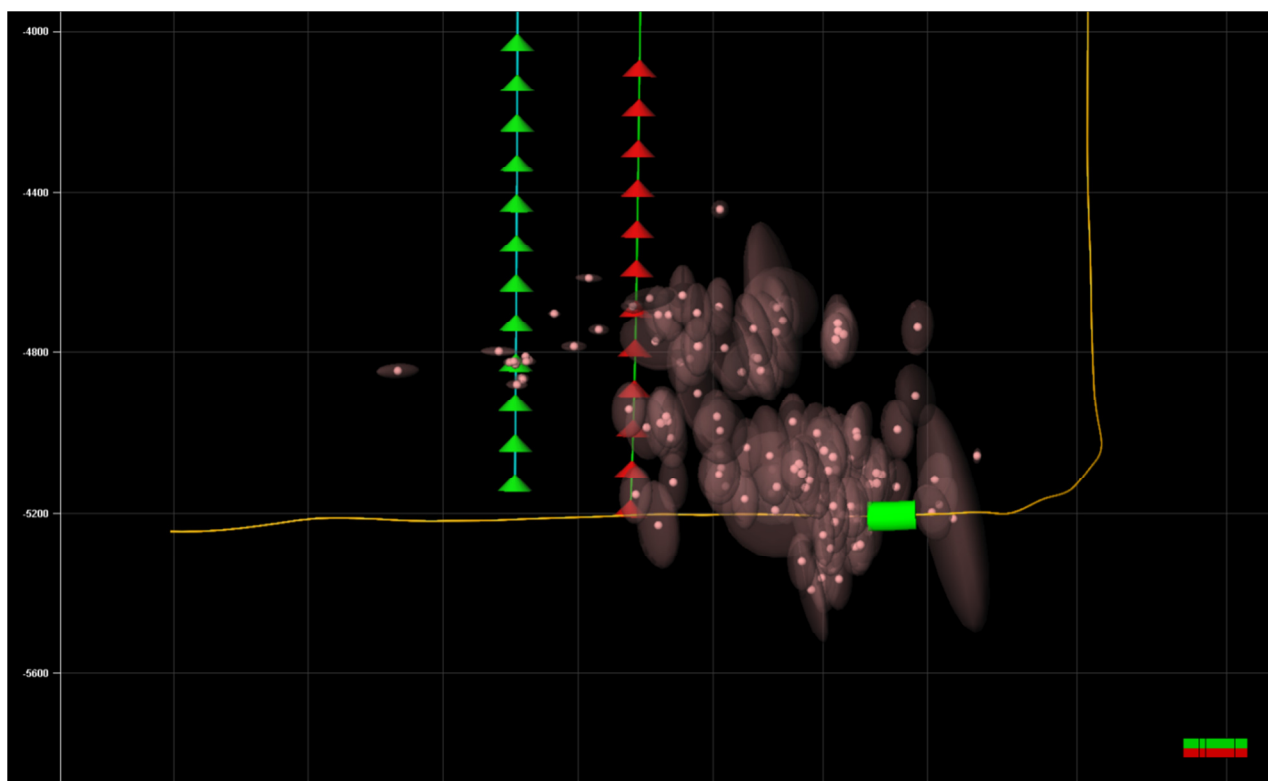


Figure 8.55 - Stage 11 event location uncertainty ellipsoids – side view

8.12 Stage 12

The Stage 12 treatment data and microseismic event rate are shown below. The microseismic events are color coded according to time as shown in the legend for each Figure 8.

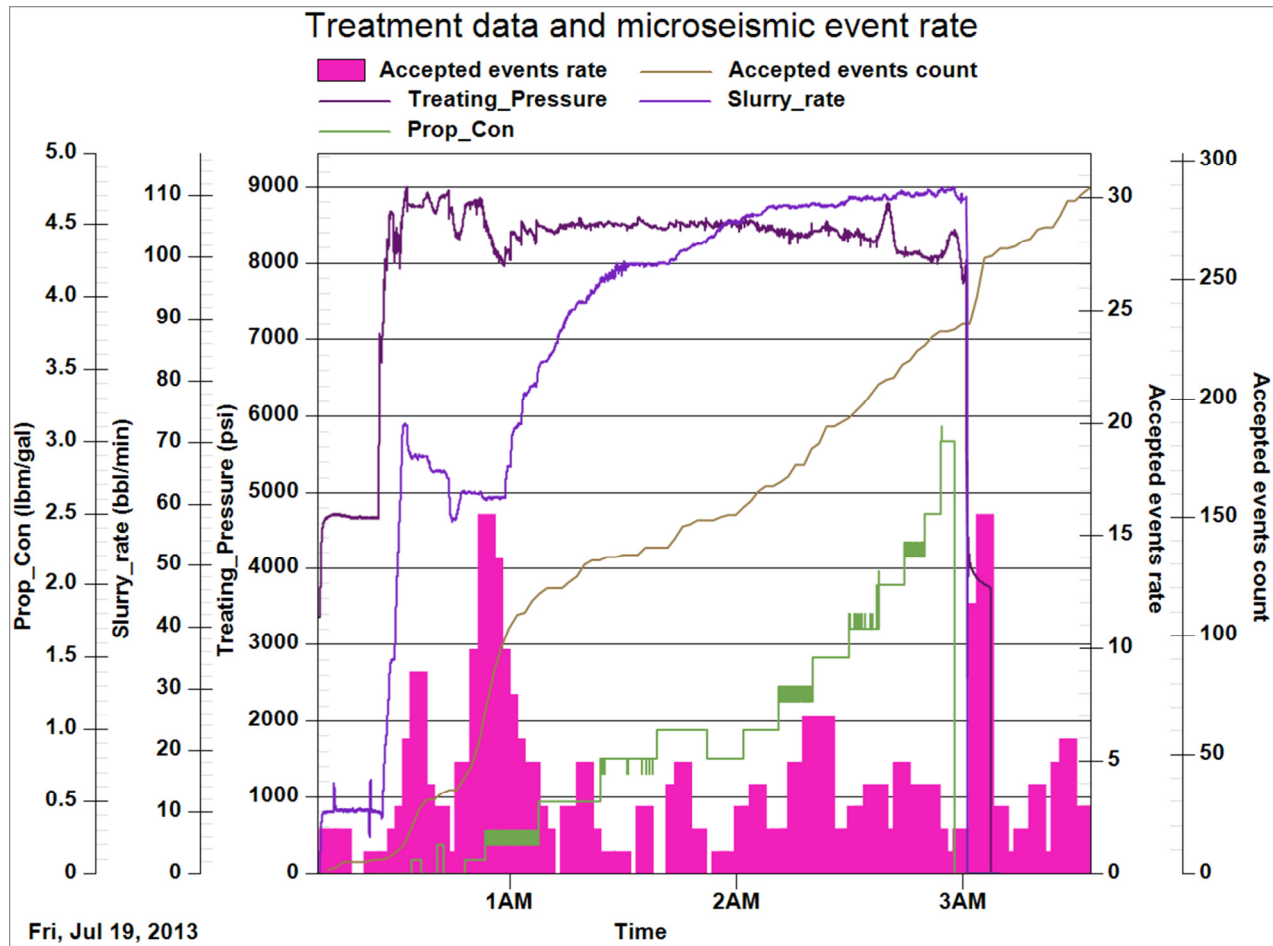


Figure 8.56 - Stage 12 treatment data and microseismic event rate

Table 8.34 - Stage 12 fracture treatment volumes

Description	Designed	Placed
Total fluids (gal)	607700	583296
Total proppants (lbm)	600500	Not used

Table 8.35 - Stage 12 treatment data summary

Description	Value
Average rate (bbl/min)	N/A
Average pressure (psi)	N/A
Pre-treatment ISIP (psi)	N/A
Post-treatment ISIP (psi)	N/A
Maximum PPA (lbm/gal)	N/A

Table 8.36 - Stage 12 microseismic event geometry

Description	Microseismic geometry
Fracture azimuth (deg)	86
MS length (ft)	2921
MS height (ft)	649
MS volume (ft3)	41903999.5

The microseismic data from Stage 12 is shown below in map and transverse views. The microseismic events are color coded according to time as shown on the plot legend. The microseismic dimensions are also shown.

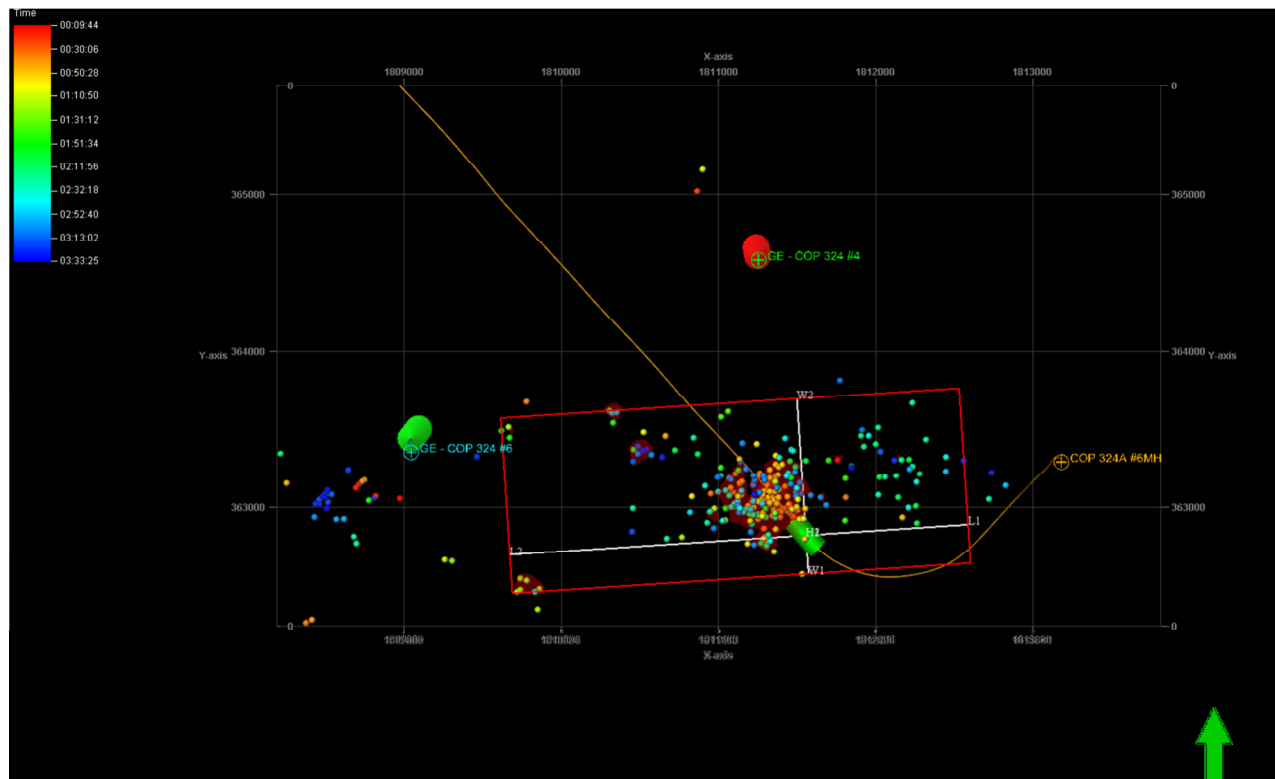


Figure 8.57 - Stage 12 map view (length and width)

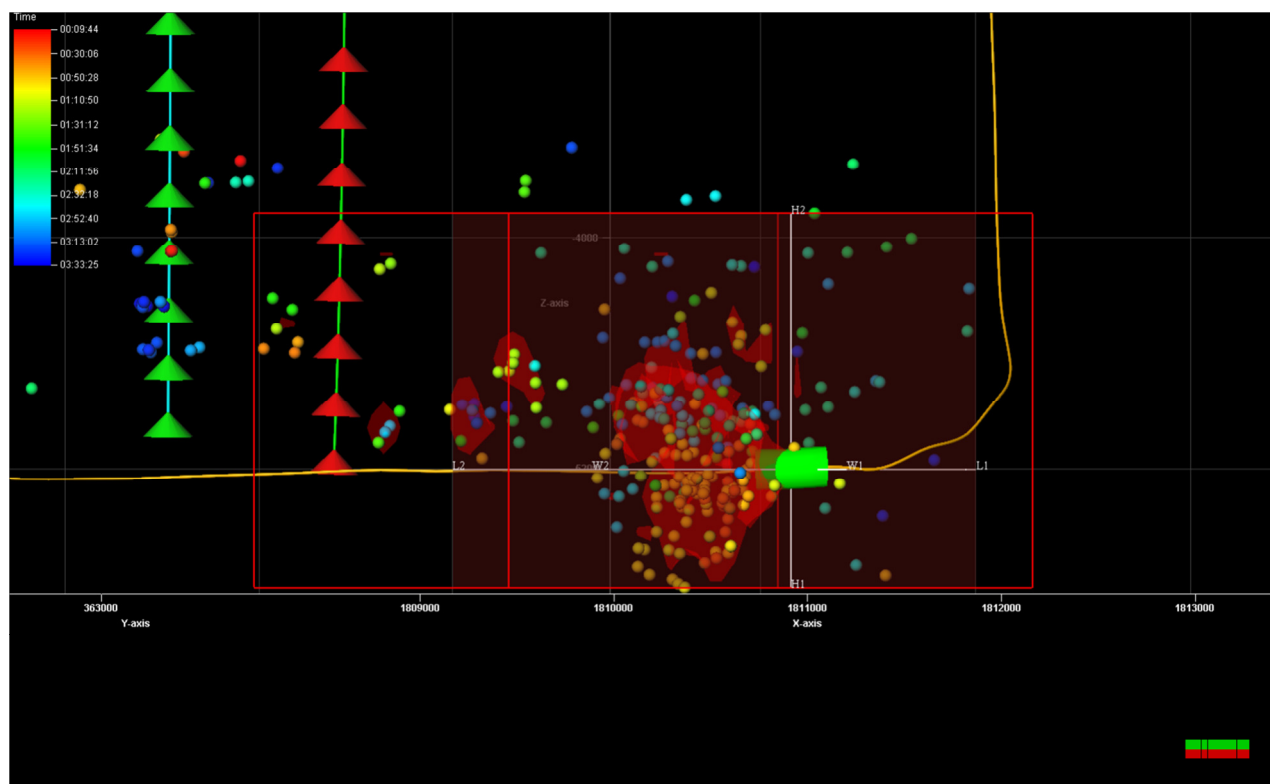


Figure 8.58 - Stage 12 transverse view (height and width)

The microseismic event location uncertainty ellipsoids for Stage 12 are shown below in map and transverse views.

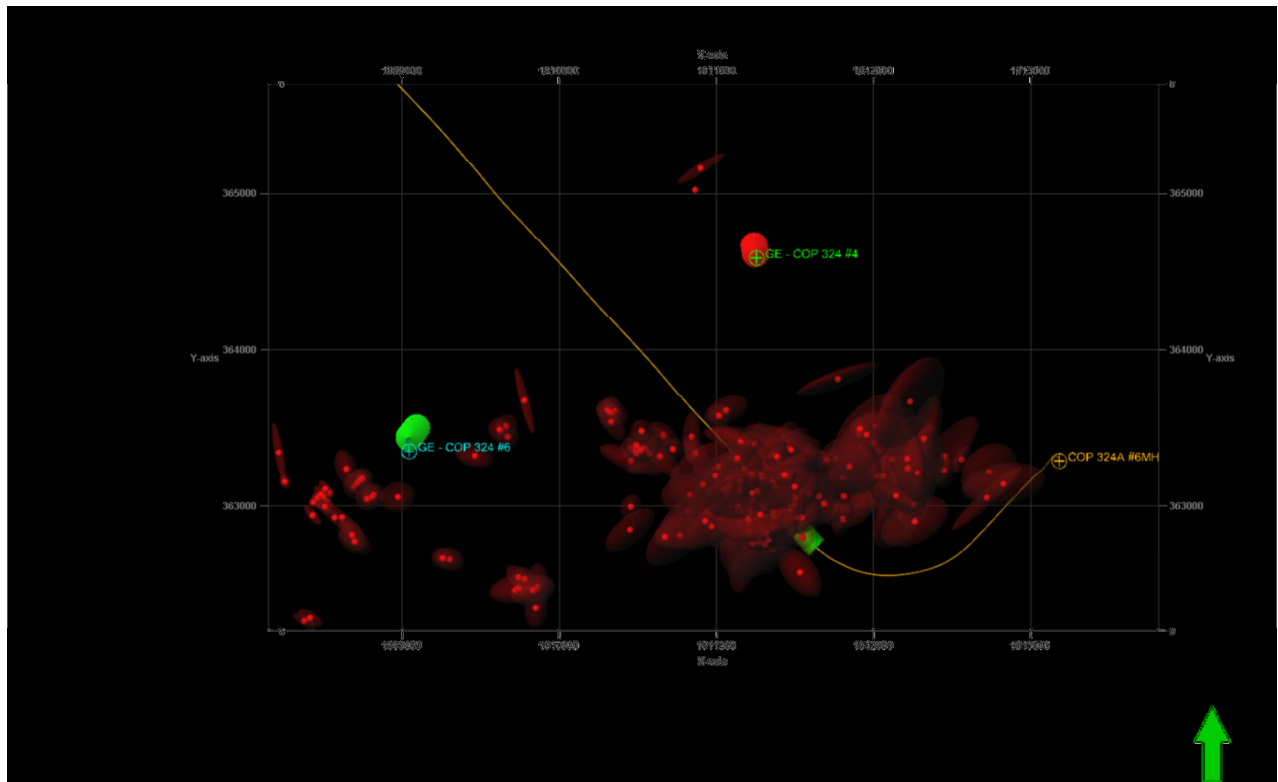


Figure 8.59 - Stage 12 event location uncertainty ellipsoids – map view

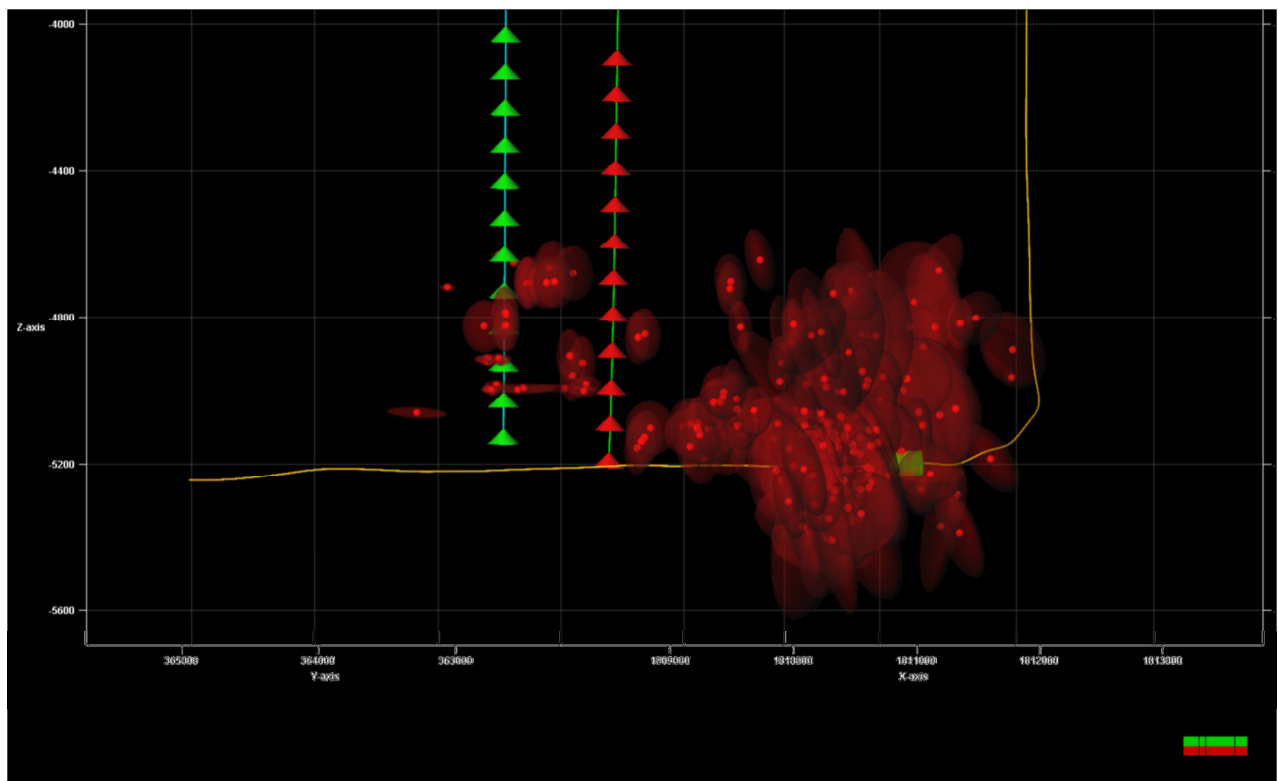


Figure 8.60 - Stage 12 event location uncertainty ellipsoids – side view

8.13 Stage 13

The Stage 13 treatment data and microseismic event rate are shown below. The microseismic events are color coded according to time as shown in the legend for each Figure 8.

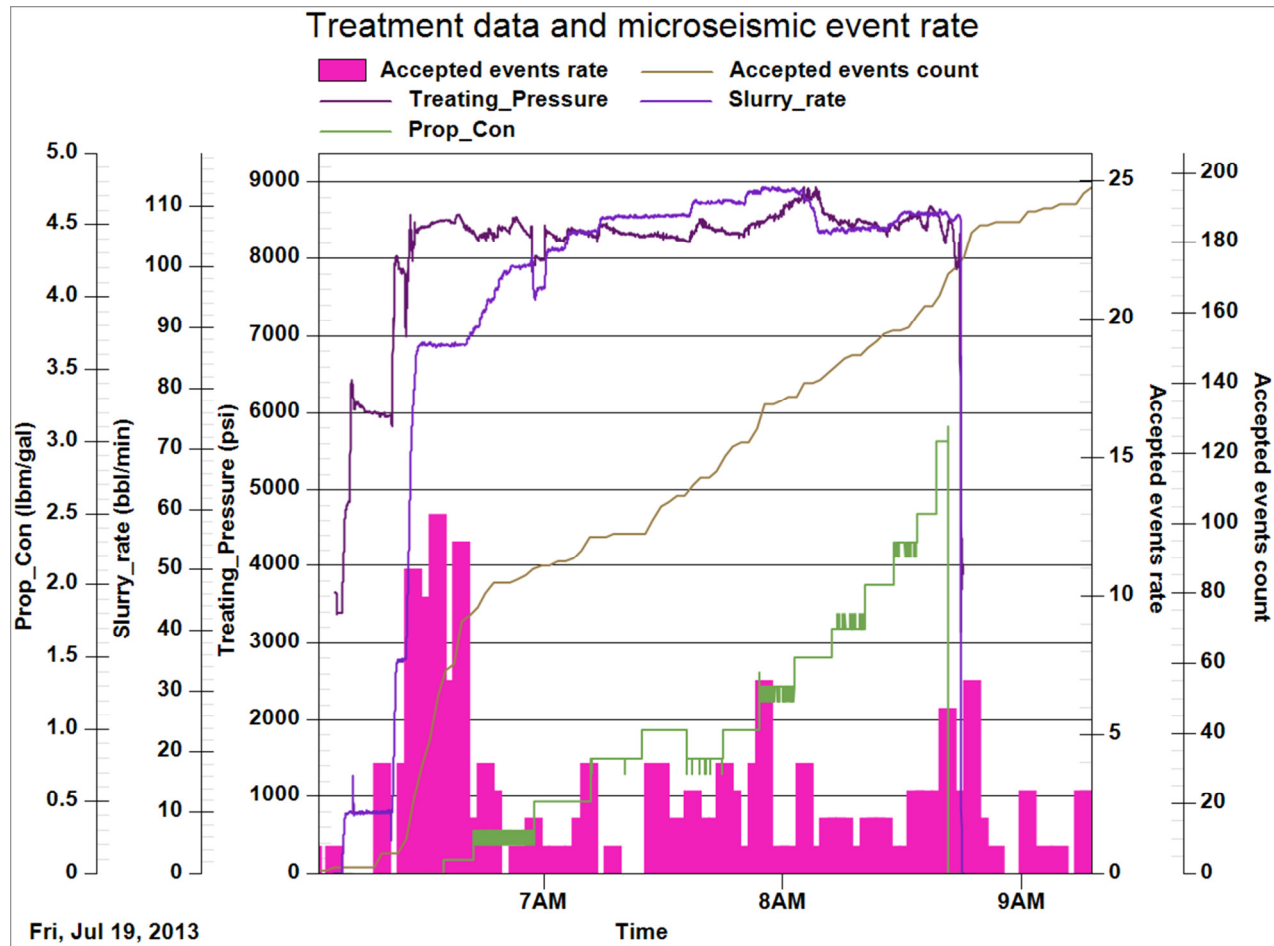


Figure 8.61 - Stage 13 treatment data and microseismic event rate

Table 8.37 - Stage 13 fracture treatment volumes

Description	Designed	Placed
Total fluids (gal)	607700	592368
Total proppants (lbm)	600500	Not used

Table 8.38 - Stage 13 treatment data summary

Description	Value
Average rate (bbl/min)	N/A
Average pressure (psi)	N/A
Pre-treatment ISIP (psi)	N/A
Post-treatment ISIP (psi)	N/A
Maximum PPA (lbm/gal)	N/A

Table 8.39 - Stage 13 microseismic event geometry

Description	Microseismic geometry
Fracture azimuth (deg)	80
MS length (ft)	2160
MS height (ft)	773
MS volume (ft3)	33263999.2

The microseismic data from Stage 13 is shown below in map and transverse views. The microseismic events are color coded according to time as shown on the plot legend. The microseismic dimensions are also shown.

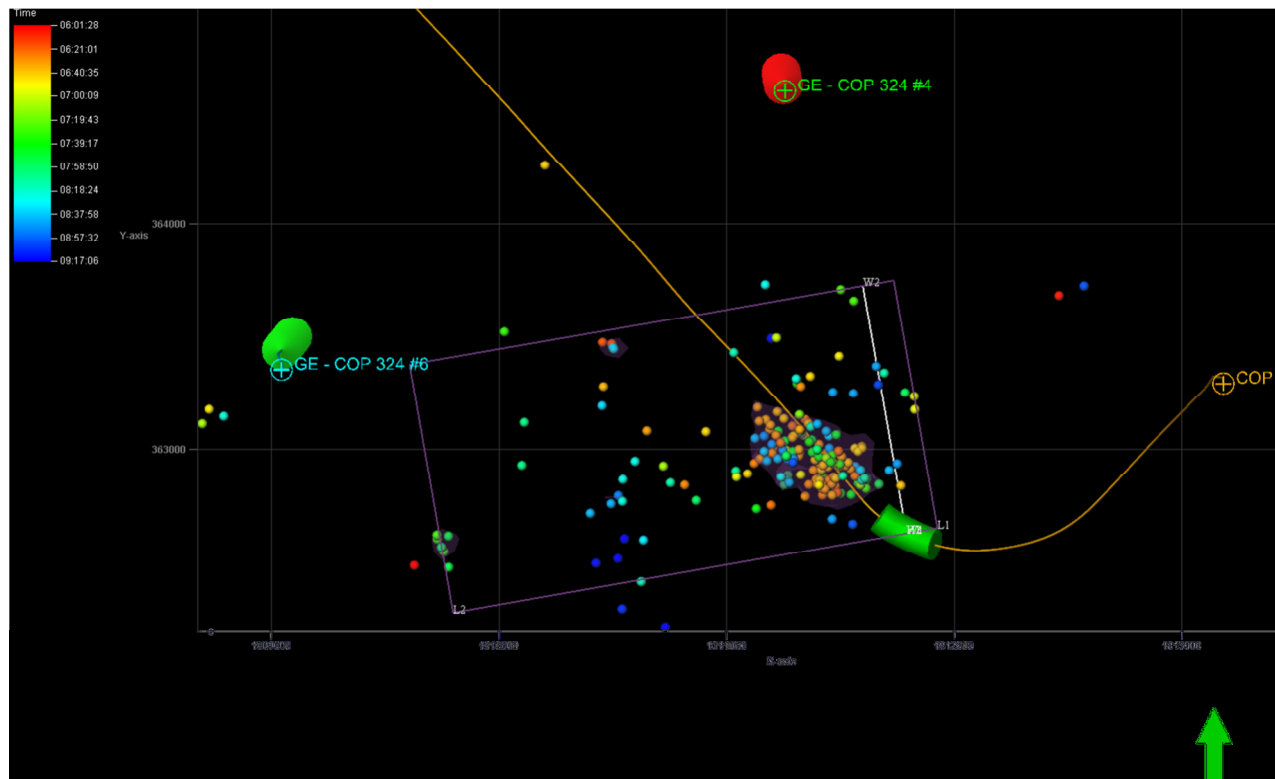


Figure 8.62 - Stage 13 map view (length and width)

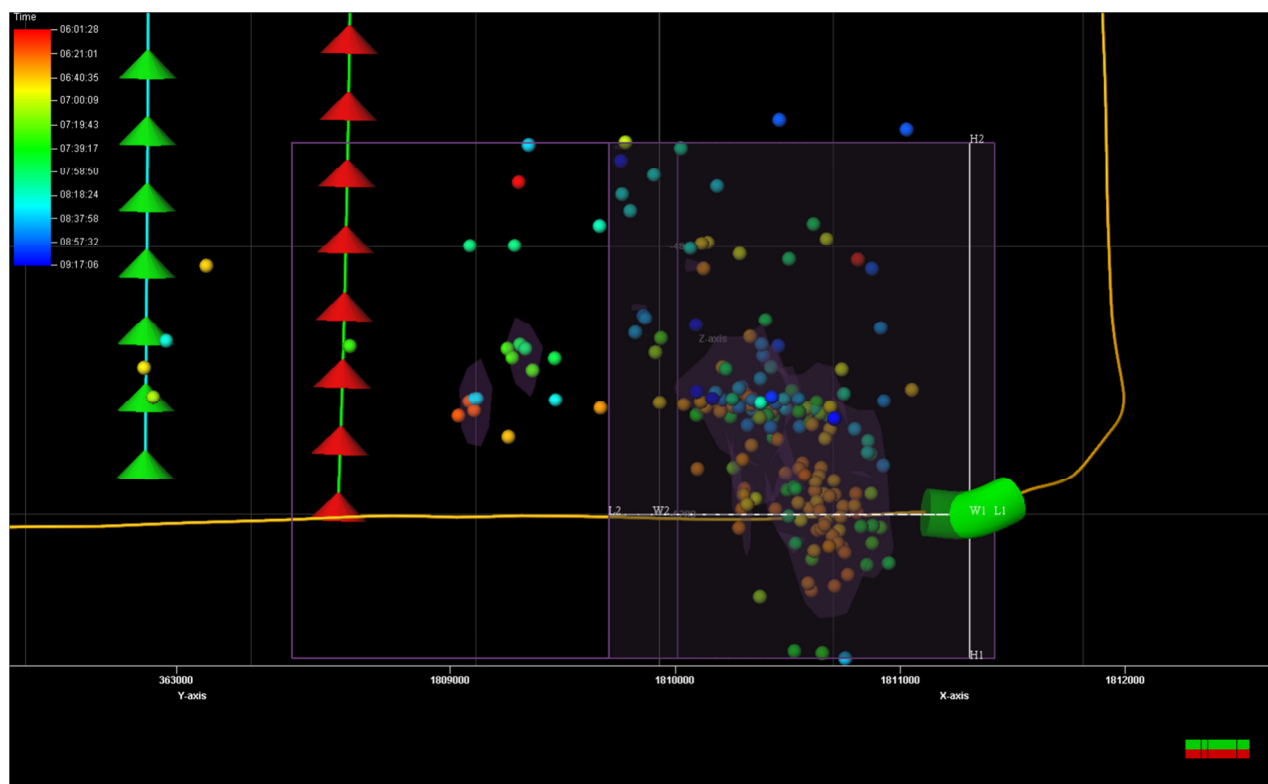


Figure 8.63 - Stage 13 transverse view (height and width)

The microseismic event location uncertainty ellipsoids for Stage 13 are shown below in map and transverse views.

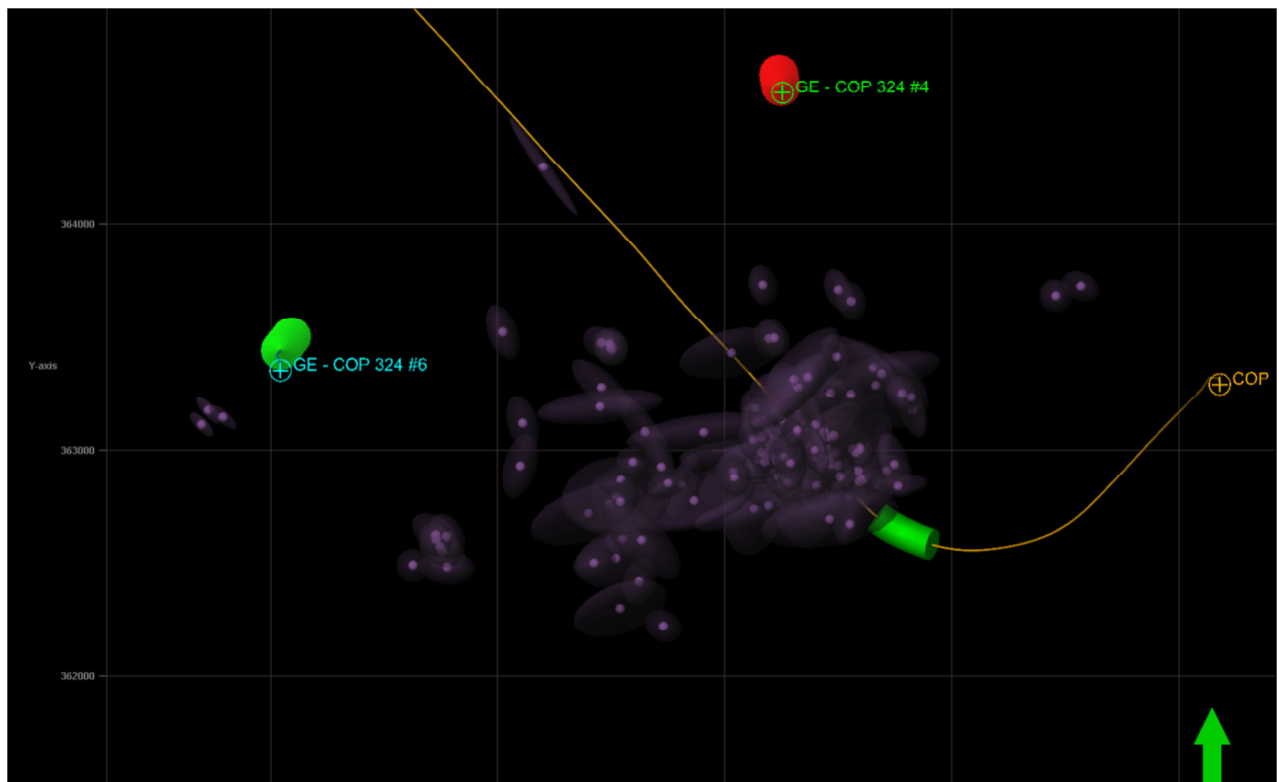


Figure 8.64 - Stage 13 event location uncertainty ellipsoids – map view

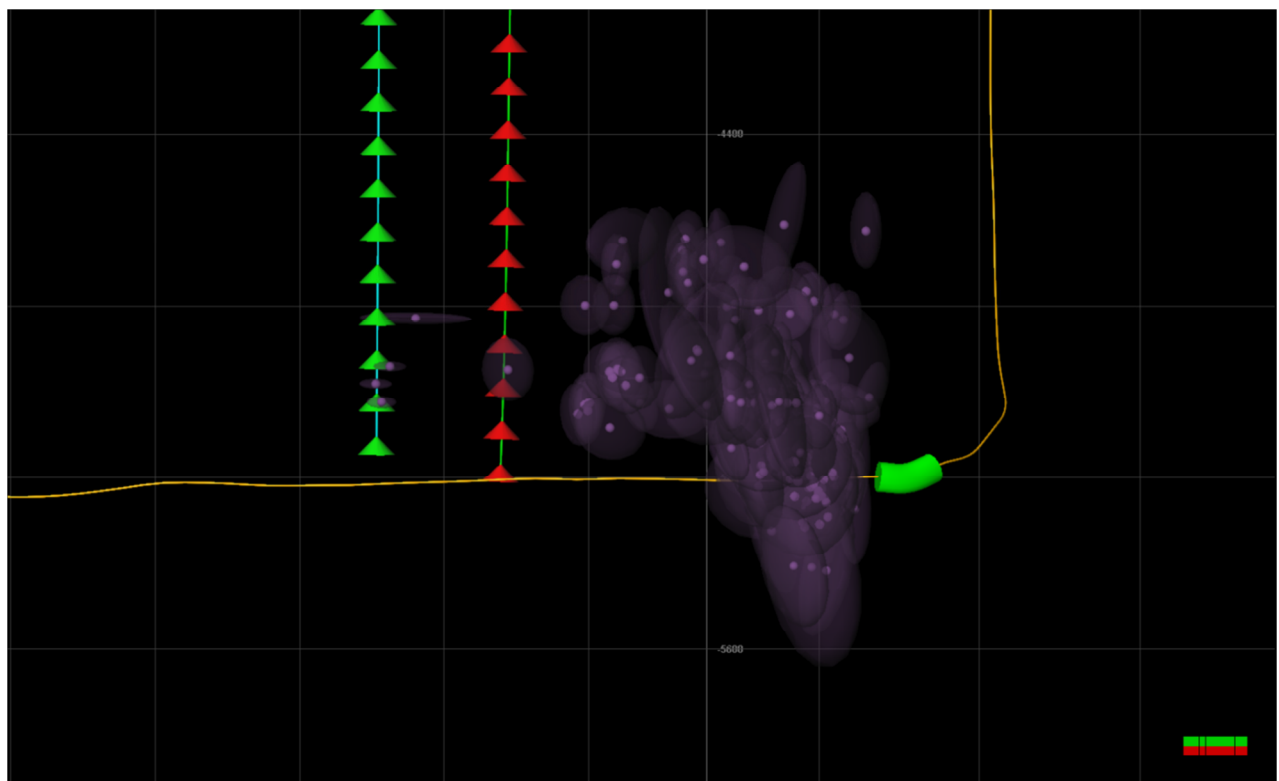


Figure 8.65 - Stage 13 event location uncertainty ellipsoids – side view

9 Geophysics Processing Report

The total data set was scanned with an event detector algorithm which first detects signals above a given signal-to-noise threshold on each shuttle. For each detected signal, the known velocity model can be used to calculate a range of expected signal arrival times for the other shuttles. Signals arriving in these expected time ranges are said to be associated, meaning they come from the same microseismic event. If signals are detected on a given minimum number of shuttles, an event is declared and stored in an event file for further processing.

Coalescent Microseismic Mapping, or CMM, is an innovative Schlumberger method for micro-earthquake hypocenter determination. Event locations are calculated without manual P and S picking. CMM determined P and S times are visually reviewed and edited for quality control only. Results are usually as good as or better than would be possible with tedious and slow manual picking.

Table 1 – Surface locations (NAD 27, Pennsylvania North, US ft)

Well Name	KB (ft)	Easting (ft)	Northing (ft)
Monitoring well: COP 324 #4	2111	1811255	364583
Monitoring well: COP 324 #6	2173	1809044	363353
Treatment well: COP 324 A #6MH	2146	1813181	363292

Three tool positions were used as described in Table 2.

Table 2 – Stages monitored and tool parameters

Monitoring Well	Stages Monitored	Tool Parameters
COP 324 #4	Stages 1-13	Vertical VSI-12 receiver array, 100 ft spacing, 0.5 ms sampling, 6200-7300 ft MD
COP 324 #6	Stages 1-13	Vertical VSI-11 receiver array, 100 ft spacing, 0.5 ms sampling, 6200-7300 ft MD

Calibration Overview

The 3C sensor array is deployed in the monitor well via wireline cable. Each 3C sensor forms a random 3 axis local coordinate system. Calibration of the 3C sensor array orientation is accomplished by recording shots from known location(s), allowing for rotation of each sensor into a global coordinate system.

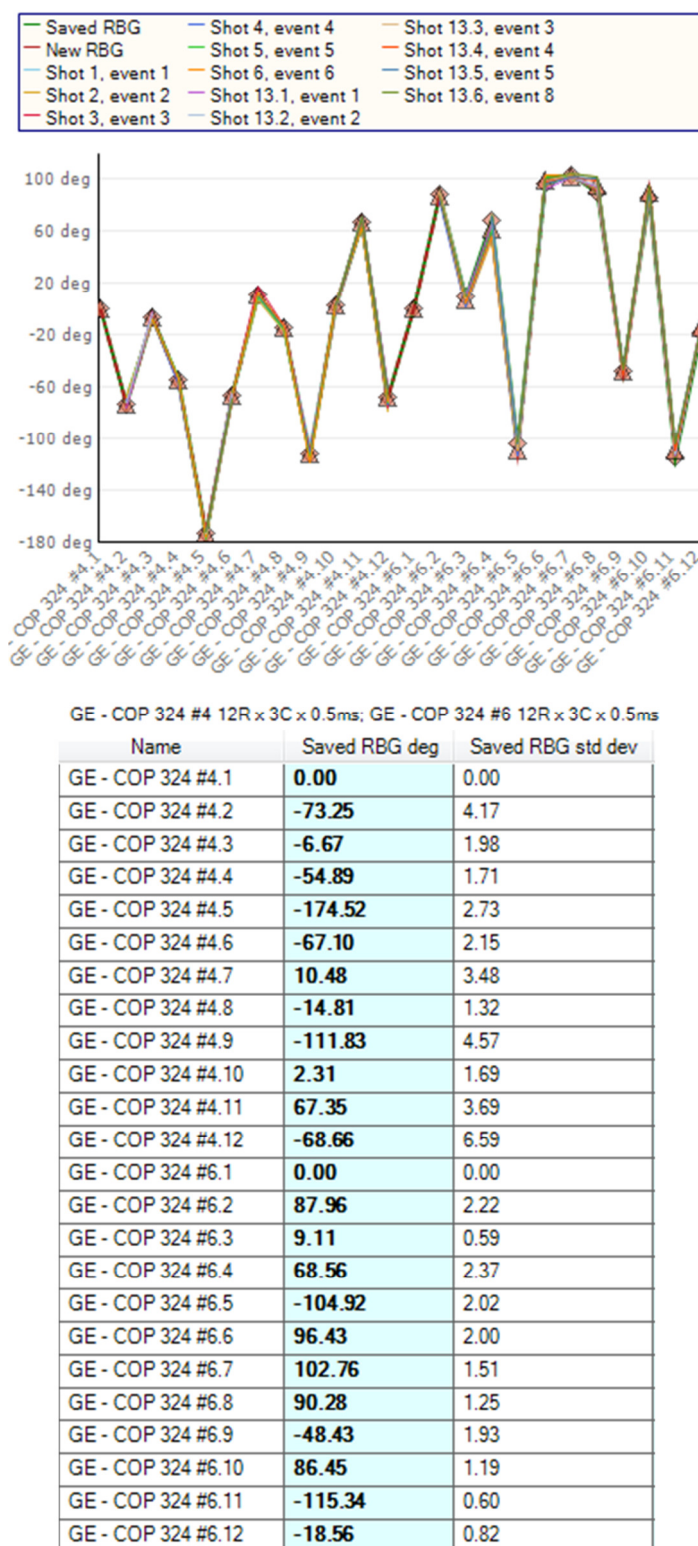


Figure 1 – Sensor orientations of the COP 324 #4 and COP 324 #6 receiver arrays

Suitable orientation shots can be:

- Perforation shots in the treatment well
- String shots (backoff shots) from the treatment well
- String shots in a nearby well.
- Vibrator shots from one or more known surface locations

Accurate calibration of the 3C sensor orientation depends on accurate knowledge of the location of the shot point in 3D space (X,Y,Z) as well as accurate location of the 3C sensor stations. Wellhead locations verified by GPS and gyro well deviation survey recorded from TD to surface are required measurements. Inaccuracies in these measurements lead to inaccuracy in sensor orientation.

Velocity Model Construction and Calibration

Vertical V_p and V_s are typically obtained from Sonic logs ideally run in open hole in a vertical wellbore. Logs are blocked by application of an edge detection algorithm and refined with minimum layer thickness derived from Backus averaging criteria. Optional smoothing may be applied to account for lateral uncertainty in the earth model.

Calibration of the earth model is accomplished by measurement of perforation shots or string shots from a known location(s), typically the treatment well. Time picks of the P, Sh, and optionally Sv arrivals as well as optional measurement of the T0 are input to either a manual calibration technique or automated inversion. Model times are obtained by ray tracing with an exact 1D-VTI ray tracer engine. Mismatch between the measured times and model times (Residual Time) for each phase is minimized by manual adjustment or automated inversion for Thomsen parameters in the calibration process.

Resulting Thomsen anisotropy parameters are checked for geophysical validity.

Velocity Model

The velocity model was built using the sonic logs taken from the COP 324 #4 monitor well. P- and S-wave sonic slowness logs were converted to P-wave velocity and S-wave velocity, and smoothing and blocking was applied to the velocity and density logs to build the initial isotropic model. Thomsen's gamma, epsilon, and delta values were derived by calibrating the initial velocity model to waveforms of known events (perforation shots).

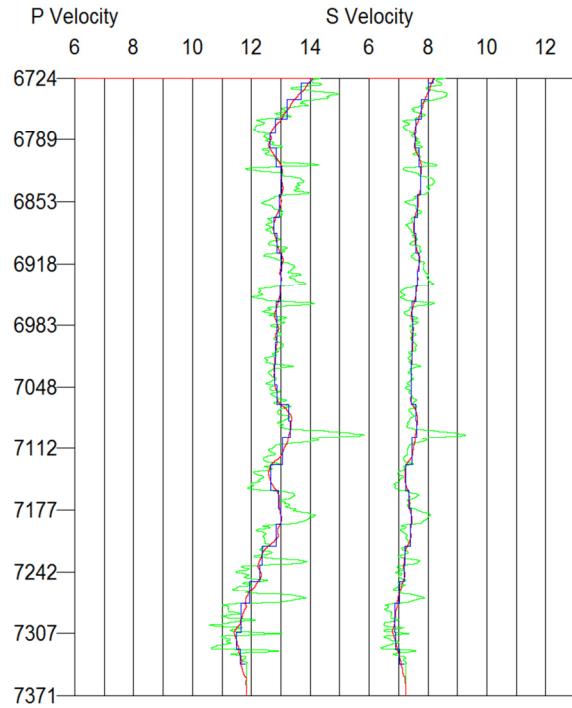


Figure 2 – Initial isotropic velocity models. Raw sonic (green) logs converted to velocity are shown with 90 ft smoothed (red) and minimum 15 ft blocked (blue) logs superimposed.

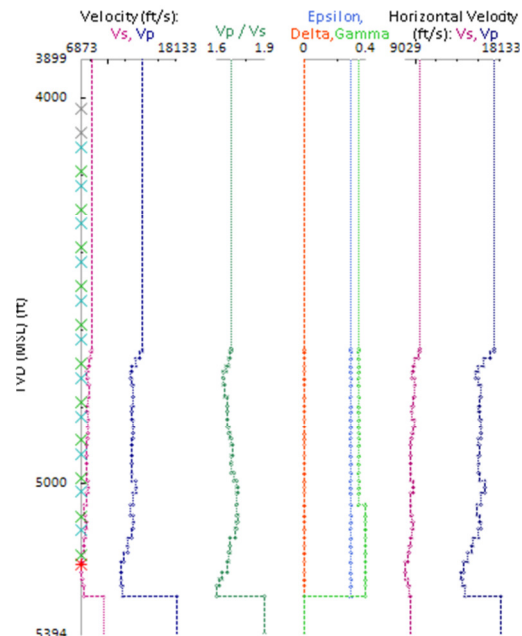


Figure 3 – Final calibrated anisotropic velocity model showing blocked (minimum 10 ft) and smoothed (50 ft) sonic velocities and calibrated Thomsen's parameters epsilon, delta, and gamma. Missing data are extrapolated at top and bottom

Calibration Shots Results

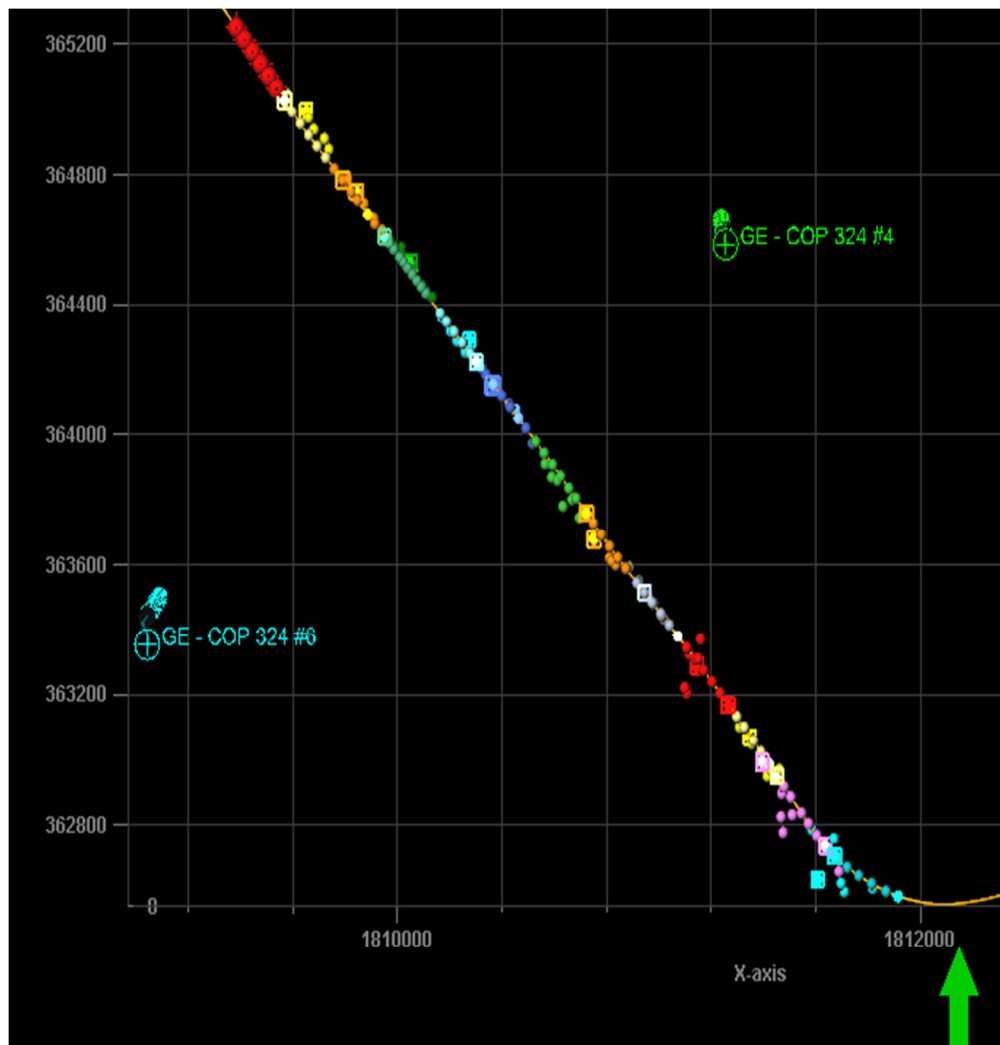


Figure 4 – Map view of located perforation shots in treatment well.

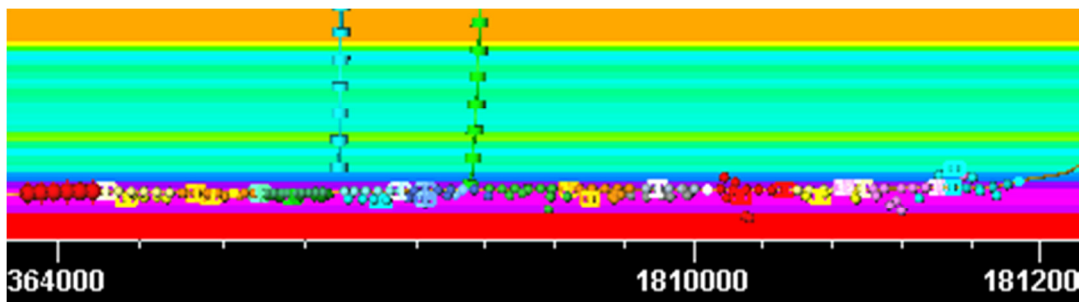


Figure 5 – Side view (N50E) of located perforation shots (expected locations shown as discs) in treatment well (violet).

Calibration Shot Waveforms

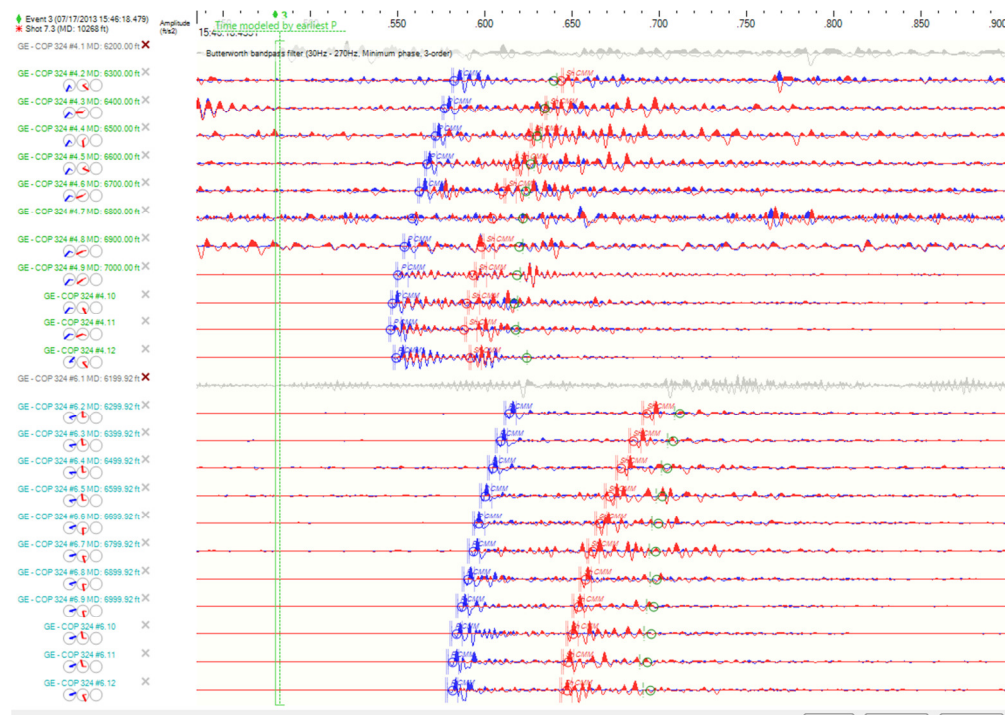


Figure 6 – Example of a relatively good quality perforation shot and calibrated model fit for stage 7.

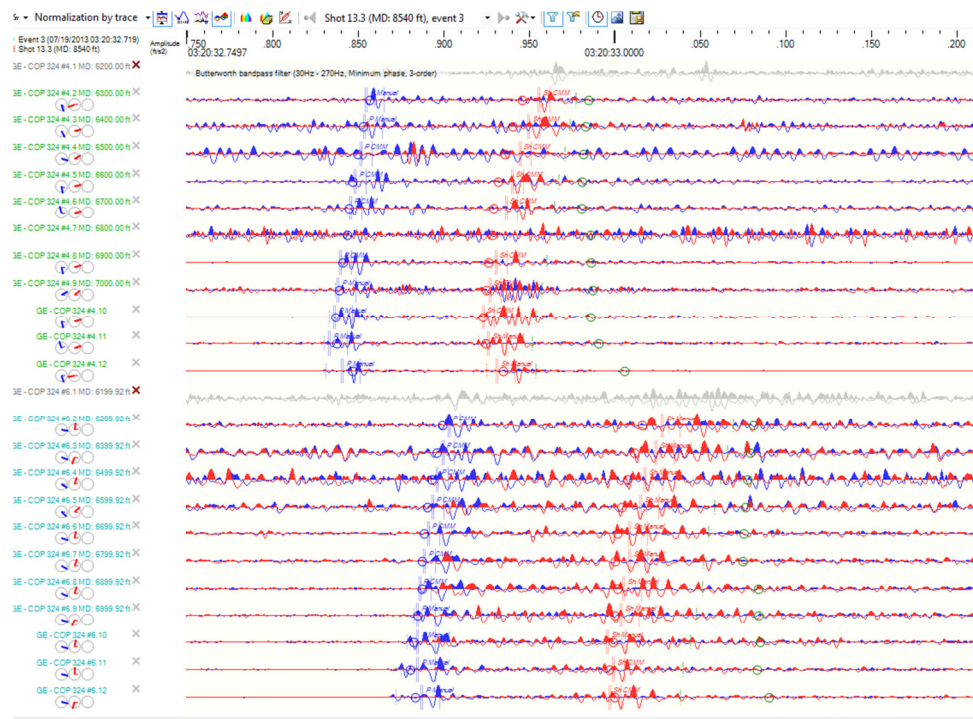


Figure 7 –Example of a poor quality perforation shot and calibrated model fit for stage 13.

Quality Indicators

SNR – Measurement of the peak value of the CMM objective function. Typical ranges 2.0 to 15.0. Generally higher values correlate to higher data quality.

Max Error – Length of the major axis of the location uncertainty ellipsoid

Mid Error – Length of the mid axis of the location uncertainty ellipsoid

Min Error – Length of the minor axis of the location uncertainty ellipsoid

Confidence Factor – Data quality indicator. This value ranges from 0 to 5. Higher values indicate higher confidence levels. Confidence Indicator is a composite of P trace quality, S trace quality, P time residual, S time residual, and P-S orthogonality.

Treatment well – stages		SNR	Magnitude	Max Error (ft)	Min Error (ft)	Radius (ft)	Confidence
COP 324 #6MH stages 1-13	Min	2	-3.1	15	1	2	1.6
	Max	74	-0.74	350	120	62	4.2

Table 3 – Quality Indicators summary.

Signal-to-noise ratio

Location confidence improves as the signal-to-noise ratio (SNR) increases. A minimum SNR threshold value is used when evaluating and interpreting microseismic events located while fracturing. Microseismic events with lower SNR values are disabled during the evaluation and are not displayed. For purposes of evaluation and interpretation the minimum signal-to-noise ratio used was 2.0.

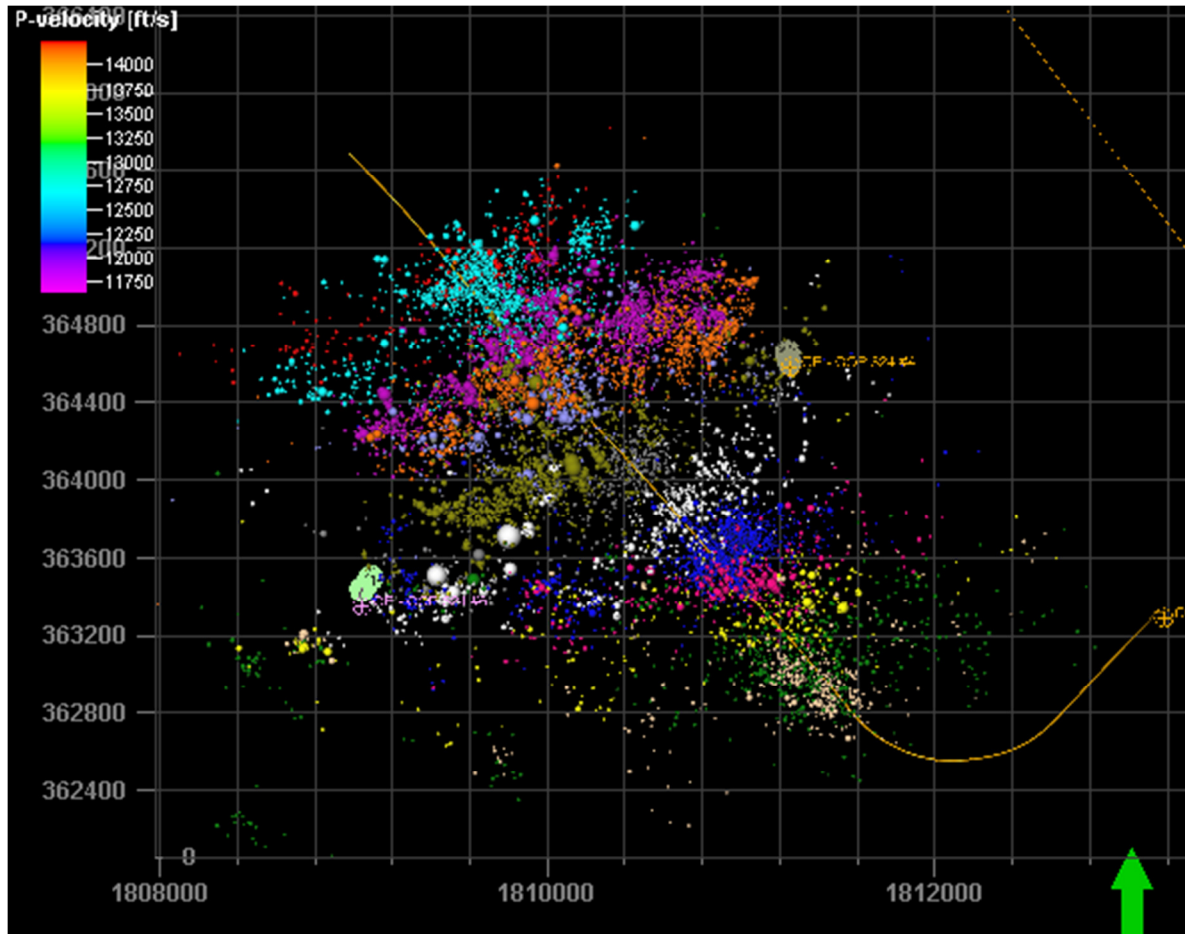


Figure 8 – Map view of SNR sized events. Event size ranges from SNR of 2 (smallest) to 74 (largest). Events are colored by stage.

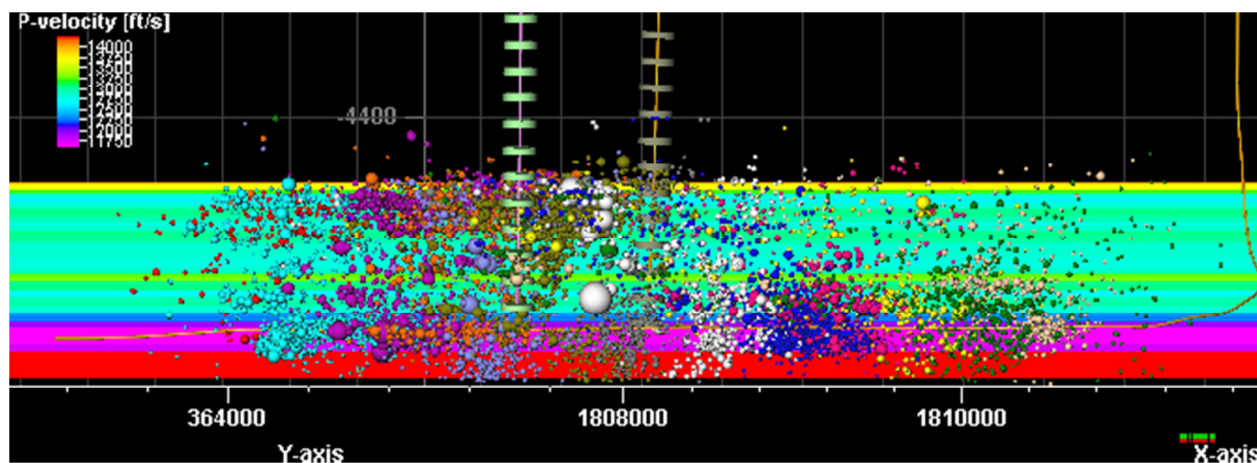


Figure 9 – Side view (from west) of SNR sized events. Event size ranges from SNR of 2 (smallest) to 74 (largest). Events are colored by stage.

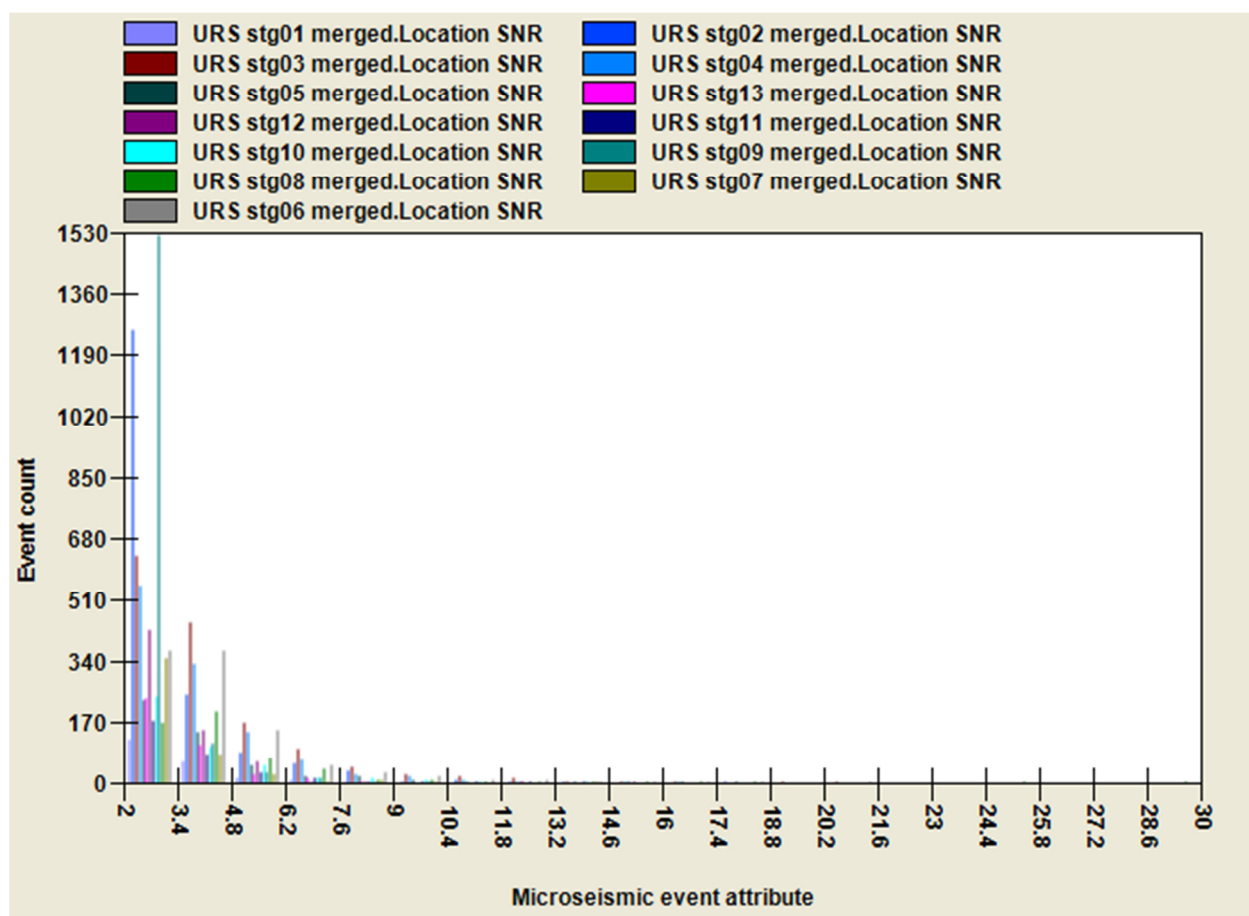


Figure 10 – SNR histogram (all stages).

Magnitude

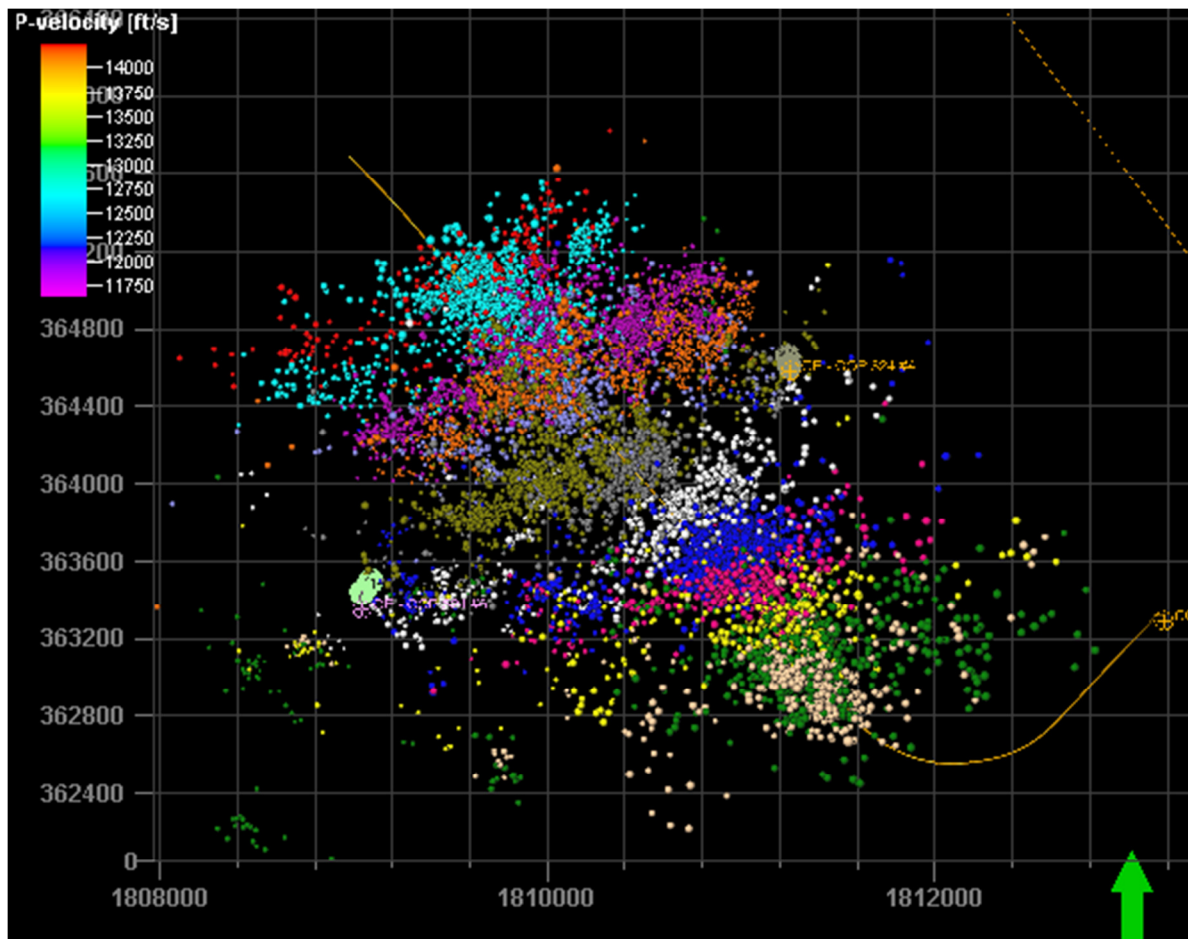


Figure 11 – Map view of relative magnitude sized events. Event magnitude size ranges from -3.1 (smallest) to -0.74 (largest). Events are colored by stage.

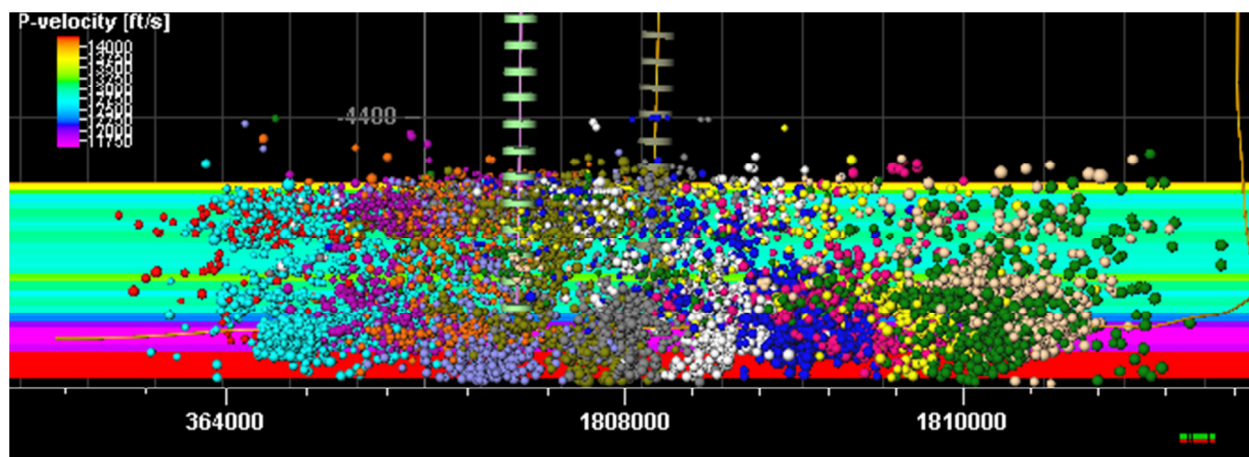


Figure 12 – Side view (N40E) of relative magnitude sized events. Event magnitude size ranges from -3.1 (smallest) to -0.74 (largest). Events are colored by stage.

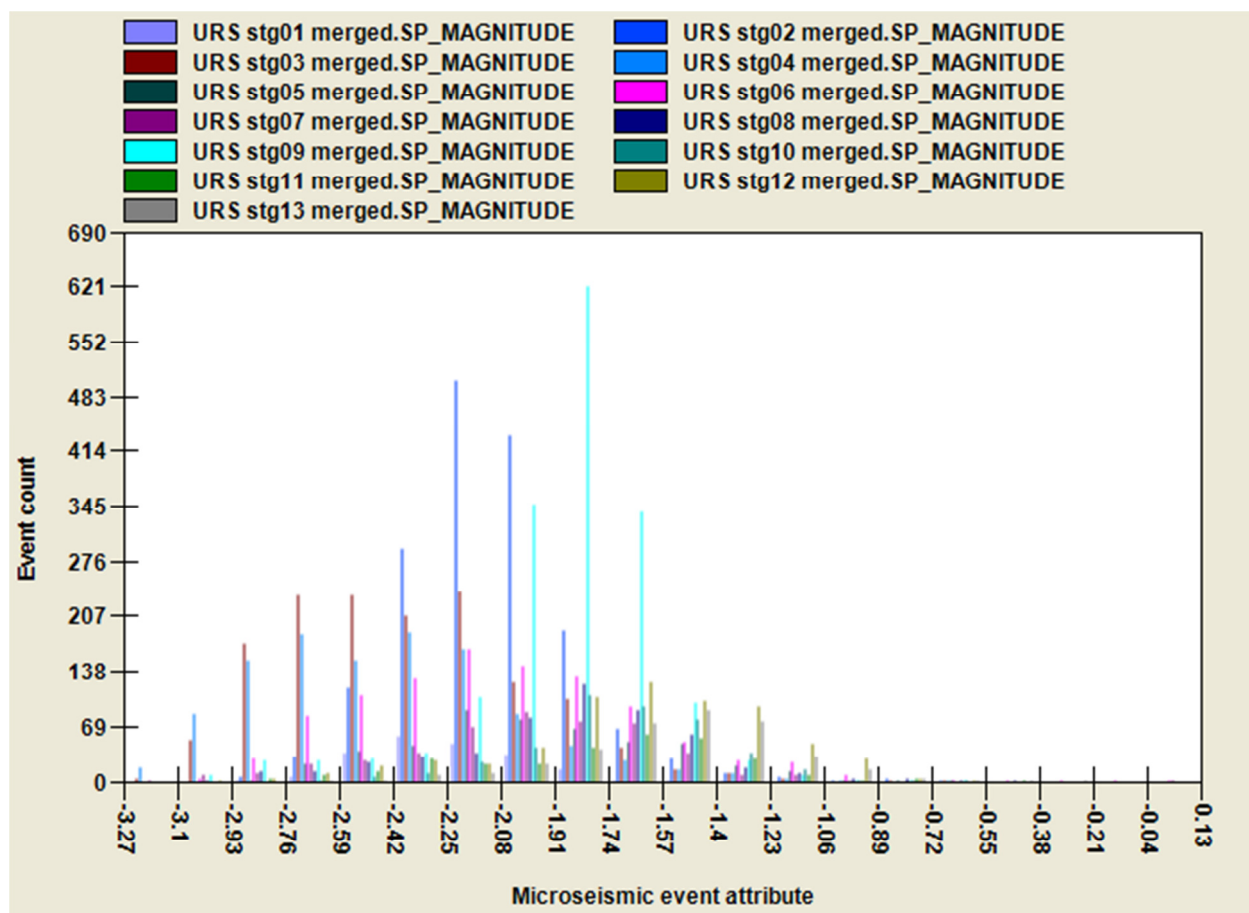


Figure 13 – Moment magnitude histogram.

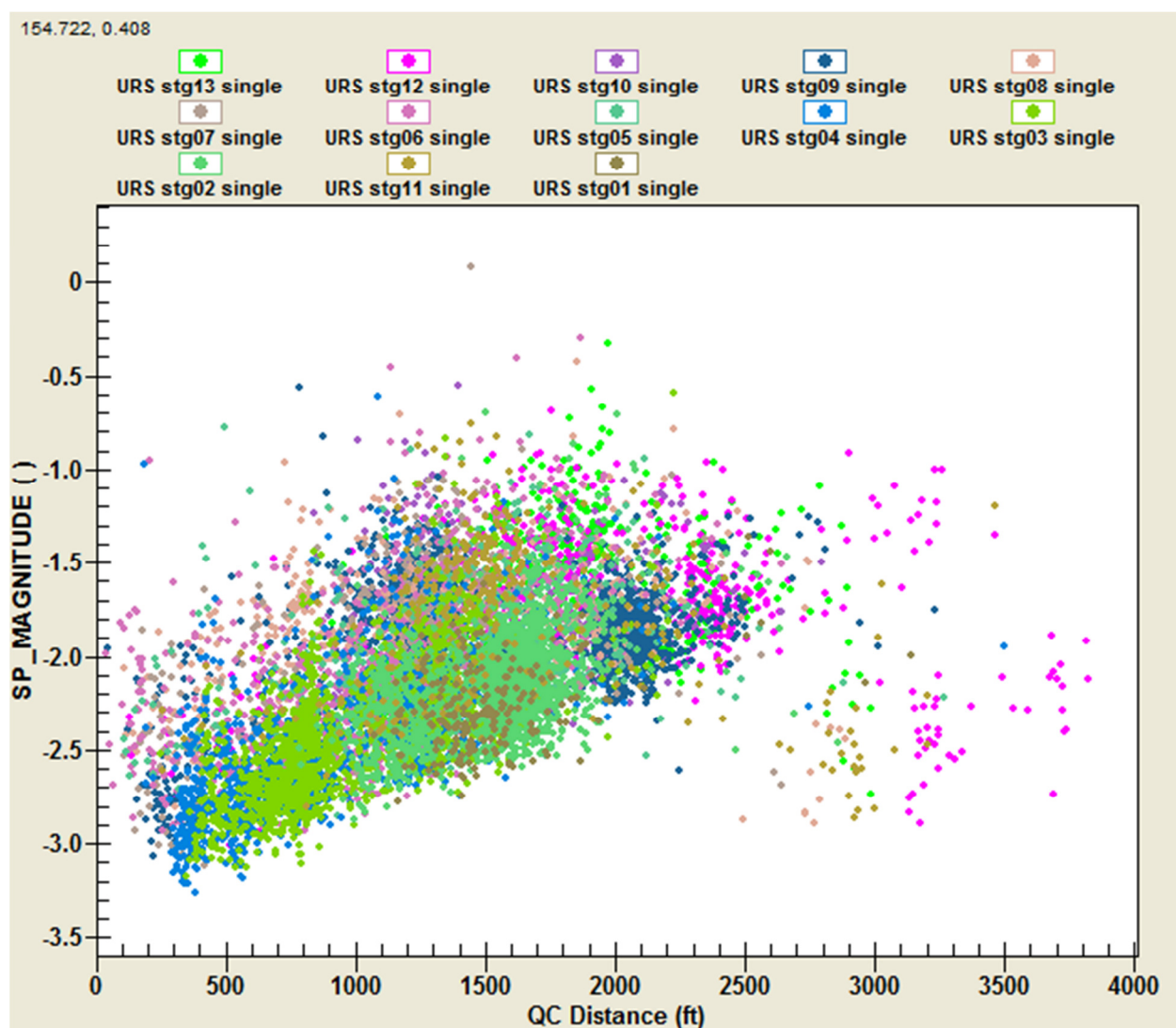


Figure 14 – Event magnitude vs. distance for all events, colored by stage.

Confidence Factor

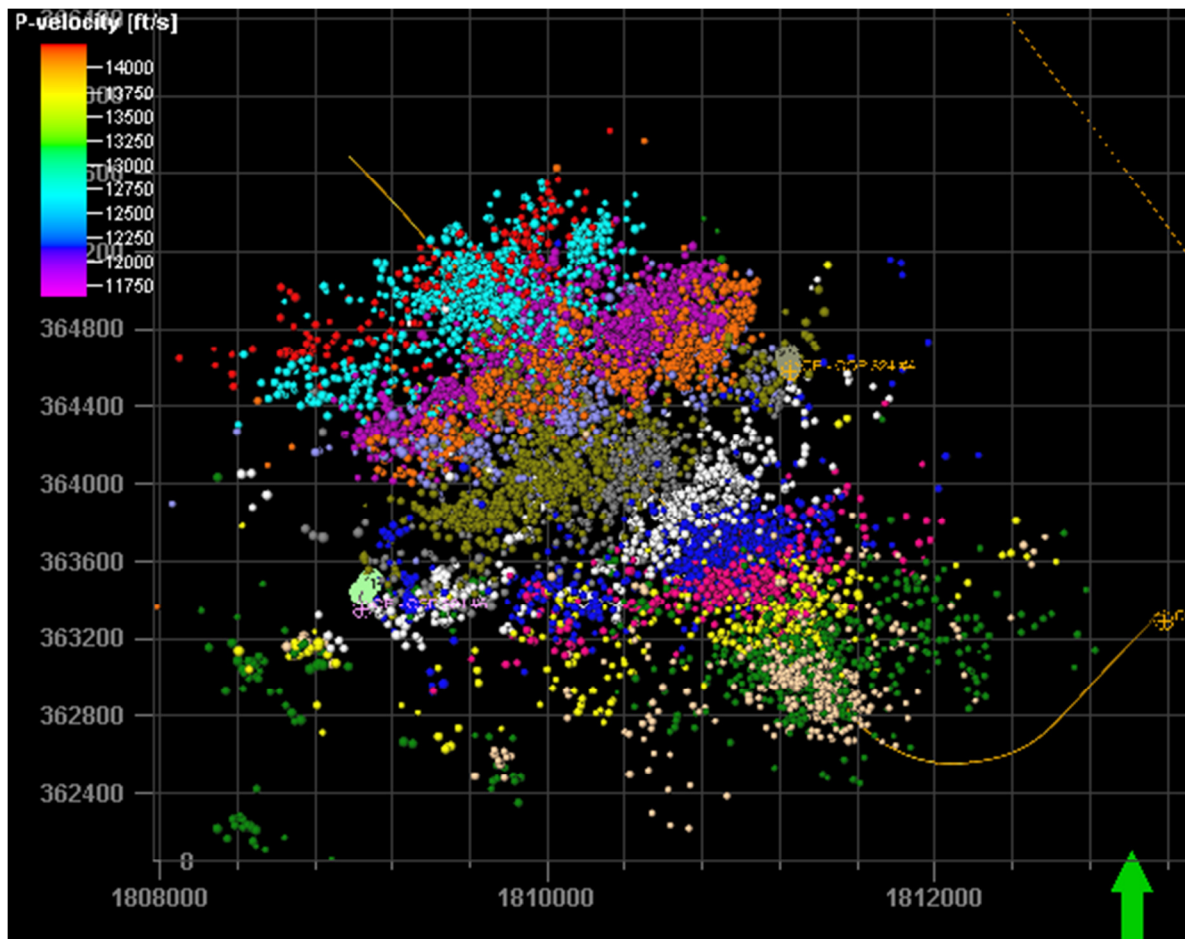


Figure 15 – Map view of events sized by confidence factor and colored by stage.

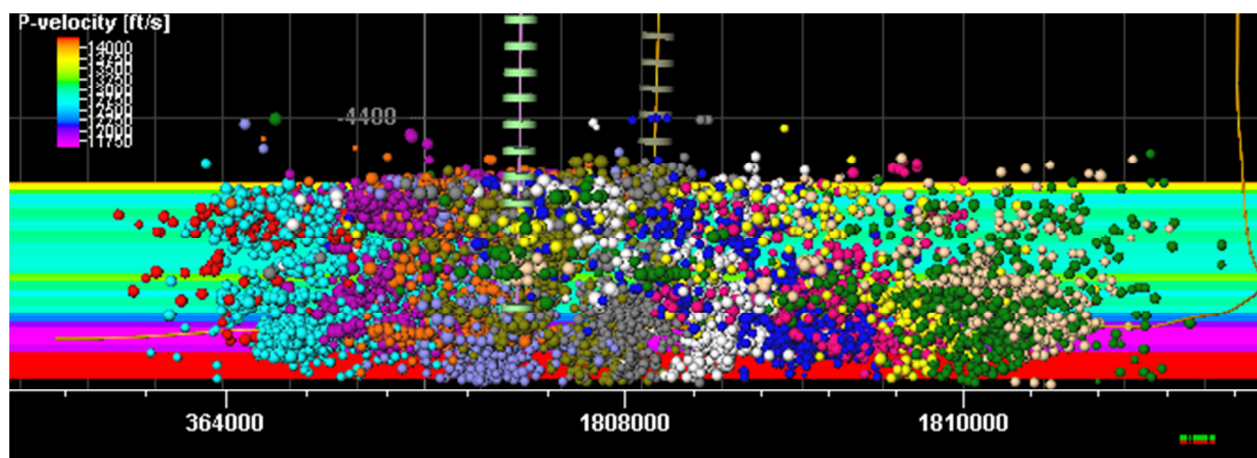


Figure 16 – Side view (N40E) of events sized by confidence factor and colored by stage.

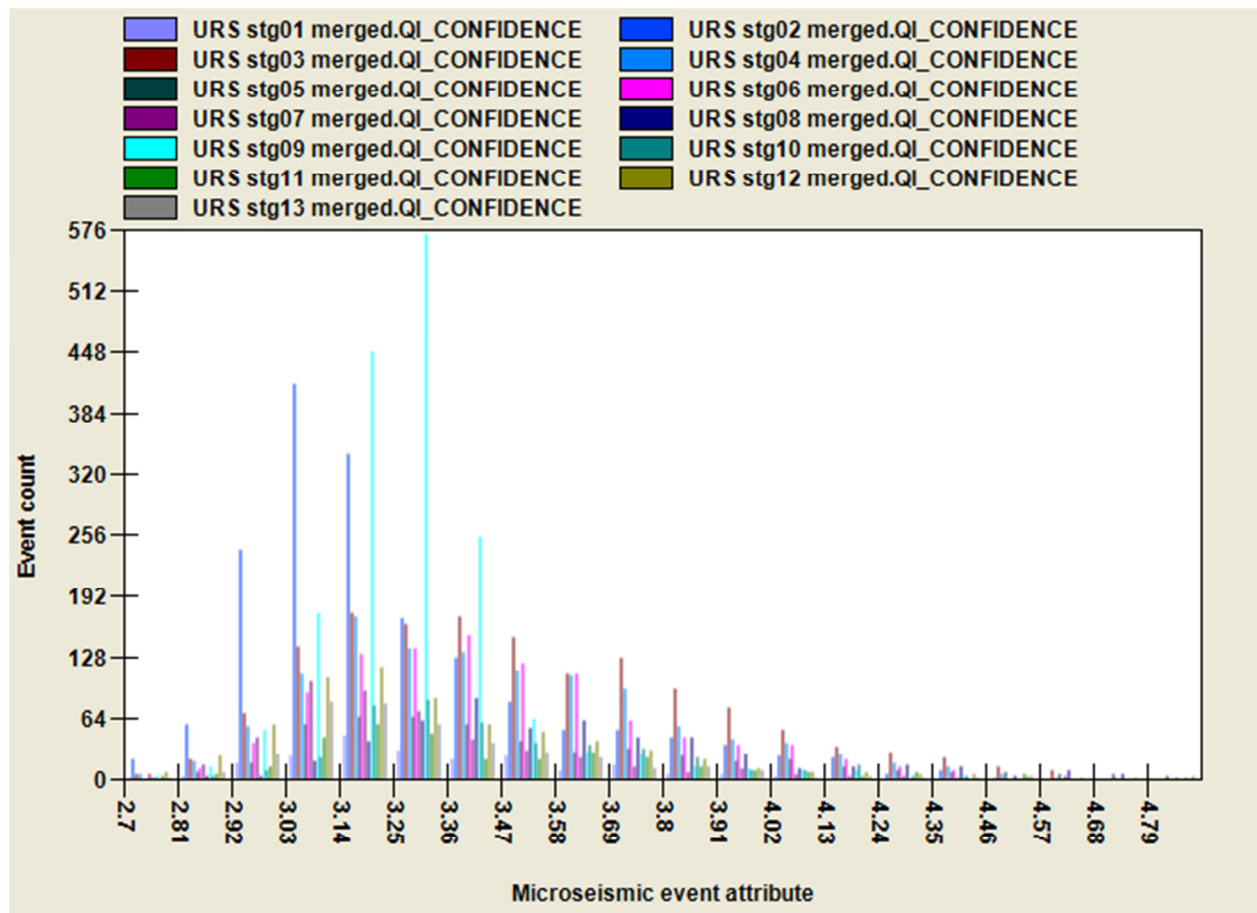
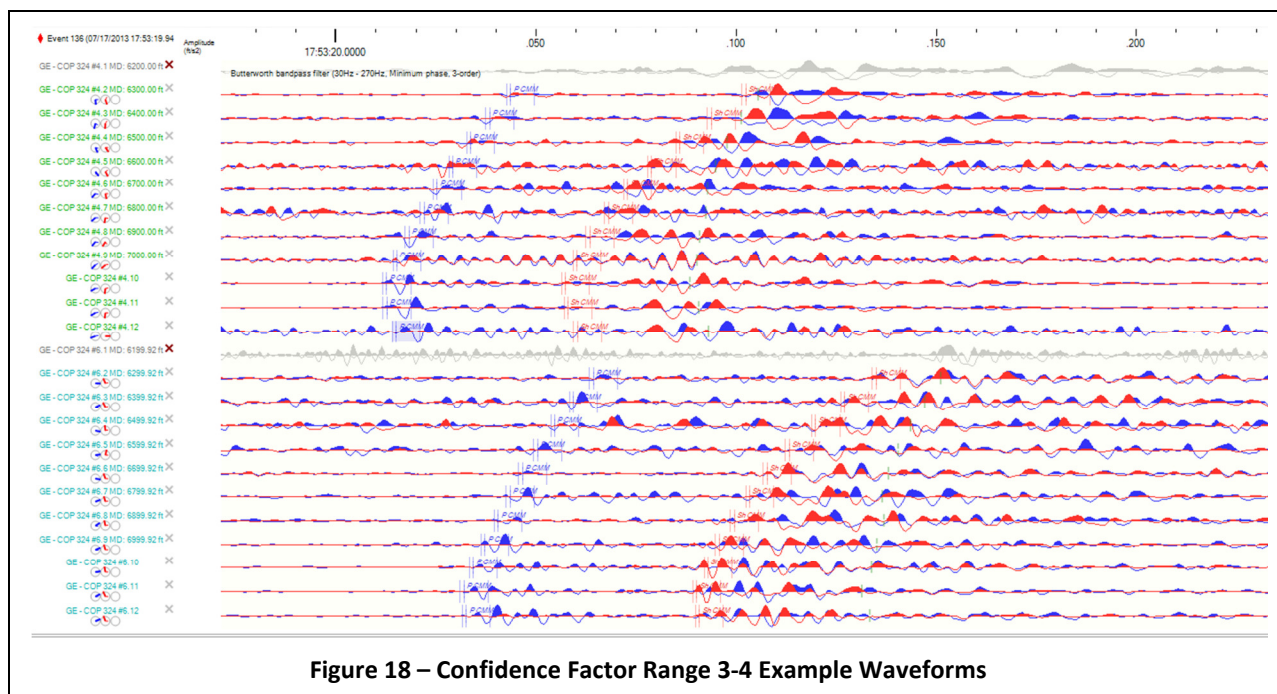
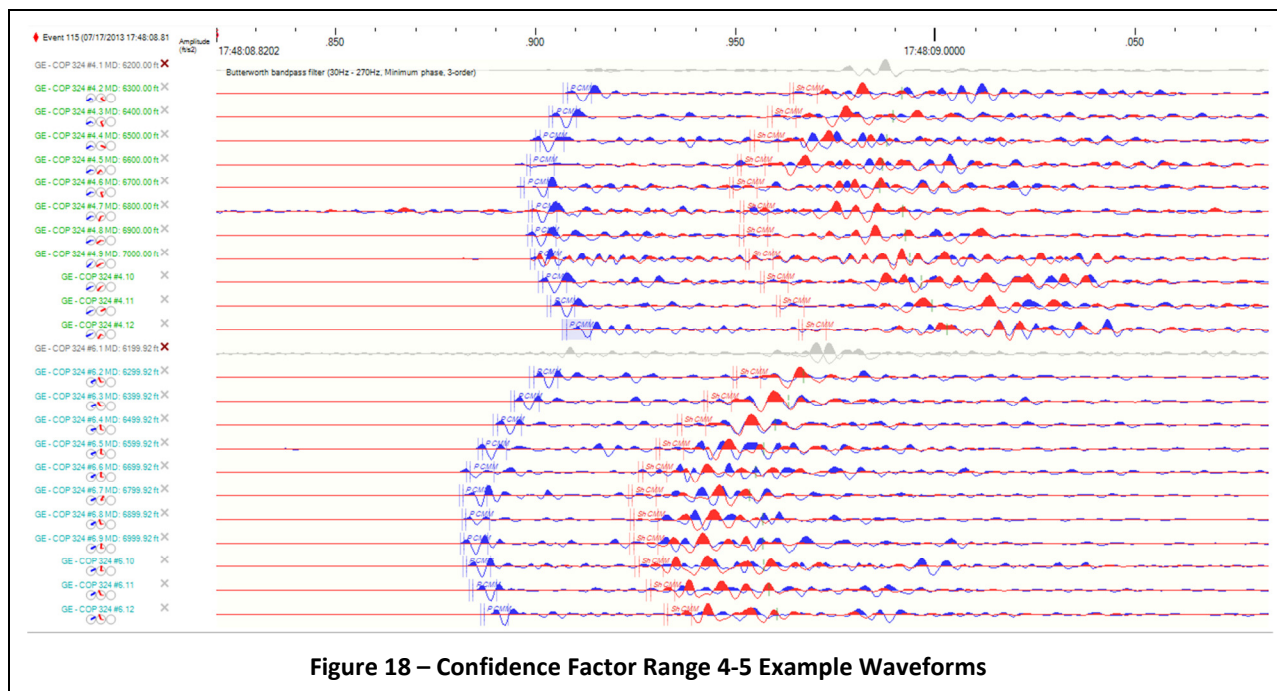
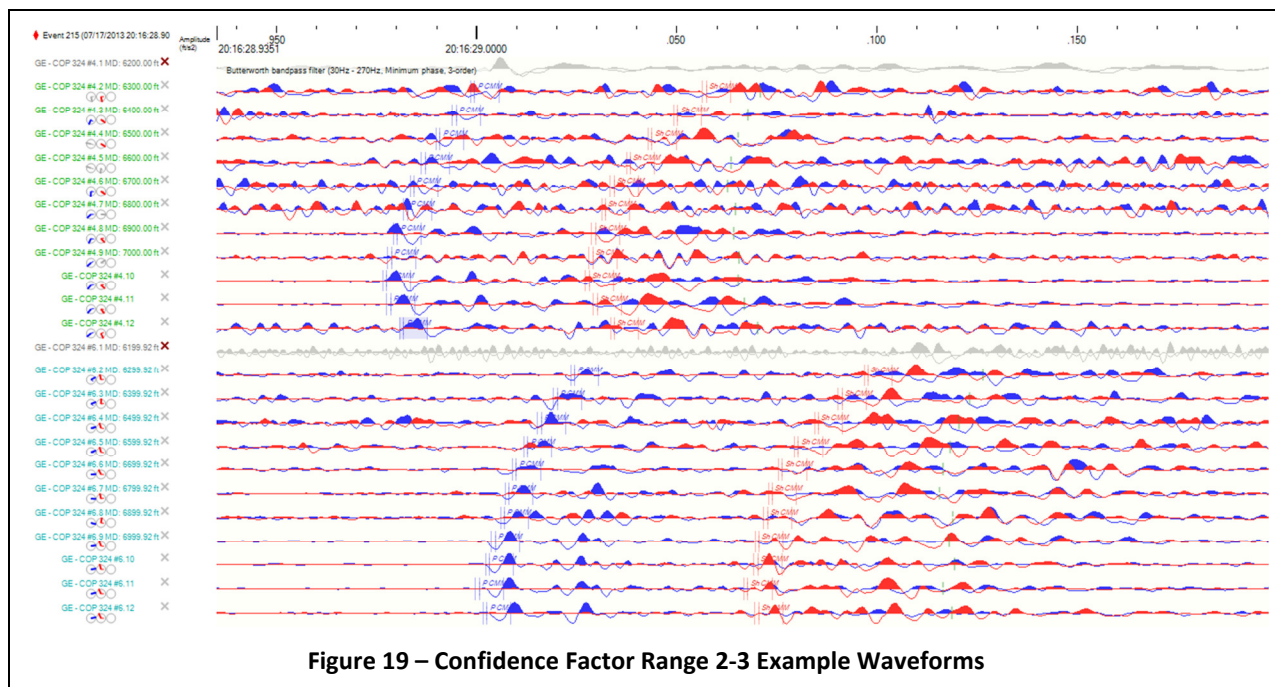


Figure 17 – Confidence factor histogram (all stages).

Example Waveforms

The following series of waveforms show selected screen shots of actual data from the project for events with different degrees of quality as designated by their confidence factor. A higher number indicates greater confidence in the event location and a lower ellipsoid of uncertainty for the event.





Uncertainty

All location estimates have an associated uncertainty due to a variety of factors, including uncertainties in time picks, wellbore location, velocity model, and a variety of other factors. During processing this uncertainty is estimated for each event. The uncertainty can be represented as the ellipsoid in space whose major axis represents the magnitude of the estimated maximum uncertainty for an event location. The major axis orientation indicates the direction that uncertainty applies.

Figure 31 shows a map view of all events located during this project for all stages, along with their associated uncertainty ellipsoids. Figure 32 shows the events from all stages and their uncertainty ellipsoids in a side view.

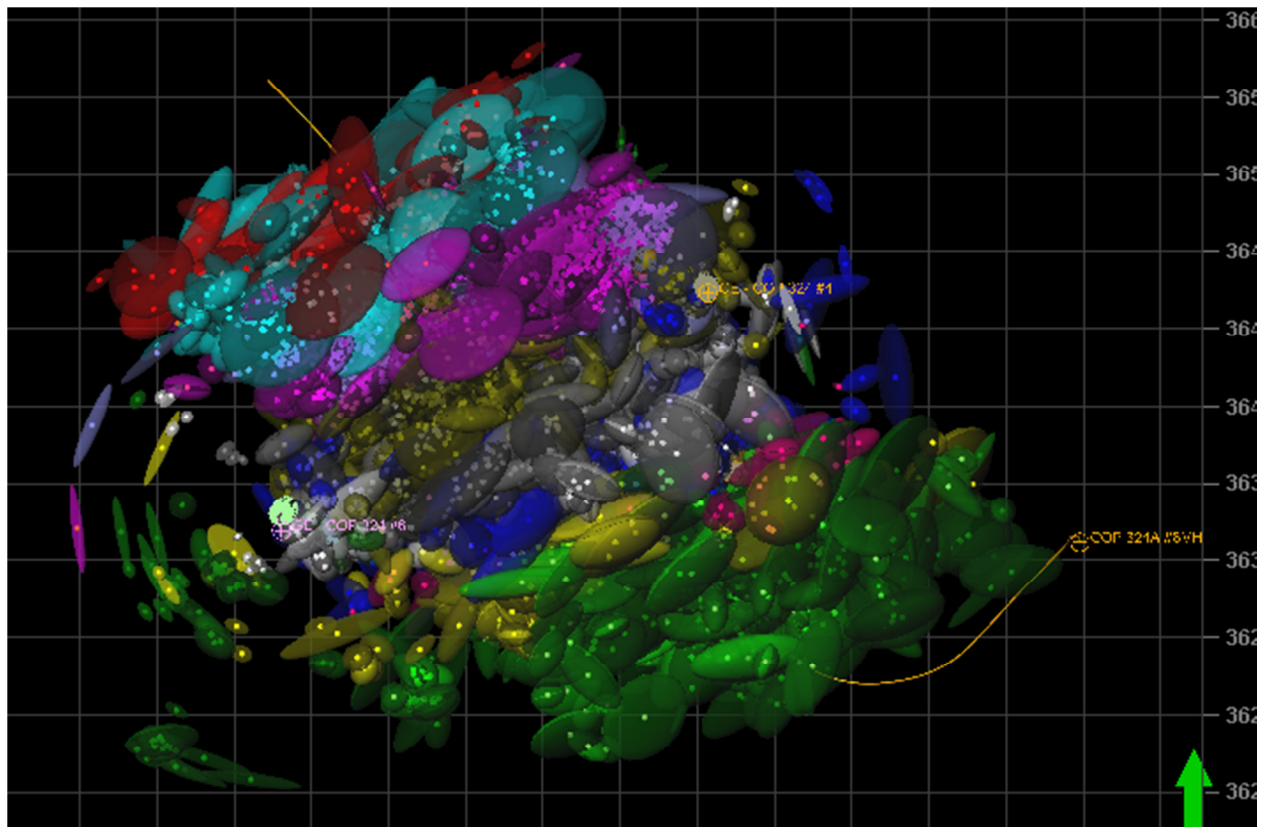


Figure 20 – Map view of event location maximum uncertainty, colored by stage.

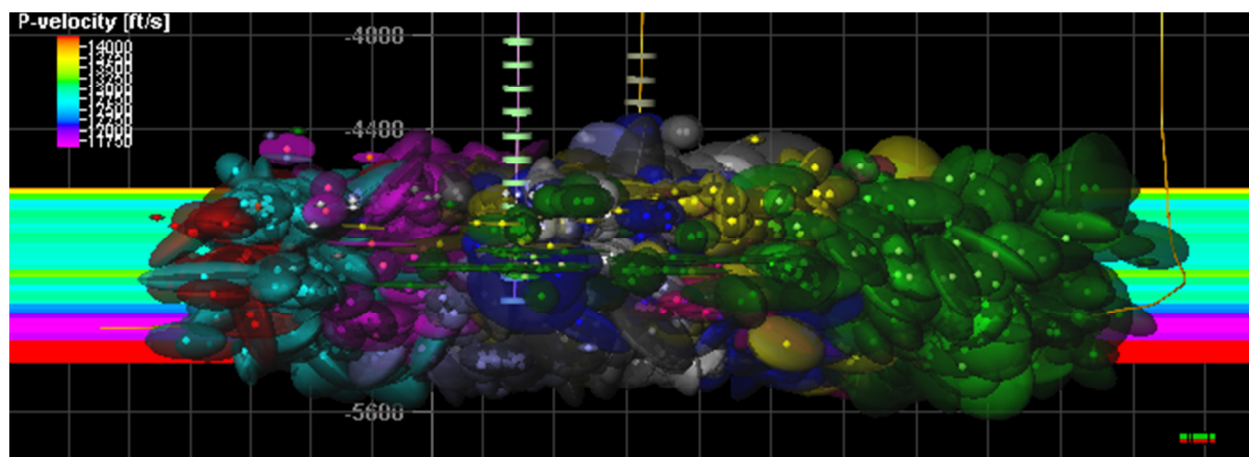


Figure 21 – Side view (N40E) of event location maximum uncertainty, colored by stage.

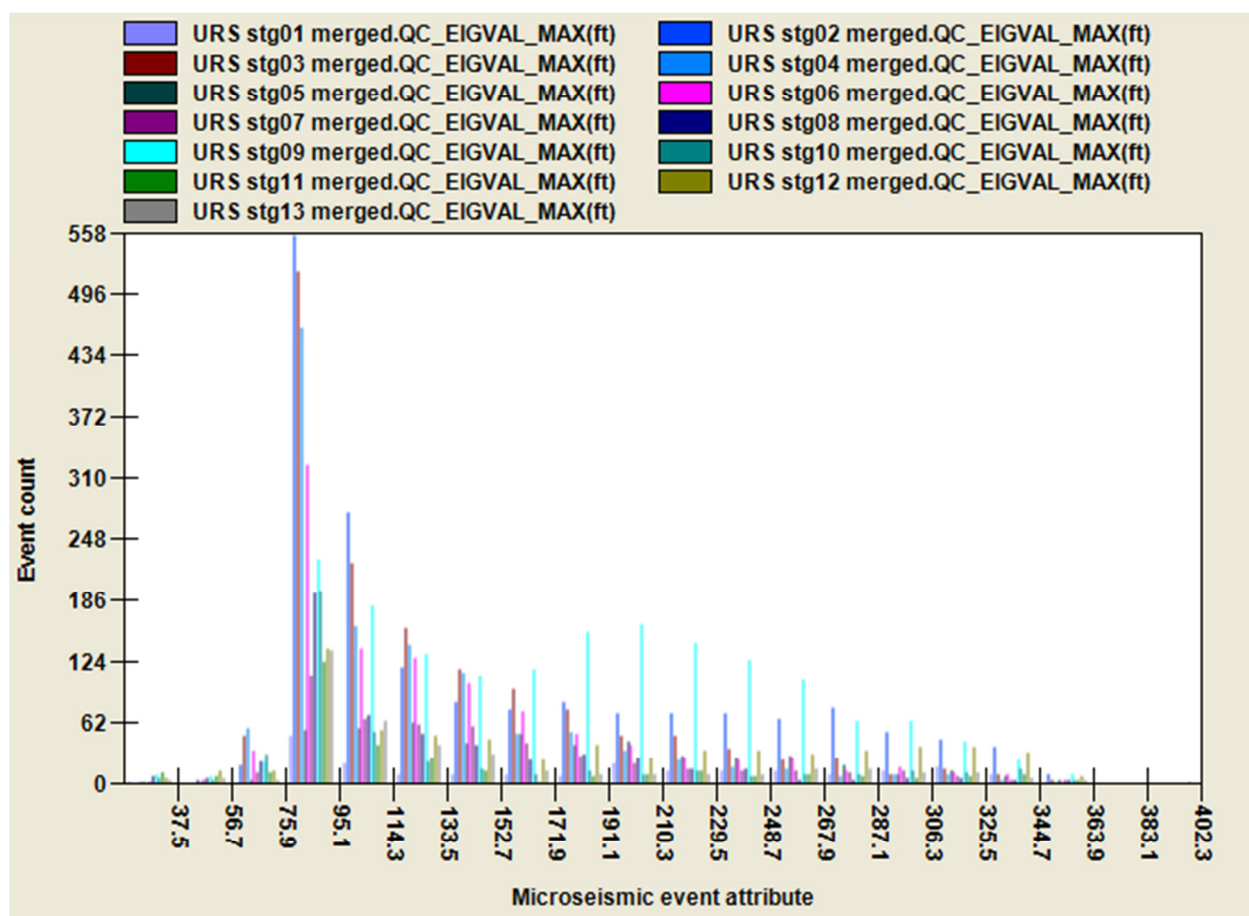


Figure 22 – Maximum uncertainty histogram (all stages).

Source Dimension

The displacement spectrum corner frequency gives an estimate of source radius by the Brune method. Since our objective is fracture geometry, the true dimensions of each microfracture are perhaps the most important factor for weighting of the events.

Figure 31 shows a map view of all events located during this project for all stages, displayed with their true diameters. Figure 32 shows the events from all stages and their diameters in a side view.

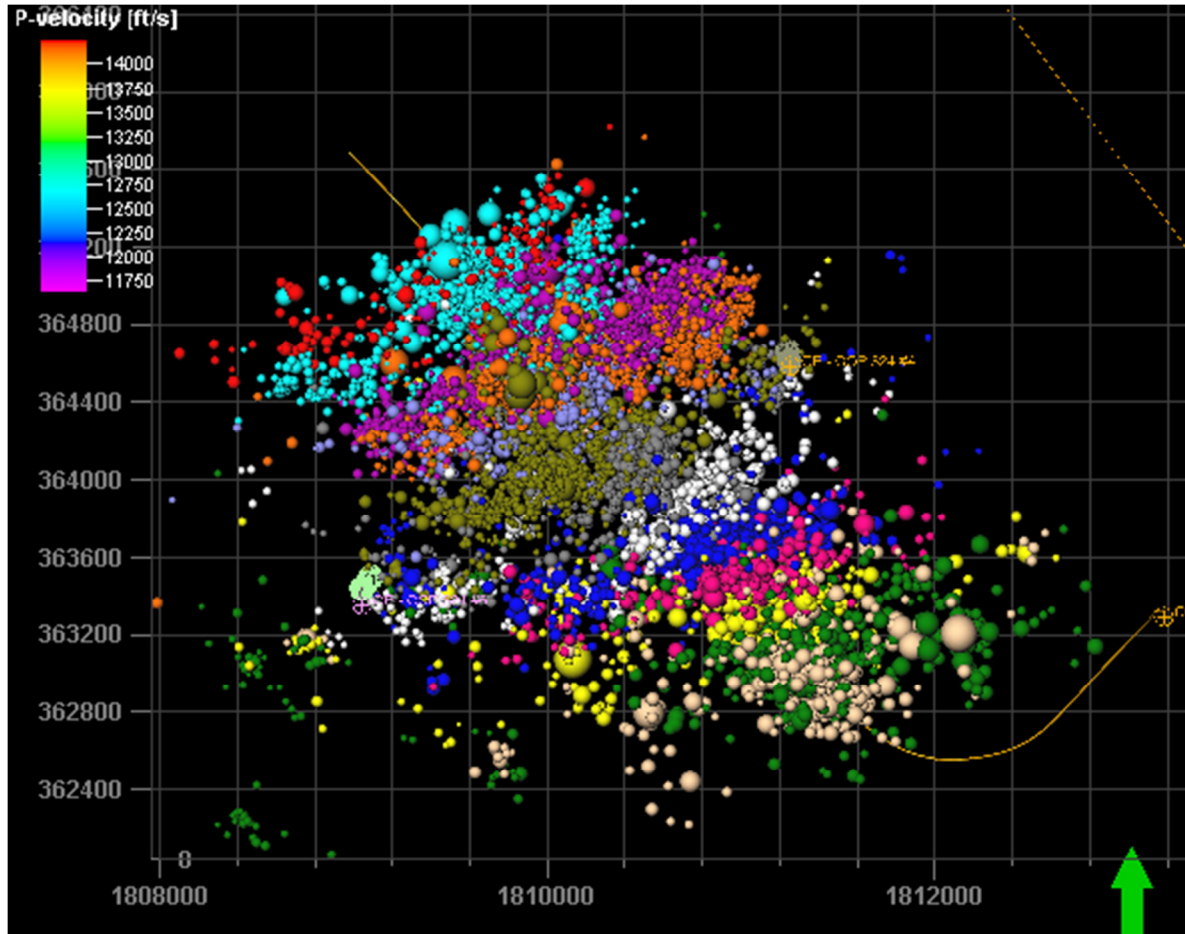


Figure 23 – Map view of events with true source dimension, colored by stage.

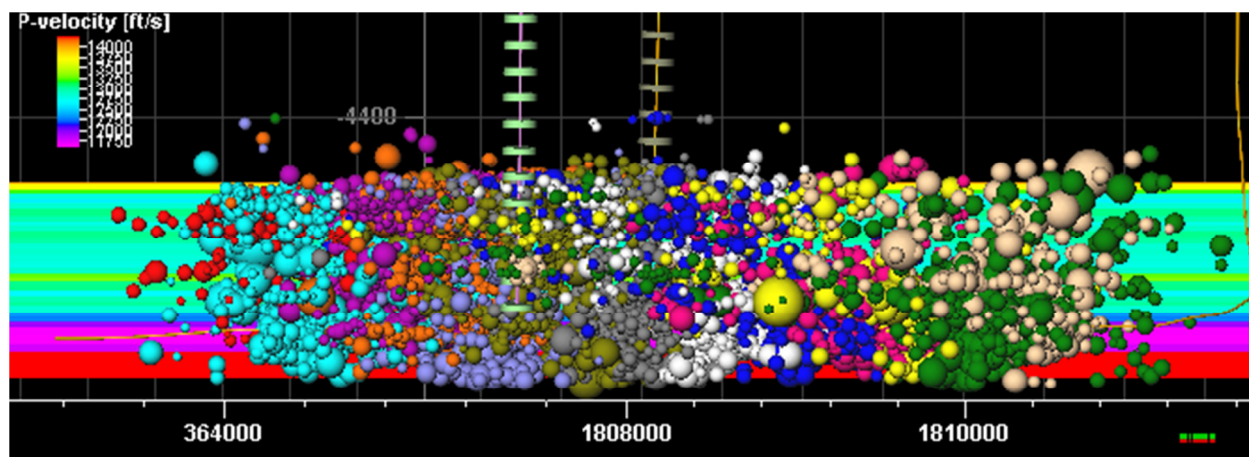


Figure 24 – Side view (N40E) of events with true source dimension, colored by stage.

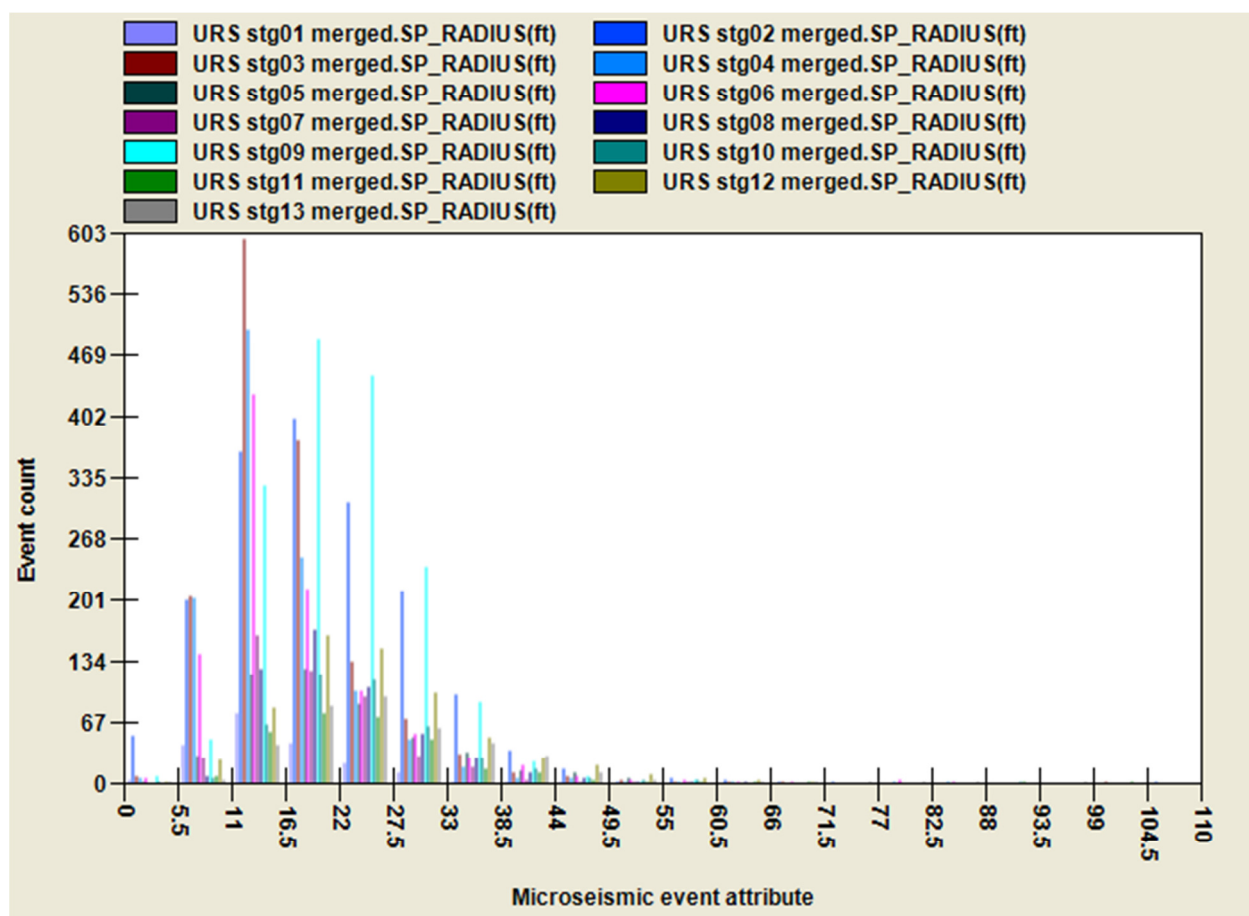


Figure 25 – Source radius histogram (all stages).